Study of the Fire Service Training Environment: Safety and Fidelity in Concrete Live Fire Training Buildings

John Regan
Robin Zevotek

UL Firefighter Safety Research Institute
Columbia, MD 21045

Study of the Fire Service Training Environment: Safety and Fidelity in Concrete Live Fire Training Buildings

John Regan
Robin Zevotek

UL Firefighter Safety Research Institute
Columbia, MD 21045

July 11, 2018

UL Firefighter Safety Research Institute
Stephen Kerber, Director

In no event shall UL be responsible to anyone for whatever use or non-use is made of the information contained in this Report and in no event shall UL, its employees, or its agents incur any obligation or liability for damages including, but not limited to, consequential damage arising out of or in connection with the use or inability to use the information contained in this Report. Information conveyed by this Report applies only to the specimens actually involved in these tests. UL has not established a factory Follow-Up Service Program to determine the conformance of subsequently produced material, nor has any provision been made to apply any registered mark of UL to such material. The issuance of this Report in no way implies Listing, Classification or Recognition by UL and does not authorize the use of UL Listing, Classification or Recognition Marks or other reference to UL on or in connection with the product or system.

Acknowledgments

The authors would like to thank the UL FSRI staff, particularly Steve Kerber, Craig Weinschenk, Dan Madrzykowski, Keith Stakes, Joseph Willi, Mike Alt, and Josh Crandall, for their help in the planning, execution, and analysis of these experiments. Additionally, Roy McLane of Thermal Fabrication was invaluable with his assistance with the fabrication and installation of instrumentation. Craig Weinschenk and Dan Madrzykowski graciously devoted their time and energy, offering review and guidance during the writing of this report. Thanks to Kerby Kerber of the Delaware County Emergency Service Training Center for allowing for the use of his facilities for the experiments and his assistance with the planning and logistics of the experiments. Fire suppression assistance was provided by Matt LeTourneau and Mark Morrissey of the Delaware County Emergency Service Training Center. Their generous help ensured that the experiments went safely and smoothly.

To assist the design and implementation of the experiments for this study, fire service experts were gathered from across the world with knowledge in fire service training. The individuals below provided direction for the project and assisted with the development of concrete conclusions. Their tireless support and effort make this project relevant to the fire service across the world. The authors would also like to acknowledge the UL LLC technical support staff for their assistance in conducting the heat release rate experiments.

This work was funded through a grant from the Department of Homeland Security's Assistance to Firefighters Grant Program under the Fire Prevention and Safety Grants: Research and Development. Without this critical funding and support, this vital fire service research would not be possible.

Fire Service Technical Panel

Name	Affiliation
Derek Alkonis	County of Los Angeles Fire Department
Brian Arnold	Oklahoma City Fire Department
Charles Bailey	Montgomery County (MD) Fire & Rescue Services
John Ceriello	Fire Department of New York
Sean DeCrane	Cleveland Fire Department (Ret.), UL LLC
James Dominick	Northeastern Illinois Public Safety Training Academy
Steve Edwards	Maryland Fire and Rescue Institute
Kenny Fent	National Institute for Occupational Safety and Health
Michael Gagliano	Seattle Fire Department
Sean Gray	Cobb County Fire Department
Bobby Halton	Fire Engineering Magazine
Todd Harms	Sacramento Metro Fire Department
Ed Hartin	Central Whidbey Island Fire & Rescue
George Healy	Fire Department of New York
Gavin Horn	University of Illinois Fire Service Institute
David Rhodes	Atlanta Fire Department
John Cunningham	North American Fire Training Directors
Ken Richards	Old Mystic Fire Department; NFPA 1403, Chair
Erich Roden	Milwaukee Fire Department
Tim Sendelbach	Firehouse Magazine
Dan Shaw	Fairfax County Fire Rescue/NFPA 1403
Denise Smith	Skidmore College
Jens Stiegel	Frankfurt am Main Fire & Rescue Services
Stefan Svensson	Lund University, Department of Fire Safety Engineering
Adam Thiel	Philadelphia Fire Department
Peter Van Dorpe	Algonquin-Lake In the Hills Fire Department
Devon Wells	International Society of Fire Service Instructors, President

Contents

List of Figures

List of Abbreviations

AFG	Assistance to Firefighters Grant program
BDP	Bi-directional Probe
DHS	U.S Department of Homeland Security
ELA	Equivalent Leakage Area
FEMA	Federal Emergency Management Agency
HGL	Hot Gas Layer
IC	Incident Commander
LODD	Line-of-Duty Death
NFPA	National Fire Protection Association
NIST	National Institute of Standards and Technology
NIOSH	National Institute of Occupational Safety and Health
OSB	Oriented Strand Board
PASS	Personal Alert Safety System
PPE	Personal Protective Equipment
RIT	Rapid Intervention Team
SCBA	Self-Contained Breathing Apparatus
TPP	Thermal Protection Performance Test
UL FSRI	UL Firefighter Safety Research Institute
UL	Underwriters Laboratories

Abstract

The goal of fire service training is to prepare students for the conditions and challenges that they face on the fireground. Among the challenges that firefighters routinely face on the fireground are ventilation-controlled fires. The hazard of these fires has been highlighted by several line-of-duty deaths and injuries in which a failure to understand the fire dynamics produced by these fires has been a contributing factor. The synthetic fuels that commonly fill contemporary homes tend to result in ventilation-controlled conditions.

While synthetic fuels are common on the residential fireground, the fuels that firefighters use for fire training are more often representative of natural, wood-based fuels. In order to better understand the fire dynamics of these training fires, a series of experiments was conducted in a concrete live fire training building in an effort to evaluate the fidelity and safety of two training fuels, pallets and OSB, and compare the fire dynamics created by these fuels to those created by a fuel load representative of a living room set with furniture items with a synthetic components. Additionally, the effects of the concrete live fire training building on the fire dynamics were examined. The two training fuel loads were composed of wooden pallets and straw, and pallets, straw, and oriented strand board (OSB).

The results indicated that the high leakage area of the concrete live fire training building relative to the fuel load prevented the training fuel packages from becoming ventilation-controlled and prevented the furniture package from entering a state of oxygen-depleted decay. The furniture experiments progressed to flashover once ventilation was provided. Under the conditions tested, the wood based fuels, combined with the construction features of this concrete live fire training building, limited the ability to teach ventilation-controlled fire behavior and the associated firefighting techniques. Additionally, it was shown that the potential for thermal injury to firefighters participating in a training evolution existed well below thresholds where firefighter PPE would be damaged.

1 Introduction

1.1 Background

Several firefighter line of duty deaths and injuries have occurred in recent years on the fireground as a result of rapid fire progression [1–4]. Among the contributing factors to these incidents was a lack of understanding of fire behavior [1–3]. Recent studies on firefighter safety [5, 6] have identified that the shift towards a higher synthetic content in modern home furnishings has resulted in fires with higher heat release rates (HRRs) than legacy fuels, which were composed mostly of natural materials. This shift has resulted in a more unforgiving fireground, where poorly timed actions such as uncoordinated ventilation can result in the rapid deterioration of conditions. Unfortunately, fire department tactics do not always reflect this changing fire environment. Among other considerations, the necessity for firefighters to understand the fire dynamics that they are likely to encounter on the fireground has been identified as essential for firefighter safety.

The National Fire Protection Association (NFPA) developed *NFPA 1403: Standard on Live Fire Training Evolutions* in response to a live fire training accident in 1982 that resulted in the deaths of two firefighters. The training evolution had featured a fuel load of tires, which ignited the combustible ceiling tiles and led to the death of two firefighters [7]. The standard offers a means of conducting live fire operations safely in both fixed-facility and acquired burn structures. The documents sets minimum requirements for live fire training evolutions, with the purpose of achieving training objectives and providing a process for conducting live fire training evolutions in a manner which minimizes the health and safety hazards for the participants.

NFPA 1403 limits the fuels that could be used to wood, clean hay, and straw. The current version of the standard specifies the types of fuels that can be used as "wood products." As a result of these guidelines, wooden pallets and straw are a common training fuel. Pallets and straw have long been used as an economical training fuel for fire training facilities because they are easy to procure and create a repeatable fire.

However, some academies and training groups have recognized that the conditions produced by these pallets and straw training fires are not representative of those observed in residential fires. Thus, in an effort to replicate the conditions experienced on the modern fireground, these organizations have begun to incorporate different fuels into their live fire training evolutions, including engineered lumber, such as pressboard, particleboard, and oriented strand board (OSB). These en-

gineered wood products combine glues or resins with smaller pieces of wood to form larger sheets or boards. The additional fuel mass and glue content of the engineered wood products are thought to produce more severe thermal conditions than traditional pallets and straw training fires, while still remaining compliant with the language in *NFPA 1403*.

The introduction of these fuels into the training environment raises the issue of balancing the fidelity of training fires with the safety of participating in such burns. Some instructors believe that *NFPA 1403* prohibits realistic training evolutions: ones that replicate the severity of conditions that students would encounter on the fireground [8]. As training fuel packages are modified to produce conditions consistent with a furnished room or fire involving the structure, the thermal environment becomes more hazardous. It is important that the thermal hazard of the training environment is considered, as several firefighter line of duty deaths (LODDs) have resulted from excessive thermal exposure during training evolutions [9–11]. Rather than mirroring the conditions experienced in a residential home using modern fuels, the goal should be to simulate the response of the fire to firefighter tactics.

1.2 Objectives

This series of experiments compared the fire conditions generated by three different types of fuel packages in a concrete live fire training building, similar to those found at many fire training academies across the United States. Two of the fuel packages contained wood based fuels and straw. The third fuel package was composed of residential furnishings such as furniture with polyurethane foam cushion, tables made of engineered lumber, polyurethane foam carpet padding, and polyolefin carpeting. The furniture fuel package is not compliant with NFPA 1403. The fire conditions resulting from the furniture fuel package will be compared with those generated by 1403 compliant fuel packages.

1. Characterize fuels commonly used in training and compare them to fuels found in the residential fire environment for both burning characteristics and potential firefighter exposure.
2. Better understand the concepts of fuel and ventilation-limited fires and research how they can be visually taught during hands-on fire training.
3. Bridge the gap between fire dynamics knowledge and the utilization of training buildings and props for hands-on training.
4. Improve firefighter safety by increasing knowledge of fire behavior.

In order to accomplish these objectives, eight full scale fire experiments were conducted with three different fuel loads in a concrete training building. Additionally, heat release rate characterization of the fuels was performed under an oxygen consumption calorimeter to compare the fuels in a configuration independent of the concrete burn building.

2 Literature Review

2.1 Standards

NFPA 1403: Standard on Live Fire Training Evolutions outlines the minimum requirements for conducting live fire training in acquired and fixed facility training structures [12]. The document discusses the responsibilities of the instructors, safety officers, and participants, and also provides guidelines for the types of fuels that can be included in the fuel package. The standard defines acceptable fuels as "pine excelsior, wooden pallets, straw, hay, and other wood-based products" [12]. The standard specifically forbids treated wood products, rubber, plastic, polyurethane foam, upholstered furniture, and chemically treated straw as fuels. *NFPA 1403* additionally makes several specific recommendations for acquired structure training burns. The standard recommends against the use of low-density particleboard and unidentified materials found within the structure. Furthermore, the document mandates that combustible materials not included in the fuel load should be moved to an area of the structure remote from the fire room.

Despite the procedures and precautions contained in *NFPA 1403*, there have been several instances where firefighters have been killed or injured during live fire evolutions. The National Institute of Occupational Safety and Health (NIOSH) investigated several of these incidents, which are described below. These incidents have resulted in a series of revisions to the document since its initial release in 1986. The 2018 Edition of *NFPA 1403* lists a series of prerequisites that students must have prior to participating in live fire training. Among these prerequisites are training on the proper use of personal protective equipment (PPE), ventilation, and fire behavior. Specifically, students should have a proper understanding of fire dynamics, including heat transfer, basic chemistry, and compartment fire behavior; the components, capabilities, and limitations of their PPE; and nozzle techniques and door control.

NFPA 1403 additionally provides guidelines for selecting an appropriate fuel load, and cautions that an excessive fuel load can result in a ventilation-controlled fire. Ventilation-controlled fires present a hazard because additional ventilation results in fire growth or flashover. It is important that firefighters understand the concept of ventilation-controlled fires, however, since most residential structure fires are ventilation-controlled. Thus, the most recent version of *NFPA 1403* includes a methodology for conducting controlled, ventilation-limited fires. These scenarios are intended to teach fire behavior, rather than to teach firefighting skills such as line advancement or search and rescue. The document stipulates that students and instructors should be positioned in a "safe

observation space," which is outside of the fire room, at the same level or below the fire room, and removed from the exhaust portion of the flow path. The observation space must have a charged hose line capable of suppressing the fire and an unimpeded path of egress. When done safely and correctly, a demonstration of a ventilation-controlled fire behavior can be a useful tool for teaching fire behavior, which is one of job performance requirements identified in *NFPA 1001: Standard for Fire Fighter Professional Qualifications* [13].

2.2 Line of Duty Deaths and Injuries

NIOSH led an investigation of a 2005 incident in Pennsylvania that resulted in the death of a 47-year-old fire instructor and attracted further studies into the hazards of the training fire environment. The instructor experienced a catastrophic failure of his facepiece lens during a live fire "train the trainer" course and died of thermal injuries two days after the event. The burn building was a two and a half story concrete block structure. Investigators attributed the facepiece failure to the high thermal conditions that were present in the basement during the evolution. The investigation emphasized the importance of using the minimum amount of fuel necessary to perform live fire training to maintain firefighter safety. Additionally, this incident demonstrated the dangers of repeated evolutions without allowing sufficient time between evolutions for the burn building and the instructor's PPE to cool down [10].

In a 2007 incident, a probationary firefighter was killed during a training evolution in a vacant end-of-the-row townhouse in Maryland. The scenario used approximately 12 wooden pallets and 11 bales of hay as fuel, and featured fire sets on all three floors of the townhouse. The victim was on the nozzle of the first hoseline and was instructed to bypass the fires on the first and second floors and make an attack on the third floor fire. When the attack team reached the stairway between the second and third floors, they were overcome by high heat conditions. Two of the participants exited the structure through a window. The victim reached the window, but was unable to get the lower half of her body out of the window. While the instructor was trying to remove her from the fire room through the window, her mask became dislodged. She was finally removed when another instructor came up the stairs and helped her legs through the window. The victim succumbed to thermal injuries and asphyxia. NIOSH attributed the outcome of the incident to several factors, including a lack of equipment, a lack of physical fitness performance requirements, and a failure to follow the requirements of *NFPA 1403* [9].

Two career firefighters were killed during a training fire in an acquired structure in Florida. The structure was a one story, single family house with three bedrooms, two bathrooms, and a kitchen. The fire was ignited in one of the bedrooms and had a fuel load of wooden pallets, straw, and a urethane foam mattress. Before ignition, other materials in the room, such as urethane foam padding, hollow core wood doors, and carpeting were not removed, and thus contributed to the fuel load. Four firefighters acted as interior safety officers throughout the duration of the incident. The victims entered the structure first and performed a primary search of the building. They were followed by the attack line. The victims passed the safety/ignition officer positioned outside of the fire room, who retreated to the living room to help the attack company while the victims

proceeded to search the fire room. Before applying water, the fire room window was vented and dark, heavy smoke exited the window. The attack company began to apply water in short bursts, and one of the safety officers exited the structure, thinking that he had been "steamed." The victims remained unaccounted for for several minutes. During this time, it is suspected that the fire room had transitioned to flashover. The location of the victims was unknown for several minutes, during the period of rapid fire growth and suppression. After the victims failed to acknowledge repeated attempts by the Incident Commander (IC) to contact them, the IC activated the rapid intervention team (RIT), who found the victims in the fire room. They were transported to a local hospital and pronounced dead. The investigation identified the fuel load and uncoordinated ventilation as contributing factors, noting that the use of fuel with unknown burning characteristics can lead to unexpected fire development and rapid fire progression [14].

In another line of duty death incident, a New York volunteer firefighter was killed during a simulated "mayday" scenario, where he and another firefighter were acting as the simulated victims. The victim had very little training prior to the incident, and had never worn a self-contained breathing apparatus (SCBA) under live fire conditions before. The training was conducted in a vacant two story duplex. The scenario called for two firefighters trapped in an upstairs bedroom in one half of the duplex, and involved the engine and rescue company making entry through the other half of the duplex, breaching a wall, and rescuing the downed firefighters. The intended fuel source was a burn barrel in one of the bedrooms, but an assistant chief ignited a foam mattress when the ignition firefighter had trouble igniting the burn barrels. The ignition of the mattress led to rapid fire growth and caused conditions throughout the duplex to deteriorate. The ignition firefighter attempted to help the two trapped firefighters, but in the process of doing so lost his gloves, received burns to his hands, and was forced to exit out of a second story window. When the engine and rescue companies arrived on scene, they both acted as RIT teams, and removed the trapped firefighters from the structure. The victim was transported to a local hospital where he was pronounced dead. The other firefighter that was removed from the structure and the ignition firefighter that jumped from the second floor were flown to a regional burn center. The investigation highlighted the importance of not using live victims during live fire training and ensuring that the fuels used in training burns are in accordance with *NFPA 1403* [11].

2.3 Previous Research

One common factor among the LODD incidents described in the previous section is the use of improper fuels or fuel loads. In several of the acquired structure burns, the addition of debris found around the house had the effect of increasing the fire size beyond what was manageable or expected. In an effort to better understand the training fuels that firefighters use, a series of research studies have aimed to quantify parts of the training fire environment.

Madrzykowski [15] investigated a pair of training fires in which firefighters had been killed. The first incident occurred during the previously mentioned incident in Florida, where two firefighters died while conducting a search when the fire room transitioned to flashover [14]. The National Institute of Standards and Technology (NIST) recreated the fire room and two adjacent spaces,

and evaluated the thermal conditions produced by five different combinations of fuel load and ventilation conditions. The results indicated that flashover conditions were reached for each fuel load, including the experiment where only pallets, straw, wood molding, and a hollow core door were used. Furthermore, the temperatures exceeded 500°F (260°C), and the heat fluxes exceeded 20 kW/m^2 during each test, indicating that the thermal conditions in the fire room were unsurvivable for even a firefighter in full PPE. An additional experiment examined the peak HRR of the pallets and straw, which was found to be 2.8 MW [15]. The author compared this HRR to the theoretical HRR required for flashover in the room and found that the HRR was sufficient to cause flashover.

The second incident that was investigated was the one which occurred in Pennsylvania during a "train the trainer" class conducted in a concrete live fire training building. After the last burn of the day, an instructor was found lying face-down on the floor in the basement with damage to his facepiece. He later succumbed to his injuries. NIST instrumented the burn building where the incident occurred and attempted to recreate the thermal conditions that were present at the time of the instructor's death. They first used a fuel load of pallets and excelsior to "pre-heat" the burn structure. Then, additional pallets and straw were added. When the fires peaked, the fuel was suppressed with a hose stream and the compartment was hydraulically ventilated. Once the compartment was cleared, additional pallets were added to the embers, and the process was repeated. The ambient heat flux at 4.9 ft. (1.5 m) from the ceiling before the last evolution was 6 kW/m^2, and the ambient temperature in the burn structure was 302°F (150°C) at 5.02 ft. (1.53 m) below the ceilings. The instructor was in the process of adding two additional pallets to the fire burning in the basement fire room. In the process he was overcome by the hot gases from the existing fire, which resulted in the catastrophic failure of his SCBA facepiece. Based on the charring of some of the neoprene components of the facepiece, it was exposed to temperatures of at least 342 C (647 F). Well above the glass transition temperature and melting temperature of the high temperature polycarbonate facepiece [10]. The recreation of the fire conditions in the training building showed peak temperatures in excess of 500 C (932 F) and peak heat flux values in excess of 20 kW/m2 at 1.5 m (5 ft) above the floor [15]. Laboratory experiments indicated that a fuel load consisting of six pallets and straw had a peak HRR of 4.5 MW.

In both fatal training fire incidents, the thermal conditions that resulted from the fuel loads exceeded the protective capabilities of the firefighters' PPE. This highlights the necessity of using discretion when determining the fuel load of training fires.

Willi et al [16] conducted a series of experiments to quantify the thermal exposure of firefighters in a concrete live fire training building. The authors constructed a portable data acquisition system capable of gathering heat flux and temperature data from a firefighter's immediate environment during live fire training exercises. The tests examined two types of firefighter training evolutions: scenarios conducted in concrete live fire training buildings, that used wooden pallets and straw as the fuel load and scenarios conducted in a metal container-based training prop known as a "flashover simulator", that had a fuel load consisting of pallets, straw, OSB, and medium density particleboard. The results indicated that routine training evolutions exhibited heat fluxes on the order of 1 kW/m^2 and temperatures close to 122°F (50°C), whereas more severe exposures showed heat fluxes between 3 kW/m^2 and 6 kW/m^2 and temperatures between 302°F (150°C) and 392°F

(200°C). Furthermore, the experiments showed that in some instances, the temperature data underpredicted the thermal hazard posed by the heat flux based on the NIST Thermal Classes, which are a method of classifying the thermal environment based on the performance of electronic equipment that first responders carry. The authors also noted that stationary temperatures located in training buildings underpredicted the overall thermal hazard encountered by the firefighters working in those buildings.

René Rossi [17] conducted a series of experiments in several types of firefighter training buildings in Switzerland to examine the effect of different thermal exposures on core temperature and sweat production. Heat flux and temperature measurements were also taken in the training buildings. Rather severe peak thermal conditions were observed during the tests, noting temperatures as high as 532°F (278°C) and heat fluxes as high as 26 kW/m^2. The more routine exposures contained temperatures between 122°F (50°C) and 266°F (130°C) and heat fluxes between and 5 kW/m^2 and 10 kW/m^2. The results indicated that relatively high heat fluxes were observed for rather moderate temperatures.

While a number of studies have examined the thermal hazards that firefighter students and instructors are exposed to in the training fire environment, there is a gap in the literature regarding the fidelity of these training fires, that is, the degree of exactness that the training fires adhere to a fire that may be encountered on the fireground. Additionally, little research has focused on new training fuels, such as OSB, particleboard, and other engineered wood products, that many training academies and organizations have begun to incorporate into live fire training. This study will attempt to bridge the gap in understanding between training fuels and fuels that are representative of those found in residential structures. Additionally, the relative thermal hazards of these fuels will be compared in an effort to place the relative severity of these fuels into context.

Safety is a critical concern for live fire training scenarios. It is imperative that safety is not compromised in the pursuit of creating fire dynamics consistent with a ventilation-controlled residential fire. This means focusing on the minimization of training-related injuries and deaths from excessive thermal exposure. Additionally, thermal conditions in which equipment, such as facepieces, helmets, and electronic equipment, may be damaged are undesirable, as the replacement of such equipment can unnecessarily burden a fire department.

Training fires are different from typical fires that fire departments respond to in the respect that firefighters involved in suppression and search and rescue operations are not the only personnel inside the burn structure. Rather, support personnel such as instructors and stokers are actively involved in the training scenarios as well. Stokers are firefighters whose specific task is the construction and maintenance of fuel packages throughout the duration of the training evolution. In contrast to a residential fire, where the suppression team would likely mitigate conditions with a hoseline before entering areas with the most severe thermal conditions, these instructors and stokers are often tasked with maintaining the fire, and may be positioned in or close to the fire room, possibly for extended periods of time. Thus, the threat that the thermal conditions in these areas pose to firefighters must be considered. Additionally, it is important for recruits to understand that although some areas are relatively safe for habitation in the training environment, the same areas in a real fire may quickly result in death or serious injury.

A variety of methods exist for evaluating the thermal conditions to which firefighters are exposed. In general, some methods divide the thermal environment into either three or four classes, with the lowest class representing conditions only slightly more severe than ambient, and the highest class representing emergency conditions that are tenable for only a few seconds before equipment failure, injury, or death are imminent. Some of these methods, such as the NIST Thermal Classes proposed by Donnelly et al. [18] are used primarily for the purpose of evaluating electronic firefighting equipment. The NIST Thermal Classes specify four classes, based on criteria listed in Table 2.1. Because these thermal classes are focused specifically on electronic equipment, Personal Alert Safety System (PASS) alarms in particular, they are not the most appropriate for evaluating the risk of thermal injury to firefighters in training fires. Additionally, heat flux and temperature are treated separately by the NIST Thermal Classes, and the consideration of only one value may give an incomplete picture of the thermal threat.

Table 2.1: NIST Thermal Classes

Thermal Class	**Maximum Time (min)**	**Maximum Temperature (°C)**	**Maximum Heat Flux (kW/m^2)**
I	25	100	1
II	15	160	2
III	5	260	10
IV	$\leq$1	$\geq$260	$\geq$10

A more appropriate method of characterizing a firefighter's thermal environment involves using the thermal operating conditions outlined by Utech [19]. Utech uses the temperature at the firefighter's height as an approximation of the convective heat transfer to the firefighter's gear and the incident heat flux as an approximation of the radiative heat transfer to the firefighter's gear from the surfaces of the room, the upper gas layer, and the fire itself. He combines these two quantities to define three fields of thermal conditions: routine, ordinary, and emergency. According to Utech, routine conditions are defined as those with a surrounding temperature between 68°F (20°C) and 158°F (70°C) with an incident heat flux between 1 kW/m^2 and 2 kW/m^2. He maintains that these conditions translate approximately to ambient conditions, such as those that would be present during the overhaul phase of a fire. As the heat flux and surrounding temperature both increase, the thermal environment crosses into the ordinary operating range. This ordinary range is defined by temperatures between 158°F (70°C) and 392°F (200°C) and heat fluxes between 2 kW/m^2 and 12 kW/m^2. Ordinary operating conditions represent more serious fire conditions, such as those next to a post-flashover room. According to Utech, firefighters are likely able to function under ordinary operating conditions from 10-20 minutes at a time, or for the working duration of an SCBA cylinder. Utech considers ordinary operating conditions those that were typical of a house fire. It is important that Utech's definition of the ordinary operating class is understood in the proper context. It is likely that a "typical fire" in the 1970's, when the thermal classes were developed,may be different than a modern fire with synthetic fuels. The final classification is emergency operating conditions, which are thermal conditions exceeding heat fluxes of 12 kW/m^2 and temperatures of

392°F (200°C). These operating conditions are intended to be consistent with an environment dangerous to a firefighter in PPE, such as a firefighter trapped in a room that is flashing over. Utech describes the emergency zone as one in which a firefighter's PPE is only be able to withstand an exposure on the order of a few seconds. Figure 2.1 offers a visual chart of the three thermal operating classes, where the x-axis is heat flux, plotted on a logarithmic scale, in kW/m^2, and the y-axis is temperature, also plotted on a logarithmic scale, in °F on the left and °C on the right .

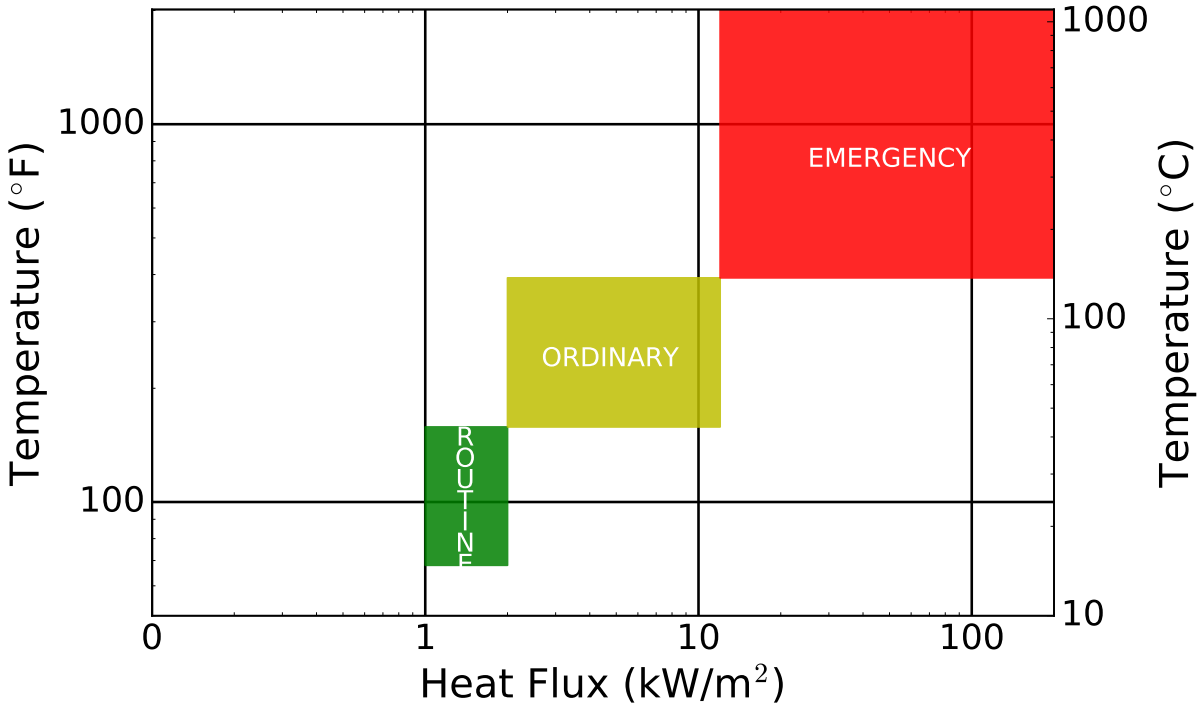

Figure 2.1: Utech's Thermal Exposure Conditions

Rather than representing the threat to electronic firefighting equipment, as the NIST Thermal Classes are intended to do, Utech's thermal operating classes estimate the potential for thermal injury to a firefighter. Utech defined the three operating classes using the results of experiments that had been conducted on 1970s-era firefighter PPE. Firefighter PPE has improved significantly since 1973, when Utech introduced the thermal classes. Modern turnout gear is required to pass a battery of standard tests that establish minimum performance criteria [20, 21]. Putorti et al. [22] conducted an investigation in 2013 to quantify the performance of firefighter SCBA facepiece lens under radiant heat flux. The study indicated that hole formation was noted at heat fluxes as low as 8 kW/m^2. As the incident heat flux was increased, the time to hole formation decreased. Figure 2.2 shows these benchmarks, as well as the 84 kW/m^2 heat flux that protective ensembles are exposed to during the thermal protective performance test [20], superimposed on the chart of Utech's thermal classes.

Comparison of Figures 2.1 and 2.2 show that the threshold between the ordinary and emergency operating classes falls between 8 kW/m^2 and 15 kW/m^2, which is the range in which hole formation would occur in an SCBA facepiece lens after several minutes of constant exposure. Exposure

criteria on the temperature axis and their relationship to PPE performance is currently a knowledge gap. Madrzykowski [23] conducted a literature review to compile previous research efforts to characterize the thermal operating environment of firefighters. The review highlighted that evaluating the operating environment of firefighters by pairing temperature and heat flux does not reflect the entire range of conditions to which firefighters may be exposed. Additionally, the thermal conditions within a structure can change from conditions where firefighters would be safe to conditions where firefighters would be in immediate danger quite rapidly. The report recommended future research should aim to improve the understanding of convective and radiative heat flux on firefighter PPE, particularly the effect of hot gas flows of various velocities on the heat transfer rate through firefighter gear. Thus, while the heat flux thresholds in Utech's thermal operating classes are representative of thermal conditions which would precipitate the failure of firefighters' PPE, there is clearly limitations to expressing the thermal exposure of firefighters by considering only the peak temperature and heat flux exposures to which a firefighter may be subjected.

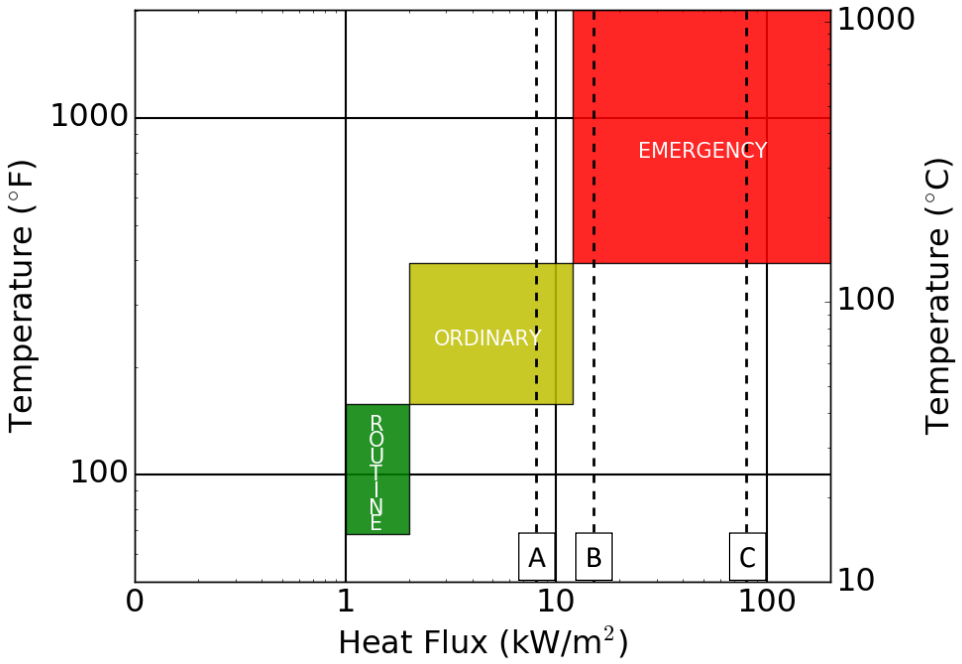

Figure 2.2: Modern PPE Performance Comparison with Utech Thermal Classes

A	8 kW/m^2 (Minimum heat flux exposure where hole formation in SCBA facepiece lens was noted in less than 20 minutes [22])
B	15 kW/m^2 (Hole formation in SCBA facepiece lens occurs between 1.5 and 4 minutes [22])
C	84 kW/m^2 (Heat flux which PPE ensemble is exposed to during Thermal Protection Performance Test (TPP) [20])

3 Experimental Approach

This chapter describes the fuel loads and ventilation configurations used in the four HRR experiments and the eight concrete live fire training building experiments. Additionally, the structure used for the concrete live fire training building experiments is detailed, and the instruments used to measure conditions during the experiments are specified.

3.1 Fuel Packages

Three fuel packages were chosen for the concrete live fire training building experiments. Two of these fuel loads, the pallets and straw package and the pallets, straw, and OSB package, were selected to be representative of training fuels that are commonly used in the fire service. The third fuel load included sofas, chairs, coffee tables, and end tables, all of which are common furnishings that would be found in a modern home. The intent was to compare the fire dynamics produced by the two common training fuel packages to those produced by the modern furnishings. Additionally, the fire dynamics of the furnished room fire can be compared to fire dynamics research that previously has been conducted in residential structures.

3.1.1 Pallets and Straw

Wooden pallets and straw are widely used as training fuels in the United States. They are appealing to use for live fire training because of their low cost, high availability, and relative predictability when it comes to fire dynamics. In addition, their ease of ignition and cleanup facilitate quick turnover between evolutions, a quality that is quite important to fire instructors aiming to maximize the amount of live fire evolutions possible during a class.

In an effort to ensure uniformity of the pallets used as fuel in these experiments, the pallets were purchased from the same lot. The pallets were weighed before each experiment except for Pallets Experiment 3. The total list of pallet weights can be found in Appendix A. Three individual pallets and one bale of straw were used for each experiment. The average weights of each component of the fuel package and the average total weight of the fuel pacakge are presented in Table 3.1. The pallets were oriented in a triangular configuration on top of a steel burn rack. The burn rack,

shown in Figure 3.1, consisted of four steel legs supporting a frame, on top of which is laid an approximately 4 ft. x 4 ft. (1.22 m x 1.22 m) flattened, perforated steel sheet, allowing air entrainment into the bottom of the pallet assembly. The frame supports the pallets so that they sit 1 ft. (0.30 m) above the floor of the fire room. The bulk of the straw was used to fill the center of the pallet configuration, and the remainder of the bale was placed beneath the stand and into the slats of the pallets. The entire assembly is shown in Figure 3.2.

Figure 3.1: Burn Rack

Table 3.1: Pallets Fuel Package Average Weights

Fuel Item	**Quantity**	**Average Weight per Item (lbs. (kg))**	**Total Weight (lbs. (kg))**
Pallets	3	38.7 (17.6)	116.6 (52.9)
Straw Bale	1	32.4 (14.7)	32.4 (14.7)
Total			149.0 (67.6)

Figure 3.2: Pallets and Straw Fuel Package

3.1.2 Pallets, Straw, and OSB

OSB is a type of engineered lumber composed of small wood chips pressed together and bonded with some type of resin. Typical resins used in OSB include phenol formaldehyde (PF), melamine fortified urea formaldehyde (MUF), or isocyanate (PMDI). Some fire academies and fire training organizations have begun to incorporate OSB, as well as other types of engineered lumber into their live fire training burns. In some training evolutions, OSB is the only fuel that is used, while in others it is used in conjunction with conventional wood-based training fuels, such as pallets and straw. The OSB experiments in this series of experiments focused on the latter case.

For ease of description, the experiments using pallets, straw, and OSB as a fuel will be referred to as the "OSB" experiments. The pallets used in the OSB experiments were from the same lot as those used in the pallets and straw experiments. Three pallets and one bale of straw were used for each experiment. The total list of pallet weights can be found in in Appendix A. The OSB sheets were 0.44 in. x 4 ft. x 8 ft. (1.1 cm x 1.2 m x 2.4 m) sheets. The average weights of each component of the fuel package, along with the average total weight of each component and the average total weight of the fuel pacakge. are presented in Table 3.2. The pallets and straw were configured in a manner identical to that described in Section 3.1.1. The OSB sheets were placed behind the pallet triangle, against the rear wall of the fire room. The pallets, straw, and OSB assembly is depicted in

Figure 3.3

Figure 3.3: Pallets, Straw, and OSB Fuel Package

Table 3.2: OSB Fuel Package Average Weights

Fuel Item	**Quantity**	**Average Weight per Item (lbs. (kg))**	**Total Weight (lbs. (kg))**
Pallets	3	42.0 (19.1)	126.0 (57.2)
Straw Bale	1	30.6 (13.9)	30.6 (13.9)
4’ x 8’ x 0.44" sheet OSB	2	46.7 (21.2)	93.3 (42.3)
Total			250.0 (113.4)

3.1.3 Furniture

The furnished room fuel package consisted of two couches, two chairs, two end tables, two lamps, one coffee table, a tall table, and carpet on top of carpet padding. The furniture was selected to simulate the living room of a modern home. The couches and chairs were purchased from a retailer and were assembled prior to the experiments. The upholstery was primarily composed of polyurethane foam, and the frame of each couch was wooden. The chairs had a polyurethane foam cushion and an expanded polystyrene frame. The end table and coffee table were made of medium density fiberboard. The weight of each item in the furniture fuel package is given in Table 3.3. The combined weight of the furnished room fuel package was approximately 309.2 lbs. (140.5 kg). The layout of the furnished room is shown in Figure 3.4.

Figure 3.4: Furniture Layout

Table 3.3: Furnished Room Contents

Furniture Item	**Quantity**	**Weight per Item (lbs. (kg))**	Total Weight (lbs. (kg))
Couch	2	50.7 (23.0)	101.4 (46.0)
Chair	2	8.4 (3.8)	16.8 (7.6)
End Table	2	17.0 (7.7)	34.0 (15.4)
Coffee Table	1	45.4 (20.6)	45.4 (20.6)
Tall Table	1	47.6 (21.6)	47.6 (21.6)
Carpet	1	34.8 (15.8)	34.8 (15.8)
Carpet Padding	1	24.0 (10.9)	24.0 (10.9)
Lamp	2	2.6 (1.2)	5.1 (2.3)
Total			309.2 (140.5)

3.2 HRR Characterization Experiments

To evaluate the HRR characteristics of the fuel packages described above, a series of experiments were performed in UL's Oxygen Consumption Calorimetry Laboratory. Two types of experiments were done: a set of free burn experiments, to characterize the individual fuels without any enclosure effects, and a set in a 12 ft. x 12 ft. (3.6 m x 3.6 m) gypsum-lined compartment, to examine the fuel packages as a whole with a common compartment and ventilation configuration.

In addition to the heat release rate, the total energy release was determined by numerically integrating the total HRR curve using the Euler scheme described in Equation 3.1. The total energy release is presented in Megajoules (MJ). A 25 second moving average was applied to the HRR graphs to minimize some of the fluctuations in the raw data.

$$E_{n+1} = E_n + \Delta T * HRR_n \tag{3.1}$$

The oxygen consumption calorimeter used for the experiments was located at UL's facility in Northbrook, IL. Four HRR experiments were performed. One experiment each was performed for the pallets and straw and the OSB fuel packages, and two replicates of the furnished rooms were performed. This was done to characterize the variability of the furnished room fuel package. Each fuel package was allowed to burn out completely. The calorimeter reported HRR in MW at 1 second intervals during the experiments. Bryant and Mullholland [24] estimate the expanded relative uncertainty of oxygen consumption calorimeters measuring high HRR fires at $\pm 11\%$. They identify several sources of error within the calorimeter, but one of the primary sources is the uncertainty in the gas concentration measurements.

3.2.1 Free Burn HRR Characterization

This section details the free burn heat release rate (HRR) experiments that were performed. These experiments offer a characterization of the fuels independent of the compartment configuration. Three free burn fuels were tested: the pallets and straw geometry used in the training fuel experiments, the barrel chair from the furnished room, and the kit couch from the furnished room. Two replicate experiments were conducted for the chair and the couch. The peak HRR and total energy release for each free burn experiment is summarized in Table 3.4

Table 3.4: Peak HRR and Total Energy Released for Free Burn Experiments

Fuel Package	**Peak HRR (MW)**	**Total Energy Released (MJ)**
Pallets and Straw	1.90	890
Barrel Chair 1	0.83	180
Barrel Chair 2	0.84	190
Couch 1	1.70	570
Couch 2	2.10	600

The pallets and straw were tested using the same geometry as the one used for the concrete burn building experiments. This configuration is shown in Figure 3.5. The results of the HRR characterization are shown in Figure 3.6. The pallets training fuel package reached a peak HRR of 1.9 MW at approximately 350 seconds from ignition. The peak slope of the HRR chart was noted in the period between ignition and the peak HRR, which was 16 kW/s. The total energy released during the experiment was 890 MJ.

Figure 3.5: Pallets and Straw Free Burn Assembly

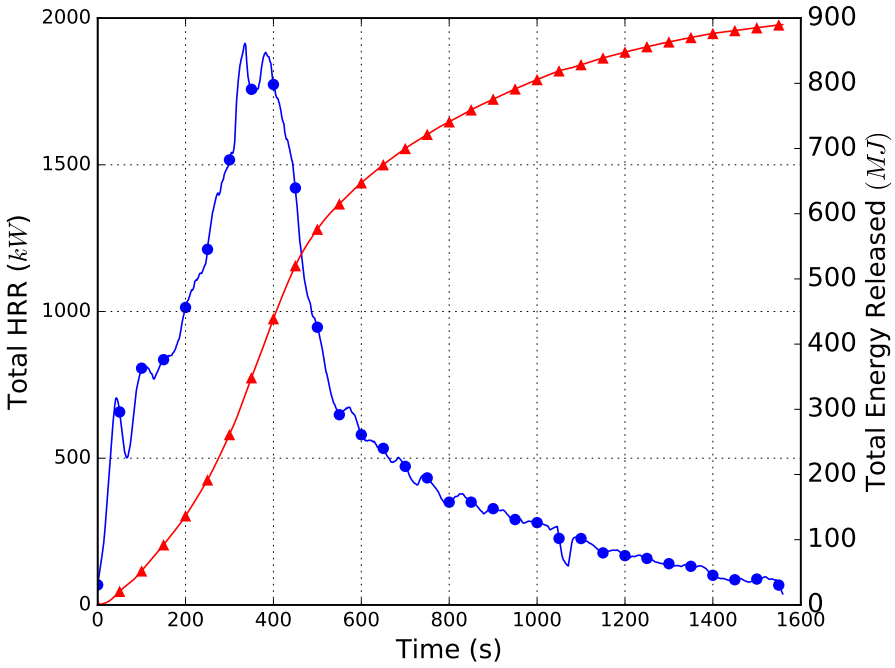

Figure 3.6: Free Burn HRR (Blue) and Total Energy Release (Red) for Pallets and Straw

The barrel type chair was composed of an expanded polystyrene foam covered with a polyurethane foam cushion, polyester batting, and polyester fabric. The chair is shown in Figure 3.7. The results of the two HRR characterization experiments are shown in Figures 3.8 and 3.9, showing the HRR and total energy release, respectively. For the first HRR experiment conducted using the chair, the peak HRR was 830 kW, which was measured approximately 150 seconds after ignition. The peak

slope of the HRR graph was 10 kW/s. The total energy released during the HRR experiment was 180 MJ. The second HRR experiment conducted on the chair exhibited similar results. The peak HRR measured was 840 kW, which was recorded 150 seconds after ignition and the total energy calculated was 190 MJ. The peak slope of the HRR graph was 14 kW/s. The percent difference in HRR and total energy release was 1% and 11% for the two replicate experiments, indicating that the chairs burned similarly.

Figure 3.7: Barrel Chair Free Burn Assembly

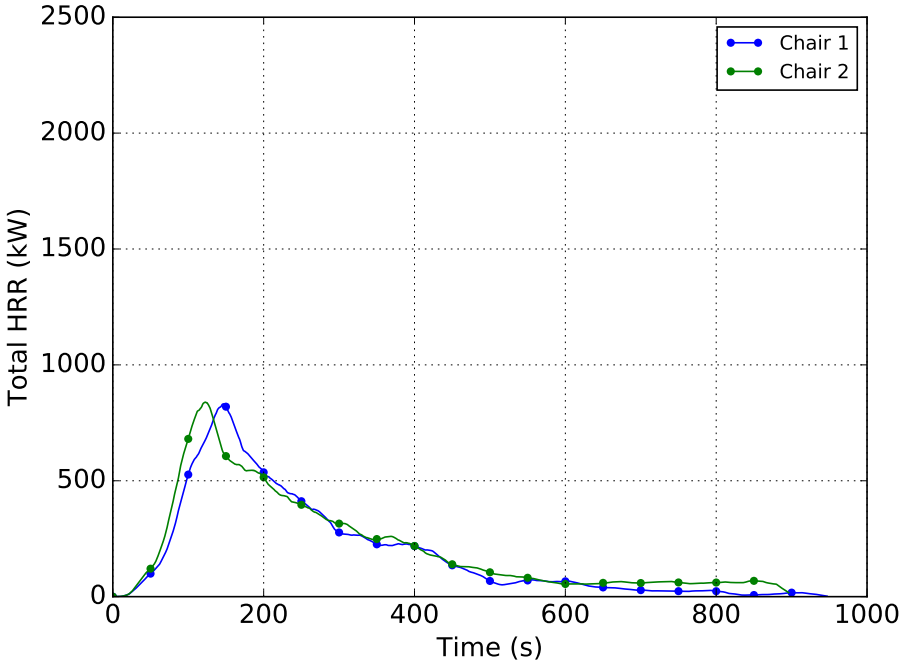

Figure 3.8: Free Burn HRR for Barrel Chair Experiments

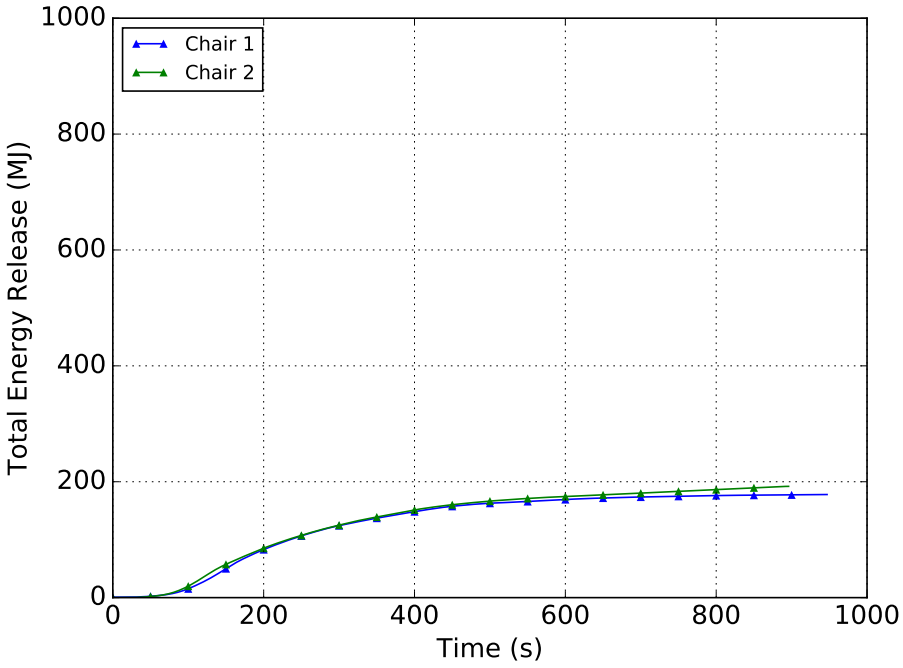

Figure 3.9: Total Energy Release for Barrel Chair Experiments

The kit couch was composed of a wooden frame with polyurethane foam cushions, polyester batting, and polyester fabric. The couch is shown in Figure 3.10. The results of the two HRR char-

acterization experiments are shown in Figures 3.11 and 3.12, showing the HRR and total energy release, respectively. For the first HRR experiment conducted using the couch, the peak HRR was 1.7 MW, which was reached 200 seconds after ignition. The peak slope of the HRR graph was 27 kW/s, which was observed prior to the peak HRR. The total energy released in the first HRR experiment using the couch was 570 MJ. The second HRR experiment using the couch had a peak HRR of 2.1 MW, a 24% higher peak HRR than the first experiment. The peak HRR was reached 225 seconds following ignition, and the peak slope of the HRR graph was 30 kW/s. The total energy released in the experiment was 600 MJ. The total energy released was similar between the 2 couches, approximately 5%. Thus, the variation in peak HRR was greater in the couches than in the barrel chairs, but the energy content for both pieces of furniture was within the error of the calorimeter.

Figure 3.10: Couch Free Burn Assembly

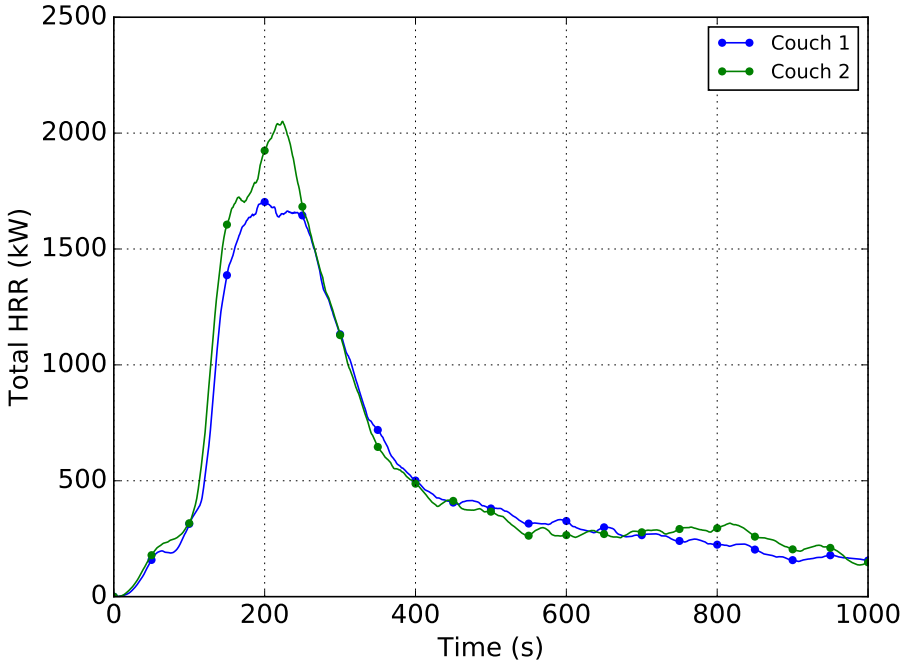

Figure 3.11: Free Burn HRR for Couch Experiments

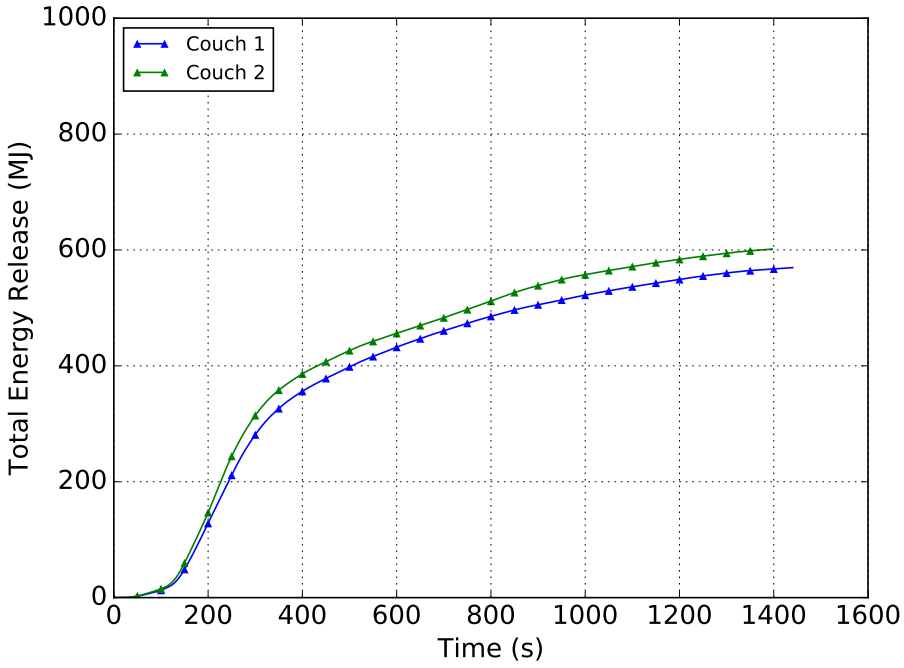

Figure 3.12: Total Energy Release for Couch Experiments

3.2.2 Compartment HRR Characterization Results

Each fuel package was arranged in a manner similar to the configuration used in the concrete live fire training building, except in place of the concrete-lined fire room, a 12 ft. x 12 ft. (3.6 m x 3.6 m) compartment with 8 ft. (2.4 m) ceilings was constructed. The compartment was framed with dimensional lumber and had an interior finish of gypsum board. The room had a 8 ft. (2.4 m) wide x 6.67 ft. (2.0 m) tall doorway to provide ample ventilation to the compartment. Because this ventilation configuration was different than that in the concrete live fire training building experiment, the HRR data are used to compare the fuels using a common ventilation configuration. The results of the HRR characterization experiments are summarized in Figures 3.13 and 3.14 and Table 3.5.

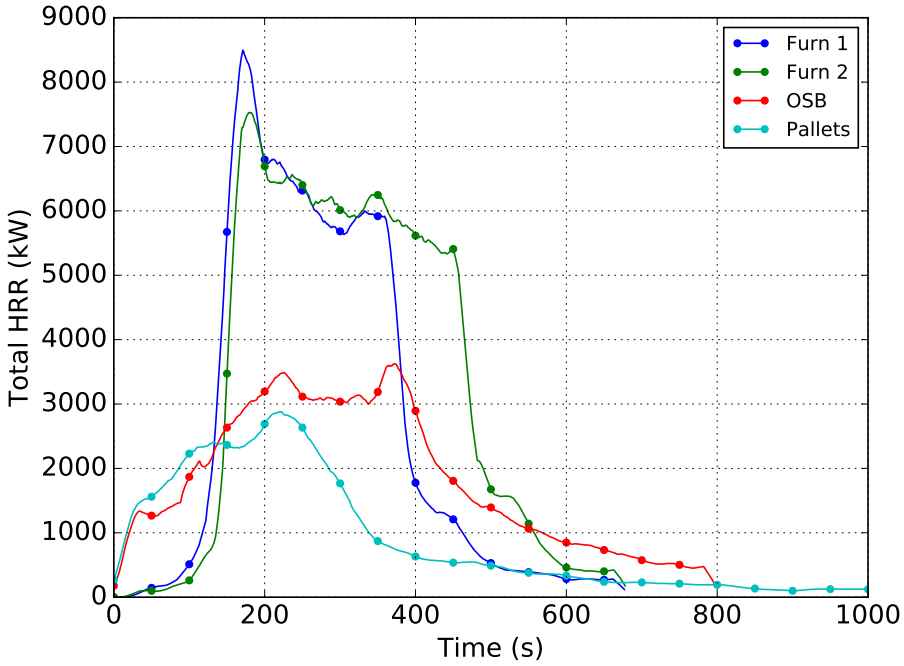

Figure 3.13: HRR vs. Time for HRR Characterization Experiments.

Table 3.5: Peak HRR and Total Energy Released for HRR Characterization Experiments

Fuel Package	Peak HRR (MW)	Total Energy Released (MJ)
Pallets and Straw	2.88	950
OSB	3.63	1440
Furnished Room 1	8.50	1790
Furnished Room 2	7.52	2190

The rate of change of the HRR in the pallets and straw experiment remained positive until approximately 250 seconds after ignition. The peak slope of the heat release curve was noted in the period

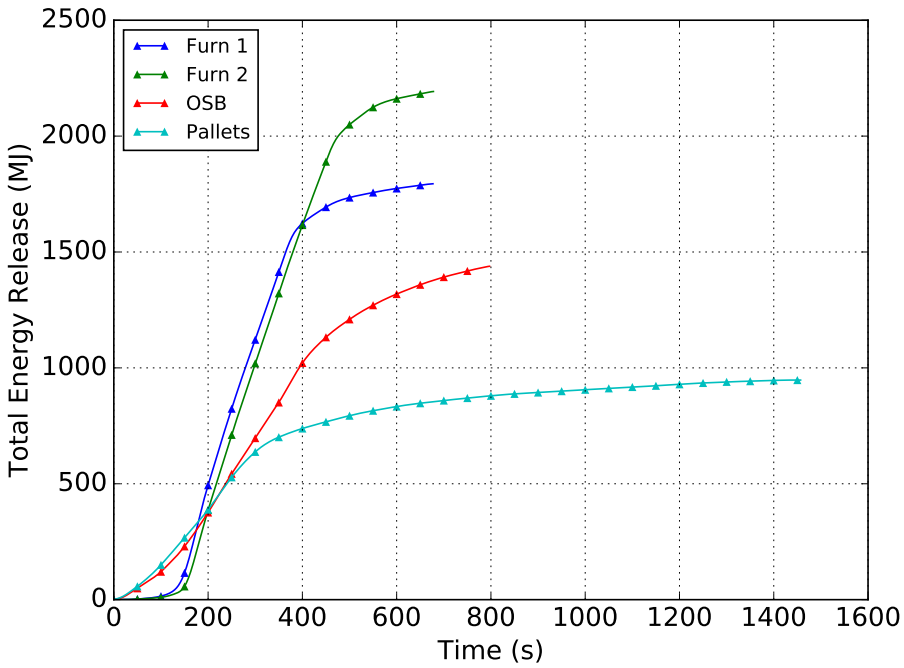

Figure 3.14: Total Energy Released vs. Time for HRR Characterization Experiments.

following the start of fire growth, where the rate of change of HRR was 30 kW/s. The peak HRR and peak slope of the HRR graph were 47% and 88% greater, respectively, than the free burn pallets HRR experiment. This indicates that the compartment had an effect on the growth of the fire, likely from re-radiation as the plume of the fire reached the ceiling and began to roll over across the ceiling. The total heat release in the pallets and straw compartment experiment was similar ($\pm$6%)to the total heat release in the free burn pallets experiment.

The rate at which the HRR increased in the period leading up to the peak HRR during the OSB fuel package test was similar to the pallets and straw with a peak slope of approximately 30 kW/s. The peak HRR observed in the OSB fuel package was 26% higher than that noted in the pallets and straw experiment. Perhaps a more significant difference can be seen in Figure 3.14, which illustrates that the total energy released by the OSB fuel package was 52% greater than that released by the pallets and straw fuel package. This trend is also manifested in Figure 3.13, looking at the OSB fuel package, after the peak HRR occurred, the HRR remained above 3 MW for another 150 seconds before beginning to decrease. Alternatively, looking at the pallets and straw plot, the HRR began to decrease almost immediately after reaching its maximum value. So, while the peak growth rates of the two training fuel packages were similar, the OSB exhibited a higher peak HRR. The additional fuel mass in the OSB fuel package enables a longer peak burning period than the pallets fuel pacakge.

Two replicate HRR tests, Furnished Room 1 and Furnished Room 2, were performed using the furnished room fuel packages with the same furnishings and layout. In both experiments, the HRR did not begin to increase significantly until after 50 seconds from the beginning of the experiment. Once this point was reached, however, the rate of HRR increase was above 150 kW/s, approx-

imately five times the rate of the training fuels. Both furnished rooms reached their peak HRR between 150 and 200 seconds. The peak HRR in Furnished Room 1 was 8.50 MW, which was 13% higher than the 7.52 MW peak observed in the Furnished Room 2. After reaching its peak, the HRR remained high, which resulted in total energy releases that were higher than both training fuels. The HRR rapidly declined after this period. In Furnished Room 1 HRRs greater than 5.5 MW were observed for approximately 200 seconds. In the Furnished Room 2, HRRs above 5.5 MW were observed for approximately 300 seconds.

The peak HRRs in Furnished Room 1 was 13% greater than the peak observed in Furnished Room 2, a value slightly greater than the combined uncertainty of the calorimeter. The difference between total energy released in the two replicates was more significant. The total energy release in Furnished Room 2 was 22% higher than Furnished Room 1. This difference can be partially explained by the longer period of sustained HRRs after peak that occurred in the furnished rooms. This longer period of sustained heat release may be the result of more of the fuel burning in the second replicate than the first, or possibly because of the difference in peak HRR behavior between the two, or some combination of both factors. The peak rate of HRR increase in both of the furnished rooms was greater than the peak rate observed in the chair or the couch, indicating that compartmentation and the amount of fuel in the room play important roles. Further, the total energy release was greater than the sum of the two chairs and two couches, indicating that the other furniture within the room (such as the tables, carpet, and carpet padding) had some contribution to the burning. Thus, in addition to exhibiting higher peak HRRs and total energies released than the OSB or pallets and straw training fuels, the furnished rooms demonstrated a peak rate of change in HRR that was nearly five times larger than that noted in the training fuels or the individual pieces of furniture.

3.3 Structure

The concrete live fire training building that was used for these experiments was located at the Delaware County Emergency Services Training Center in Sharon Hill, PA. The three-story structure had a footprint of 33.5 ft. x 28 ft (10.2 m x 8.5 m), shown in Figure 3.15. Every fire was ignited on the second floor in the designated burn room, labeled Room 201, located in the southwest corner of the fire training building. Three other rooms on the second floor, labeled Rooms 202, 203, and 204, were also instrumented. The two remaining rooms on the second floor were sealed from the rest of the space by a cement board barrier and used to stage and store fuel. Room 201 measured 18.7 ft. x 12.7 ft. (5.7 m x 3.9 m) with 8 ft. (2.4 m) ceilings. Room 201 had a wall and ceiling lining of 12 in. x 12 in. (30 cm x 30 cm) high-density refractory tiles. The walls and ceiling of the remaining rooms were protected with a 1.0 in. (25 mm) layer of calcium silicate insulation. Rooms 202, 203, and 204 had 11.1 ft. (3.4 m) ceilings. Room 202 measured 10.8 ft. x 17.2 ft. (3.3 m x 5.2 m), Room 203 measured 8.3 ft. x 17.2 ft. (2.5 m x 5.2 m), and Room 204 measured 10.9 ft. x 14.6 ft. (3.3 m x 4.5 m). The floor plan for the second floor of the concrete live fire training building is shown in Figure 3.16, which provides labels for the doorways and windows on the second floor. The dimensions of these openings are given in Table 3.6.

Figure 3.15: Front (top) and rear (bottom) of concrete live fire training building.

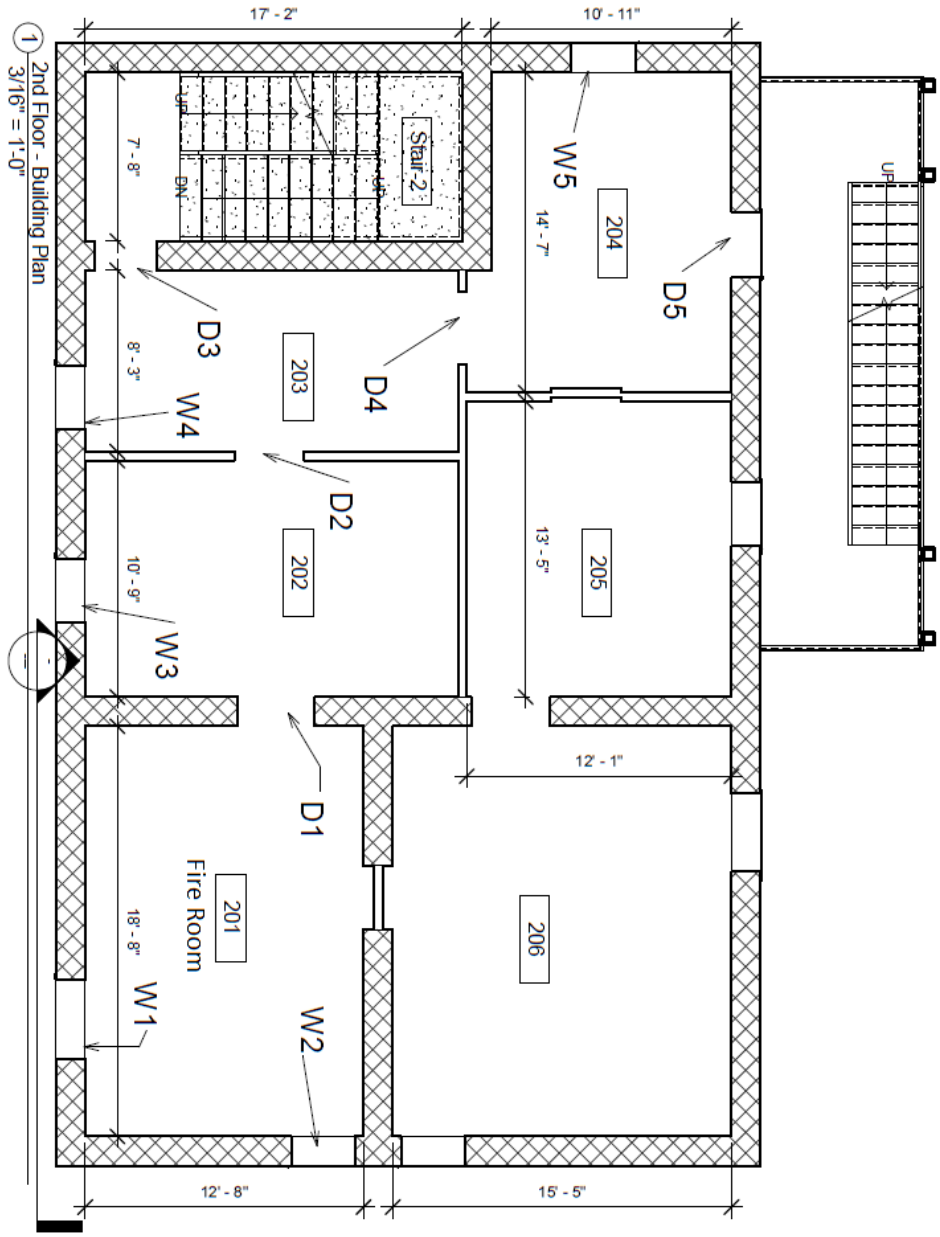

Figure 3.16: Second Floor Layout of Concrete Burn Structure

Table 3.6: Door and Window Dimensions

Item	Height ft. (m)	Width ft. (m)
D1	6.52 (1.99)	3.35 (1.02)
D2	7.13 (2.17)	3.17 (0.97)
D3	6.96 (2.12)	2.90 (0.88)
D4	7.19 (2.19)	2.94 (0.90)
D5	6.85 (2.09)	2.33 (0.71)
Front Door (Ground Level)	7.04 (2.15)	2.85 (0.87)
W1	3.38 (1.03)	3.56 (1.09)
W2	3.35 (1.02)	2.94 (0.90)
W3	4.35 (1.33)	3.92 (1.2)
W4	4.33 (1.32)	3.92 (1.2)
W5	4.33 (1.32)	3.92 (1.2)

As shown in Figure 3.16, the second floor was connected to the first and third floors by an interior staircase and an exterior stairway. The exterior door between Room 204 and the exterior stairway (D5) was never opened during any of the experiments, but the exterior door at the base of the staircase was used for ventilation in some of the experiments. Other ventilation openings included the windows in Rooms 201, 202, 203, and 204. Room 201 had two windows, although one was never opened during any of the experiments. Additionally, several of the rooms featured scuppers, which are built-in openings along the base of the exterior walls that facilitate water drainage and cleanup following a training evolution. A picture of a scupper is shown in Figure 3.17. A total of four scuppers were located on the second floor of the building. Room 204 had a scupper that measured 16.5 in. (41.9 cm) long by 8 in. (20.3 cm) high. Rooms 201, 202, and 203 each contained a square scupper with a side length of 8 in. (20.3 cm). On the ground floor, there were four circular scuppers, each with a 5 in. (12.7 cm) diameter.

Figure 3.17: Example of scupper along base of wall on second floor of concrete live fire training building

3.4 Concrete Live Fire Training Building Experiments

A total of eight experiments were conducted in the concrete live fire training building previously described in Section 3.3. Each experiment combined one of the fuel packages described in previous sections with a specific ventilation configuration in an effort to explore the effects of different ventilation configurations on the behavior of the training fire. Three configurations were studied: no vent, near vent, and remote vent. In the no vent case, all exterior doors and windows remained closed for the duration of the experiment. This was done in an effort to examine the fuels with minimal outside influence of ventilation. In the near vent case, the window in Room 201, shown in Figure 3.18, was opened to examine the effect of ventilation close to the fire. No exterior doors were opened in the near vent case. In the remote vent case, the door on the ground floor was opened in conjunction with the window in Room 204 to examine the effect of a ventilation point far from the seat of the fire, creating a flow path with the front door as the inlet and the far window as the exhaust. The two vent openings for this configuration are shown in Figure 3.19.

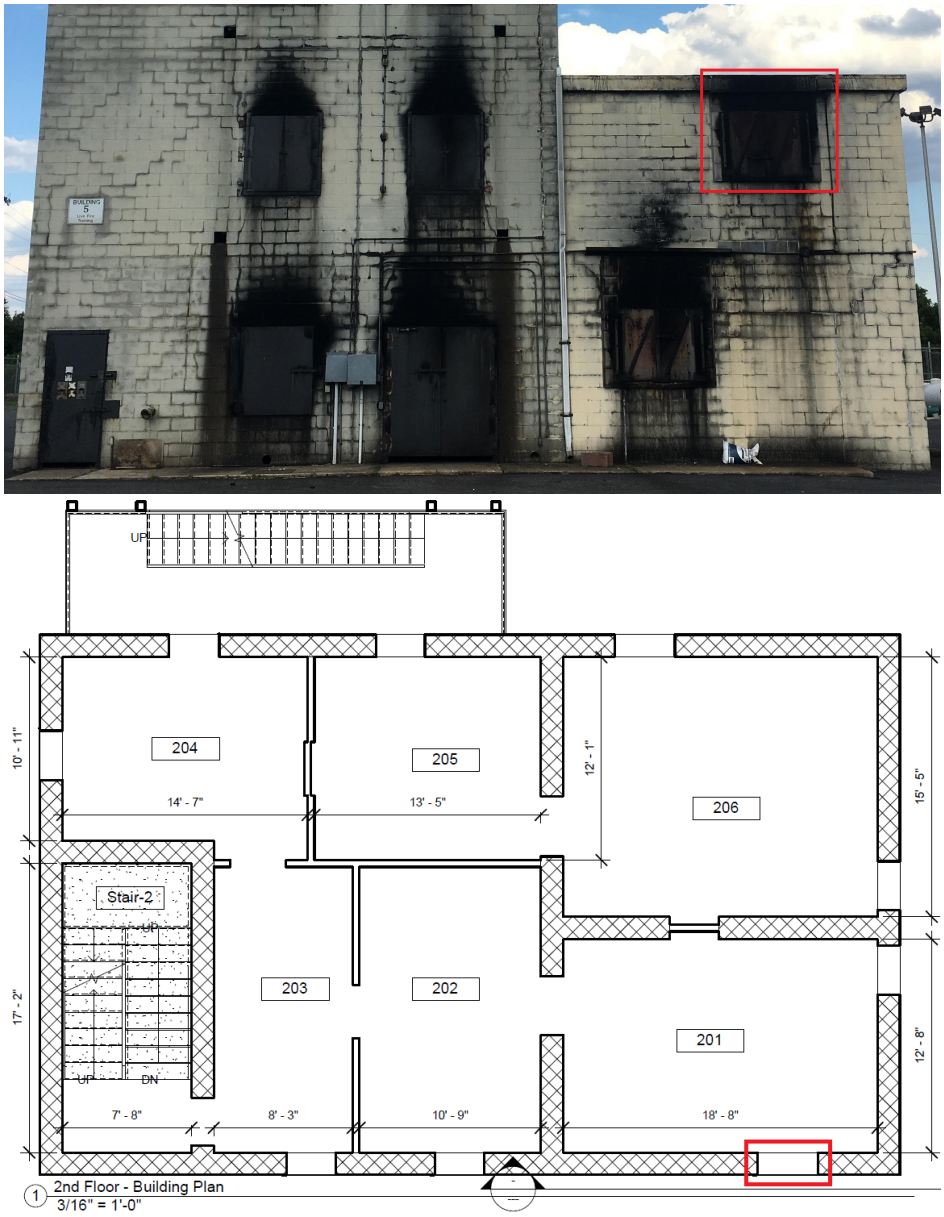

Figure 3.18: Near Ventilation Case

Table 3.7 lists the eight experiments with their respective fuel package, ventilation configuration, and time at which ventilation was performed. Ventilation times were determined by monitoring the oxygen concentrations at the 2 ft. and 6 ft. levels, performing ventilation when the concentrations reached a minimum value. It should be noted that the no ventilation experiment was not performed for the OSB fuel package due to time constraints for this experiment series. While a no ventilation case for the OSB fuel package would have been useful, it was assumed that the fire dynamics of the OSB would have been bounded by the pallets and straw no vent case and the furniture no vent case.

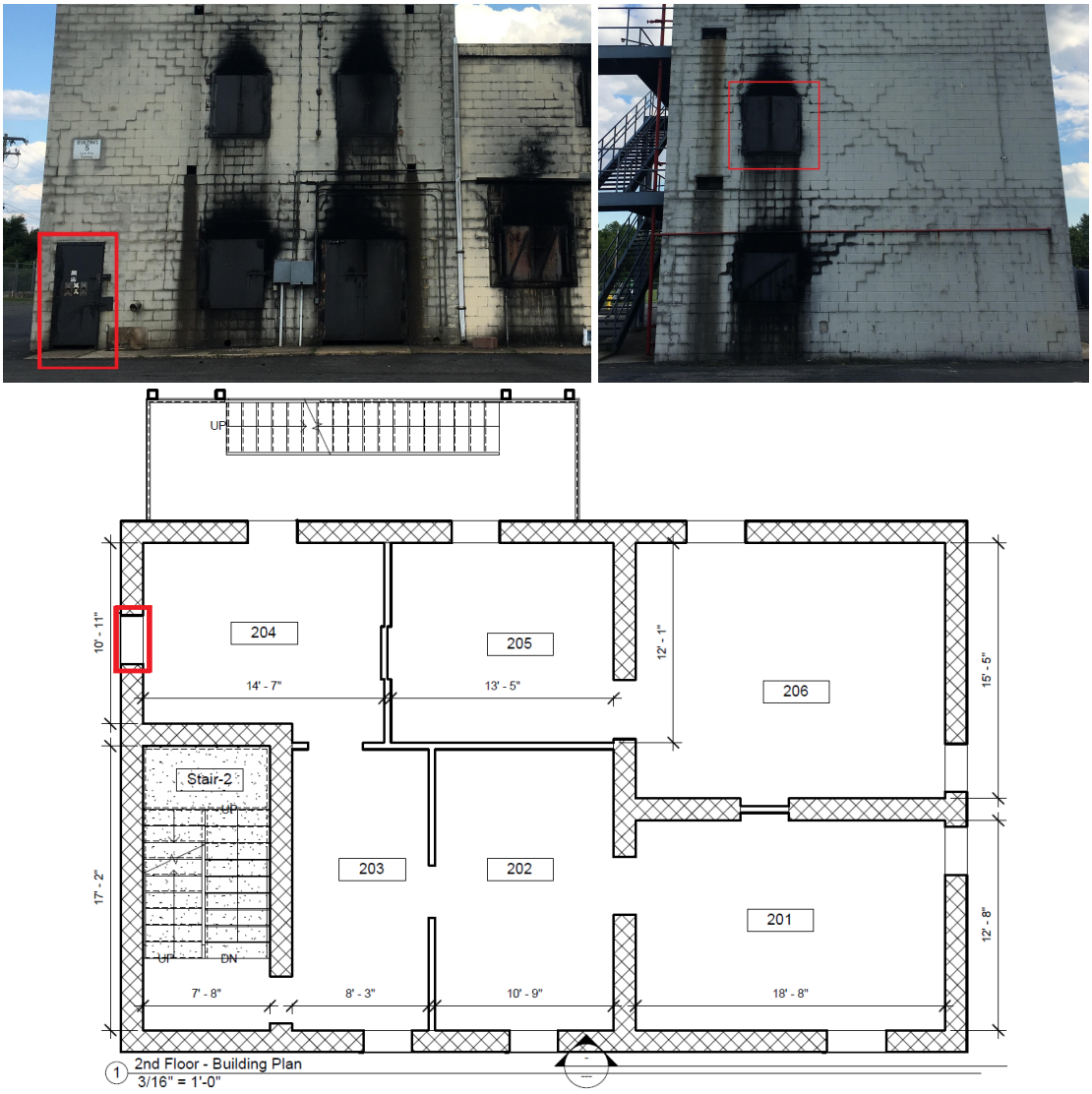

Figure 3.19: Far Ventilation Case. Red box on floor plan denotes the window to Room 204. The exterior door on the front of the structure, at ground level, was also opened in the remote vent case.

Table 3.7: Experiment Matrix

Experiment	**Fuel**	**Vent Scenario**	**Vent Time (s)**
Pallets Experiment 1	Pallets and Straw	No Vent	-
Pallets Experiment 2	Pallets and Straw	Near Vent	480
Pallets Experiment 3	Pallets and Straw	Remote Vent	240
OSB Experiment 1	OSB	Near Vent	250
OSB Experiment 2	OSB	Remote Vent	300
Furniture Experiment 1	Furniture	No Vent	-
Furniture Experiment 2	Furniture	Near Vent	420
Furniture Experiment 3	Furniture	Remote Vent	510

3.5 Instrumentation

This section details the equipment used during the concrete live fire training building experiments to measure the gas temperature, heat flux, gas velocity, and oxygen concentration at various locations throughout the structure. The layout of these instruments is given in Figure 3.20.

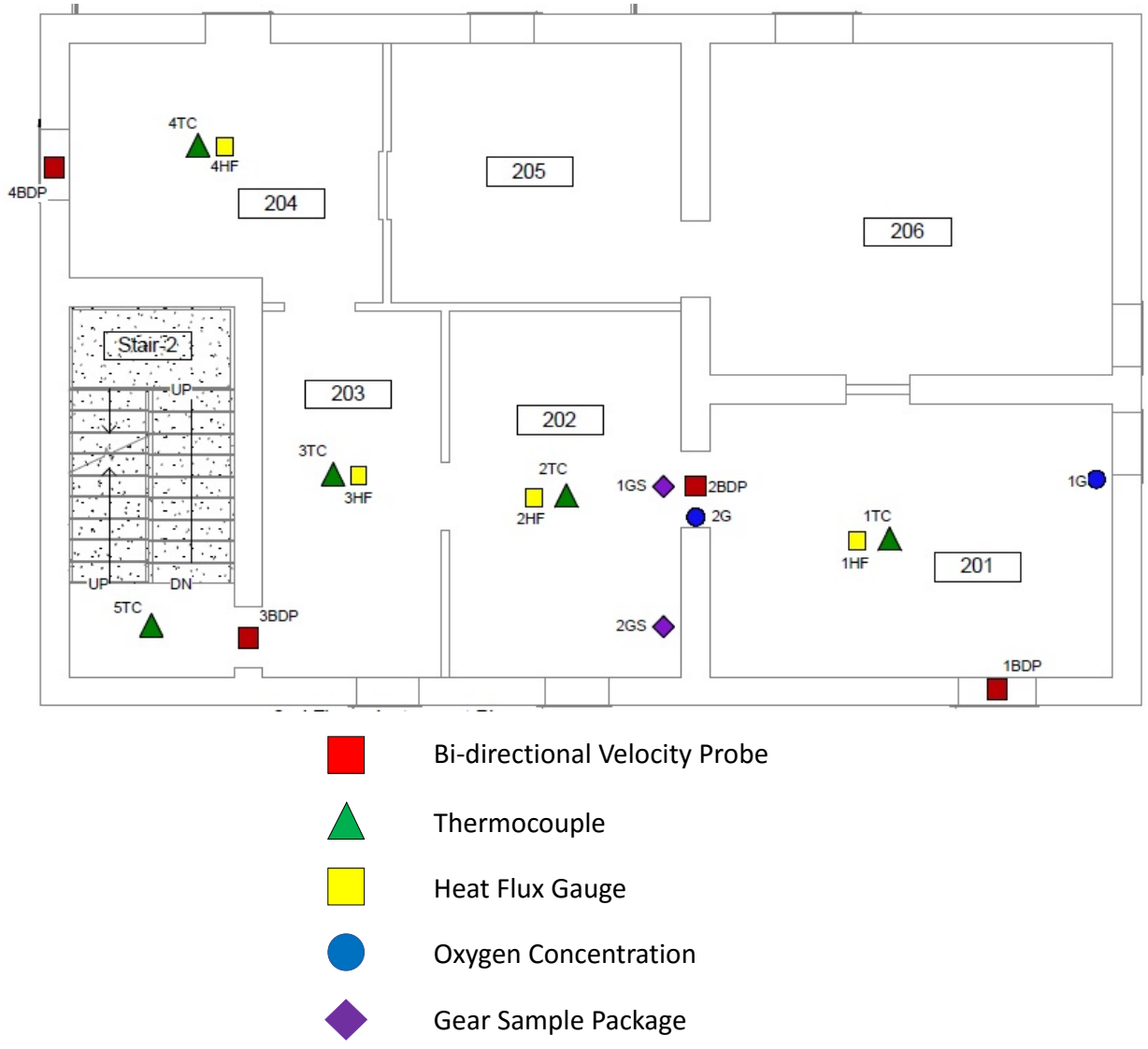

Figure 3.20: Instrument locations on second floor of concrete live fire training building

3.5.1 Thermocouple

The thermocouples used in these experiments were chromel-alumel, Type K thermocouples. The thermocouple wire was manufactured by Omega Engineering and had a nominal 0.02 in. (0.5 mm)

diameter. The individual thermocouple wires were arranged into vertical arrays of thermocouples spaced at 1 ft. (0.31 m) increments from the floor to the ceiling of each room. In Room 201, the arrays had seven thermocouples and in Rooms 202, 203, and 204, the arrays had twelve thermocouples. The locations of these thermocouple arrays are denoted by green triangles in Figure 3.20.

According to Omega, the uncertainty of the thermocouple wire is ±4.0°F (2.2°C) for temperatures below 559°F (293°C) and ±0.75% for temperatures above this range [25] The variation of the temperature in the environment surrounding the thermocouple is known to be much greater than that resulting from the wire uncertainty. Expanded uncertainties as high as 20 % for upper layer temperatures measured by a 0.5 mm bare-bead type K thermocouple have been reported by researchers at NIST [26, 27]. Small diameter (approximately 0.03 in. (0.65 mm)) thermocouples were used during these experiments to limit the impact of radiative heating and cooling. The total expanded uncertainty associated with the temperature measurements from these experiments is estimated to be ± 15 %.

3.5.2 Heat Flux Gauge

Total heat flux was measured using a nominal 1 in. (2.54 cm) diameter, water-cooled, Schmidt-Boelter heat flux gauge. The gauges were oriented towards the ceiling in an effort to measure the total heat flux (both convective and radiative) from the hot gas layer in the room. The radiative heat transfer portion of the total heat flux is largely a function of the hot gas layer temperature, while the convective heat transfer portion is dependent on both the ambient temperature and the velocity of the gas flow. The locations of the heat flux gauges are shown by yellow squares in Figure 3.20.

Medtherm Corporation, the manufacturer of the heat flux gauges, lists the uncertainty as ±3%. Each gauge has a unique calibration curve that is used to convert the voltage signal output into a heat flux. Such gauges are NIST-traceable, and must be re-calibrated from time to time to ensure accuracy. A study on the uncertainty of measurements from heat flux gauges quantified the expanded uncertainty for these instruments as ±8% [28].

3.5.3 Gear Sample Packages

In an effort to characterize the thermal protection that is afforded to firefighters by their turnout gear, turnout gear sample packages were instrumented with heat flux gauges and temperature sensors. Two heat flux gauges, one horizontal and one vertical, were mounted in a metal container. The containers were insulated with ceramic wool and were water-cooled using copper tubing to prevent damage from high thermal conditions. For each gear sample package, two heat flux boxes were positioned side-by-side. One of the boxes was covered in a PPE ensemble consisting of an outer shell, a moisture barrier, and a thermal layer, and the other was covered with a ceramic wool blanket and aluminum foil. The outer shell of the PPE ensemble was a TenCate Advance, composed of a Kevlar and Nomex blend; the moisture barrier was a Crosstech Black moisture barrier;

and the thermal liner was a TenCate Caldura SL2i thermal barrier. The turnout gear was sewn into a pouch to encapsulate the heat flux box. Type K thermocouples were sewn into the outside of the outer shell and the inside of the thermal liner in locations adjacent to the two heat flux gauges. This setup yielded eight measurement points per gear sample: uncovered heat flux in the horizontal and vertical directions, covered heat flux in the horizontal and vertical directions, exterior surface temperature in the horizontal and vertical directions, and interior surface temperature in the horizontal and vertical directions.

Gear sample packages were placed in two locations, as indicated by the purple diamonds in Figure 3.20. Each gear sample package was placed directly on the ground, with the vertical gauges elevated approximately 8 in. (20 cm) from the floor and the horizontal gauges elevated approximately 4.5 in. (11 cm) from the floor. One sample was placed in the doorway between Rooms 201 and 202, with the horizontal gauges and thermocouples oriented towards Room 201. The second sample was placed in the corner of Room 202, in a location that was intended to be isolated from the flow path. The horizontal gauges and thermocouples of the second sample were oriented towards the the gauge in the doorway, parallel to the walls dividing Rooms 201 and 202. As discussed in Sections 3.5.1 and 3.5.2, the combined uncertainty of the temperature and heat flux measurements are $\pm 15\%$ and $\pm 8\%$, respectively.

3.5.4 Bi-directional Probes

Bi-directional probes paired with single type K, inconel-sheathed thermocouples were used to measure gas velocity. The bi-directional probes used pressure transducers similar to those used to measure differential pressure as discussed in the previous subsection. A gas velocity measurement study examining flow through doorways in pre-flashover compartment fires yielded expanded uncertainties ranging from $\pm$ 14 % to $\pm$ 22 % for measurements from bi-directional probes similar to those used during this series of tests [29]. The total expanded uncertainty for gas velocity measured during these experiments is estimated to be $\pm$ 18 %.

Arrays of BDPs were installed in the window to Room 201, the doorway between Rooms 201 and 202, the stairwell doorway, and the window in Room 204. Each array contained five probes centered laterally in their respective openings. The vertical probe spacings for each of the arrays are listed in Table 3.8. The locations of the bi-directional probe arrays are shown by red squares in Figure 3.20.

Table 3.8: Bi-directional Probe Spacings

Array	Location	Probe Spacings (in. from bottom)	Probe Spacings (cm. from bottom)
1BDP	Room 201 Window	6.75, 13.5, 20.25, 27, 33.75	17.1, 34.3, 51.4, 68.6, 85.7
2BDP	Room 201/202 Door	13, 26, 39, 52, 65	33, 66, 99, 132, 155
3BDP	Stairwell Door	14, 28, 42, 56, 70	35.6, 71.1, 106.7, 142.2, 177.8
4BDP	Room 204 Window	8.5, 17, 25.5, 34, 42.5	21.6, 43.2, 64.8, 86.4, 108

3.5.5 Gas Analyzers

Gas samples were collected at heights of 2 ft. and 6 ft. (0.61 m and 1.83 m) above the floor in two locations in Room 201, shown by the blue circles in Figure 3.20. The samples were collected by stainless steel tubes, which were run from their respective measurement locations to the exterior of the structure, where they passed through a coarse paper filter (Solberg Model 8242) followed by a condensing trap to remove moisture. The samples were then run through a nominal 0.75 CFM pump (Cole Palmer Model L-79200-30), followed by a drying tube (Perma Pure Model FF-250-SG-2.5G) and a fine filter (FF-250-E-2.5G) before finally reaching the OxyMat6 Siemens Gas Analyzers.

The measurement range for the oxygen concentrations in the OxyMat6 was 0-25%. The gas sampling instruments used throughout the series of tests discussed in this report have demonstrated a relative expanded uncertainty of ± 1 % when compared to span gas volume fractions [30]. According to a study by Lock et al. [31], the non-uniformities and movement of exhaust gases in addition to the limited set of sampling points considered in a given experiment result in an estimated expanded uncertainty of $\pm$ 12 %.

4 Experimental Results

This chapter presents the measurements from the concrete live fire training building experiments described in the previous chapter. During the course of firefighter training, it is typical for several fire evolutions to be conducted in the same day, therefore, several concrete live fire training building experiments were conducted per day. Table 4.1 lists the temperatures in the fire room prior to ignition; computed as the average across the thermocouple array in the fire room; the order in which each test was conducted that day; the time since the previous test; and the ambient temperature outside of the building for each of the experiments in chronological order.

Table 4.1: Initial Temperatures

Experiment	**Test of day**	**Time Since Previous Test (hours)**	**Average Initial Temperature °F(°C)**	**Ambient Temperature °F (°C)**
Furniture Experiment	1	-	90±7 (32±4)	91 (33)
Pallets Experiment	2	2	102±7 (39±4)	84 (29)
OSB Experiment	1	-	91±2 (33±1)	91 (33)
Furniture Experiment	2	6	93±5 (34±3)	84 (29)
Pallets Experiment	1	-	90±2 (32±1)	90 (32)
Pallets Experiment	2	2	104±7 (40±4)	93 (34)
OSB Experiment	3	2	109±9 (43±5)	97 (36)
Furniture Experiment	4	3	108±7 (42±4)	90 (32)

Table 4.1 shows that tests later in the day contained a higher average initial fire room temperature and a higher standard deviation from the average than tests which were conducted in the morning. This can be attributed to the nature of the concrete burn building, which has a tendency to hold heat after live fire training evolutions. Since at least two hours were allowed between experiments, these temperature differences are only on the order of a few degrees with a maximum difference of 12°F (7°C) between initial average fire room temperatures of the first and last tests of each day. Thus, it is not expected that the changes had a substantial effect on the experimental results. Typically, the time between training evolutions would be less than 2 hours. Therefore, the temperature increase would be expected to be higher than what is documented here.

4.1 Pallets and Straw Experiments

Three training fuel experiments were conducted using pallets and straw as a fuel. In these experiments, three ventilation cases were considered: no vent, vent close to the seat of the fire, and vent remote from the seat of the fire. This section presents the fire room (Room 201) temperature, heat flux, gas velocity, oxygen concentration, and pressure for these experiments. Temperature data for rooms remote from the fire room are located in Appendix B.1.

4.1.1 Pallets and Straw Experiment 1 (No Vent)

Pallets and Straw Experiment 1 started with all exterior doors and windows closed. The windows and doors remained closed for the duration of the experiment. Figures 4.1 and 4.2 show the fire room temperatures and floor heat flux. Fire room temperatures began to rise shortly after ignition, followed by fire room heat flux. The fire room temperatures close to the ceiling (6 ft. and 7 ft. (1.8 m and 2.1 m)) and heat flux reached a peak at approximately 200 seconds after ignition, remaining steady until approximately 400 seconds after ignition before decreasing. The fire room temperatures closer to the floor (1 ft. - 4 ft. (0.3 m - 1.2 m)) were considerably lower, and reached a peak at approximately 400 seconds after ignition. Following the peak thermal conditions in the fire room, the temperatures and heat flux began to decrease, reaching a steady state at approximately 500 seconds, which continued until the end of the experiment at 700 seconds. Figure 4.3 shows the heat fluxes in the remote rooms on the second floor.

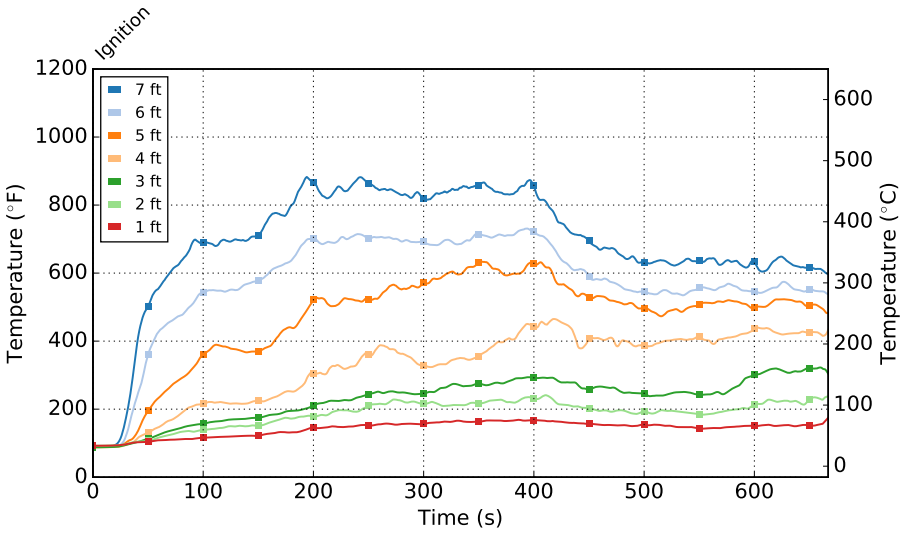

Figure 4.1: Fire room temperatures for Pallets and Straw Experiment 1.

This steady peak period corresponded to the minimum 6 ft. (1.8 m) oxygen concentration that was observed in the experiments, which occurred at approximately 300 seconds after ignition, as shown in Figure 4.4. The minimum concentrations at the 6 ft. (1.8 m) level were approximately

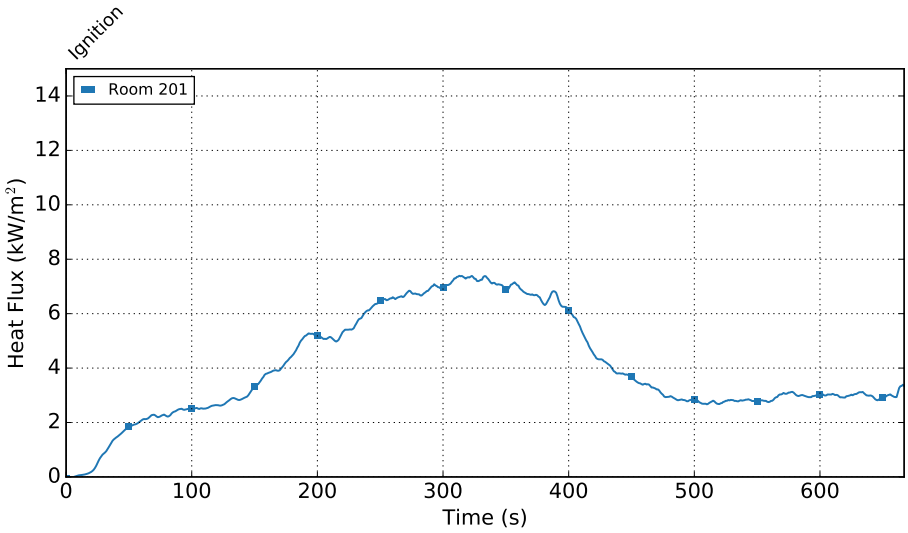

Figure 4.2: Fire room heat flux for Pallets and Straw Experiment 1.

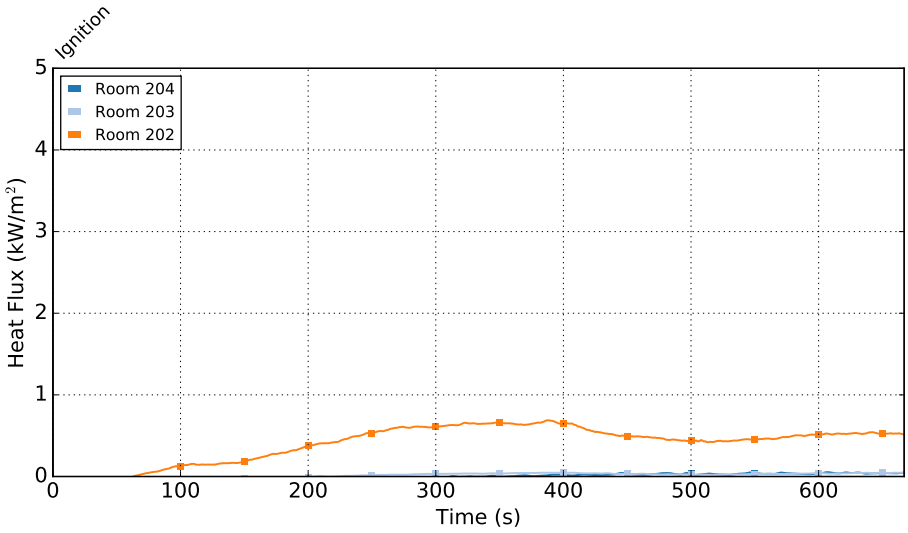

Figure 4.3: Remote heat fluxes for Pallets and Straw Experiment 1.

10%. Flaming combustion of most fuels begins to cease at oxygen concentrations below 15%. After reaching their minimum values, the 6 ft. (1.8 m) oxygen values rebounded, reaching a steady value close to 18% by the end of the experiment. In contrast to the oxygen concentrations at the 6 ft. (1.8 m) level, the oxygen concentrations at the 2 ft. (0.6 m) level remained above 20% for the duration of the experiment.

There were no significant pressure spikes in the fire room during the experiment, as shown in Figure 4.6. As the fire grew, producing products of combustion, a bi-directional flow was established through the front door. This can be seen in the data from the BDPs in the fire room doorway (Figure 4.5). The positive velocities measured at the top two BDP locations in the array indicated

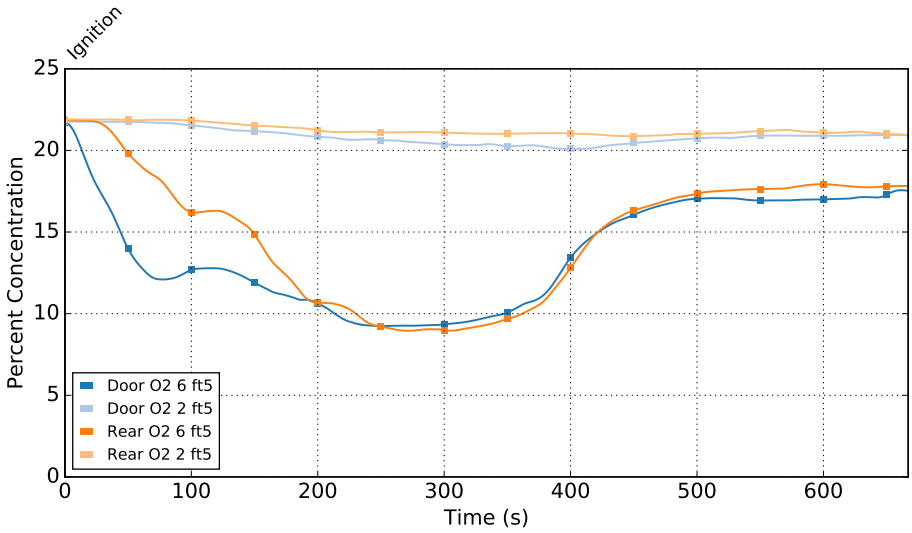

Figure 4.4: Fire room O_2 Concentration (%) for Pallets and Straw Experiment 1.

that the top of the doorway was exhaust, while the negative velocity in the bottom location in the array indicates an inlet close to the floor. The middle and bottom middle BDP locations indicated that the flow in the middle of the doorway was negligible. The bi-directional flow through the doorway and lack of a pressure build-up in the fire room indicate that a two-layer environment was present in the fire room for the duration of the experiment, with a hot upper layer and cooler lower layer. This can additionally be seen in the temperature and oxygen data, where fire room temperatures close to the floor are significantly lower than those close to the ceiling, and oxygen depletion close to the floor is negligible. Although all exterior doors and windows were open, the significant amount of leakage into the structure allowed a sufficient amount of air in and products of combustion out to prevent a significant pressure buildup or oxygen depletion close to the floor.

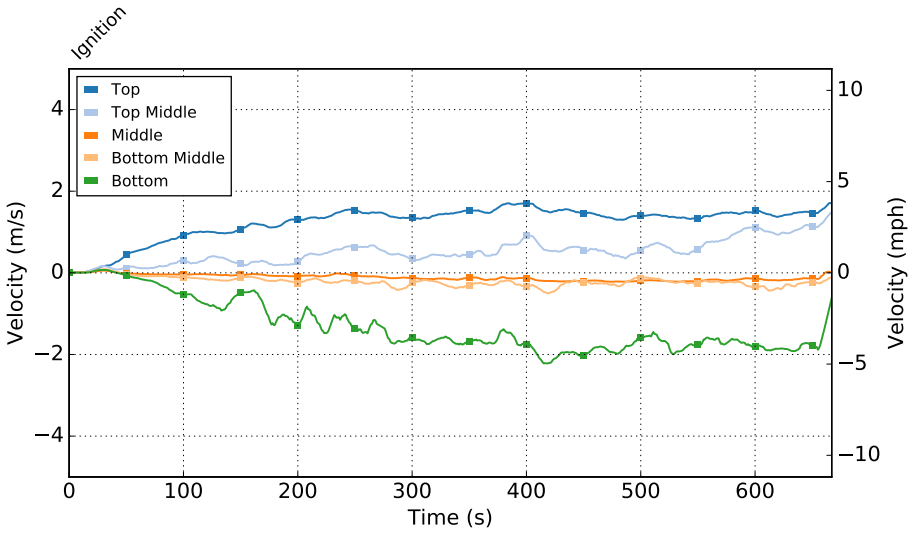

Figure 4.5: Fire room doorway velocities for Pallets and Straw Experiment 1.

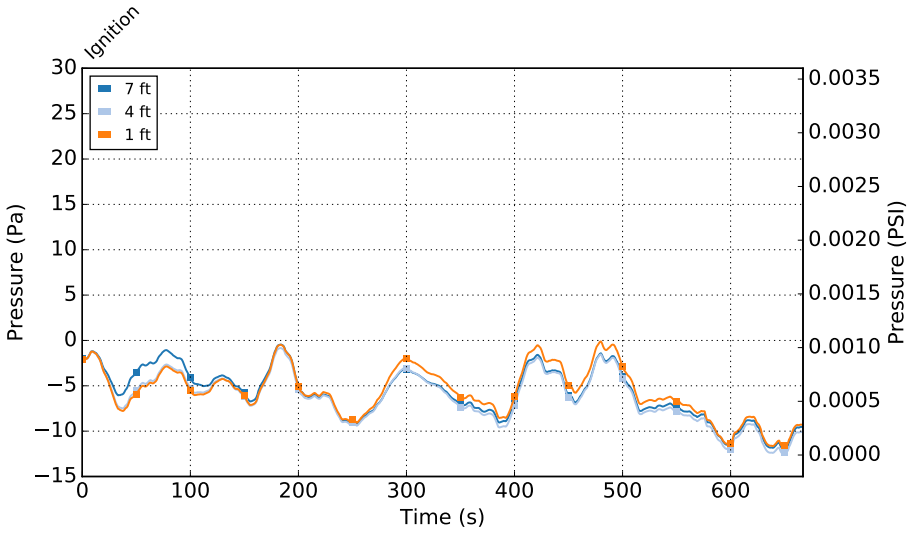

Figure 4.6: Fire room pressure for Pallets and Straw Experiment 1.

4.1.2 Pallets and Straw Experiment 2 (Near Vent)

Pallets and Straw Experiment 2 started with all exterior doors and windows closed. At 480 seconds after ignition, the fire room window was opened. Figures 4.7 and 4.8 show the fire room temperatures and floor heat flux. Both temperatures and heat fluxes in the fire room climbed steadily in the pre-ventilation period, reaching a steady maximum values between 400 and 450 seconds after ignition. The peak temperature and heat flux in the fire room were observed later in the experiment than in Pallets and Straw Experiment 1. Additionally, the growth was not as rapid as the other pallets and straw tests. The reason for this may be that all of the straw was not ignited early in

the incipient phase of the fire, possibly because it was too densely packed. Because of this, most of the burning was concentrated on one side of the pallets, until approximately 180 seconds after ignition, when the remainder of the straw became involved. Figure 4.9 shows the heat fluxes in the remote rooms on the second floor. Temperatures and heat fluxes remote from the fire room were considerably lower than those measured within the fire room.

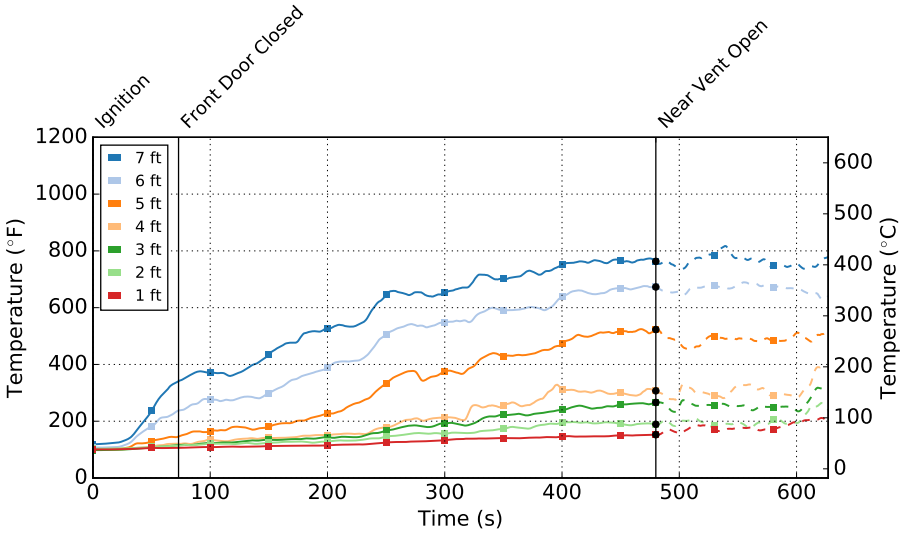

Figure 4.7: Fire room temperatures for Pallets and Straw Experiment 2. Pre-ventilation data is denoted by a solid line. Post-ventilation data is denoted by a dashed line of the same color as the corresponding solid line.

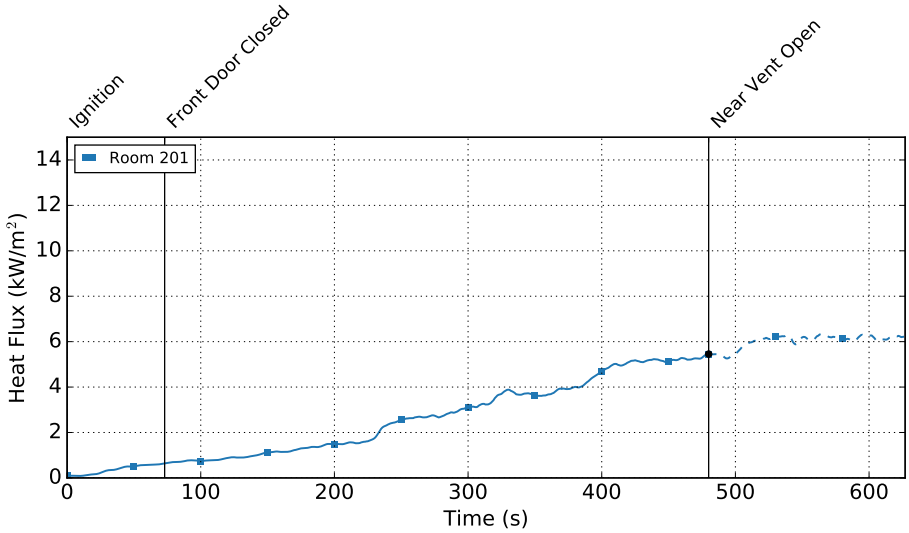

Figure 4.8: Fire room heat flux for Pallets and Straw Experiment 2. Pre-ventilation data is denoted by a solid line. Post-ventilation data is denoted by a dashed line of the same color as the corresponding solid line.

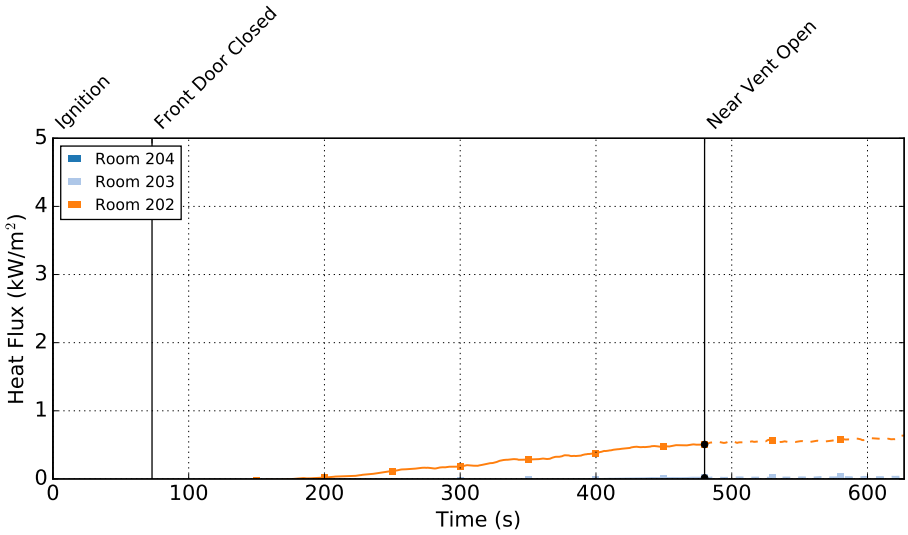

Figure 4.9: Remote heat fluxes for Pallets and Straw Experiment 2.

The peak thermal conditions occurred in the same time period that the minimum oxygen concentrations were measured at the 6 ft. (1.8 m) level, as shown in Figure 4.10. The minimum values in both the front and rear of the room were between and 10% and 15%. The 6 ft. (1.8 m) oxygen concentrations began to rebound after reaching the minimum value, increasing to above 15% by the end of the test. The 2 ft. (0.6 m) oxygen concentrations remained above 20% for the entire duration of the test. Similarly to Pallets and Straw Experiment 1, a constant bi-directional flow was maintained for the duration of the experiment, as indicated by the BDP data in Figure 4.11. The flow, oxygen, heat flux, and fire room temperature data indicated that two distinct zones existed in the fire room for the duration of the experiment, as was noted in Pallets and Straw Experiment 1. The temperature data indicates that the neutral layer was between 4 ft. and 5 ft. (1.2 m and 1.5 m).

The BDP data from the fire room window and doorway, shown in Figures 4.13 and 4.5, respectively, show that once the window was opened, the majority of flow through the window is inlet and the majority of the flow through the doorway is exhaust. This flow data, along with video of the experiment, indicates that the wind had an influence on the flow through the fire room. The nearly uni-directional flow into the fire room through the window was punctuated by momentary oscilations of exhuast, which were accompanied by local pressure peaks, as seen in Figure 4.6. While this pulsing flow behavior due to wind affected the flow through the fire room, it did not correspond with any notable growth in temperatures or heat flux within the fire room.

4.1.3 Pallets and Straw Experiment 3 (Remote Vent)

Pallets and Straw Experiment 3 started with all exterior doors and windows closed. At 240 seconds after ignition, the front door and remote window in Room 204 window were opened. Figures 4.14 and 4.15 show the fire room temperatures and floor heat flux. The growth was similar to Pallets

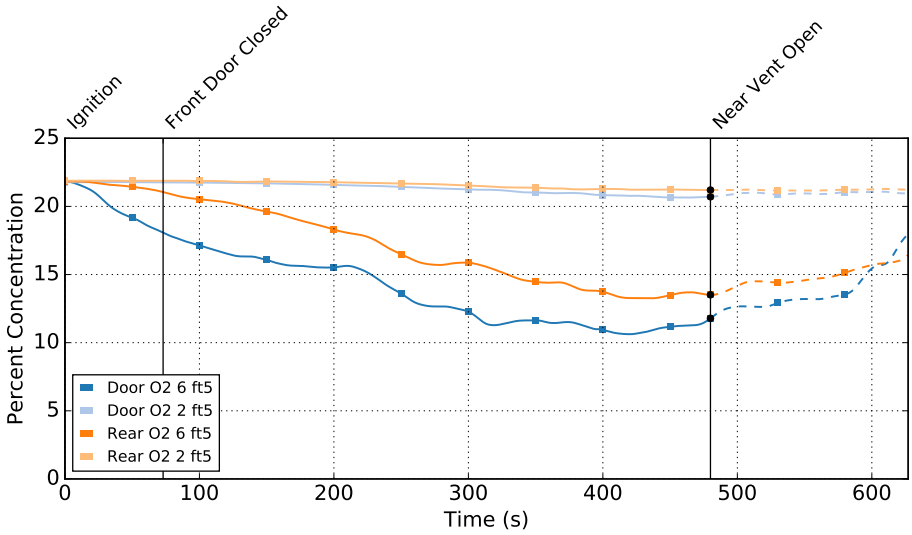

Figure 4.10: Fire room O_2 Concentration (%) for Pallets and Straw Experiment 2. Pre-ventilation data is denoted by a solid line. Post-ventilation data is denoted by a dashed line of the same color as the corresponding solid line.

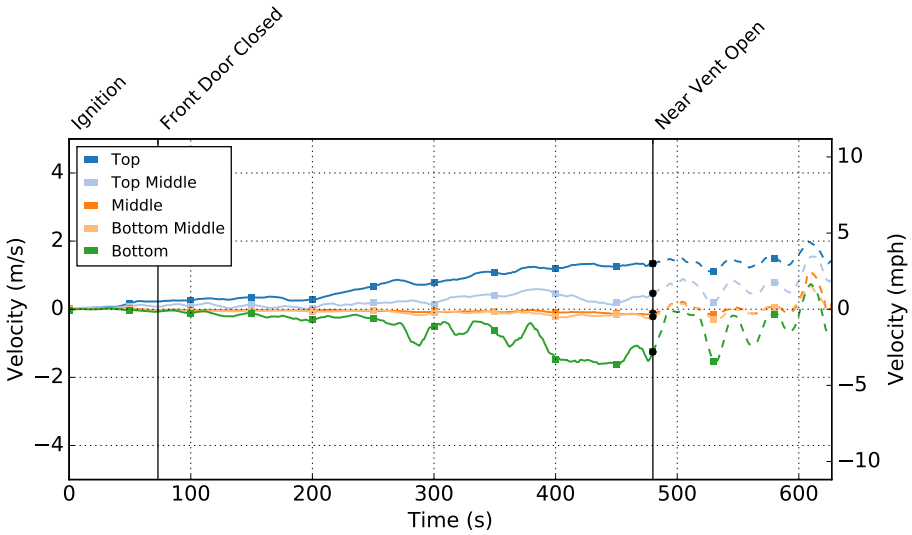

Figure 4.11: Fire room doorway velocities for Pallets and Straw Experiment 2. Pre-ventilation data is denoted by a solid line. Post-ventilation data is denoted by a dashed line of the same color as the corresponding solid line.

and Straw Experiment 1, with the peak temperature occurring at approximately 300 seconds, and the peak fire room heat flux occurring at approximately 350 seconds. Temperatures and heat fluxes remote from the fire room were lower than those observed in the fire room, as shown in Figure 4.16. These peaks corresponded to the minimum oxygen concentrations at the 6 ft. (1.8 m) level, which occurred at approximately 300 seconds, as shown in Figure 4.17. The minimum oxygen concentrations at the 6 ft. (1.8 m) level were approximately 10%. The 2 ft. (0.6 m) oxygen

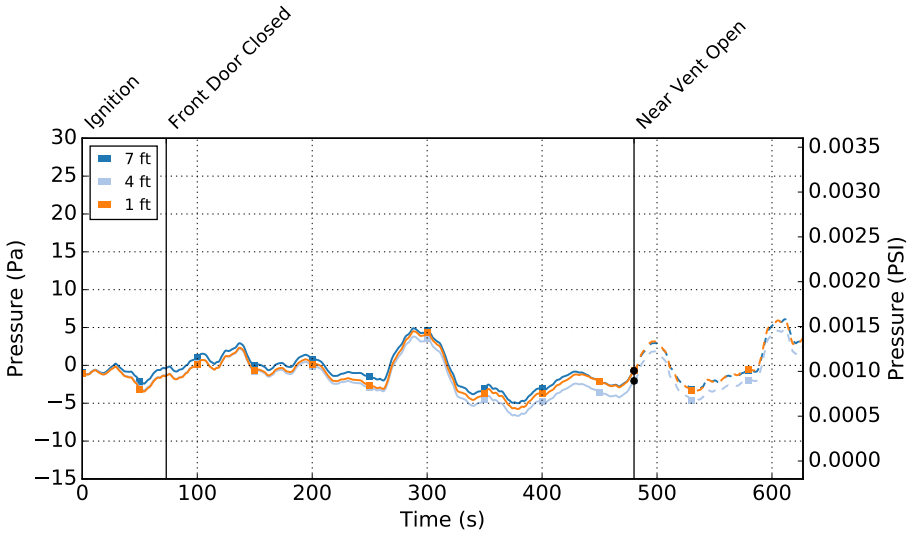

Figure 4.12: Fire room pressure for Pallets and Straw Experiment 2. Pre-ventilation data is denoted by a solid line. Post-ventilation data is denoted by a dashed line of the same color as the corresponding solid line.

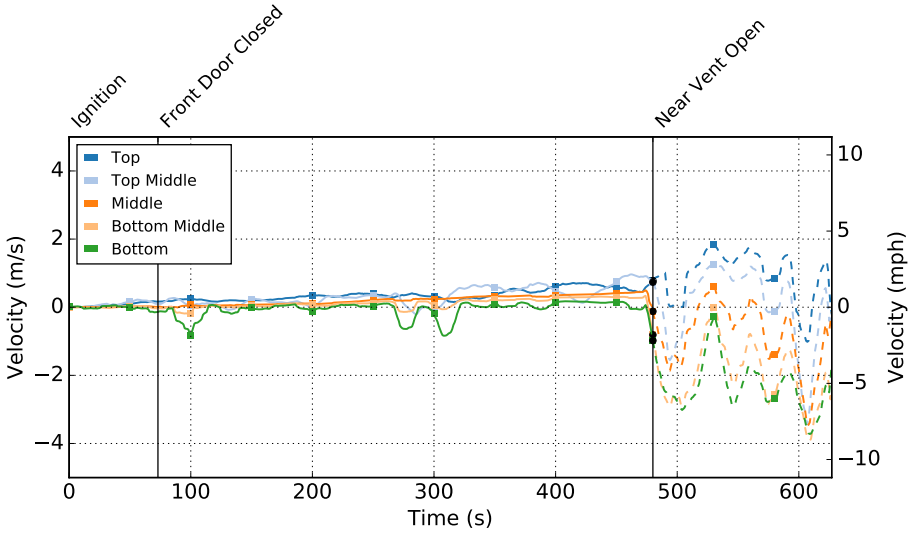

Figure 4.13: Fire room window velocities for Pallets and Straw Experiment 2. Pre-ventilation data is denoted by a solid line. Post-ventilation data is denoted by a dashed line of the same color as the corresponding solid line.

concentrations remained above 20% for the duration of the experiment. Following the peak thermal conditions in the fire room, the temperatures and heat flux began to decrease, reaching a steady state at approximately 500 seconds, which continued until the end of the experiment.

Similarly to the other two pallets and straw experiments, a bi-directional flow was maintained through the doorway for the duration of the experiment. Figure 4.18 shows that the two top BDPs

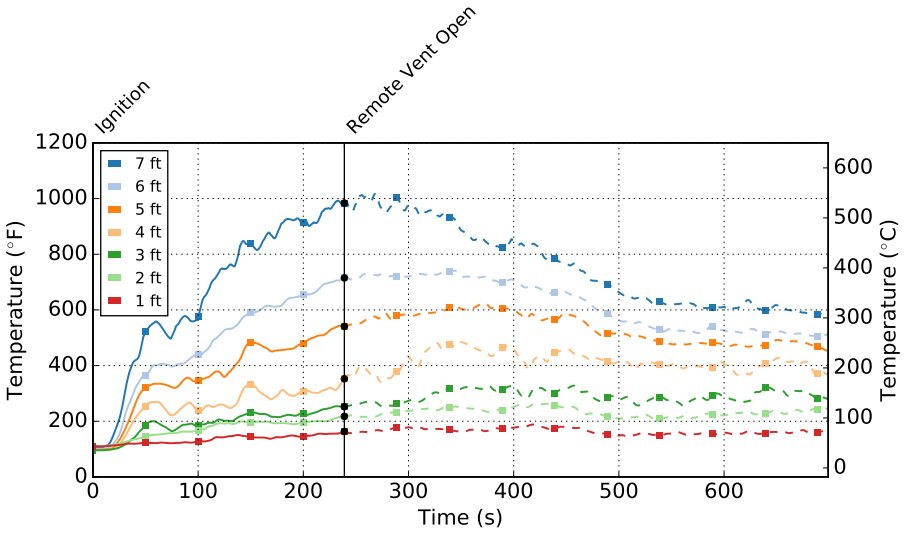

Figure 4.14: Fire room temperatures for Pallets and Straw Experiment 3. Pre-ventilation data is denoted by a solid line. Post-ventilation data is denoted by a dashed line of the same color as the corresponding solid line.

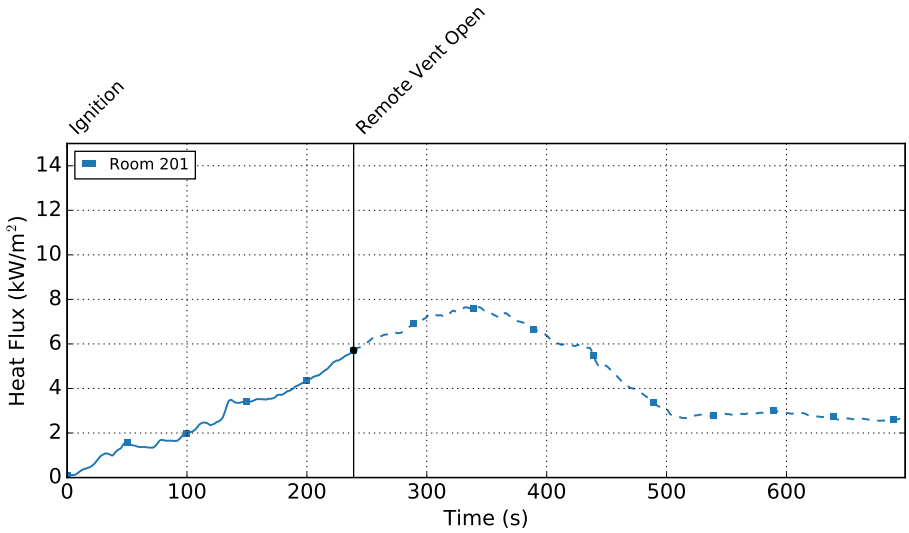

Figure 4.15: Fire room heat flux for Pallets and Straw Experiment 3. Pre-ventilation data is denoted by a solid line. Post-ventilation data is denoted by a dashed line of the same color as the corresponding solid line.

in the array had positive velocities, indicating exhaust from the fire room, while the bottom BDP in the array was an inlet, with the middle and bottom middle probes registering negligible flow. The bi-directional flow in the doorway, combined with the temperature, oxygen, and heat flux data, indicates that two distinct zones exist, similarly to those observed in the other two pallets and straw experiments.

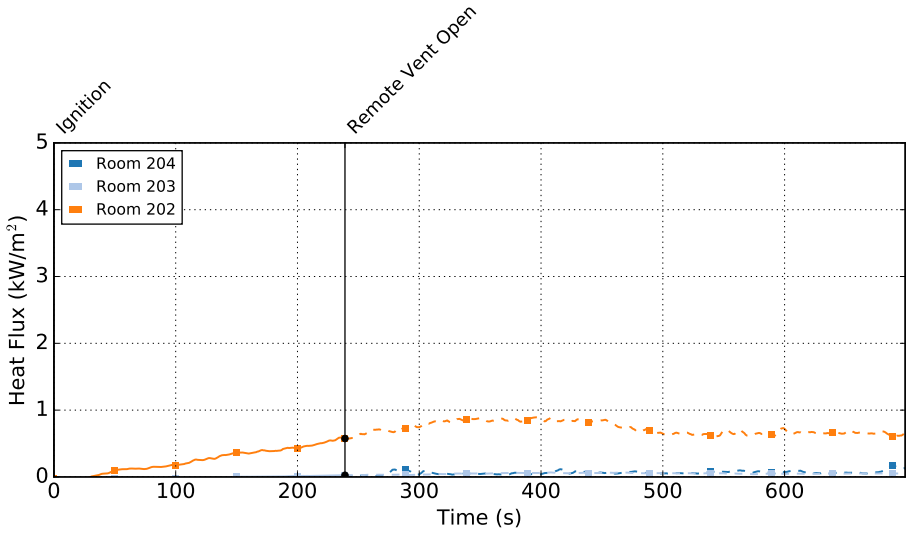

Figure 4.16: Remote heat fluxes for Pallets and Straw Experiment 3.

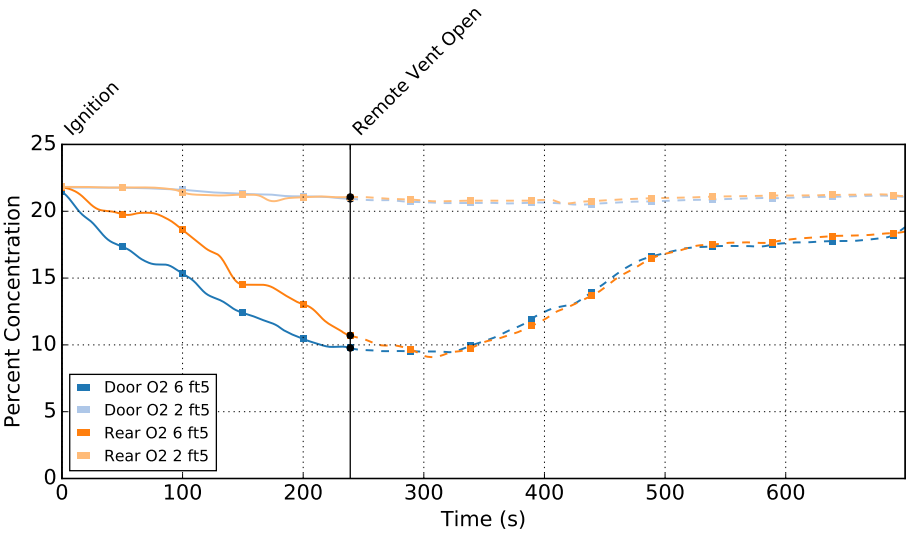

Figure 4.17: Fire room O_2 Concentration (%) for Pallets and Straw Experiment 3. Pre-ventilation data is denoted by a solid line. Post-ventilation data is denoted by a dashed line of the same color as the corresponding solid line.

Following ventilation of the front door and Room 204 window, there was no significant change in the flow through the fire room door. Additionally, there was no major increase in fire room temperatures or heat flux values. In the period following ventilation, the fire held a steady state before decaying in a manner similar to Pallets and Straw Experiment 1 (no vent case). No major rises in fire room pressure (Figure 4.19) were observed over the duration of the fire room experiment.

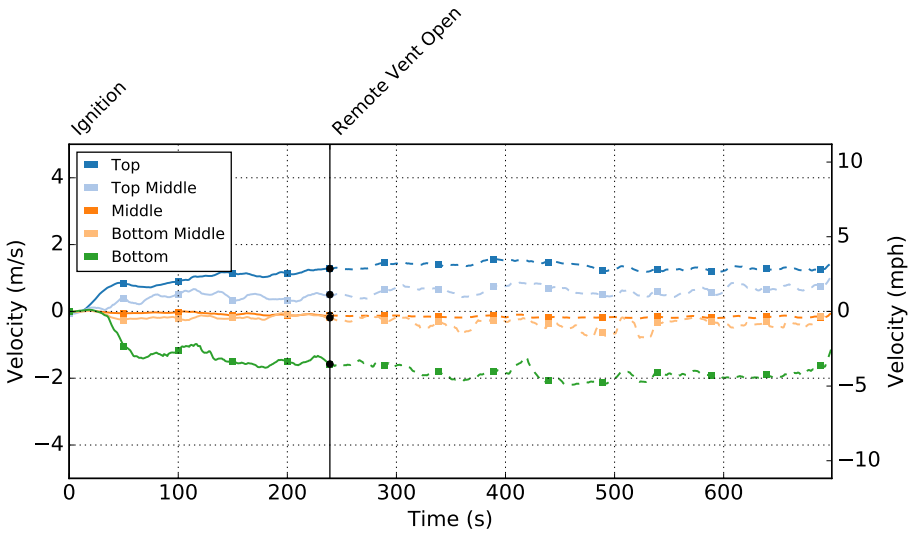

Figure 4.18: Fire room doorway velocities for Pallets and Straw Experiment 3. Pre-ventilation data is denoted by a solid line. Post-ventilation data is denoted by a dashed line of the same color as the corresponding solid line.

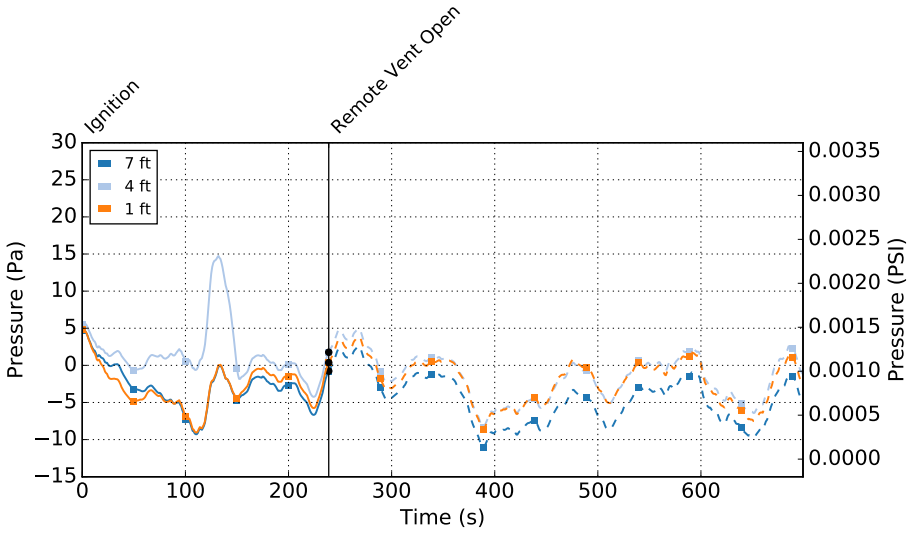

Figure 4.19: Fire room pressure for Pallets and Straw Experiment 3. Pre-ventilation data is denoted by a solid line. Post-ventilation data is denoted by a dashed line of the same color as the corresponding solid line.

4.2 OSB Experiments

Two training fuel experiments were conducted using pallets, straw, and OSB as a fuel. In these experiments, two ventilation cases were considered: vent close to the seat of the fire, and vent remote from the seat of the fire. This section presents the fire room temperature, heat flux, gas velocity, oxygen concentration, and pressure measurements for these experiments. Temperature data for rooms remote from the fire room are located in Appendix B.1.

4.2.1 OSB Experiment 1 (Near Vent)

OSB Experiment 1 began with all exterior doors and windows closed prior to ignition. The fire room window was opened 250 seconds after ignition. Figures 4.20 and 4.21 show the fire room temperature and heat flux as a function of time. The peak temperature and heat flux were both observed at roughly 350 seconds after ignition, after the fire room window was ventilated. Following ventilation of the window, there was a significant increase in temperature at the 3 ft., 4 ft., and 5 ft. (0.9 m, 1.2 m, and 1.5 m) levels, as well as in the fire room heat flux, which increased from 10 kW/m^2 to 15 kW/m^2 in roughly 50 seconds. The temperatures in the fire room were generally higher than those measured in the pallets and straw experiments, although the peak values were observed at approximately the same time. Temperatures and heat fluxes remote from the fire room were less severe than those measured in the fire room, as shown in Figure 4.22.

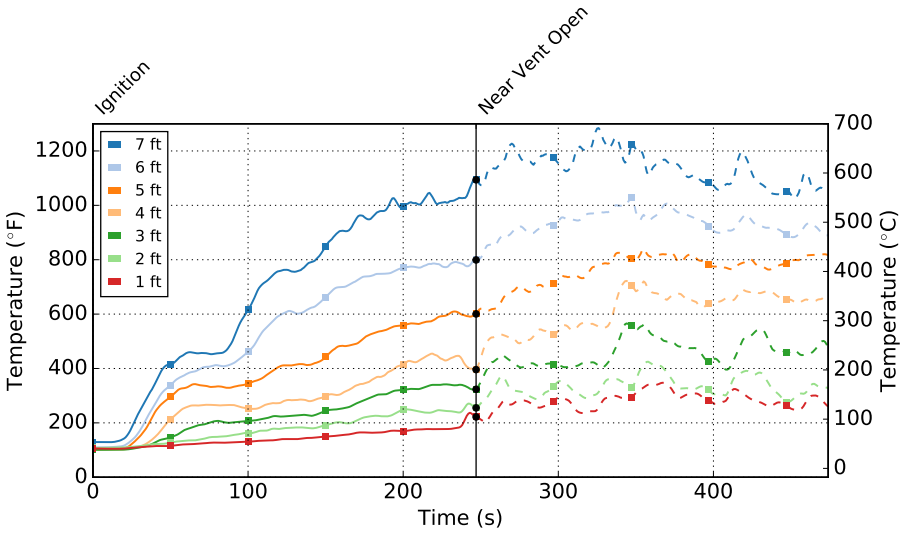

Figure 4.20: Fire room temperatures for OSB Experiment 1. Pre-ventilation data is denoted by a solid line. Post-ventilation data is denoted by a dashed line of the same color as the corresponding solid line.

Figure 4.23 shows that the oxygen concentrations at the 6 ft. (1.8 m) level reached a minimum value immediately before the fire room window was ventilated. Following fire room ventilation,

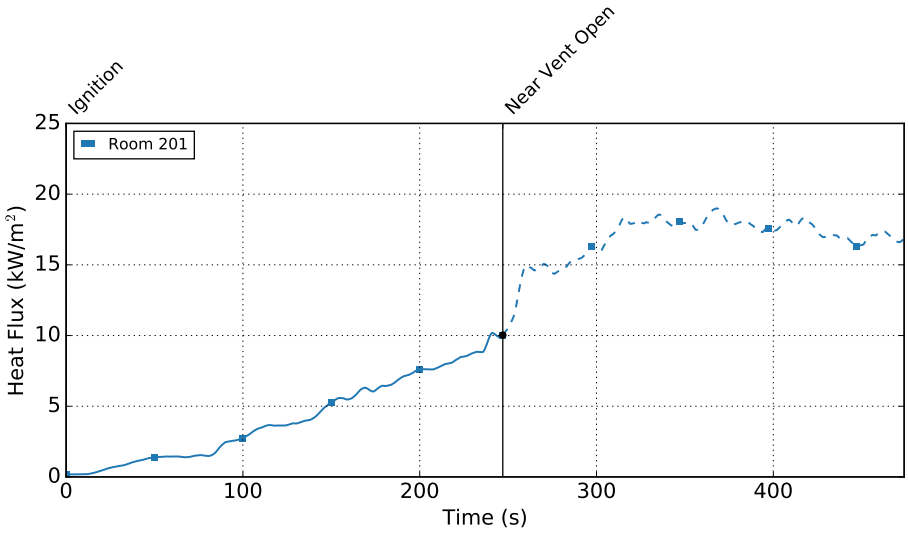

Figure 4.21: Fire room heat flux for OSB Experiment 1. Pre-ventilation data is denoted by a solid line. Post-ventilation data is denoted by a dashed line of the same color as the corresponding solid line.

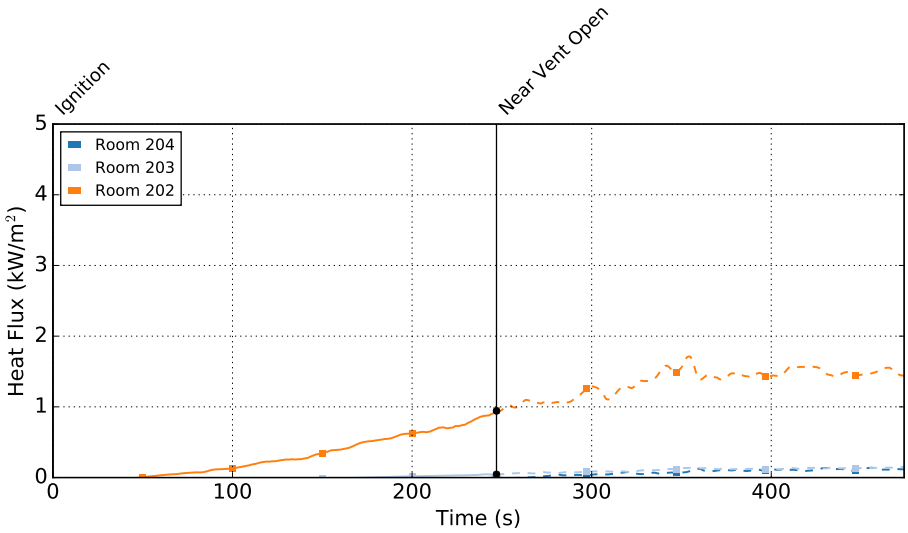

Figure 4.22: Remote heat fluxes for OSB Experiment 1.

the oxygen concentrations at the 6 ft. (1.8 m) level remained low until approximately 400 seconds after ignition, when they began to rebound. This behavior is similar to the behavior of the 6 ft. (1.8 m) oxygen concentrations in the pallets and straw experiments, although the minimum values are sustained for slightly longer. This may be a result of the increased fuel weight, which could sustain the peak for longer. The 2 ft. (0.6 m) oxygen concentrations were also very similar to the pallets and straw experiments, remaining above 20% for the duration of the experiment.

The top two probes in the array indicated exhaust while the bottom probe indicated an inlet, with

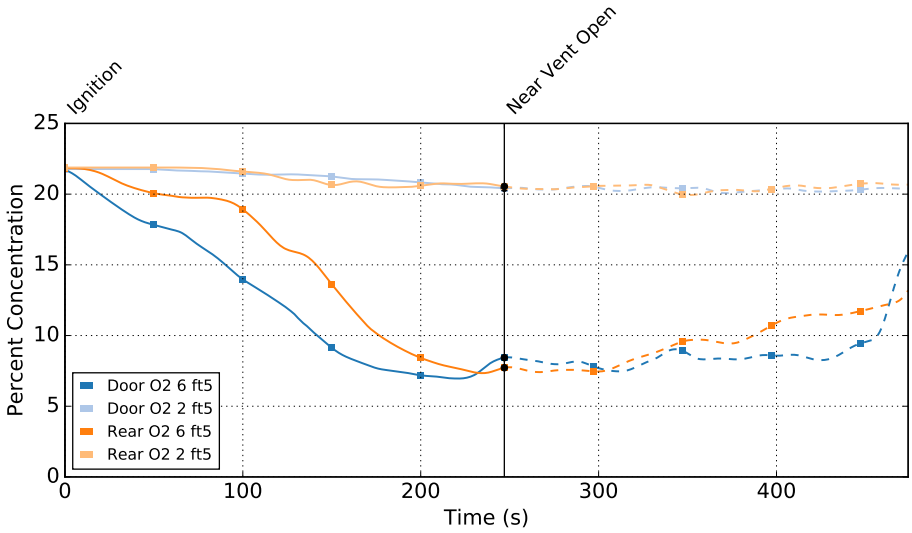

Figure 4.23: Fire room O_2 Concentration (%) for OSB Experiment 1. Pre-ventilation data is denoted by a solid line. Post-ventilation data is denoted by a dashed line of the same color as the corresponding solid line.

minimal flow in the middle two probes, which is similar to the behavior exhibited in the pallets and straw experiments. Following ventilation, all five probes have positive readings, indicating uni-directional exhaust from the fire room. Following this event, the velocities stabilize to their pattern prior to ventilation.

The BDPs in the doorway to the fire room showed that bi-directional flow at the vent was maintained for the pre-ventilation period (Figure 4.24).T After ventilation, the BDP data from the fire room window and doorway, shown in Figures 4.25 and 4.24, respectively, show that the majority of flow through the window is inlet and the majority of the flow through the doorway is exhaust. This flow data, along with video of the experiment, indicates that the wind had an influence on the flow through the fire room. The nearly uni-directional flow into the fire room through the window was punctuated by momentary oscilations of exhuast, which were accompanied by local pressure peaks, as seen in Figure 4.26. It is possible that the additional flow into the fire room due to wind was responsible for the growth in thermal conditions observed in this period.

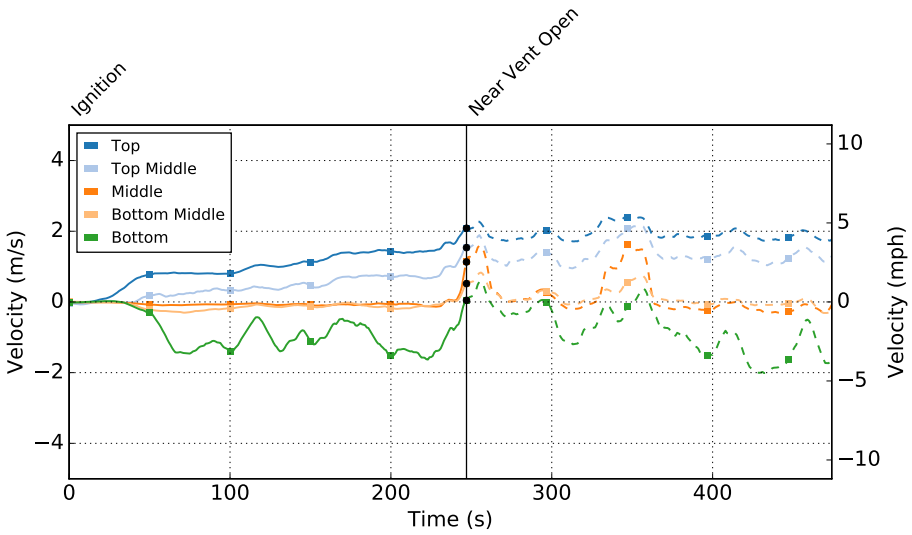

Figure 4.24: Fire room doorway velocities for OSB Experiment 1. Pre-ventilation data is denoted by a solid line. Post-ventilation data is denoted by a dashed line of the same color as the corresponding solid line.

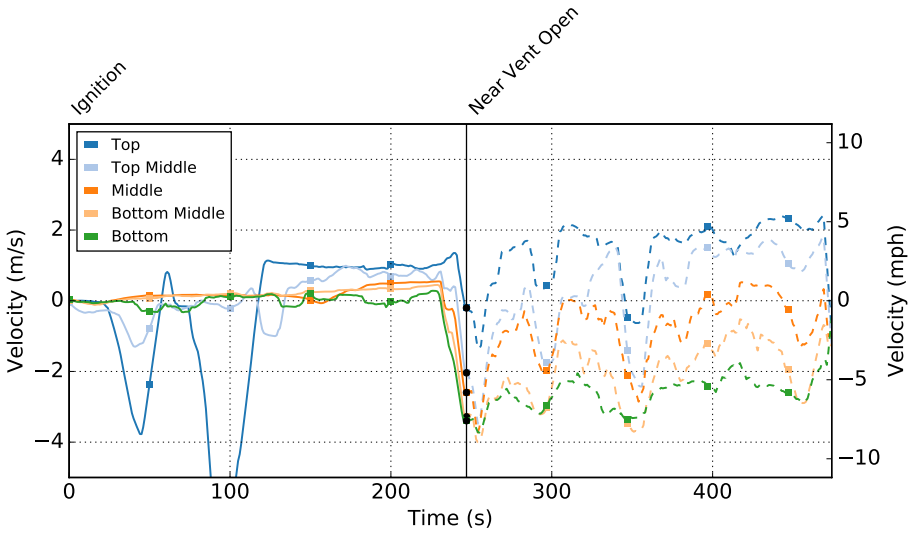

Figure 4.25: Room 201 Window Velocity for OSB Experiment 1

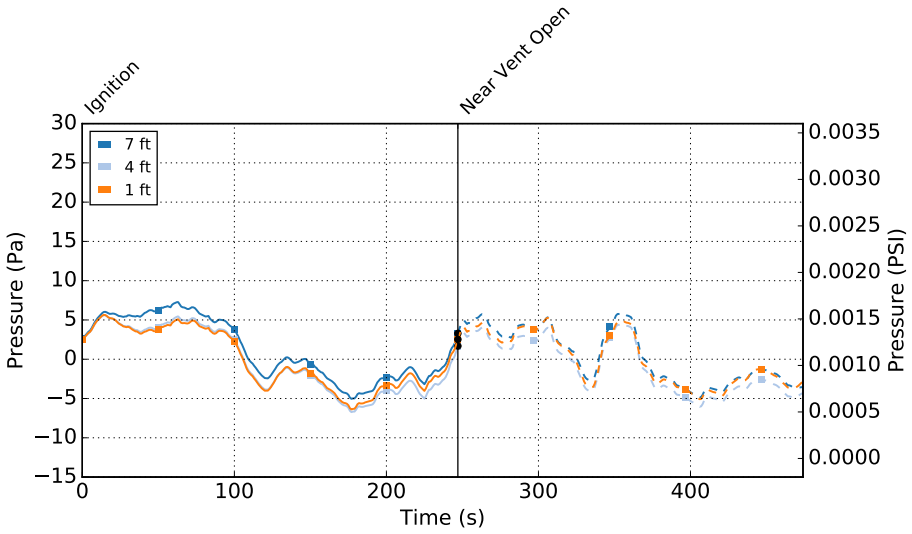

Figure 4.26: Fire room pressure for OSB Experiment 1. Pre-ventilation data is denoted by a solid line. Post-ventilation data is denoted by a dashed line of the same color as the corresponding solid line.

4.2.2 OSB Experiment 2 (Remote Vent)

OSB Experiment 2 began with all exterior doors and windows closed prior to ignition. At 300 seconds after ignition, the front door and remote window in Room 204 window were opened. Figures 4.27 and 4.28 show the fire room temperatures and heat flux The fire growth in the 100 seconds following ignition was different in this experiment than in the four other training fuel experiments, where the fire room temperatures reached an approximately steady state between 100 seconds and 150 seconds, before continuing their growth. A similar trend was noted in the fire room heat flux. Both of these periods corresponded with a spike in pressure within the fire room, as shown in Figure 4.29. This temperature behavior and increase in pressure could be related to the point at which the fuel package transitions from mostly straw burning to pallets, OSB, and straw burning. The temperature profile observed in the fire room was similar to the fire growth in OSB Experiment 1, although there was no significant rise in temperature and heat flux following remote ventilation. The heat fluxes in rooms remote from the fire room are shown in Figure 4.30.

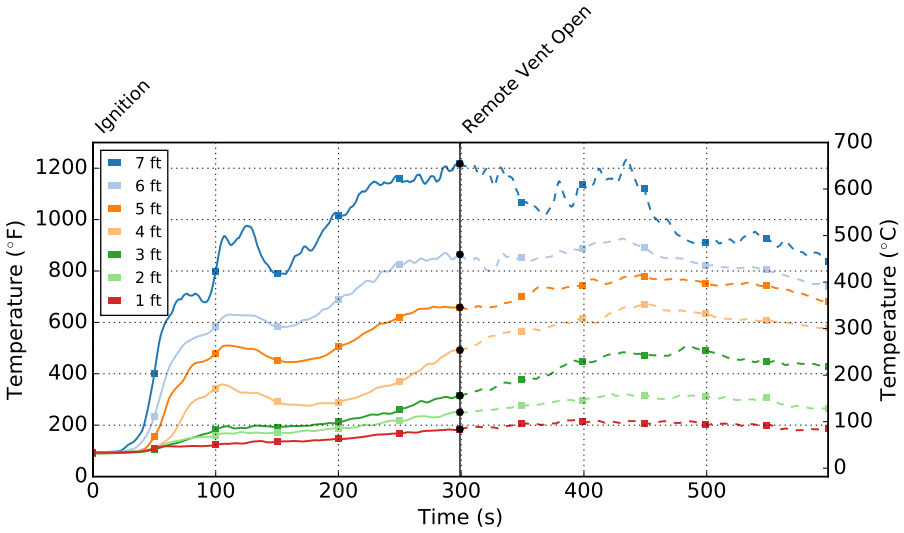

Figure 4.27: Fire room temperatures for OSB Experiment 2. Pre-ventilation data is denoted by a solid line. Post-ventilation data is denoted by a dashed line of the same color as the corresponding solid line.

The oxygen concentration behavior at the 2 ft. (0.6 m) and 6 ft. (1.8 m) level was similar to that observed in OSB Experiment 1 and the pallets and straw experiments. Oxygen concentrations at the 6 ft. (1.8 m) level fell below 10%, while 2 ft. (0.6 m) concentrations remained above 20% for the duration of the experiment. A bi-directional flow path was maintained for the duration of the experiment, as shown in Figure 4.32 with the pre-ventilation behavior being similar to the pallets and straw experiments and OSB Experiment 1. Following ventilation, there is a slight change in doorway velocities. The velocity increases in the positive direction in the top middle BDP in of the array and the magnitude of the velocity increases in the negative direction for the bottom two BDPs in the array, indicating that both the inlet and exhaust flow rates are increasing.

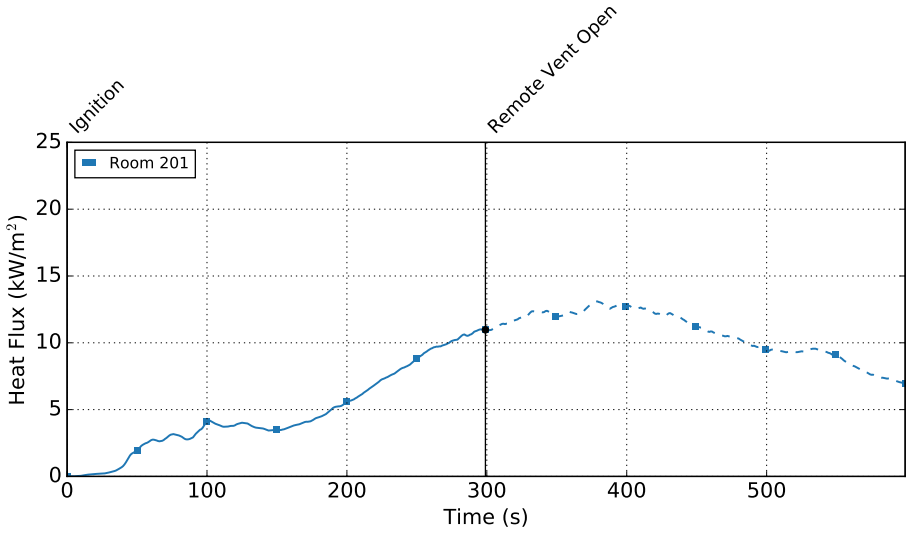

Figure 4.28: Fire room heat flux for OSB Experiment 2. Pre-ventilation data is denoted by a solid line. Post-ventilation data is denoted by a dashed line of the same color as the corresponding solid line.

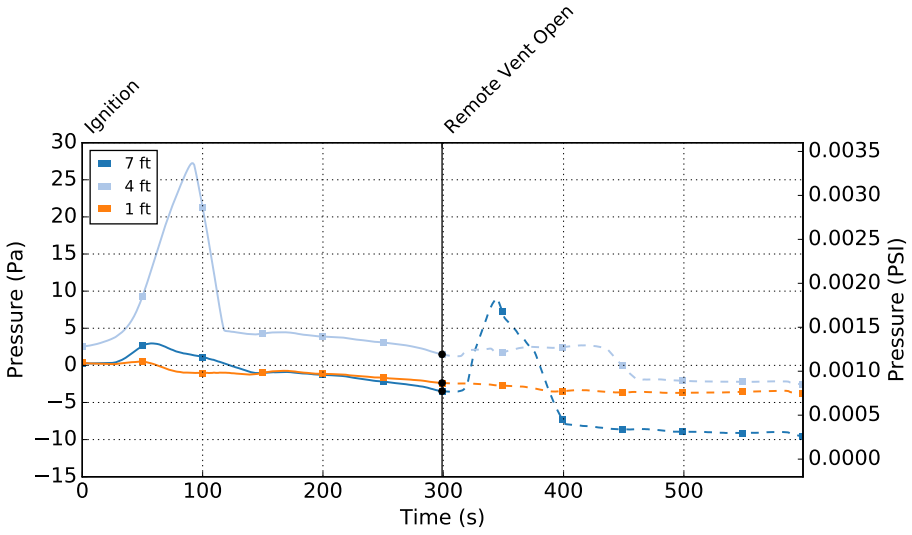

Figure 4.29: Fire room pressure for OSB Experiment 2. Pre-ventilation data is denoted by a solid line. Post-ventilation data is denoted by a dashed line of the same color as the corresponding solid line.

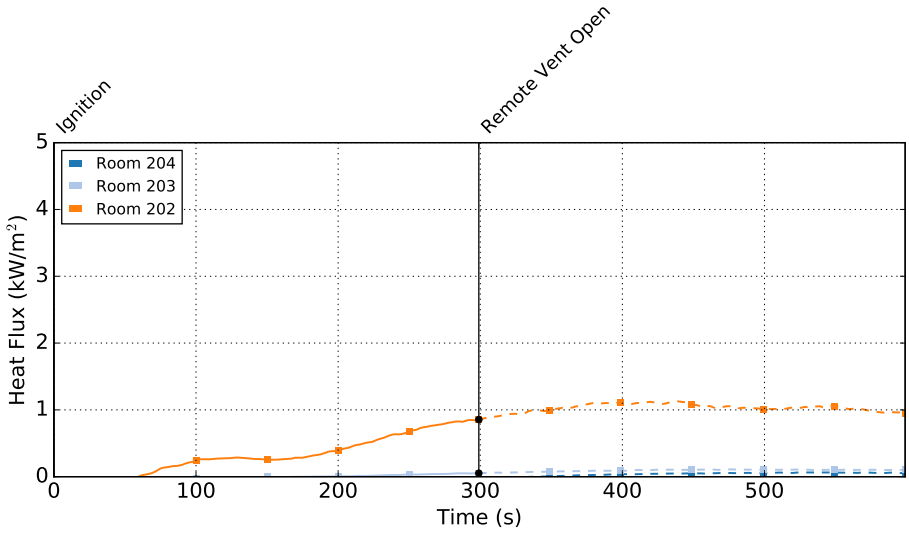

Figure 4.30: Remote heat fluxes for OSB Experiment 2.

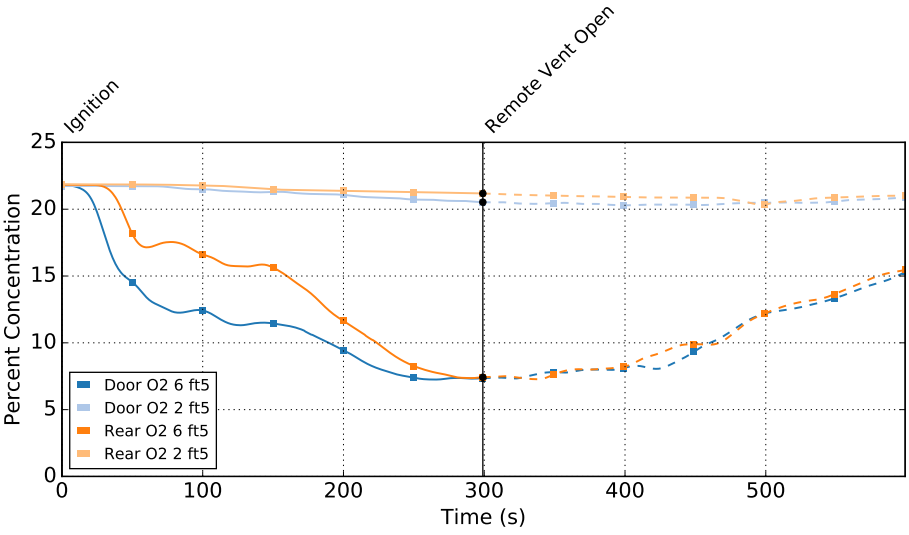

Figure 4.31: Fire room O_2 Concentration (%) for OSB Experiment 2. Pre-ventilation data is denoted by a solid line. Post-ventilation data is denoted by a dashed line of the same color as the corresponding solid line.

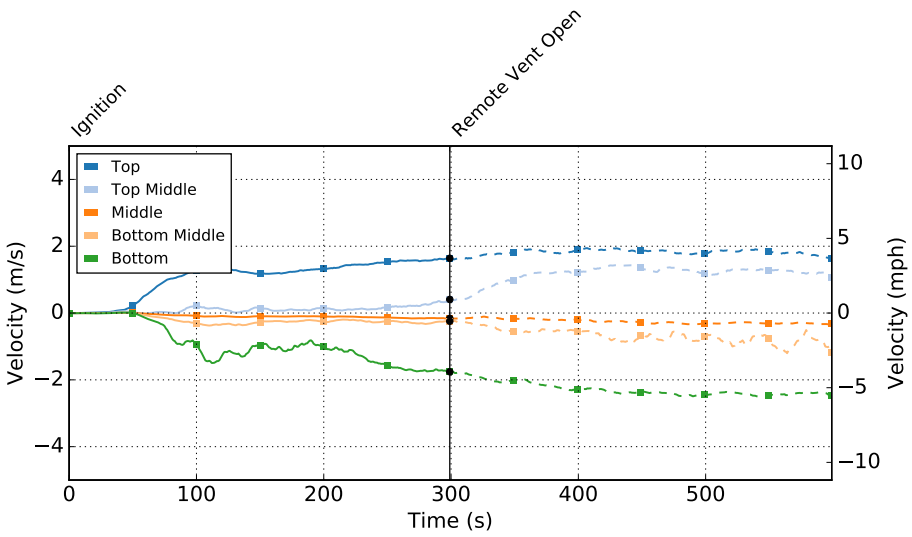

Figure 4.32: Fire room doorway velocities for OSB Experiment 2. Pre-ventilation data is denoted by a solid line. Post-ventilation data is denoted by a dashed line of the same color as the corresponding solid line.

4.3 Furniture Experiments

Three experiments were conducted using common residential furnishings as a fuel. These fuels are not intended to be used as training fuels, but rather to evaluate the fire dyanamics produced by fuels similar to those that firefighters would find in their workplace, within concrete live fire training building. In these experiments, three ventilation cases were considered: no vent, vent close to the seat of the fire, and vent remote from the seat of the fire. This section presents the fire room temperature, heat flux, gas velocity, oxygen concentration, and pressure measurements for these experiments. Temperature data for rooms remote from the fire room are located in Appendix B.1.

4.3.1 Furniture Experiment 1 (No Vent)

Furniture Experiment 1 had all exterior doors and windows closed at the time of ignition. These doors and windows remained closed for the duration of the experiment. The fire room temperatures and heat fluxes were significantly more severe than those noted in the pallets and straw and OSB experiments. The peak temperature and heat flux were observed at approximately 400 seconds after ignition. This peak time is later than the peak times for the pallets and OSB experiments, but, unlike those experiments, the peak temperature was maintained for the duration of the experiment. Fire room temperatures and heat fluxes were sustained in excess of 1000°F (540°C) and 30 kW/m^2, respectively, for the remainder of the experiment. Additionally, the cooler temperatures close to the floor which were measured in the training fuel experiments were not observed in Furnished Room Experiment 1. Rather, the temperatures were more consistent with a single zone of elevated temperature. The peak floor heat flux in the room adjacent to the fire room was close to 4 kW/m^2, as shown in figure 4.35. This is higher than the peak observed in any of the training fuel experiments, although floor heat fluxes in rooms more remote from the fire room remained quite low.

The minimum oxygen concentrations at the 6 ft. (1.8 m) level were observed at approximately the same time as the peak thermal conditions in the fire room. While this behavior is similar to the training fuel experiments discussed in previous sections, the oxygen concentrations remained low, close to 5%, for the remainder of the experiment. The 2 ft. (0.6 m) oxygen concentrations also exhibited different behavior than was noted in the training fuels. In the rear of the room, the 2 ft. (0.6 m) oxygen concentration decreased to 5%, as shown in Figure 4.36. The oxygen concentration in the doorway was significantly higher than the other three sample points in the fire room, but was still lower than the 2 ft. (0.6 m) concentrations. The 2 ft. (0.6 m) doorway concentrations reached a steady value at approximately 15%. The oxygen concentrations were insufficient for combustion to occur at higher elevations in the room or rear in the room, but the higher oxygen concentration in the doorway indicates that the oxygen is being supplied to the fire through the doorway to the fire room. This is further supported by the BDP data from the fire room doorway. Much like the training fuel experiments, a bi-directional flow was maintained through the fire room doorway for the duration of the experiments. The profile of the flow, however, was different in this experiment. In the training fuel tests, the most common flow profile featured the top two BDPs in the array

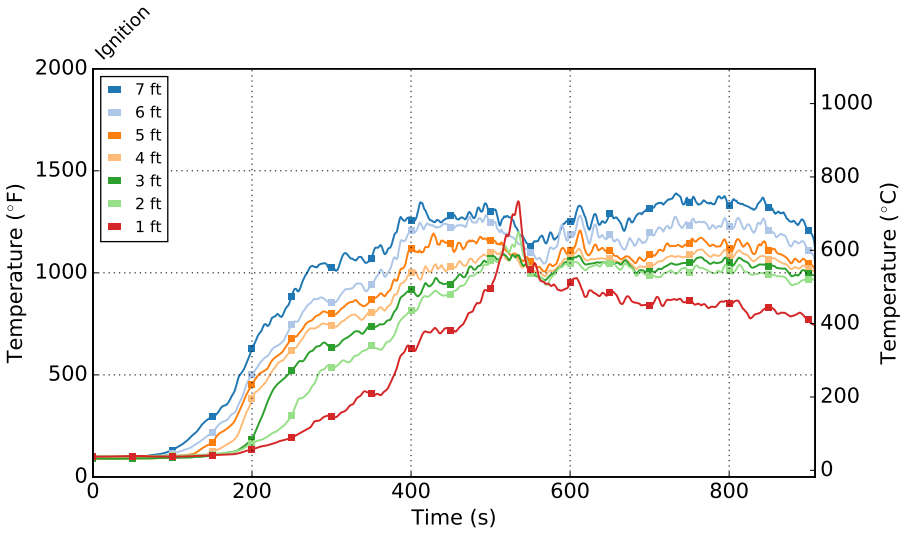

Figure 4.33: Fire room temperatures for Furniture Experiment 1.

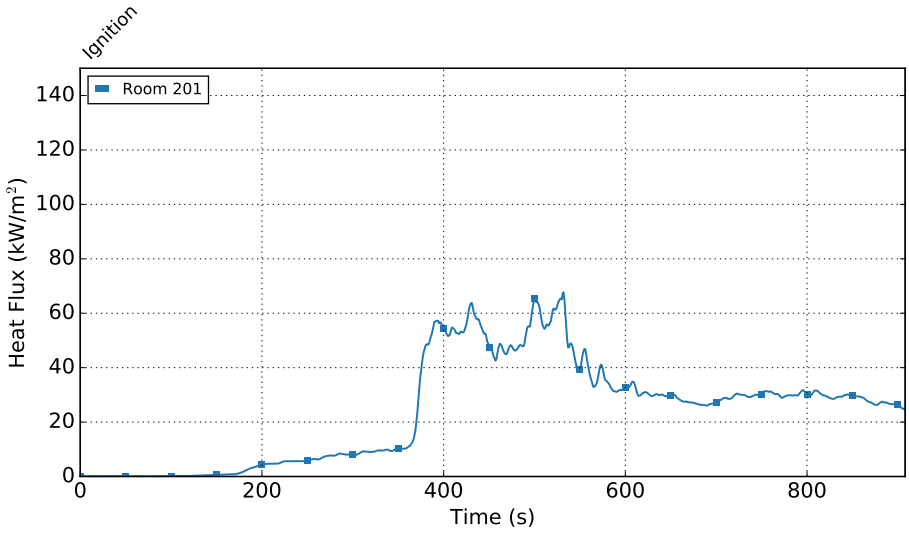

Figure 4.34: Fire room heat flux for Furniture Experiment 1.

exhausting products of combustion from the fire room and the bottom probe in the array indicating an inlet into the room for fresh air, with minimal flow in the middle and bottom middle probes in the array. In this experiment, the top three probes in the array indicated exhaust, while the bottom two probes in the array indicated intake into the room. Thus, more products of combustion were being exhausted from the fire room than fresh air being drawn in. Despite the higher rate of combustion products being produced in the furniture fuel package, as indicated by the higher temperatures and exhaust from the fire room, there was no significant pressure spikes in the experiment, as seen in Figure 4.38.

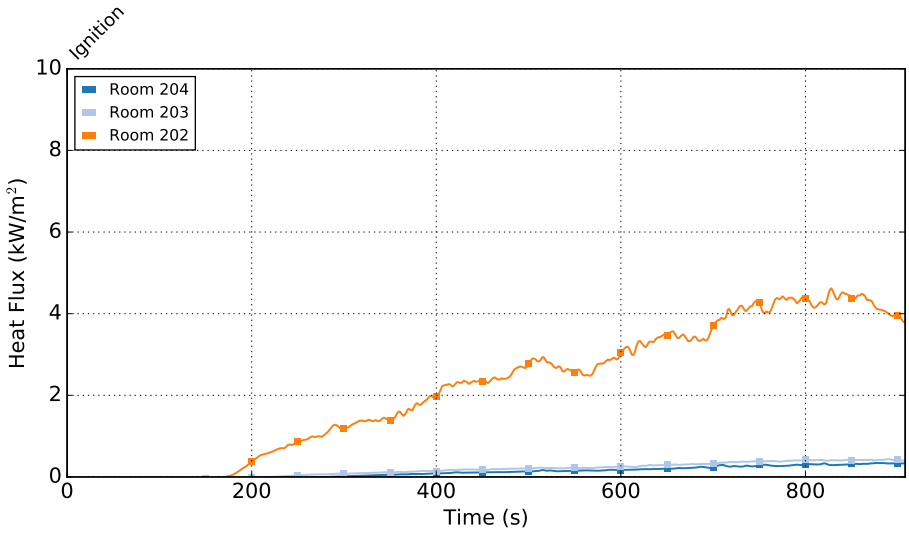

Figure 4.35: Remote heat fluxes for Furniture Experiment 1.

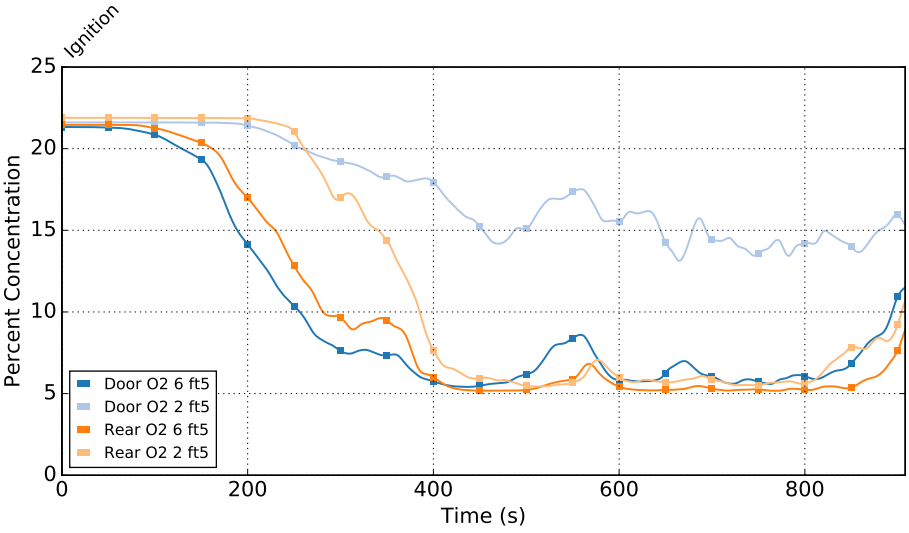

Figure 4.36: Fire room O_2 Concentration (%) for Furniture Experiment 1.

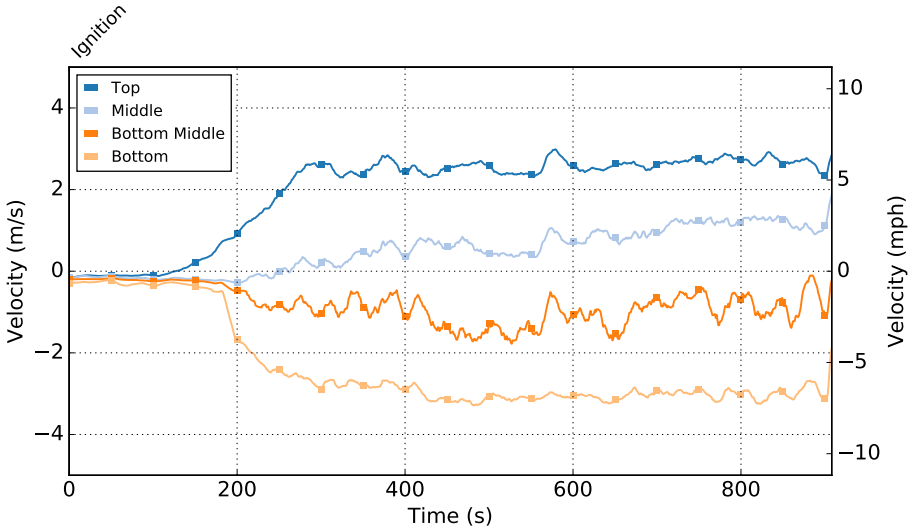

Figure 4.37: Fire room doorway velocities for Furniture Experiment 1. Note that the top middle sensor experienced an error during the test and was excluded from the chart.

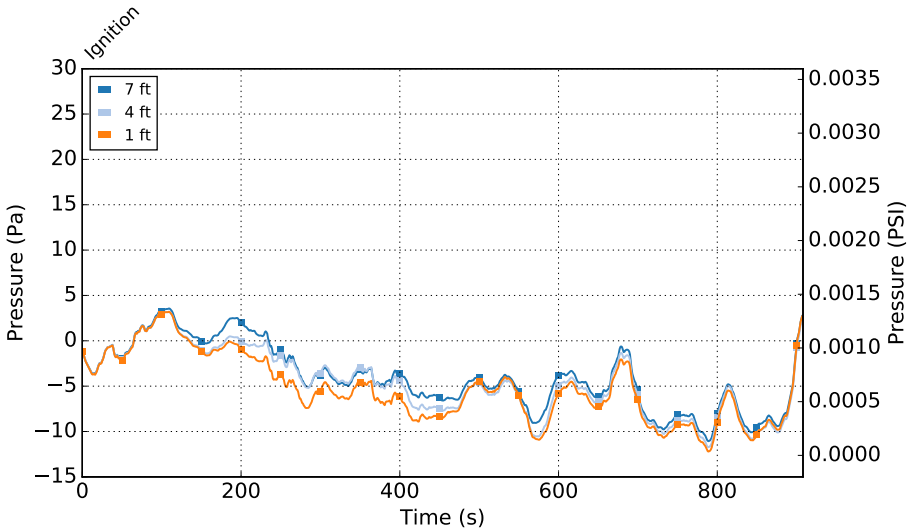

Figure 4.38: Fire room pressure for Furniture Experiment 1.

4.3.2 Furniture Experiment 2 (Near Vent)

Furniture Experiment 2 had all exterior doors and windows closed at the time of ignition. The fire room window was opened at 420 seconds after ignition. While the fire growth prior to ventilation was similar to that in Furniture Experiment 1, the fire room temperatures and heat fluxes that were observed in the post-ventilation period were the most severe in this series of experiments, as shown in Figures 4.39 and 4.40. Immediately after ventilation of the fire room window, fire room temperatures and heat flux increased to conditions consistent with flashover. The time of ventilation approximately corresponded with the time at which the peak temperatures were observed in Furniture Experiment 1. Remote heat fluxes demonstrated a similar behavior to Furniture Experiment 1, with a peak in Room 202 close to 4 kW/m^2 and negligible peaks in the remaining two rooms on the second floor, as shown in Figure 4.41. The increase in temperature and heat flux

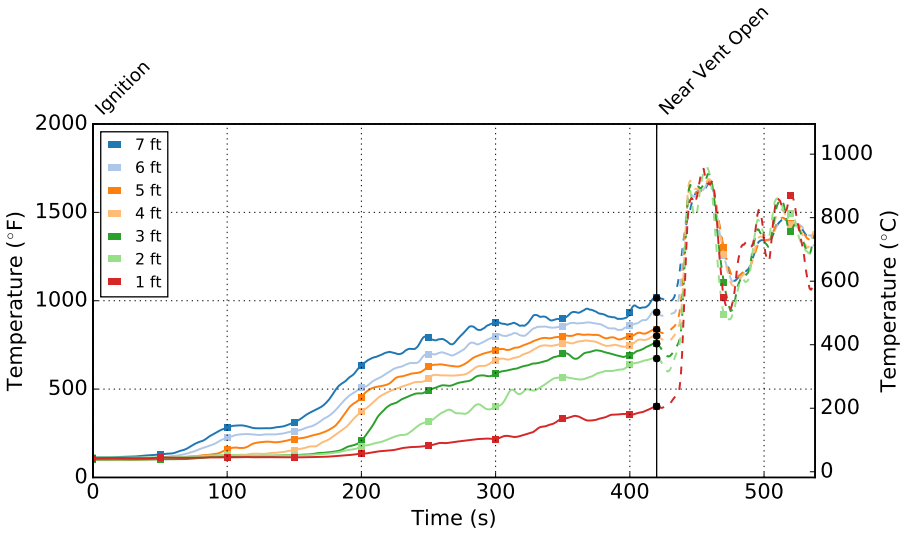

Figure 4.39: Fire room temperatures for Furniture Experiment 2. Pre-ventilation data is denoted by a solid line. Post-ventilation data is denoted by a dashed line of the same color as the corresponding solid line.

following ventilation was accompanied by oxygen concentrations close to 5% for both 6 ft. (1.8 m) sample points and the 2 ft. (0.6 m) sample point in the rear of the fire room. The 2 ft. (0.6 m) oxygen concentration remained higher, as shown in Figure 4.42, indicating that the primary source of oxygen for the fire was through the fire room doorway, similar to Furniture Experiment 1. This is corroborated by the fire room door velocities (Figure 4.43, which indicate that the bottom three BDPs in the array act as an intake prior to ventilation. After ventilation, there is a pressure spike in the fire room (Figure 4.44) just before 450 seconds after ignition. This pressure spike corresponds to a moment of unidirectional exhaust from the fire room.

The significant increase in temperature, heat flux, pressure and decrease in oxygen concentration following ventilation of the fire room window reflects a massive increase in combustion as a result of the additional entrained air. Despite the constant supply of oxygen to the fire room through the doorway, ventilation of the window allowed for additional fire growth, a phenomenon which was

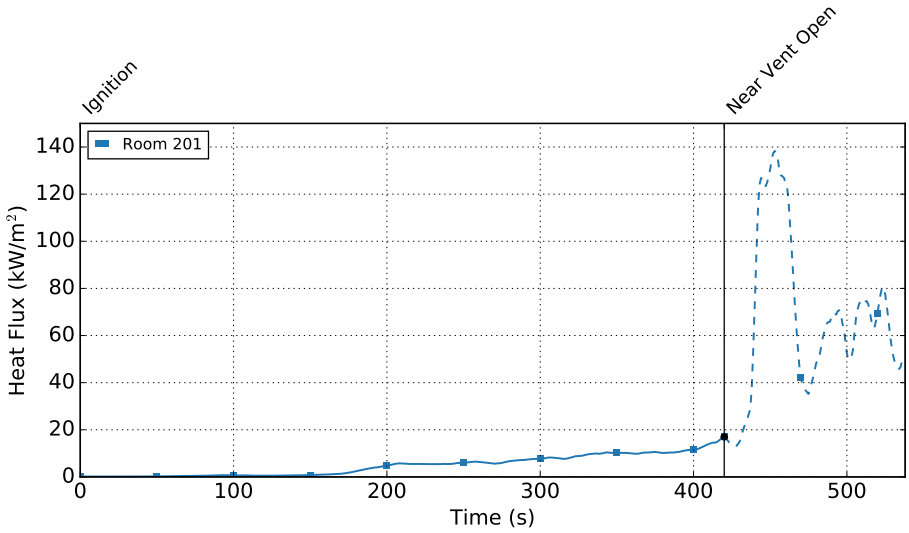

Figure 4.40: Fire room heat flux for Furniture Experiment 2. Pre-ventilation data is denoted by a solid line. Post-ventilation data is denoted by a dashed line of the same color as the corresponding solid line.

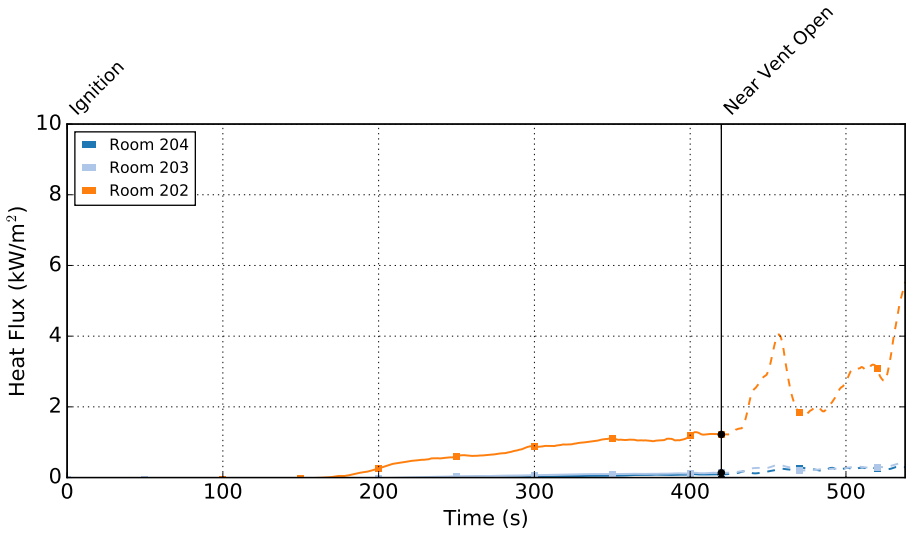

Figure 4.41: Remote heat fluxes for Furniture Experiment 2.

not noted in the training fuel experiments. Furthermore, the depletion in oxygen in the 2 ft. (0.6 m) oxygen concentration sample points indicate that the fuel rich smoke layer descended much lower to the floor than in the training fuel experiments, where the oxygen concentrations close to the floor remained close to ambient. All of this indicates that in Furniture Experiment 2, the fire was ventilation controlled.

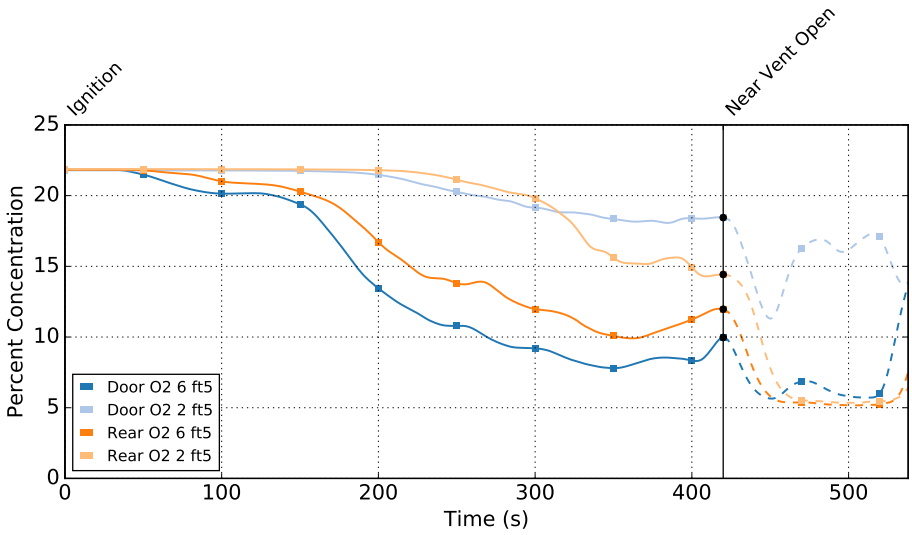

Figure 4.42: Fire room O_2 Concentration (%) for Furniture Experiment 2. Pre-ventilation data is denoted by a solid line. Post-ventilation data is denoted by a dashed line of the same color as the corresponding solid line.

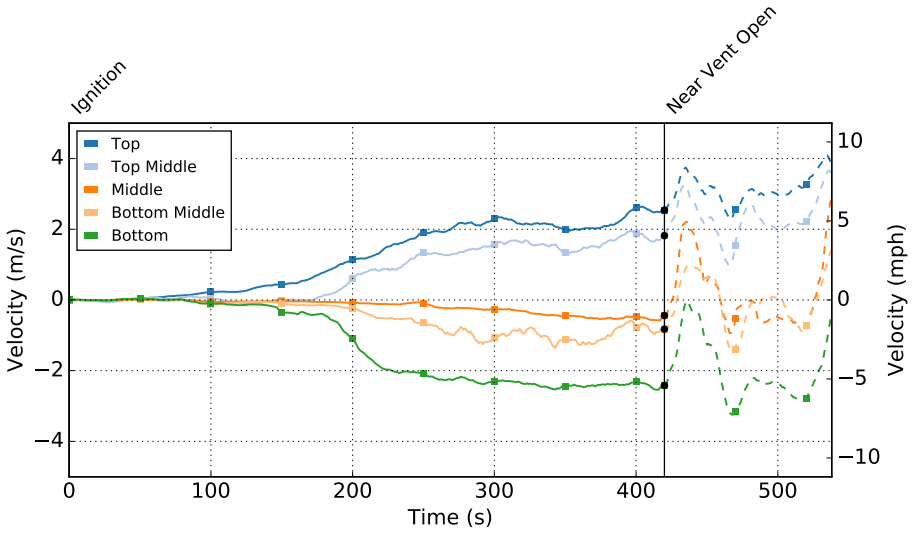

Figure 4.43: Fire room doorway velocities for Furniture Experiment 2. Pre-ventilation data is denoted by a solid line. Post-ventilation data is denoted by a dashed line of the same color as the corresponding solid line.

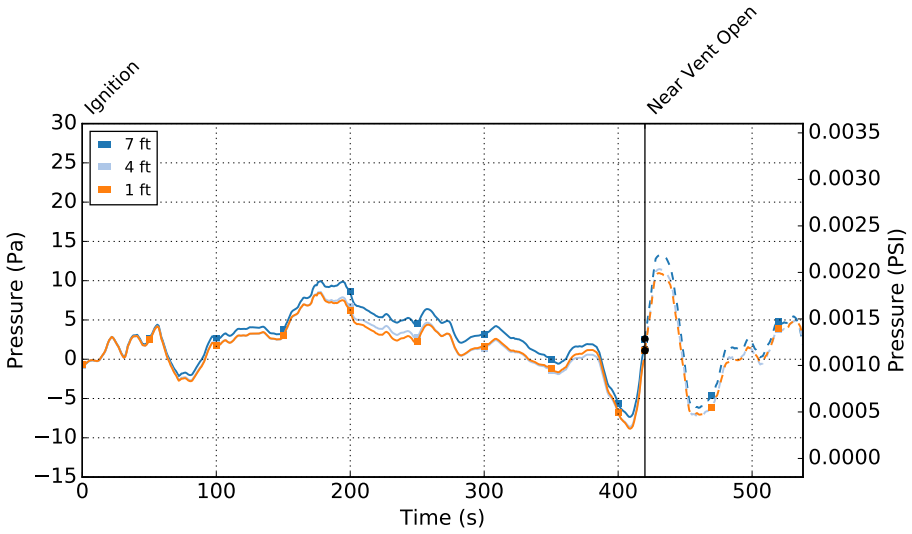

Figure 4.44: Fire room pressure for Furniture Experiment 2. Pre-ventilation data is denoted by a solid line. Post-ventilation data is denoted by a dashed line of the same color as the corresponding solid line.

4.3.3 Furniture Experiment 3 (Remote Vent)

Furniture Experiment 3 began with all exterior doors and windows closed prior to ignition. At 510 seconds after ignition, the front door and remote window in Room 204 window were opened, in an effort to create a flow path through the fire room. The growth of the fire in the pre-ventilation period was similar to the other two furnished room experiments, as shown in Figures 4.45 and 4.46. The most severe temperatures and heat fluxes measured in the fire room occurred after ventilation, at approximately 650 seconds. Fire room temperatures and heat flux did not peak immediately after ventilation, like in the near vent case in Furniture Experiment 2, but took approximately 140 seconds to reach a peak. Although the peak temperatures and heat fluxes were not observed until later in the experiment, once observed their severity was on the same order of magnitude as the other furnished room experiments, with fire room temperatures exceeding 1100°F (600°C) and heat fluxes exceeding 60 kW/m^2. Figure 4.47 shows that remote ventilation did not result in significant heat fluxes in Rooms 203 or 204, and the peak heat flux observed in Room 202 was of a similar magnitude to the peak in the other two furniture experiments.

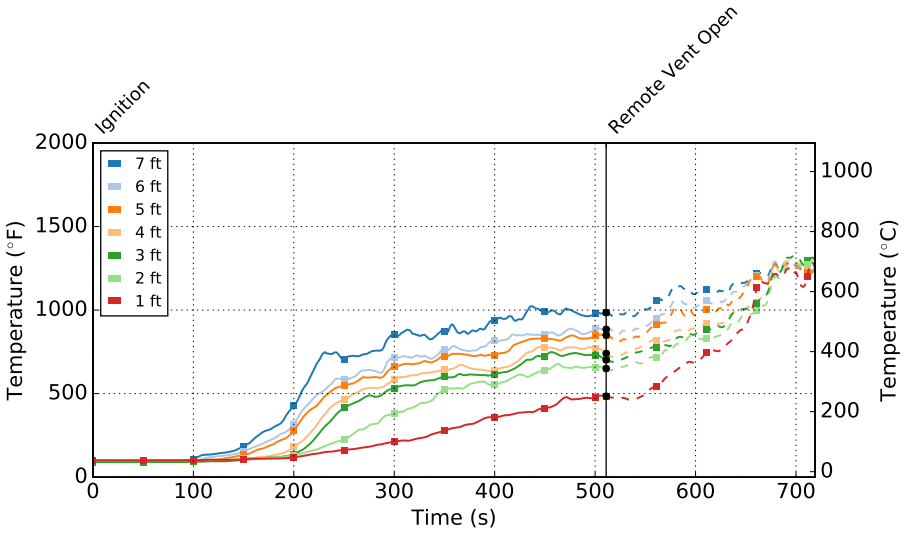

Figure 4.45: Fire room temperatures for Furniture Experiment 3. Pre-ventilation data is denoted by a solid line. Post-ventilation data is denoted by a dashed line of the same color as the corresponding solid line.

The 6 ft. (1.8 m) oxygen concentrations were the lowest in the fire room at the time of ventilation were close to 10%, while the 2 ft. (0.6 m) oxygen concentration in the rear of the room was higher, close to 15%, and the doorway oxygen concentration was the highest, just below 20%. The minimum oxygen concentrations observed corresponded with the peak thermal conditions, at which point all of the oxygen sample points except the 2 ft. (0.6 m) point in the doorway measured concentrations close to 5%, while the 2 ft. (0.6 m) oxygen concentration in the doorway was approximately 17%. Just as with the other two furniture experiments, the high oxygen concentration at the 2 ft. (0.6 m) level in the doorway indicates that the oxygen is being supplied to the fire through the doorway. The doorway velocities (Figure 4.49) show that a bi-directional flow was

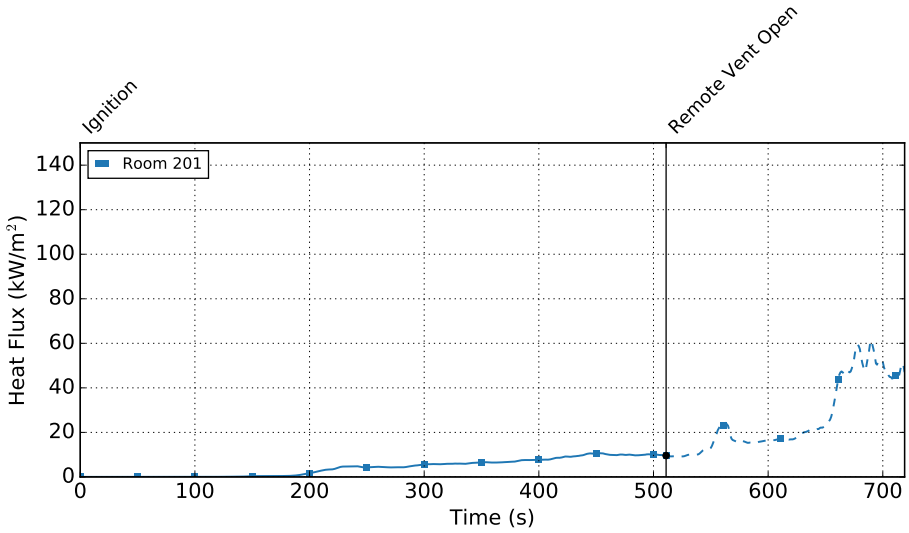

Figure 4.46: Fire room heat flux for Furniture Experiment 3. Pre-ventilation data is denoted by a solid line. Post-ventilation data is denoted by a dashed line of the same color as the corresponding solid line.

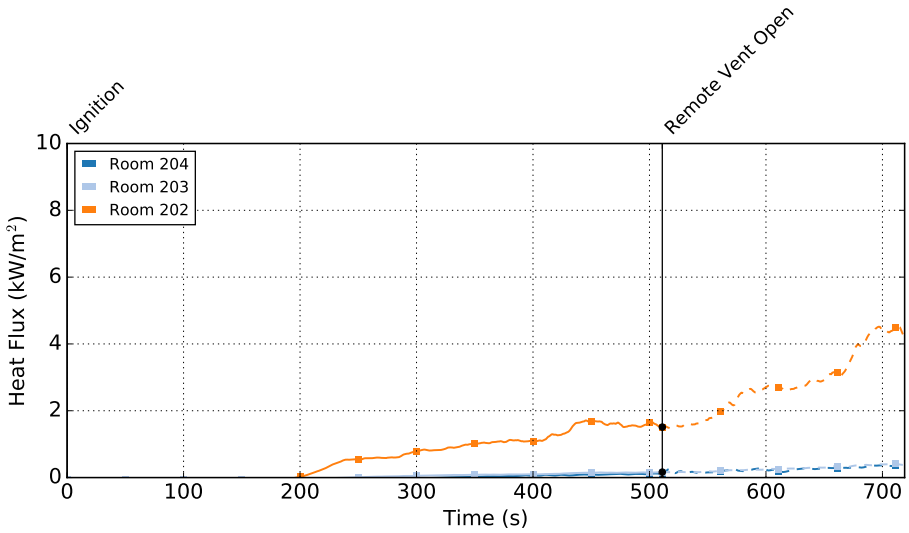

Figure 4.47: Remote heat fluxes for Furniture Experiment 3.

maintained through the doorway for the duration of the experiment. Following ventilation, there was no major change in the magnitude of the velocities into the fire room. This behavior is more similar to the no vent case in Furniture Experiment 1 than the near vent case in Furniture Experiment 2, where the increase in burning resulted in a pressure buildup, causing unidirectional flow out of the fire room. The fire room pressures, shown in Figure 4.50 did not indicate any significant pressure spikes during the experiment.

While the magnitude of the peak thermal conditions observed in the remote ventilation case were

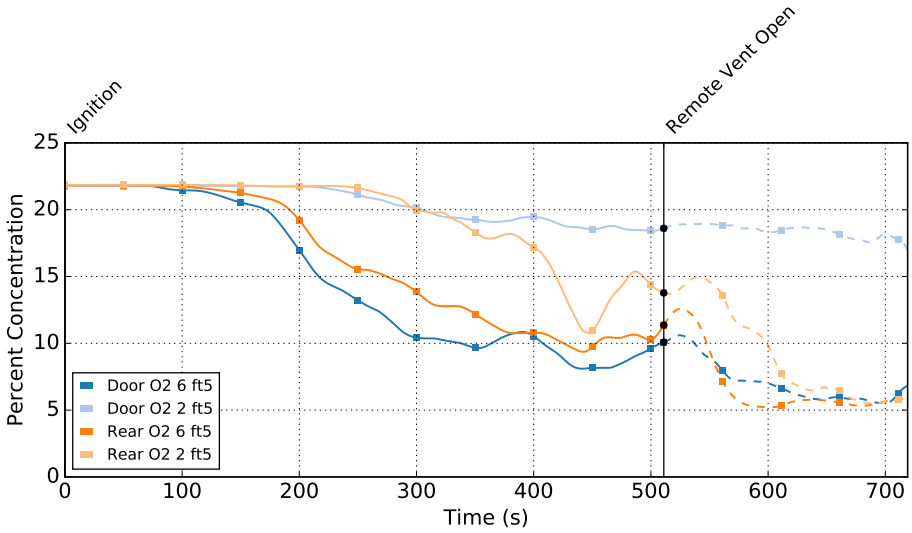

Figure 4.48: Fire room O_2 Concentration (%) for Furniture Experiment 3. Pre-ventilation data is denoted by a solid line. Post-ventilation data is denoted by a dashed line of the same color as the corresponding solid line.

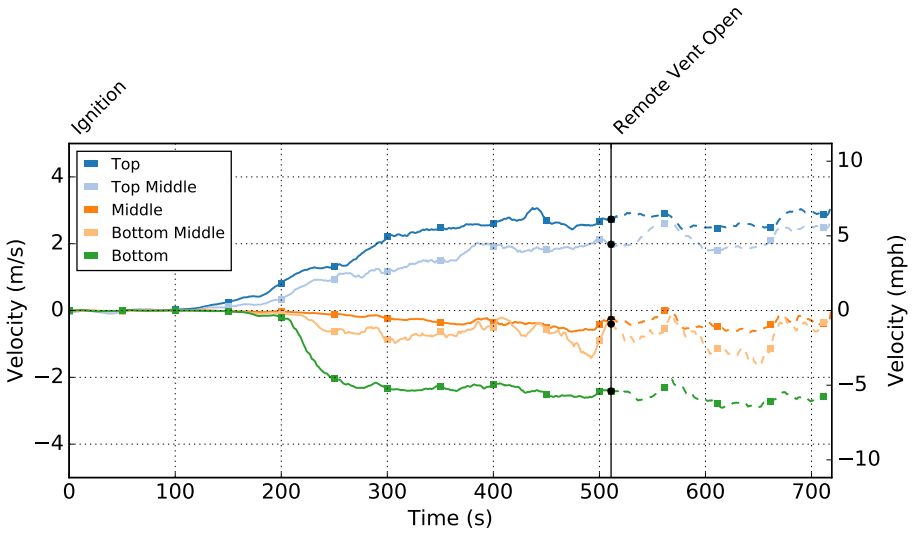

Figure 4.49: Fire room doorway velocities for Furniture Experiment 3. Pre-ventilation data is denoted by a solid line. Post-ventilation data is denoted by a dashed line of the same color as the corresponding solid line.

similar to those observed in the other two conditions, the peak occurred later in the test than when ventilation was close to the fire. One possible reason for this is the different flow paths that were established by the two ventilation configurations. In the near vent case, the flow path was very efficient because air could be entrained both through leakage into the structure and through the window directly into the fire room, while products of combustion could be exhausted both out the window and the top of the fire room doorway. In the remote ventilation case however, fresh air had

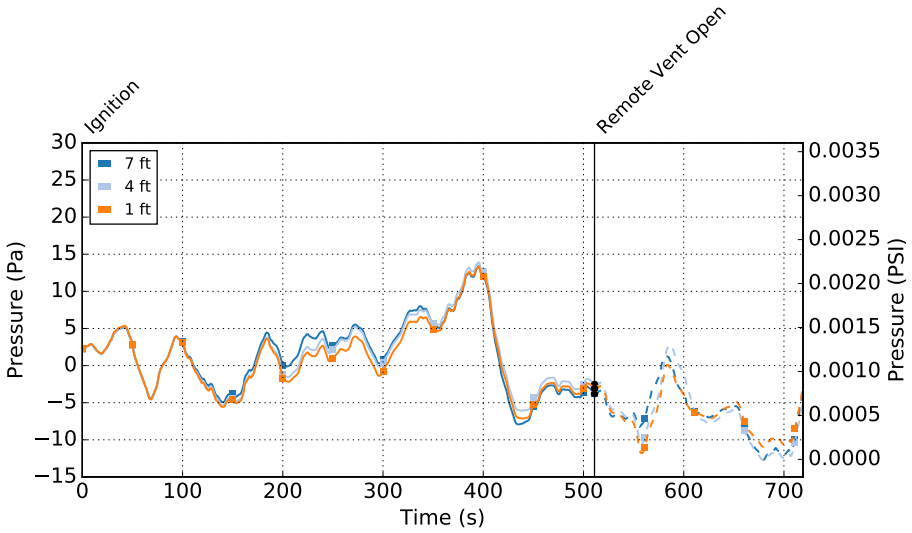

Figure 4.50: Fire room pressure for Furniture Experiment 3. Pre-ventilation data is denoted by a solid line. Post-ventilation data is denoted by a dashed line of the same color as the corresponding solid line.

to travel a longer distance to reach the fire room from the front door, and had the potential to mix with products of combustion along the way. Nevertheless, the additional air still resulted in fire growth, indicating that the furniture fires were ventilation controlled.

4.4 Gear Sample Packages

This section presents the results from the turnout gear samples placed in the doorway between Rooms 201 and 202 and in the corner of Room 202 next to the doorway. Tables 4.2 through 4.7 present the peak thermal conditions that were observed for each of the three fuel packages. The complete temperature-time profiles for each of the gear sample packages can be found in Appendix C.

Table 4.2 and 4.3 shows the peak over-gear and under-gear thermal conditions that were observed in the pallets and straw experiments. The most severe heat flux was measured by the horizontal, uncovered gauges for the near ventilation and no ventilation experiments, exhibiting fluxes of 3.7 and 3.5 kW/m^2, respectively. The maximum surface temperatures were noted during the remote ventilation experiment, where the exposed vertical temperature was 192°F (89°C) and the exposed horizontal temperature was 252°F (122°C). For the gear sample package isolated from the flow path, temperatures and heat fluxes were significantly reduced, with heat fluxes less than 1 kW/m^2 and temperatures less than 130°F (55°C) for all orientations.

The covered heat flux and temperature sensors experienced lower peak values than the unprotected results summarized in Table 4.2. In the doorway, heat flux values below 1 kW/m^2 and tempera-

Table 4.2: Peak Over-Gear Thermal Conditions for Gear Sample Packages in Pallets and Straw Experiments

Experiment	In Doorway			
	Heat Flux (kW/m^2)		Temperature °F (°C)	
	Side-facing	Top-facing	Side	Top
1 (No Vent)	3.5	1.7	169 (76)	138 (59)
2 (Near Vent)	3.7	1.5	185 (85)	154 (68)
3 (Remote Vent)	1.7	1.2	252 (122)	192 (89)
Experiment	**Out of Doorway**			
	Heat Flux (kW/m^2)		Temperature °F (°C)	
	Side-facing	Top-facing	Side	Top
1 (No Vent)	≤ 1	≤ 1	111 (44)	124 (51)
2 (Near Vent)	≤ 1	≤ 1	113 (45)	126 (52)
3 (Remote Vent)	≤ 1	≤ 1	106 (41)	129 (54)

tures between 131°F (55°C) and 154°F (68°C) were observed. These were higher than the peak temperatures and heat fluxes recorded out of the doorway, where heat fluxes were negligible, and temperatures ranged between 100°F and 104°F (38°C and 40°C.)

Table 4.3: Peak Under-Gear Thermal Conditions for Gear Sample Packages in Pallets and Straw Experiments

Experiment	In Doorway			
	Heat Flux (kW/m^2)		Temperature °F (°C)	
	Side-facing	Top-facing	Side	Top
1 (No Vent)	≤ 1	≤ 1	138 (59)	131 (55)
2 (Near Vent)	≤ 1	≤ 1	140 (60)	136 (58)
3 (Remote Vent)	≤ 1	≤ 1	154 (68)	136 (58)
Experiment	**Out of Doorway**			
	Heat Flux (kW/m^2)		Temperature °F (°C)	
	Side-facing	Top-facing	Side	Top
1 (No Vent)	-	≤ 1	100 (38)	102 (39)
2 (Near Vent)	-	≤ 1	102 (39)	104 (40)
3 (Remote Vent)	-	≤ 1	100 (38)	104 (40)

For the OSB experiments, the heat flux to the gear package in the doorway was more severe in the near ventilation experiment than in the remote ventilation case, while the surface temperatures

recorded in the remote ventilation case were greater than those noted in the near ventilation case. The peak heat fluxes from the near ventilation case were over twice the value of the peaks recorded in the pallets and straw experiments. Additionally, the most severe exterior surface temperatures recorded in the OSB tests were higher than those observed in the pallets and straw experiments. For the gear sample isolated from the doorway, heat fluxes and surface temperatures were less severe, with a peak of 1.7 kW/m^2 and surface temperatures between 115°F and 192°F (46°C and 89°C).

Table 4.4: Peak Over-Gear Thermal Conditions for Gear Sample Packages in OSB Experiments

Experiment	**In Doorway**			
	Heat Flux (kW/m^2)		**Temperature °F (°C)**	
	Side-facing	**Top-facing**	**Side**	**Top**
1 (Near Vent)	8.8	5.3	262 (128)	212 (100)
2 (Remote Vent)	2.3	3.1	291 (144)	239 (115)
Experiment	**Out of Doorway**			
	Heat Flux (kW/m^2)		**Temperature °F (°C)**	
	Side-facing	**Top-facing**	**Side**	**Top**
1 (Near Vent)	1.2	1.7	129 (54)	138 (59)
2 (Remote Vent)	≤ 1	1.2	115 (46)	192 (89)

The heat fluxes for the protected doorway turnout gear packages in the near ventilation case were higher than those observed in the remote ventilation case, although the interior surface temperatures were similar between the two cases. Similarly to the pallets and straw experiments, the gear sample packages isolated from the flow path exhibited considerably lower temperatures and heat fluxes compared to those in the doorway.

The most severe thermal insult to the gear sample packages was observed in the furnished room experiments. The most severe heat fluxes were noted in the near ventilation experiment, with peaks of 33.6 kW/m^2 and 21.2 kW/m^2 for the horizontal and vertical gauges, respectively. This is consistent with the severity of conditions noted in the fire room from Section 4.3. The heat fluxes in the remote ventilation and no ventilation experiments were not as high as the near ventilation case. The exterior surface temperatures noted for the gear sample packages within the doorway ranged between 396°F and 545°F (202°C and 285°C). For the out of doorway gear sample, the thermal conditions were also more severe than those observed in either the pallets and straw or the OSB experiments. The peak heat fluxes that were observed for this gear package ranged from 1.7 kW/m^2, observed in the remote ventilation case, to 4.3 kW/m^2, observed in the near ventilation case. The peak surface temperatures measured for this package ranged between 189°F and 243°F (87°C and 117°C).

The severity of the under-gear thermal conditions reflects those of the unprotected thermal conditions for the furnished rooms. For the doorway turnout gear samples, heat fluxes of 3.1 kW/m^2

Table 4.5: Peak Under-Gear Thermal Conditions for Gear Sample Packages in OSB Experiments

Experiment	In Doorway			
	Heat Flux (kW/m^2)		Temperature °F (°C)	
	Side-facing	Top-facing	Side	Top
1 (Near Vent)	1.7	1.1	178 (81)	176 (80)
2 (Remote Vent)	≤ 1	≤ 1	171 (77)	154 (68)
Experiment	**Out of Doorway**			
	Heat Flux (kW/m^2)		Temperature °F (°C)	
	Side-facing	Top-facing	Side	Top
1 (Near Vent)	-	≤ 1	108 (42)	113 (45)
2 (Remote Vent)	-	≤ 1	102 (39)	108 (42)

Table 4.6: Peak Over-Gear Thermal Conditions for Gear Sample Packages in Furnished Room Experiments

Experiment	In Doorway			
	Heat Flux (kW/m^2)		Temperature °F (°C)	
	Side-facing	Top-facing	Side	Top
1 (No Vent)	3.2	7.9	451 (233)	453 (234)
2 (Near Vent)	33.6	21.2	482 (250)	396 (202)
3 (Remote Vent)	6.8	9.0	545 (285)	455 (235)
Experiment	**Out of Doorway**			
	Heat Flux (kW/m^2)		Temperature °F (°C)	
	Side-facing	Top-facing	Side	Top
1 (No Vent)	2.0	3.3	208 (98)	243 (117)
2 (Near Vent)	3.8	4.2	189 (87)	237 (114)
3 (Remote Vent)	1.7	2.8	194 (90)	226 (108)

and 2.9 kW/m^2 were recorded in the near vent and no vent cases, respectively. Note that these are higher peaks than were recorded for any of the training fuels. Further, each of the furnished room experiments had interior surface temperatures in excess of 212°F (100°C). The heat fluxes noted in the gear sample package isolated from the flow path were higher than those observed for the training fuels as well, although these heat fluxes were still less than 1 kW/m^2. The interior surface temperatures for the turnout gear package out of the doorway ranged between 129°F and 160°F (54°C and 71°C).

Table 4.7: Peak Under-Gear Thermal Conditions for Gear Sample Packages in Furnished Room Experiments

Experiment	In Doorway			
	Heat Flux (kW/m^2)		Temperature °F (°C)	
	Side-facing	Top-facing	Horizontal	Top
1 (No Vent)	2.1	2.9	297 (147)	307 (153)
2 (Near Vent)	3.1	2.0	250 (121)	228 (109)
3 (Remote Vent)	≤ 1	1.9	273 (134)	164 (129)
Experiment	**Out of Doorway**			
	Heat Flux (kW/m^2)		Temperature °F (°C)	
	Side-facing	Top-facing	Side	Top
1 (No Vent)	-	≤ 1	151 (66)	160 (71)
2 (Near Vent)	-	≤ 1	129 (54)	142 (61)
3 (Remote Vent)	-	≤ 1	136 (58)	154 (68)

5 Discussion

This section uses the data presented in the Section 4 to compare the training fuel loads to the furniture fuel loads for the eight fire experiments.

5.1 Fidelity

5.1.1 Fire Growth

In Pallets Experiments 1 and 3, the temperatures and heat flux began to rise shortly after ignition, reaching peaks approximately 300 seconds following ignition. Pallets Experiment 2 grew at a slower rate, reaching a peak after 400 seconds. The different growth behavior observed in Pallets Experiment 2 is because the fire did not completely propagate through the straw in the center of the fuel set. Rather, it only burned on the side of the teepee away from the fire room wall. In the other two pallets experiments, the fire did propagate completely through to the wall of the fire room. This allowed the fuel package to burn uniformly, whereas in Pallets Experiment 2, the burning was concentrated to the side away from the wall until later in the experiment. This can be seen in Figure 5.1, which shows the IR view of the pallets and straw fuel package 60 seconds after ignition.

Figure 5.1: Comparison of IR view 60 seconds after ignition in fire room for Pallets Experiments 1 (left), 2 (center), and 3 (right). Note that in Pallets Experiment 2, the burning is concentrated on the side of the fuel package away from the wall, while the burning for the other two experiments is more uniform throughout the fuel package. This explains the slower growth rate observed in Pallets Experiment 2.

The difference in fire dynamics between Pallets Experiment 2 and the other two pallets and straw

experiments indicates that the rapid growth shortly after ignition that was observed in both the HRR experiments and the concrete live fire training building experiments for the pallets and straw fuel package is mostly due to the straw burning. If packed loosely, the high surface-to-mass ratio of the straw makes it easily ignitable, and allows the fire to spread through it rapidly. If the straw is packed too densely, not enough air can be entrained for combustion to occur. Although the straw is responsible for the rapid initial growth, the pallets are responsible for the majority of the energy released by the fire. Consider the average weights (m_{fuel}) of pallets and straw described in Section 3.1, which were 116.6 lbs. and 32.4 lbs. (52.9 kg and 14.7 kg), respectively. Since the pallets comprise 78% of the total weight of the fuel package, they also are responsible for the majority of the energy released. HRR experiments indicated that the effective heat of combustion (ΔH_c) of the pallets and straw fuel package is 13.9 MJ/kg. Equation 5.1 can be used to calculate the theoretical total energy release of the pallets and straw fuel package using the effective ΔH_c and the average total weight of the fuel package. This theoretical energy release is calculated as 0.94 GJ, quite close to the measured value of 0.95 GJ.

$$Q = \Delta H_c m_{fuel} \tag{5.1}$$

Fire growth following ignition in the OSB experiments was similar to the pallets and straw experiments, reaching peak values at a similar time. Although the peak temperatures and heat flux values were reached at approximately the same time as the pallets and straw experiments, the peak thermal conditions were higher than in the pallets and straw experiments. This is indicative of the higher HRR of the OSB fuel package. In the pallets and straw experiments, the straw was largely responsible for the rapid growth following ignition. In the OSB experiments, the early involvement of the vertically oriented OSB sheets results in a higher energy release early in the experiment, which explains the higher temperatures and heat fluxes observed in the fire room. The addition of the two OSB sheets results in a 67% higher average total fuel weight compared to the pallets and straw fuel package. HRR experiments indicated that, like the pallets and straw, the effective ΔH_c of the OSB package is 13.9 MJ/kg. Using this value and the average total weight of the OSB fuel package, a theoretical total energy release of 1.57 GJ is computed, which is relatively close to the measured value of 1.44 GJ from HRR testing. Thus, the higher peak thermal condition observed for the OSB training fuel package can be attributed to the additional fuel mass when compared to the pallets training fuel package.

The peak thermal conditions for the furniture fuel package occurred later in the experiment than in the training fuel packages. In Furniture Experiment 1, the no ventilation case, the peak was reached approximately 400 seconds after ignition. In the other two experiments, the peak thermal conditions were measured after ventilation, but the growth of the fires prior to ventilation was similar. Geometric differences between the furniture fuel package and the training fuel packages contribute to the later peak observed in the furniture experiments. In the furnished room, the fuel is located low in the room and is spread out, and surfaces are heated primarily from radiation, initially from the origin point of the fire and later from the thermal layer as it descends. This is when the period of most rapid growth is seen in the training fires. More important than the timing of fire growth in the furniture fires is the rate at which the fire grows.

The HRR characterization experiments indicated that the furniture fire grows 5 times faster than either of the training fuel packages. The reason for this increased rate of growth is synthetic materials, such as polyurethane and polystyrene, that make up the furniture. These materials have different combustion characteristics than wood-based material [32]. HRR characterization of the training fuel packages indicated that the effective ΔH_c of the pallets and OSB fuel packages was similar and within the range commonly cited for wood-based products. The heat of combustion of synthetic materials, however, are commonly higher than wood-based products. For example, the polyurethane foam found in the cushions of the couch and chair has a heat of combustion of 23.90 MJ/kg [32]. Recall from Section 3.2.1 that the peak free burn total energy release of the couch was between 570 and 600 MJ and the peak free burn total energy release of the barrel chair was between 180 and 190 MJ. Thus, the theoretical heat release of the 2 couches and 2 chairs alone is close to that of the OSB fuel package. This includes neither the carpet and carpet padding nor the wooden tables in the furniture fuel package. In addition to the higher-energy fuels within the furniture fuel package, the fuel load is significantly larger than either of the other two fuel loads, and this larger amount of fuel also helps contribute to the growth.

The differences between the training fuel packages and the furniture fuel package are significant because the ventilation-limited fires that firefighters respond to are characterized by growth which may occur more rapidly than the time firefighters need to recognize it. Indeed, there have been several line-of-duty deaths and injuries where failure to identify worsening conditions has been listed as a contributing factor. By design, the training fuel packages that firefighters use during their live fire training evolutions, such as pallets and straw and OSB, do not have the same potential for this rapid growth. The discrepancy between these training fuels, which quickly reach a steady state following the initial fire growth, and the plastic- and foam- based fuels commonly found on the fireground, which have the potential for rapid growth, leave an important gap in understanding in firefighters' knowledge of fire behavior.

5.1.2 Ventilation-Controlled Fires in Concrete Live Fire Training Buildings

Ventilation controlled fires are defined in NFPA 1403 as "fires in which the heat release rate or growth is controlled by the amount of air available to the fire" [12]. In other words, for a ventilation-controlled fire, additional air will cause an increase in the size of the fire. Since many structure fires that firefighters respond to are ventilation-limited fires, it is important that firefighters understand them, and how they might respond to intervention that they may perform.

In the pallets and straw experiments, 6 ft. oxygen concentrations remained at or above 10% and 2 ft. oxygen concentrations remained close to ambient for each of the three experiments, indicating that there were two distinct zones in the fire room: a smoke-filled hot upper layer and a cooler lower layer. A constant bi-directional flow was also maintained through the fire room door for the duration of the experiment, indicating that fresh air was entering the room through the lower half of the door while products of combustion were exhausted through the top portion of the door. Because the oxygen concentrations at the 2 ft. level were not depleted and the fire room was constantly being supplied with oxygen through the front door, the pallets and straw fires were not ventilation-

controlled. This is further evidenced by the growth in Pallets Experiments 1 and 3, which were similar, despite the opening of the remote window and front door in Pallets Experiment 3.

The oxygen concentrations in the fire room exhibited a similar behavior in the OSB experiments. The 6 ft. concentrations were slightly lower in the OSB experiments than in the pallets experiments, reaching a minimum value below 10%, but the 2 ft. oxygen concentrations remained above 20% for the duration of the experiment. The lower oxygen values at the 6 ft. level is indicative of an increased concentration of products of combustion at this elevation in the room, which was due to the larger amount of fuel in the OSB fuel package. In both of the OSB experiments, a bi-directional flow was maintained through the door for the pre-ventilation portion of the experiment. In OSB experiment 2, the remote vent case, there was no change in the slope of the temperature or heat flux graphs in the fire room following ventilation, indicating that the additional air provided by remote ventilation did not have a major effect on fire growth. In the near vent case in OSB Experiment 1, however, there was an increase in 7 ft. temperature from 1112°F to 1320°F (600°C to 715°C) and in fire room heat flux from 10.7 kW/m^2 to 19.3 kW/m^2. This increase in thermal conditions was accompanied by a decrease in the magnitude of the velocities in the lower part of the doorway and an increase in velocities in the upper part of the doorway, indicating a decrease in inlet and an increase in exhaust. Although two distinct layers were maintained in the fire room, as evidenced by the high oxygen concentrations close to the floor, ventilation of the fire room window, which resulted in additional air to be entrained into the fire room, resulted in fire growth. The reason for this additional growth may be the additional fuel mass in the package, which resulted in a more fuel-rich upper layer, or the wind that is suspected to have impacted the flow through the fire room following window ventilation.

The ambient oxygen concentrations at the 2 ft. level that were observed in the pallets and OSB experiments were not seen in the furniture experiments. In the furniture experiments, all of the gas sample points in the fire room with the exception of the 2 ft sensor in the doorway reached minimum oxygen concentrations of 5% or less. Despite the oxygen depletion at these sample locations, a bi-directional flow was maintained through the fire room door for the duration of the furniture experiments. Prior to ventilation, temperatures in the fire room ranged from 752°F to 1112°F (400°C to 600°C), with heat fluxes between 10 and 15 kW/m^2. After ventilation, conditions consistent with flashover were observed, with temperatures at all heights of the fire room in excess of 1112°F (600°C) and sustained heat fluxes in excess of 50 kW/m^2 at the floor of the fire room. Post-flashover conditions were also observed without any exterior doors or windows open in Furniture Experiment 1. The time offset between ventilation and flashover was longer in the remote ventilation case than in the near ventilation case, which is consistent with previous research in residential structures [6].

In all of the experiments, including those where no exterior doors or windows were opened, a bi-directional flow was maintained through the fire room door for the duration of the experiment. This constant flow is indicative of the large amount of leakage in the concrete live fire training building.

Leakage into the fire building is high because of built-in openings such as scuppers. While these built-in openings are small when compared to a window or door, the total area of these openings

sums becomes significant, as shown in Table 5.1. The total leakage area across the three floors of the building is 5.7 ft^2 (5300 cm^2), which would be equivalent to a small window. These openings allow the free flow of air into the structure, meaning that instead of a fixed amount of oxygen present in the building, as would be the case in a well-sealed residential structure [33], there is a constant source of fresh air for the fire to draw upon. In the concrete burn building experiments, this constant flow of air was confirmed by the bi-directional probes in the fire room doorway.

Table 5.1: Leakage Areas for Concrete Structure

Floor	**Leakage Area (in^2)**
1	145.5
2	404
3	272

The constant supply of air through leakage points affects the oxygen concentrations and fire dynamics in the fire room. In the furnished room experiments, the bulk of burning materials was in the center of the room, meaning that oxygen from the doorway was not able to reach in the rear of the room, which explains the low oxygen concentrations at those sample points for most of the duration of the experiment. On the other hand, the oxygen concentrations in the doorway were close to 15% during this period. This means that oxygen was being provided to the fire room at a high enough concentration to sustain burning in that area, which is the reason for the maintenance of high temperatures in the fire room. In the pallets and OSB experiments, the oxygen concentrations close to the floor remained close to ambient concentrations because the fire was not consuming as much oxygen, as was the case in the furnished room.

Built-in leakage points, such as the scuppers in the concrete burn building, are not a feature of the homes to which firefighters would be responding. In a residential home, minimizing the amount of air leakage between the house and the environment is desirable, as it makes the home the most efficient in terms of energy [33]. For the same reason, the amount of air that is able to be entrained into a home is quite small. Thus, in a building such as this, if no exterior ventilation openings are available for air exchange between the structure and the environment, the only oxygen that is available for the fire to burn is in the air that is in the structure prior to ignition.

The high leakage into the concrete live fire training building, combined with the comparatively low fuel load, prevents the pallets and straw training fuel package from becoming ventilation-controlled. The temperature and heat flux histories show that there was no growth following ventilation in Pallets Experiments 2 or 3. Furthermore, there was never a decrease in oxygen concentration at the 2 ft. level in the pallets and straw experiments, including the no vent experiment.

For the OSB experiments, growth was observed after ventilation for the near vent case (OSB Experiment 1), but not in the remote vent case (OSB Experiment 2). The difference between these

two experiments is the flow path that is established by ventilation. in the near ventilation case, the flow path is efficient, with air provided by the fire room window located close to the fuel package location supplemented by leakage air. Further, the flow data presented in Section 4.2.1 indicates that the wind had an impact on the flow through the window, allowing for the entrainment of additional air into the fire room. In the remote ventilation case, the flow path is not as efficient, because fresh air must travel from the front door to the fire room, and products of combustion must travel through three adjacent rooms to be exhausted through the window. The less efficient flow path in the remote ventilation case did not cause a significant growth in the fire following ventilation.

In contrast to both of the training fuel packages, the furniture fuel package is clearly ventilation-controlled, as evidenced by the depleted oxygen concentrations and growth to post-flashover conditions in Furniture Experiments 2 (near vent) and 3 (remote vent). The reason for the ventilation-controlled behavior observed in the furniture fuel package is the weight and composition of fuel in the furniture fuel package. In addition to having nearly 2 times more fuel by weight than the pallets fuel package and 1.25 times more fuel by weight than the OSB fuel package, the composition of the fuel in the fuel package is different. The majority of the weight of the pallets and OSB fuel packages is wood, while the couches and chair include polyurethane foam and other synthetic materials. These materials have a higher oxygen demand for combustion than wood. Table 5.2 lists the stoichiometric oxygen to fuel mass ratios (Ψ_O) for three wood products (pine, oak, and Douglas fir) and four types of flexible polyurethane foam, representative of the foam that would be found in the couches or chairs in the furnished room. On average, the polyurethane products require just less than twice as much oxygen for complete combustion than the wood products. This means that, for equal masses of fuel and a constant rate of air entrainment, combustion of polyurethane results in less efficient combustion.

Table 5.2: Coefficients for Stoichiometric Combustion of Fuels

Material	**Formula**	Ψ_O
Wood (pine)	$CH_{1.7}O_{0.83}$	1.21
Wood (oak)	$CH_{1.7}O_{0.72}N_{0.001}$	1.35
Wood (Douglas fir)	$CH_{1.7}O_{0.74}N_{0.002}$	1.32
GM21 PU Foam	$CH_{1.8}O_{0.30}N_{.05}$	2.24
GM23 PU Foam	$CH_{1.8}O_{0.35}N_{.06}$	2.11
GM25 PU Foam	$CH_{1.8}O_{0.32}N_{.07}$	2.16
GM27 PU Foam	$CH_{1.8}O_{0.30}N_{.08}$	2.21

These ratios in Table 5.2 can be used to estimate the amount of air required for stoichiometric combustion of the fuel packages used in these experiments. The Ψ_O values for pine can be used to approximate the wood products, such as pallets, straw, and the wooden furniture, and polyurethane can be used to represent the synthetic materials, such as the couches and chairs. Note that this method assumes that the couch and chairs are homogeneously made of polyurethane, which is not the case, since the couches have a wood frame. Since the exact weights of each component of the

furniture items is unknown; however, this assumption will suffice. Equation 5.2 shows how the product of the Ψ_O values in Table 5.2 and the weight of the fuel component give the total mass of oxygen that is required for stoichiometric combustion. Dividing this value by the density yields the volume of oxygen required, which can then be divided by the volume fraction of oxygen in ambient air to find the volume of air at STP that is required for stoichiometric combustion of the fuel package. Table 5.3 lists these results for the three fuel packages, assuming all wood is pine and all polyurethane foam is GM 25, which was chosen because of its intermediate value of Ψ_O.

$$V_{O_2,stoich} = \frac{m_{fuel}\Psi_O}{\rho_{O_2}} \tag{5.2}$$

$$V_{air,stoich} = V_{O_2,stoich}/\Phi_{air} \tag{5.3}$$

Table 5.3: Required Oxygen for Stoichiometric Combustion vs. Available Oxygen in Structure

Material	**Mass of Fuel (kg)**	**Vol. O_2 Required for Stoich. combustion (m^3)**	**Vol. Air Required for Stoich. Combustion (m^3)**
Pallets	67.6	61	292
OSB	113.4	103	491
Furniture	59.9 (wood) 80.6 (polyurethane)	183	868

The pallets and straw fire requires the least amount of oxygen for complete combustion to occur. The larger fuel mass in the OSB fuel package required a corresponding greater volume of oxygen for complete combustion. The furnished room required the most oxygen for complete combustion, roughly 2 times more than OSB and 3 times more than pallets. This large difference is a result of both the larger weight of fuel in the furnished room but also the increased amount of oxygen that is needed for these fuels to burn to completion.

Compare these figures to the volume of the concrete burn structure, which is approximately 537 m^3 (18964 ft^3). If the amount of oxygen present at the time of ignition inside of the structure is less than the amount that is required, the fire will become underventilated, and decay if no additional ventilation is provided. Previous research [5, 6] has emphasized that the high oxygen demand of the synthetic fuels and plastics that are increasingly found in residential structures can result in an initial decay phase due to a lack of ventilation. The growth of these ventilation-controlled fires, demonstrated by the curve on the right in Figure 5.2 is drastically different than the growth of a fuel-controlled fire, as shown on the left of Figure 5.2. This difference is important for firefighters to understand, as any additional ventilation that they provide to a ventilation-controlled fire can result in a rapid increase in fire growth.

Although the fire in each of the furniture experiments were ventilation-controlled, no ventilation-controlled decay consistent with the right curve in Figure 5.2 was observed. Even in the no vent case, the fire did not enter a state of ventilation-controlled decay, because of the constant supply

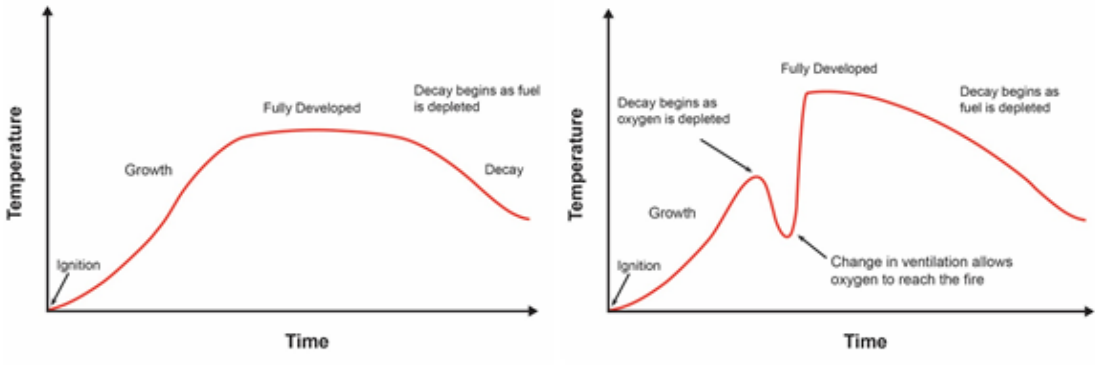

Figure 5.2: Idealized Fuel-Controlled Fire (left) vs. Idealized Ventilation-Controlled Fire (right)

of fresh air through the leakage points in the building. Thus, while the furniture fuel package was able to achieve a ventilation-controlled fire, it had a much higher oxygen demand and total fuel weight than the two training fuel packages, which were not able to achieve ventilation-controlled conditions. Although the furniture fires were ventilation-controlled, they did not have a stage of decay as a result of oxygen depletion. Previous studies conducted in residential structures [5, 6] have shown a distinct decay stage as a result of oxygen depletion. Thus, concrete live fire training buildings with large amounts of air leakage prevent them from being a useful tool for teaching ventilation-controlled fire behavior to firefighters.

5.1.3 Peak Thermal Conditions in Adjacent Rooms

The most severe thermal conditions in each of the experiments were observed in the fire room. As distance from the fire room increased, the peak heat fluxes and temperatures decreased. Table 5.4 summarizes the peak 3 ft. temperatures and heat fluxes that were measured in each room on the second floor of the concrete live fire training building.

The fire room thermal conditions were the least severe for the pallets experiments. The highest peak 3 ft. temperature and heat flux were 329°F (165°C) and 7.8 kW/m^2, respectively. Thermal conditions were more severe in the OSB experiments, particularly in the near vent scenario, where an increase in temperature and heat flux was observed following ventilation of the fire room window. The peak 3 ft. temperature and heat flux for the OSB fuel package were 581°F (305°C) and 19.3 kW/m^2, respectively. The furniture fuel package resulted in the most severe thermal conditions in the fire room. In the near vent and remote vent experiments (Furniture Exps. 2 and 3), peak temperatures and heat fluxes in the fire room were consistent with post-flashover fire conditions. In Furniture Experiment 1, the no vent scenario, the peak thermal conditions were similarly severe, but the rapid temperature growth associated with flashover was not noted. Rather, the fire in this experiment was consistent with a fully-developed, ventilation controlled fire.

The peak floor heat fluxes were substantially lower in the room adjacent to the fire room. The highest floor heat fluxes for each of the fuel packages were 1.0, 1.9, and 5.8 kW/m^{2}for the pallets, OSB, and furniture fuel packages, respectively. The peak 3 ft. temperatures were 167°F, 237°F, and

245°F (75°C, 114°C, and 245°C) for the pallets, OSB, and furniture fuel packages, respectively. The highest heat flux and 3 ft. temperature out of all the experiments were observed in Furniture Experiment 2, where post-flashover conditions were observed in the next room for an extended period. Thermal conditions in the remaining two rooms on the second floor were negligible in all eight experiments, with heat fluxes less than 1 kW/m^2 and 3 ft. temperatures less than 172°F (78°C).

Table 5.4: Peak Heat Temperatures and Heat Fluxes in Rooms on Second Floor of Concrete Live Fire Training Building

Experiment	Fire Room		Adjacent Room		2 Rooms Away		3 Rooms Away	
	3 ft. Temp °F (°C)	**Heat Flux kW/m^2**	**3 ft. Temp °F (°C)**	**Heat Flux kW/m^2**	**3 ft. Temp °F (°C)**	**Heat Flux kW/m^2**	**3 ft. Temp °F (°C)**	**Heat Flux kW/m^2**
Pallets Exp. 1 (No Vent)	327 (164)	7.7	167 (75)	≤ 1	104 (40)	≤ 1	102 (39)	≤ 1
Pallets Exp. 2 (Near Vent)	322 (161)	6.7	160 (71)	≤ 1	113 (45)	≤ 1	106 (41)	≤ 1
Pallets Exp. 3 (Remote Vent)	329 (165)	7.8	162 (72)	≤ 1	109 (43)	≤ 1	117 (47)	≤ 1
OSB Exp. 1 (Near Vent)	581 (305)	19.3	237 (114)	1.2	132 (56)	≤ 1	127 (53)	≤ 1
OSB Exp. 2 (Remote Vent)	513 (267)	13.4	316 (158)	1.9	93 (34)	≤ 1	90 (32)	≤ 1
Furniture Exp. 1 (No Vent)	1116 (602)	80.2	351 (177)	4.7	129 (54)	≤ 1	126 (52)	≤ 1
Furniture Exp. 2 (Near Vent)	1751 (955)	150.2	473 (245)	5.8	172 (78)	≤ 1	142 (61)	≤ 1
Furniture Exp. 3 (Remote Vent)	1339 (726)	69.3	327 (164)	4.7	154 (68)	≤ 1	135 (57)	≤ 1

5.2 Safety

Utech's thermal operating classes were used to quantify the severity of the thermal conditions present in the training fires and the furniture fires. In order to quantify the most serious conditions that were present in each experiment, the peak temperature at the 3 ft. (0.9 m) level and the heat flux value at 8 in. (0.2 m) that was recorded at the same time as this peak temperature were used to classify the thermal hazard according to Utech's method. The vertical and horizontal error bars in Figures 5.3-5.12 represent the measurement uncertainty of the heat flux or temperature measurements.

5.2.1 Thermal Exposure to Firefighters

Figure 5.3 shows where the peak values listed in Table 5.4 for each of the furniture, OSB, and pallets and straw experiments fell on Utech's chart. The highest heat fluxes and 3 ft. (0.9 m) temperatures were observed in the furniture experiments, which were in excess of 1112°F (600°C) and 60 kW/m^2. The lowest peak heat flux and 3 ft. (0.9 m) temperatures were observed in the pallets experiments, which were less than 330°F (165°C) and 8 kW/m^2. The OSB experiments had peaks fire room thermal conditions between the furniture and the pallets fuel packages, with 3 ft. (0.9 m) temperatures between 513°F and 581°F (267°C and 305°C) and the fire room heat flux is between 13 kW/m^2 and 19 kW/m^2.

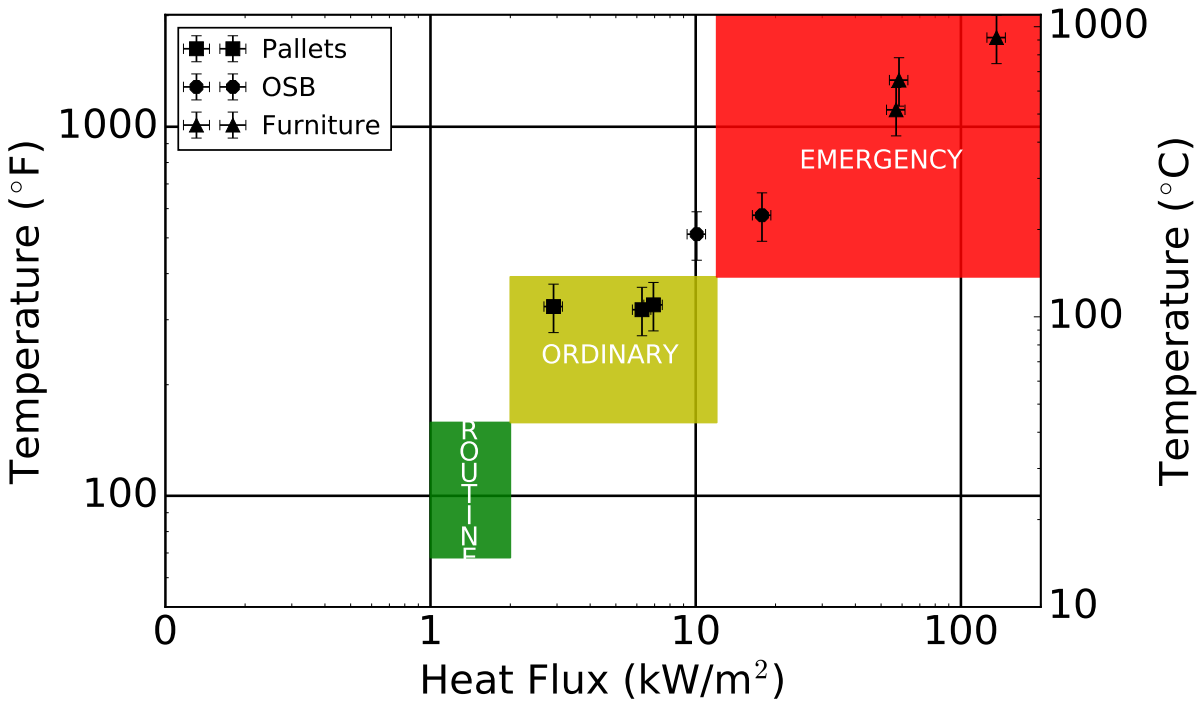

Figure 5.3: Thermal Operating Conditions in Fire Room (Room 201)

The increase in fuel weight from the pallets and straw fuel package to the OSB fuel package resulted in a corresponding increase in the severity of the peak thermal conditions. The peak thermal conditions in the pallets and straw fuel packages were consistent with Utech's definition of ordinary operating conditions, whereas the peak thermal conditions observed during the OSB experiments exceeded the criteria for ordinary operating conditions. Like the furniture experiments, the most severe conditions in the OSB experiments were consistent with the criteria for emergency operating conditions. In the OSB and furniture fuel package experiments, the high heat flux and temperatures would likely make the fire room untenable for firefighters in full PPE after a short period of time, whereas in the pallets experiments, a firefighter in full PPE would likely be able to operate for a longer period of time before risking injury. Thus, if the objectives of a particular training evolution include being able to operate in the fire room without an immediate risk of injury, instructors should take care to limit the fuel load.

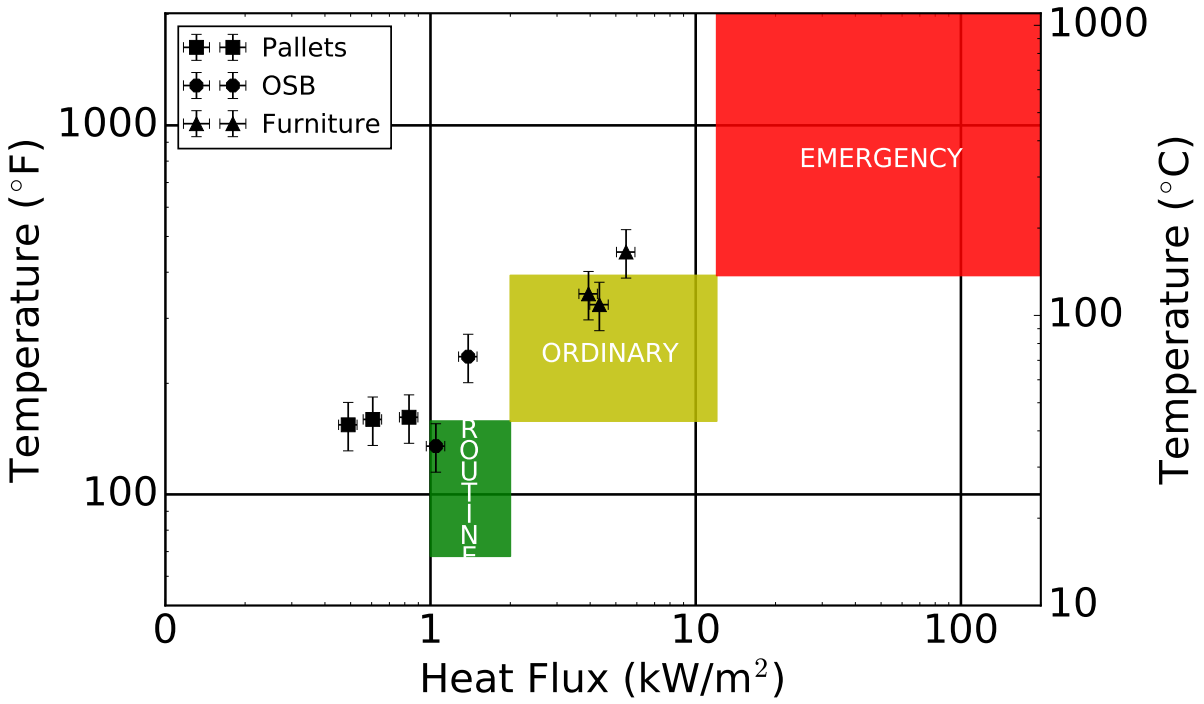

Figure 5.4: Thermal Operating Conditions in Room 202

As the distance from the fire room increases, the peak heat flux and 3 ft. (0.9 m) temperatures decreases. Figure 5.4 shows the thermal operating class that the peak temperature and the heat flux recorded at this time fall into for each experiment. Like in the fire room, the furniture experiments had the highest peak heat flux and temperatures recorded in the adjacent room, with peak heat fluxes greater than 4.7 kW/m^2 and peak 3 ft. (0.9 m) temperatures greater than 327°F (164°C). The peak conditions in the training fuels were considerably lower, with heat fluxes less than 1 kW/m^2 and 3 ft. (0.9 m) temperatures less than 167°F (75°C). The addition of OSB resulted in a significantly higher 3 ft. (0.9 m) temperatures, between 240°F and 315°F (115°C and 158°C), but only a slight increase in floor heat flux, with peak values between 1 kW/m^2 and 2 kW/m^2.

When comparing these peak values to their location according to Utech's chart, it is evident that the heat flux and temperature do not always fall into the same operating class. In particular, for the training fuels, the floor heat flux values were quite low, even when the local temperature corresponded to ordinary operating conditions. One possible explanation for these low peak heat flux measurements is that fresh air flowing across the remote gauges to the fire room cools the gauge, affecting the measurement. Another possibility is the high ceilings and thick walls removing energy from the gases traveling from the fire room, decreasing the temperature of the layer and, subsequently, the radiation. In Rooms 203 and 204, the peak heat fluxes were less than 1 kW/m^2, even with flashover conditions present a few rooms away. Figure 5.5 shows that the peak thermal conditions two and three rooms away from the fire room met the criteria for Utech's routine operating conditions for all three fuel packages considered.

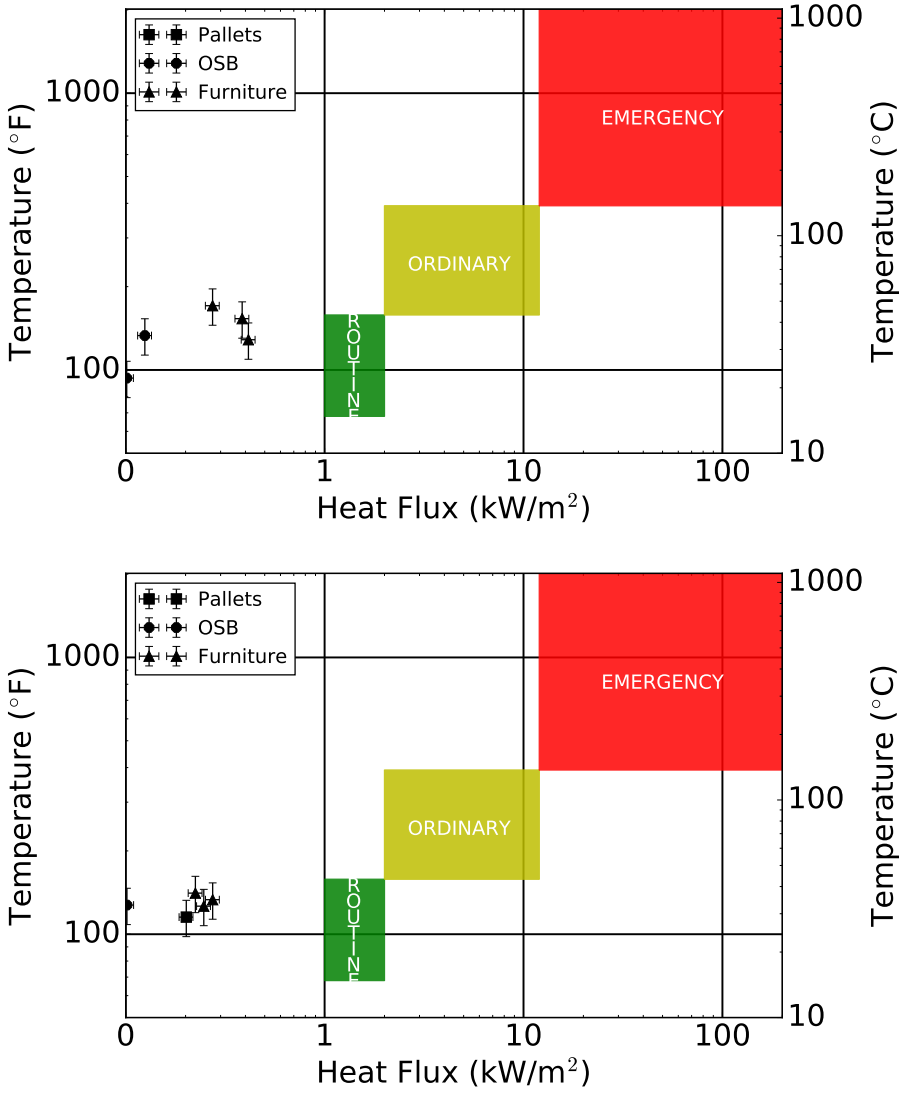

Figure 5.5: Thermal Operating Conditions Rooms 203 (top) and 204 (bottom)

In all eight experiments, a bi-directional flow was maintained through the door between Rooms

201 and 202 for the duration of all of the training fire experiments. Comparing the turnout gear packages placed in the doorway and out of the flow path, next to the doorway emphasizes the additional thermal insult that occurs to a target within the flow path. Figures 5.6 through 5.8 show where the horizontal and vertical peak heat flux and temperature measurement for the samples placed in and out of the flow path.

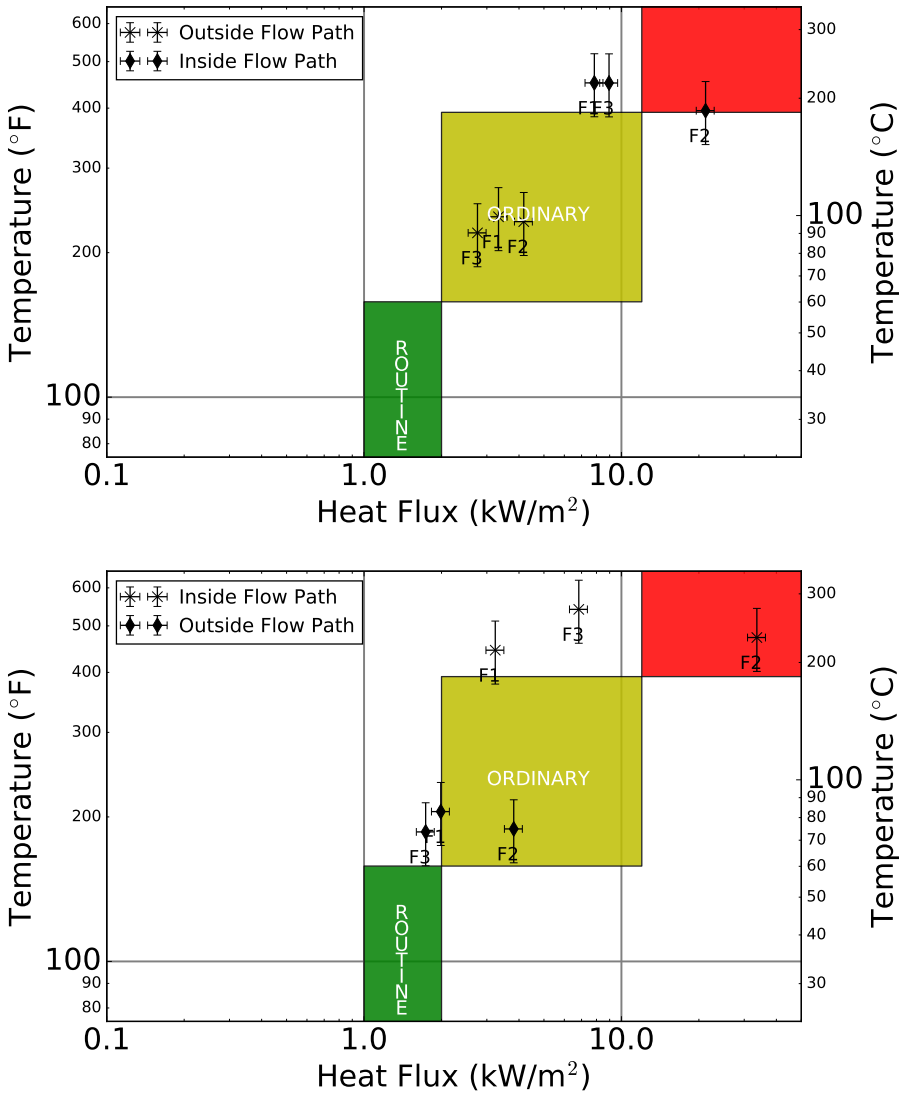

Figure 5.6: Comparison of Turnout Gear Samples In vs. Out of the Flow Path for Furniture at Vertical (top) and Horizontal (bottom) Orientations

The high-temperature gases escaping the fire room in the furniture experiments, and in particular the near vent case, resulted in the largest difference between turnout gear sample exposures in and out of the flow path. Figure 5.6 shows that different exposures were noted for the horizontal and vertical orientations in the flow path, but in both cases, the near ventilation case exhibited the peak exposures which were consistent with thermal conditions in the doorway of a flashed over room, and were within the emergency operating zone. In the other two furnished room experiments,

peak conditions were observed which met the heat flux criteria for ordinary operating conditions but met the temperature criteria for emergency operating conditions. For the turnout gear package isolated from the flow path, the thermal conditions were notably less severe. The vertical heat flux and temperature indicated a thermal operating class well within the ordinary operating class, with heat fluxes less than 5 kW/m^2 and temperatures below 248°F (120°C). For the horizontal heat flux gauge and surface thermocouple, the temperatures met the criteria for ordinary operating conditions, but only the near ventilation experiment met the heat flux criteria for the ordinary class. The other two experiments had heat fluxes less than 2 kW/m^2.

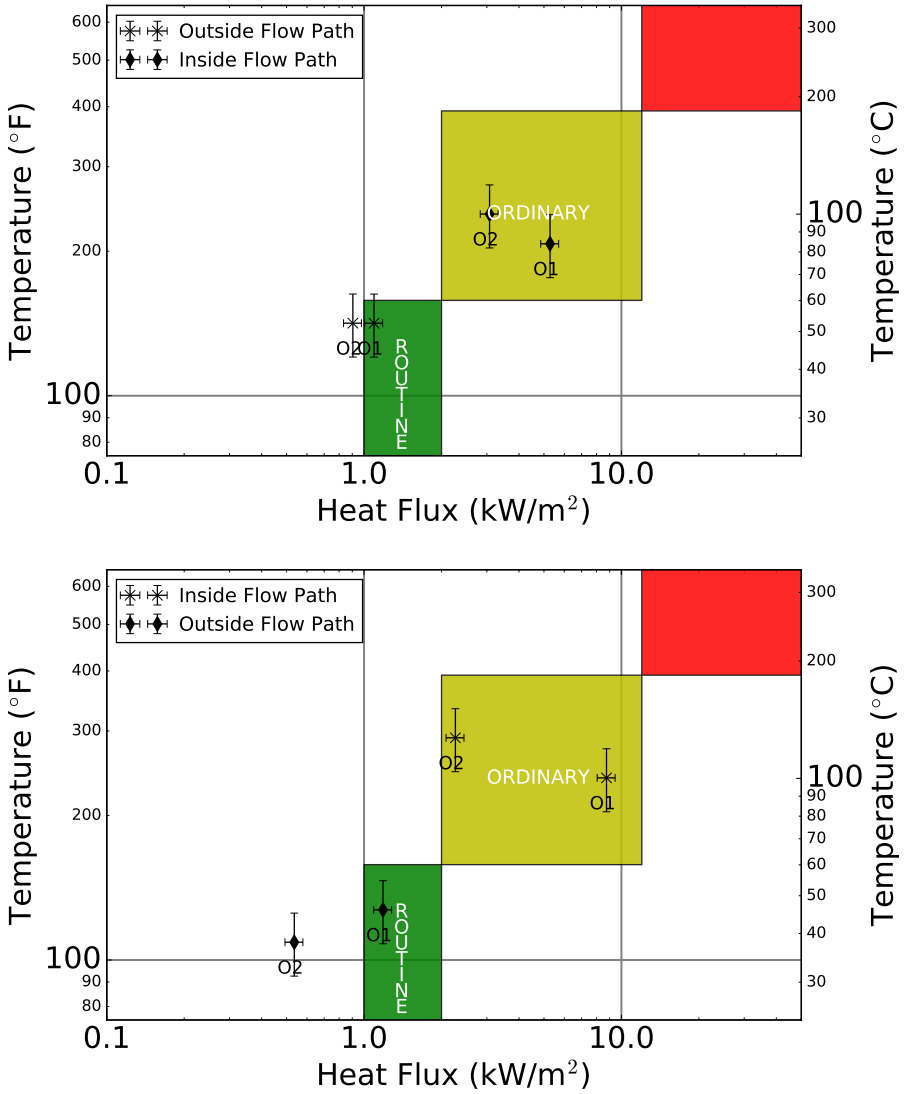

Figure 5.7: Comparison of Turnout Gear Samples In vs. Out of the Flow Path for OSB at Vertical (top) and Horizontal (bottom) Orientations

A similar reduction in severity was seen in the experiments where OSB was the fuel, as shown in Figure 5.7. The gear samples placed in the doorway experienced peak thermal exposures consistent with ordinary operating conditions. The samples isolated from the flow path, on the other

hand, exhibited heat fluxes that were 1.0 kW/m^2 or less, and temperatures that were within routine operating conditions. Inspection of the figure indicates that the horizontally-facing heat flux gauge and thermocouple recorded more severe conditions than the corresponding vertical gauge. This indicates that the direct radiative heat transfer from the fuel package is the predominant form of heat transfer to the target.

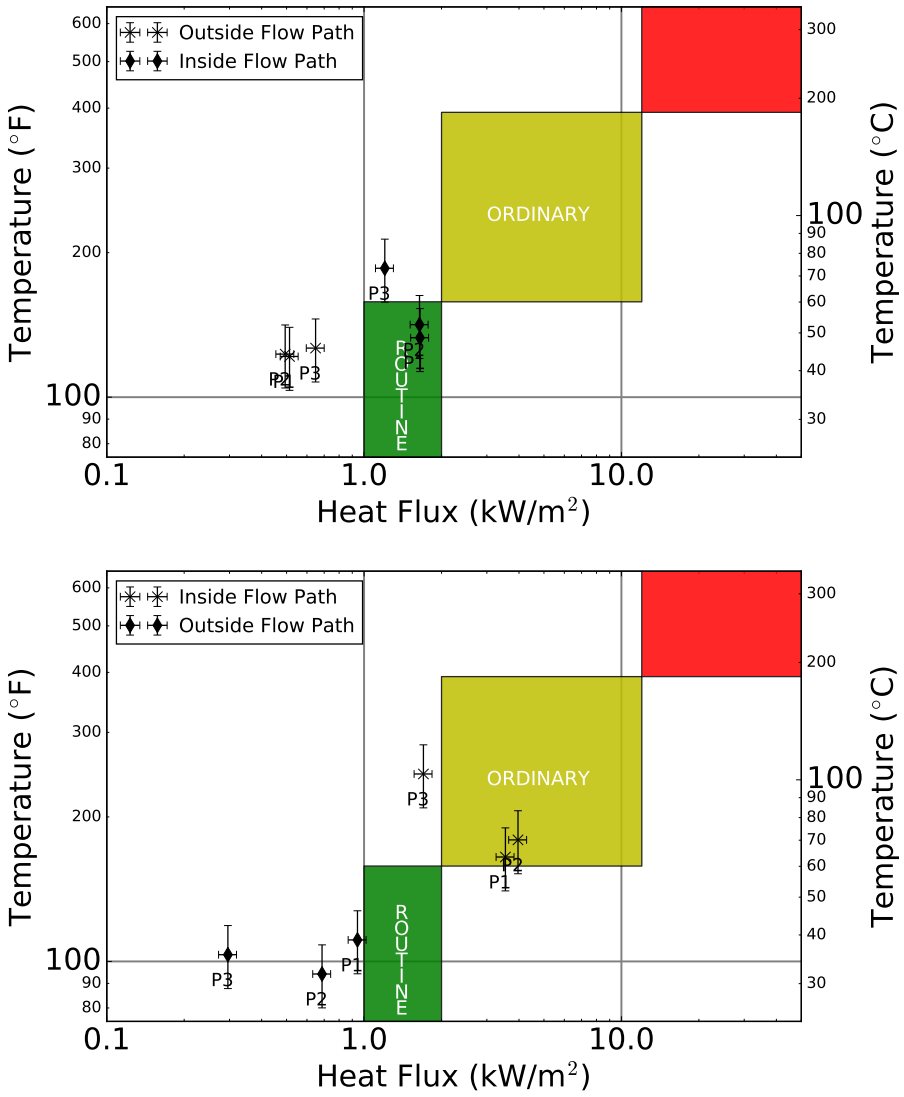

Figure 5.8: Comparison of Turnout Gear Samples In vs. Out of the Flow Path for Pallets and Straw at Vertical (top) and Horizontal (bottom) Orientations

The least severe thermal insult was observed with the turnout gear samples in the pallets and straw experiments. Figure 5.8 shows the thermal operating conditions corresponding to the peak exposures for the vertical and horizontal orientations in and out of the flow path. For the vertically oriented heat flux gauge and thermocouple in the doorway, the near ventilation and no ventilation experiments fell into the routine thermal operating class, while the remote ventilation case met the heat flux criteria for the routine class, but the temperature criteria for the ordinary operating

class. The horizontal orientation had a more severe thermal exposure, with the near vent and no vent cases falling into the ordinary operating class, and the remote ventilation experiment meeting the temperature criteria for the ordinary operating class, but the heat flux criteria for the routine class. As was the case in the OSB experiments, this larger horizontal exposure is likely a result of the direct radiant exposure to the burning fuel package, which the gear samples which are isolated from the flow path do not experience. In the pallets and straw experiments, the isolated samples all fell within the routine operating zone.

For each of the three fuel types, a firefighter positioned in the doorway of the fire room experiences a more severe thermal exposure than if the same firefighter had been positioned a short distance away, out of the flow path. This increase in severity can be attributed to the higher convective heat transfer, from the transport of hot gases from the fire room, and to higher radiant heat transfer from the gas layer and from the fuel package itself. The convective heat flux to a target is expressed by Equation 5.4, where $\dot{q}''_c$ is the convective heat flux, T_s is the surface temperature of the target, T_∞ is the environmental temperature, and h_c is the convective heat transfer coefficient. This heat transfer coefficient is dependent on flow conditions, and can vary considerably with height. Tanaka and Yamana [34] conducted a series of small-scale experiments in an effort to characterize convective heat transfer in fires. Among their findings was that h_c increases as the heat release rate of the fire increases and as the compartment size decreases. This trend, in addition to the higher temperatures close to the turnout gear packages in the doorway, is indicative of higher convective heat transfer rates in the OSB and furniture fuel packages, where higher heat release rates were noted, as discussed in Section 3.2.2. The effect of the increased thermal conditions due to convective heat transfer within the flow path was not as pronounced in the pallets and straw experiments as in the OSB and furnished room tests. Numerous firefighter fatality investigations [35, 36] have identified convection from high velocity, high temperature flows as a significant factor in firefighter line of duty deaths.

$$\dot{q}''_c = h_c(T_s - T_\infty) \tag{5.4}$$

In each of the experiments, radiation to the target occurs from the hot upper gas layer. The magnitude of this heat transfer is a function of the gas layer temperature. Radiation also occurs from the burning fuel package itself, and the severity of this radiation can vary depending on the density of the smoke between the fuel package and the target. As the smoke becomes more optically dense, the less efficient the radiative heat transfer to the target. In the pallets and straw and OSB experiments, obscuration of the fuel package was not as severe as was noted in the furnished room experiments. Consider Figures 5.7 and 5.8, where in several cases, the horizontal heat flux in the doorway was higher than the vertical heat flux. This would indicate that a firefighter in the doorway experiences a more severe radiative exposure from the flaming gases near the fuel package rather than from the hot gas layer above the firefighter.

Using Utech's definition as a method of assessing the thermal insult to firefighters indicates that as the fuel load increases, the severity of thermal conditions within the fire room also increases. For the furniture and OSB experiments, the peak thermal conditions threaten the limits of firefighter PPE [20, 21] and have the potential to cause thermal injury to firefighters exposed for short dura-

tions. The peak fire room thermal conditions in the pallets and straw experiments would have been tolerable for longer periods of time without risking thermal injury. As distance from the fire room increases, the severity of thermal conditions at firefighter operating height decreases. Conditions in rooms remote from the fire room were within the routine operating zone, even when post-flashover conditions were observed in the fire room. This is significant because instructors in remote parts of the building may not fully appreciate the severity of the thermal conditions that their students are advancing towards.

Similarly, there is a significant difference between the thermal exposures in and out of the flow path. Because of the inherent leakage within the concrete burn building, there is always a flow path through the fire room door. The combination of convective heat transfer to the firefighter from gases flowing from the fire room and the direct radiant transfer from the fuel package results in a greater amount of heat transfered to a firefighter situated in the doorway compared to one residing out of the doorway. Thus, if an instructor or safety officer spends an excessive amount of time close to the fire room or situated in the flow path or in the direct view of the fuel package, their gear will become saturated with heat more quickly than if they were in a remote area of the burn building, or if they were isolated from the flow path. So, while it is possible to create conditions in the fire room consistent with post-flashover conditions in a residential house, the severity of these conditions decreases in rooms immediately adjacent to the fire room, due to the heat loss to the high ceilings and concrete walls.

5.2.2 Duration of Thermal Exposures

One important element that is missing from the thermal operating classes proposed by Utech is the time component. The peak temperatures in Figures 5.3-5.5 offer a mere snapshot in time of the thermal conditions to which instructors and students would be exposed. Consider Figure 5.9, which shows the heat flux and temperature data plotted at the time of ventilation, and at intervals of 30s, 60s, 90s, and 120s. The grouping for the pallets and straw experiments is concentrated in this region over the time interval, indicating that the pallets and straw fire remains stagnant in the ordinary region in the two minutes following ventilation. In the furnished room, the thermal conditions within the fire room are already in the emergency operating range at the time of ventilation, although the severity of conditions increases following ventilation, remaining in the emergency operating zone for the two minute period. In the OSB experiment, the ordinary conditions were in the ordinary operating range at the time of ventilation. Over the next two minutes, the severity of these conditions increase into the emergency operating range.

A similar trend can be seen in the remote ventilation experiments, as seen in Figure 5.10. Just as in the near ventilation case, the pallets and straw experiments maintain a tight grouping for the 150 seconds following ventilation. At the time of ventilation, the conditions in the furnished room met the heat flux criteria for the ordinary operating range and the temperature criteria for the emergency operating range. After the first 60 seconds, the temperature crossed into the emergency operating range. The OSB exhibited a similar trend, starting in the ordinary operating class at the time of ventilation, before increasing into the emergency operating class until the heat flux

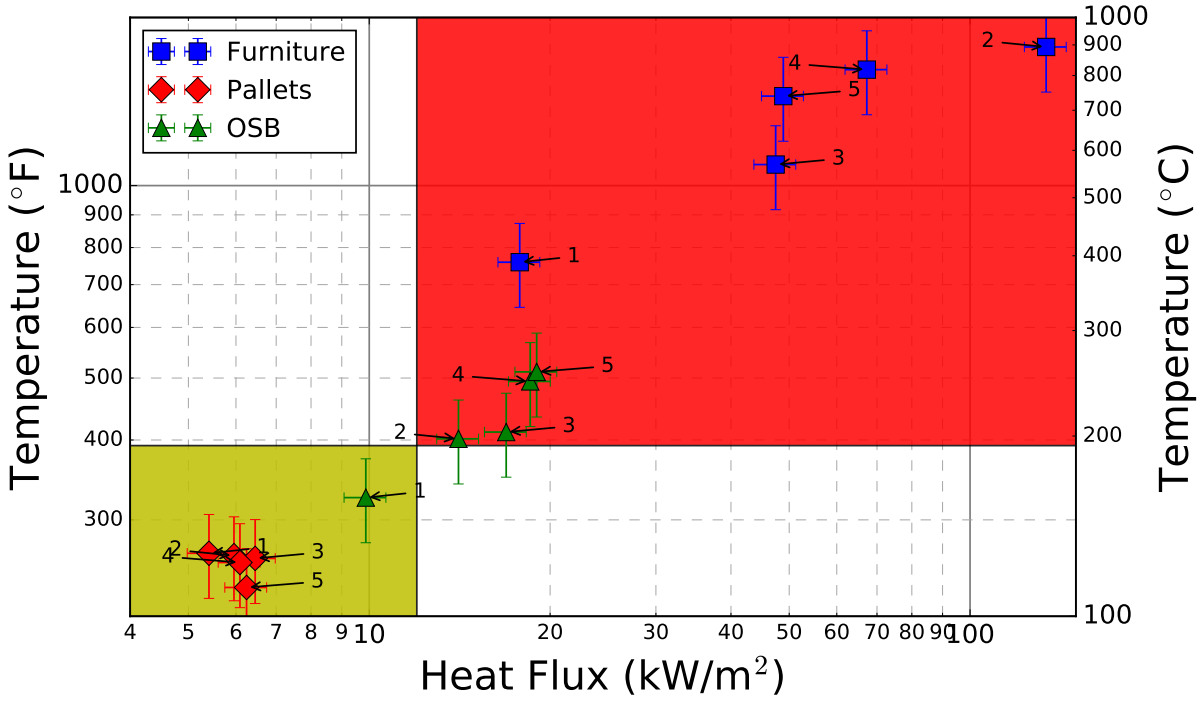

Figure 5.9: Ventilation response of fire for near vent experiments. Points are labeled 1, 2, 3, 4, and 5, corresponding to the temperature and heat flux at 0 s, 30 s, 60 s,90 s, and 120 s after ventilation, respectively. The yellow and red portions of the chart indicate the ordinary and emergency operating zones, respectively.

began to decrease, bringing the thermal conditions into the area where the temperature exceeds ordinary operating conditions, but the heat flux meets these criteria. Note also that while the OSB thermal conditions do increase, they increase at a more consistent rate than was noted in the near ventilation scenario. This further illustrates the difference between the near ventilation experiment and the remote ventilation experiment for the OSB.

Figures 5.9 and 5.10 demonstrate the importance of the time component of evaluating the thermal response to firefighters, and highlight the differences in ventilation between the three fuel packages. The pallets and straw thermal conditions are steady following ventilation, so students or instructors would feel little change from the action. An increase in the severity of thermal conditions was noted in the OSB experiments, but this change was more gradual than the rapid change that was observed in the furnished rooms. Consider the near ventilation case. If OSB was used as a fuel, students and instructors would be exposed to a gradual increase in conditions from roughly 320°F (160°C) and 10 kW/m^2 at the time of ventilation to 510°F (265°C) and 19 kW/m^2 after two minutes. In the furnished room, thermal conditions increased from 758°F (403°C) and 17 kW/m^2 at the time of ventilation to 1650°F (900°C) and 130 kW/m^2 after only 30 seconds. The increase in conditions in the furnished room is larger in magnitude and occurs over a shorter span of time, meaning that firefighters would have less time to react to the worsening conditions. The experiments conducted by Mensch et al. [22] indicated that the time to SCBA facepiece failure is dependent on the severity

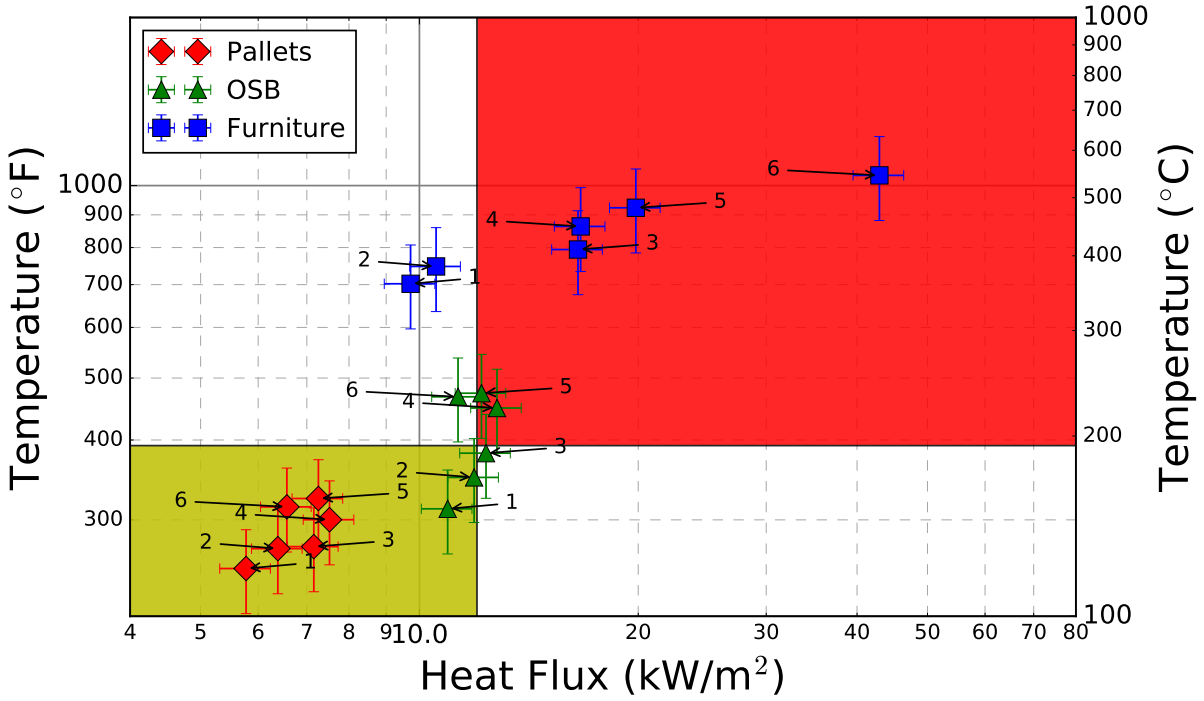

Figure 5.10: Ventilation response of fire for remote vent experiments. Points are labeled 1, 2, 3, 4, and 5, corresponding to the temperature and heat flux at 0s, 30s, 60s, 90s, 120s, and 150s after ventilation, respectively. The yellow and red portions of the chart indicate the ordinary and emergency operating zones, respectively.

of the thermal exposure. Thus, although the thermal conditions in the OSB experiments and the furnished room experiments are in the emergency operating range and conditions within these rooms could eventually cause failure of a firefighter's PPE, the length of time that a firefighter would have until their PPE was compromised may vary significantly.

The variations in thermal conditions that occur over the duration of the experiments as well as the time of exposure highlight an important gap in understanding in the thermal operating class method of evaluating firefighter safety. In defining each class, Utech lists a reference time. The ordinary operating class is defined as being an area where firefighters could operate for the entire 20 or 30 minute duration of a fire incident [19]. He describes the emergency operating class as one in which a firefighter can survive in for only a few minutes before suffering burn injuries. As discussed in Chapter 2, while firefighter PPE has improved since the time that Utech proposed the thermal operating classes, the thresholds that he defined still correspond to the critical temperatures and heat fluxes of various pieces of firefighter PPE. Furthermore, Figures 5.9 and 5.10 demonstrate that the thermal operating class is not stagnant for the duration of a fire. In addition to considering the variation of the thermal exposure with time, it is important to consider the cumulative exposure to the firefighter during a training scenario, and how this exposure can affect the firefighter.

Prior to the introduction of the Thermal Performance Test (TPP) into NFPA 1971 for turnout en-

sembles, PPE was required to have a minimum thickness. The TPP was introduced as it was considered [37] to be a more realistic exposure, giving a more realistic estimation of the thermal protection afforded by bunker gear. The TPP exposes a sample of turnout gear to a radiant and convective heat flux of 84 kW/m^2 from two separate sources. A copper calorimeter mounted behind the sample measures the amount of heat that is transmitted through the sample, and compares it to the amount of heat required to cause second degree burns. The threshold of burn injuries is dependent on both the amount of heat that is delivered through the gear and the rate at which it is conducted. This test is intended to simulate a short, high intensity thermal exposure, consistent with a firefighter operating in the area of a flashover.

This same principle of the cumulative energy transfer through the turnout gear can be applied to longer-duration exposures, such as those that would occur to an instructor or student during a longer training evolution. Figure 5.11 shows the cumulative heat exposure to the gear package over the duration of each experiment. This total energy term, similar to that measured in the TPP test, is determined by numerically integrating the vertical and horizontal heat flux using an Euler scheme. The x-axis shows the exposure from the horizontal gauge and the y-axis shows the exposure from the vertical gauge.

For the furnished room tests, the peak thermal conditions, and particularly the peak heat flux noted in Figure 5.6, were more severe for the near ventilation and remote ventilation experiments than for the experiment where no ventilation was provided. When the total energy is considered however, the largest vertical exposure occurs in the no ventilation case. While the peak exposure in Furniture Experiment 1 (no vent) was not as high as in Experiments 1 (near vent) and 5 (remote vent), the experiment had a longer duration, meaning that the firefighter was exposed for longer. The furnished room experiments had the highest cumulative exposure in the vertical direction, ranging from 1680 kJ/m^2 to 3500 kJ/m^2, while the pallets and straw experiments had the lowest, between 500 and 650 kJ/m^2. The OSB experiments exhibited cumulative vertical exposures between the furnished room experiments with exposures of 1055 kJ/m^2 and 1150 kJ/m^2. Since the vertical exposure is strongly influenced by the temperature of the gas layer above the gauge, this trend is consistent with expectations. The most severe horizontal exposures were noted in the furnished room and OSB experiments, with cumulative exposures of 2425 kJ/m^2 and 1895 kJ/m^2, respectively. Among the lowest cumulative horizontal exposures were the remote ventilation experiments, which had exposures of 715 kJ/m^2, 890 kJ/m^2, and 1014 kJ/m^2 for pallets, OSB, and furniture, respectively. As discussed in the previous section, the more severe heat exposures in the horizontal direction are likely because these gear samples have a direct line of sight to the seat of the fire, and thus would be exposed to direct radiation from the flames, particularly if the smoke is not dense, obscuring direct radiation. Figure 5.11 shows how the total thermal insult to the turnout gear package in the doorway is dependent not only on the peak thermal exposures, but also the time history of the exposure, as well as the total duration.

Figure 5.11 illustrates the total thermal insult to which a firefighter in PPE would be exposed in the path to the fire room, but in order to understand the level of protection that PPE affords a firefighter, consider the total energy exposure from the covered heat flux packages, as shown in Figure 5.12. These measurements are all considerably lower than the total amount of heat that is transferred to the outside of the gear. This demonstrates the mechanism by which turnout gear

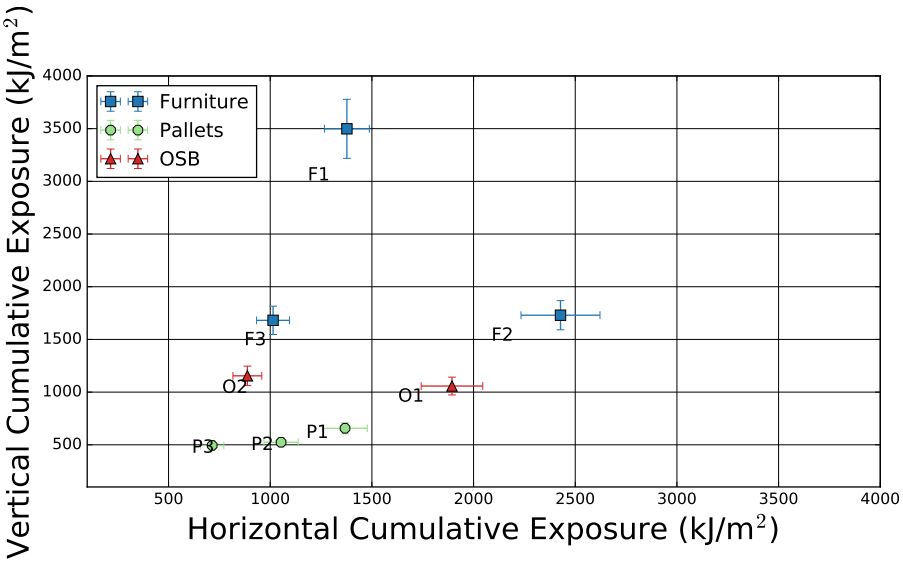

Figure 5.11: Cumulative Energy Exposure to Gear Sample in Doorway

protects the firefighter from thermal insult. Turnout gear consists of three layers: An outer shell for abrasion resistance, a moisture barrier, and a thermal liner [38]. This thermal liner is typically a material with a low net thermal conductivity. As the ensemble is exposed to an incident heat flux, some of the energy is stored within the thermal liner, increasing the temperature of the material. Even when the incident heat flux is removed, the energy remains in the gear until the heat is lost. Two mechanisms by which this heat loss can occur are convective cooling to the environment or conduction to the firefighter. This second mechanism can be hazardous and result in burn injuries if the contact exceeds the minimum duration for injury [39]. This conduction to the firefighter becomes particularly hazardous as the duration and severity of the thermal exposure increases and the thermal layer begins to approach equilibrium with the thermal conditions to which it is exposed. Since heat transfer is a transient process, momentary, severe exposures can be within the tolerance of the PPE, as long as the ensemble is removed from these conditions after the short duration. If the turnout gear ensemble is not removed fromt he environment, the interior conditions will continue to worsen until the PPE is no longer providing enough protection to prevent injury.

Figure 5.12, which summarizes the peak heat flux and surface temperature recorded beneath the turnout gear for each orientation, reveals that the cumulative exposure in Furniture Experiment 1 is over three times higher than those observed in the other experiments. This is likely a result of the extended exposure in this experiment, since neither of the other two furnished rooms had under-gear exposures that were nearly as high, although the peaks were of similar magnitudes. The consequence of this heat exposure to the firefighter wearing the gear would be dependent on the rate at which it is transferred, although the conditions on the inside of the gear sample, listed in Table 5.5, can give some insight into the injury potential for the firefighter.

The surface temperatures on the inside of the turnout gear samples can be compared to two benchmark temperatures, 111°F and 162°F (44°C and 72°C), which are the hot surface temperatures corresponding to the minimum temperature at which epidermal damage is observed in a 6-hour

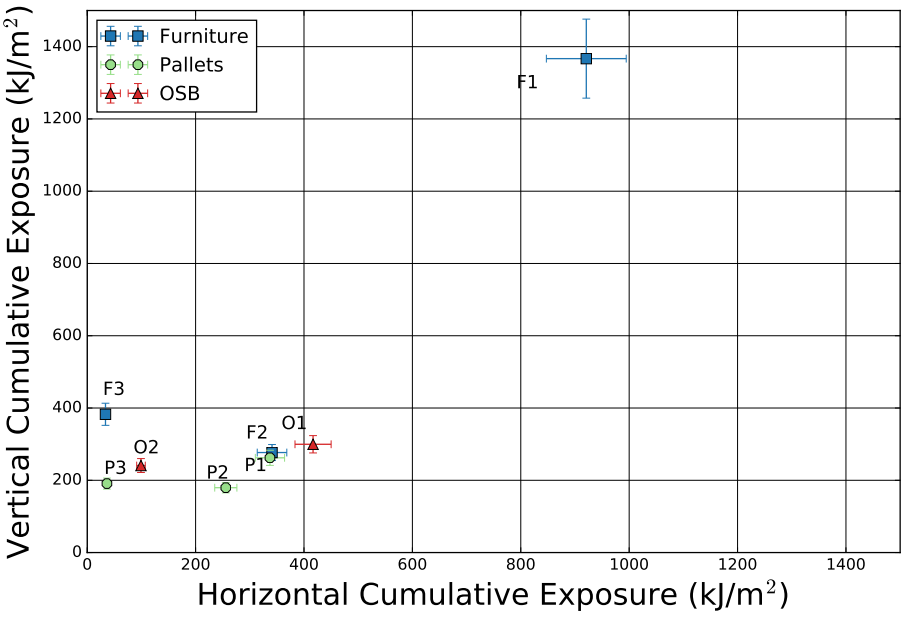

Figure 5.12: Cumulative Energy Exposure Beneath Turnout Gear for Samples in Doorway

Table 5.5: Peak Under Gear Temperatures and Heat Fluxes Measured in Doorway Gear Sample Package

Experiment	**Surface Temp. °F (°C)**		**Heat Flux (kW/m^2)**	
	Horizontal	**Vertical**	**Horizontal**	**Vertical**
Pallets 1	138 (59)	131 (55)	≤ 1	≤ 1
Pallets 2	140 (60)	136 (58)	≤ 1	≤ 1
Pallets 3	154 (68)	136 (58)	≤ 1	≤ 1
OSB 1	178 (81)	176 (80)	1.7	1.1
OSB 2	171 (77)	154 (68)	≤ 1	≤ 1
Furniture 1	297 (147)	307 (153)	2.1	2.9
Furniture 2	250 (121)	228 (109)	3.1	2.0
Furniture 3	273 (134)	264 (129)	≤ 1	1.9

period and the temperature at which complete transdermal necrosis occurs instantly [40]. It is important to note that these benchmarks are typically used as contact temperatures for industrial processes, and are provided as reference points for different levels of injury, rather than as strict thresholds.

The peak heat fluxes measured below the turnout gear samples for both the horizontal and vertical orientations were below 4.5 kW/m^2. However, both the OSB and furnished roomfires generated temperatures greater than 162°F (72°C) on the interior surface of the turnout gear samples. In particular, the furnished rooms all demonstrated interior surface temperatures in excess of 212°F

(100°C). None of the pallets and straw experiments exhibited interior surface temperatures in excess of 162°F (72°C), although the peak values did fall above the 111°F (44°C) minimum threshold. Since a firefighter operating in this environment would be encapsulated by turnout gear, it is not unreasonable to assume that they may directly contact the interior surface of the gear. The interior surface temperatures that were measured in the furnished room and OSB experiments are within the range of temperatures where contact could result in burn injuries to the skin, although it is difficult to conclude the extent of these injuries and the duration required to sustain them.

The method used above to evaluate the potential for thermal injury to the firefighters has several limitations. The profile of the turnout gear packages is much different than that of a firefighter, and the packages themselves sit lower in the door. Since the turnout gear ensemble is not air tight, the airflow between the firefighter and the garment may be different than that between the heat flux box and the turnout gear sample. Furthermore, the thresholds described above for skin injury are intended primarily for use with solid surfaces in industrial settings. Since the thermal properties of the thermal liner are different, it will affect the conduction characteristics, but these temperatures serve as reasonable reference temperatures. Additionally, the turnout gear packages did not move for the duration of the experiment, whereas a firefighter participating in a training evolution would be moving. This movement may compress certain areas of their PPE, accelerating the rate of heat transfer to the skin. Further research is needed to better quantify the relationship between thermal exposure to a firefighter's PPE and the onset of thermal injuries, although it is reasonable to conclude that the potential exists for burns to occur, even under conditions which do not necessarily exceed PPE performance criteria. Thus, in order to fully capture the thermal risk to firefighters during a training evolution, the analysis would not only have to consider the peak heat flux and peak temperature, but rather a fractional approach, similar to toxicity calculations, where the time history of the temperature and heat flux could be considered.

Therefore, the most appropriate way of characterizing a firefighter's thermal exposure would be to develop a time-dose relationship, which would consider the transient nature of the thermal conditions at firefighter operating height, the time-dependent transfer of heat through turnout gear, and the threshold of burns to the skin, or the failure of various pieces of PPE. In this series of experiments, even the training fuels exhibited surface temperatures on the interior of the turnout gear ensemble that had the potential for thermal injury, despite the comparatively lower peak thermal conditions. This potential for injury is driven not only by the magnitude of the thermal insult, but also by the duration of the exposure. Turnout gear is designed to provide protection for a high-intensity, but short duration exposure, as might be experienced on the fireground. In live fire training exercises, on the other hand, students and instructors may be exposed to less intense exposures, but for a longer period of time. In training evolutions such as these, the exposure of participants should be monitored to avoid thermal injury.

6 Training Considerations

This section uses the analysis from Section 5 to develop a series of training considerations for use by firefighters. These considerations are based on the fuel packages that were used in experiments, which were chosen to be representative of fuel packages used by the fire service. Additionally, these considerations should be read in the context of concrete live fire training buildings similar to the one in which these excperiments were conducted. The fire dynamics produced in these types of buildings may be quite different than those produced in different types of training props due to differences in ventilation or construction. The fidelity of these fuel packages in a concrete live fire training building is the degree of exactness with which they replicate the fire dynamics of a contemporary residential structure furnished with items composed of foams, plastics, and other synthetic materials. This report is one section of a four-part series of experiments examining training fires, and other sections of the report will examine different types of training structures.

6.1 Wood-Based Training Fuels Are Different Than Synthetic Fuels

Training fuels permissible by *NFPA:1403* are primarily wood-based, making them different than many foams, plastic, and other synthetic fuels typically found in residential homes. These wood-based fuels produce different fire dynamics than the synthetic fuels commonly found in residential furniture. These different fire dynamics can be attributed to both the geometry of the fuel packages and the chemistry of the components themselves.

Fire growth and the rate at which it occurs is an important element when considering the fidelity of a training fuel. Figure 6.1 compares the 7 ft. temperature growth in the fire room for each of the three fuel packages for the remote ventilation experiments. For both the pallets and the OSB fuel packages, the highest rate of growth occurred immediately following ignition. Temperature rise at the 7 ft. level is not observed until later in the furnished room experiments, with the first appreciable growth roughly 100 seconds following ignition. While the period of most rapid growth was noted earlier in the training fuel package experiments than in the furniture experiments, it was far less than the peak rate of growth in the furniture fires. Table 6.1 shows the results of the HRR characterization tests for each of the fuel packages. The results indicated that the peak rate of HRR increase was approximately five times faster in the furniture than in either training fuel package.

The high growth rate early in the training fuel package experiments is a result of the geometry of the fuel package, particularly the high surface-area-to-mass ratio of the straw. The fire is ignited in the straw, propagating rapidly and releasing enough energy to ignite the pallets and OSB. The pallets and OSB provide the bulk of the weight of their respective fuel packages, and therefore provide more longevity to the burn. The importance of the straw to the growth rate can be seen in the pallets experiments. In Pallets Experiment 2 the straw was packed more densely between the pallets, inhibiting total involvement of the straw and resulting in a slower growth rate than the other two experiments. The peak growth in the furniture fuel package is observed later in the experiment because the growth is hindered by the configuration of the fuel. The components of the furniture fuel package do not have a high surface area-to-mass ratio like the straw, and are located closer to the floor, in the coolest part of the room. This limits the surfaces that are exposed to high heat fluxes, inhibiting flame spread. In the case of the furniture fuel package, the rapid growth is a result of the high heat of combustion of the components, rather than the geometry. The heat of combustion of polyurethane foam is 23.9 MJ/kg, compared to 13.9 MJ/kg for wood-based training fuels. This means that for every kilogram of polyurethane foam that is burned, 72% more energy is released than if the same mass of pine had been burned.

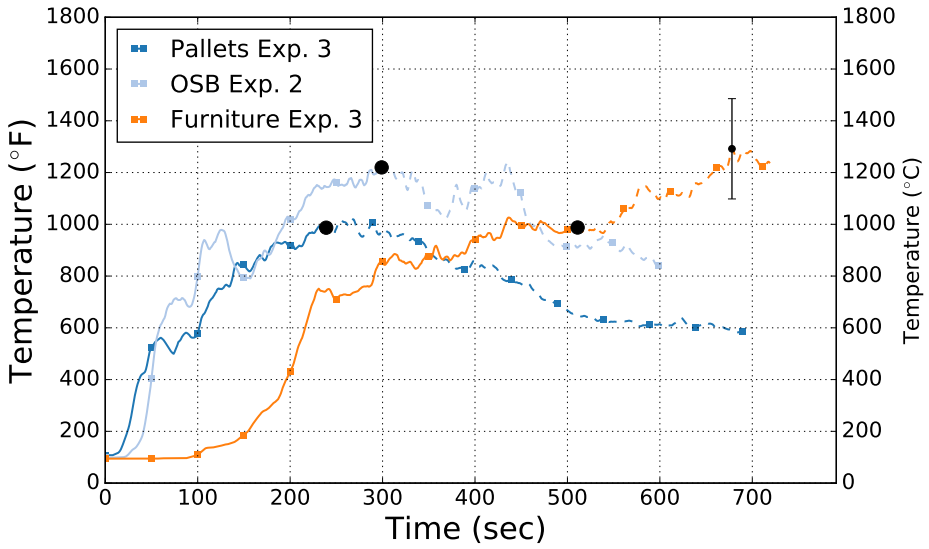

Figure 6.1: Comparison of 7 ft. Temperature Growth for Training Fuel and Furniture Fuel Packages

Table 6.1: HRR Results Comparison

Fuel Package	**Peak Rate of Increase (kW/s)**	**Peak HRR (MW)**
Pallets	30	2.88
OSB	30	3.63
Furnished Room 1	160	8.50
Furnished Room 2	150	7.52

For each kilogram of oxygen consumed in combustion, 13.1 MJ of energy is released. Thus, the

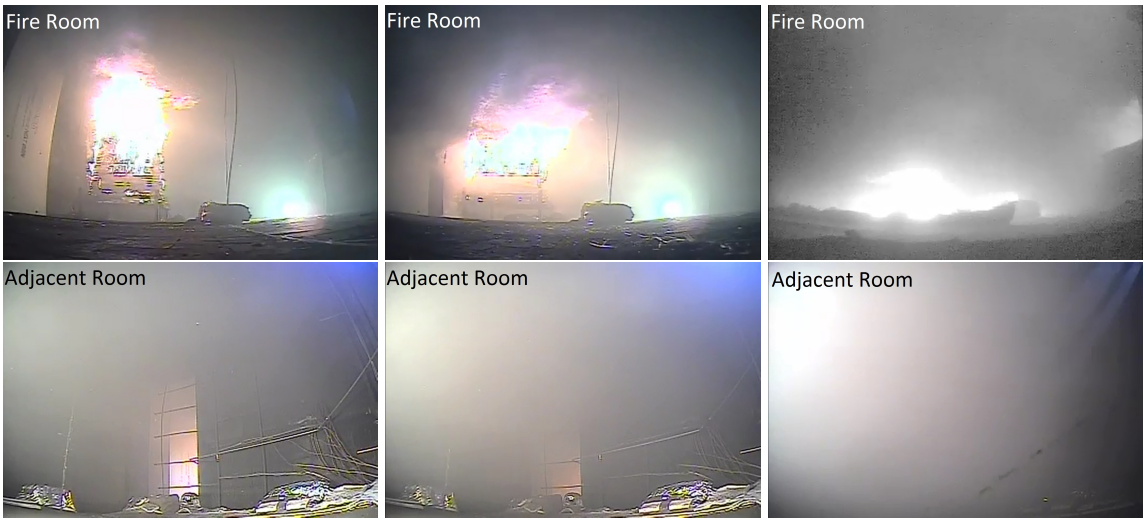

Figure 6.2: Comparison of Smoke Conditions in Fire Room Ventilation Experiments for Pallets (left), OSB (center), and Furniture (Right)

higher heats of combustion of the synthetic fuels dictates that these fuels also have a higher oxygen demand. Consider one of the 3.8 kg barrel chairs in the furniture fuel package. If the chair were composed entirely of wood, it would require 3.0 m^3 of oxygen for combustion, whereas if the chair were composed of polyurethane foam, it would require 6.9 m^3 of oxygen. These masses translate to 14.4 m^3 and 24.7 m^3 of air for pine and polyurethane, respectively. Thus, for the same mass of fuel, the synthetic material requires more oxygen for complete combustion. In order to satisfy the higher HRR's of the furniture fuel packages, a greater supply of oxygen is needed. An insufficient oxygen supply to these fuels can result in inefficient combustion and ventilation-controlled conditions, as were observed in the furniture experiments.

Fires in modern residential structures are often characterized by low visibility conditions due to optically dense smoke [41]. Thus, if one of the objectives of the training evolution is to create realistic visibility conditions, the fuel package should also aim to produce such conditions. Figure 6.2 compares the visibility conditions in the near ventilation experiments for each of the three fuel loads. Visibility conditions are the highest in the pallets experiment, where a firefighter in the room adjacent to the fire room would be able to see most of the doorway between the two rooms and a firefighter in the doorway would have an obscured line of sight to most parts of the fire room. In the OSB experiment, visibility is not as high in the room adjacent to the fire room. Only the lower part of the fire room doorway can be seen, however, qualitatively, visibility in the fire room doorway was similar between the pallets and OSB experiments. In the furnished room experiments, visibility is drastically lower than either training fuel fire. A firefighter approaching the fire room would not be able to see the doorway. Visibility conditions were similarly reduced in the doorway to the fire room, where a firefighter would only be able to make out the burning beneath the furniture.

The low visibility conditions is a result of the inefficient combustion in the furniture fuel package. The oxygen demand of the large mass of fuel in the furniture fuel package and the high oxygen demand of its synthetic components is too high for complete combustion, resulting in depletion

of oxygen close to the floor and low visibility because of the fuel-rich smoke produced by incomplete combustion. This oxygen depletion close to the floor was not observed in the training fuel experiments, where oxygen concentrations remained close to ambient throughout the experiment.

Visibility remained higher in the training fuel experiments as well. Thus, if low visibility conditions are desired, similar to those that may be encountered in a residential structure with a synthetic fuel load, then instructors may choose to use alternative methods of increasing the smoke density, such as wet excelsior or smoke barrels.

6.2 Building Construction Affects Fire Behavior

Many concrete live fire training buildings are built for durability to withstand repeated live fire training evolutions rather than to replicate the types of residential structures to which firefighters may respond. Some of the aspects of the construction of concrete live fire training buildings have a pronounced effect on fire dynamics. Previous fire service research [5, 6] has documented the fire dynamics typical of room and contents fires in residential structures. One of the structures used in these studies was an 8-room, 1200 ft^2 ranch house constructed to be representative of a home constructed in the mid-twentieth century. The walls and ceiling of the ranch house were lined with two layers of gypsum board (5/8 in. base layer and 1/2 in. surface layer).

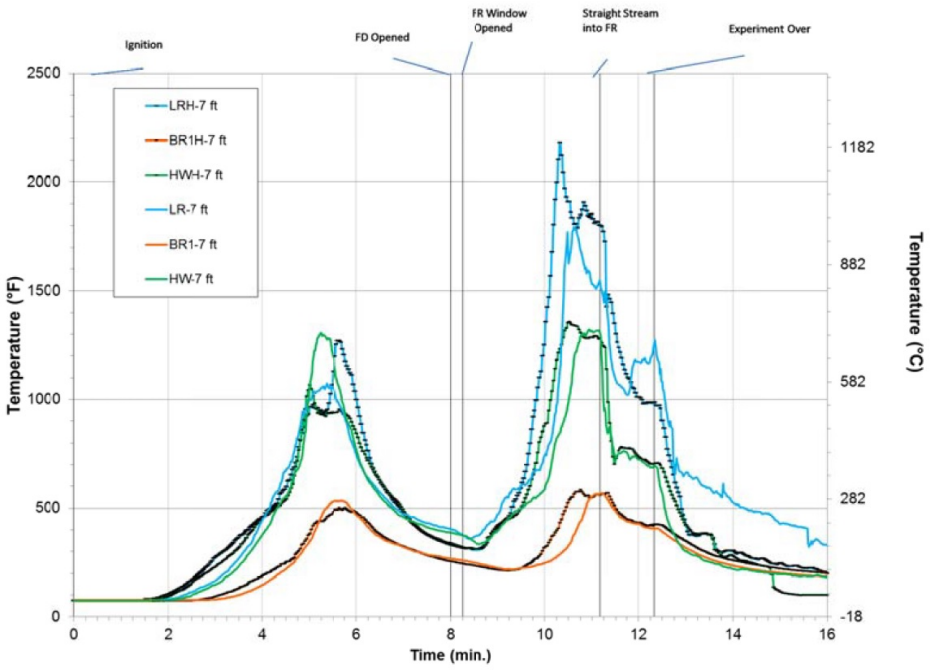

Figure 6.3: 7 ft. temperature comparison for replicate ranch house experiments from DHS 2008 and DHS 2010 projects. The front door and living room window were opened 8 minutes (480 seconds) following ignition.

Figures 6.3, 6.4, and 6.5 compare the 7 ft. temperatures, oxygen concentrations, and pressures for

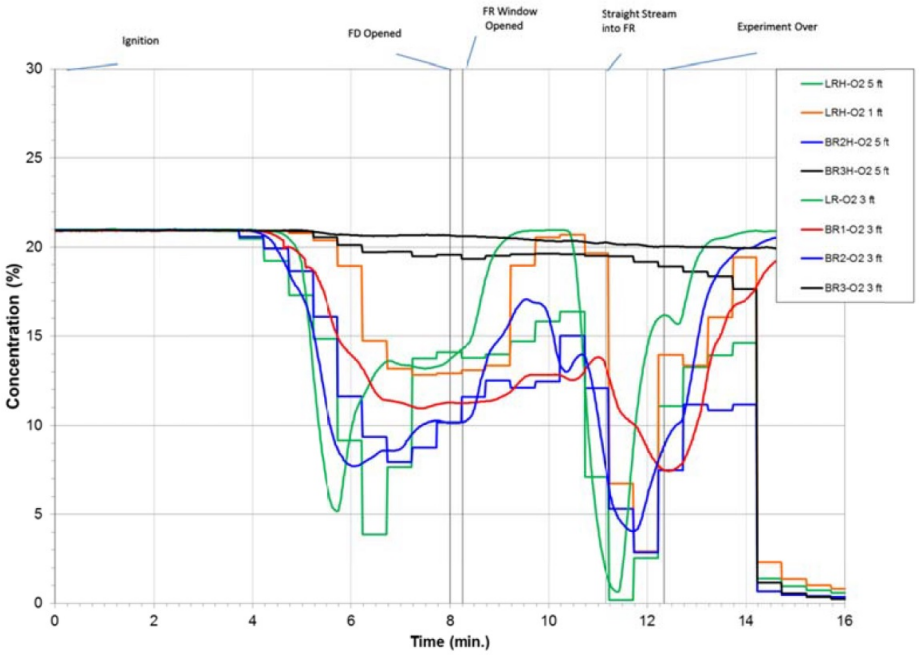

Figure 6.4: O_2 concentration comparison for replicate ranch house experiments from DHS 2008 and DHS 2010 projects. The experiment began with all exterior windows and doors closed, and the fire was ignited in the living room. The front door and living room window were opened 8 minutes (480 seconds) following ignition.

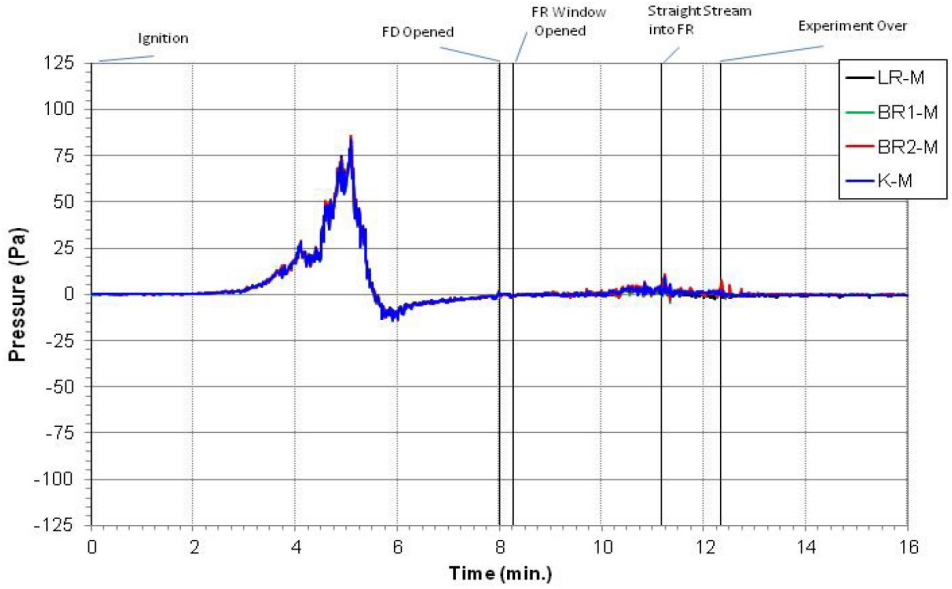

Figure 6.5: Pressure throughout Ranch Structure from Experiment 1, DHS 2010

two experiments where a fire was ignited in the living room. In each of the experiments, temperatures began to increase, reaching a peak. This local peak temperature corresponds to the minimum oxygen concentration in the fire room, which is close to 5%, and a pressure spike above 75 Pa.

After the peak, pressure throughout the structure became negative, which was accompanied by a decrease in temperatures and increase in oxygen concentration in the living room. This behavior indicates that the fire had an insufficient supply of oxygen to sustain combustion and tried to draw air in through leakage points in the structure, resulting in a decrease in burning and corresponding decrease in temperatures. Following ventilation of the front door and living room window, the living room fire is provided with a fresh source of oxygen and temperatures increase and flashover conditions are observed in the living room approximately 150 seconds after ventilation. After flashover, 7 ft. temperatures throughout the ranch structure reach peaks above 500°F (260°C) with the highest temperatures observed in the living room at approximately 1800°F (980°C).

The fire dynamics that were observed in the furniture experiments in the concrete live fire training building differed from those documented in the ranch structures in [5, 6], particularly concerning the decay due to oxygen depletion in the ranch homes. The period of decreasing temperatures and increasing oxygen concentrations prior to ventilation was not noted in any of the furniture experiments. Rather, the temperatures in the fire room approach a steady state until the time of ventilation. After ventilation, temperatures increase to flashover. This contrast in fire dynamics between the ranch houses in [5, 6] and the concrete live fire training building is illustrated in Furniture Experiment 2 (near vent), which has a similar fuel package (a living room furniture set) and ventilation configuration (a window in close proximity to the fire in the living room). The 7 ft. temperature profiles on the second floor of the concrete live fire training building are shown in Figure 6.6 and the fire room oxygen concentrations are shown in Figure 6.7. In addition to the lack of a decay because of oxygen depletion, flashover conditions were observed approximately 50 seconds sooner after ventilation than in the ranch house.

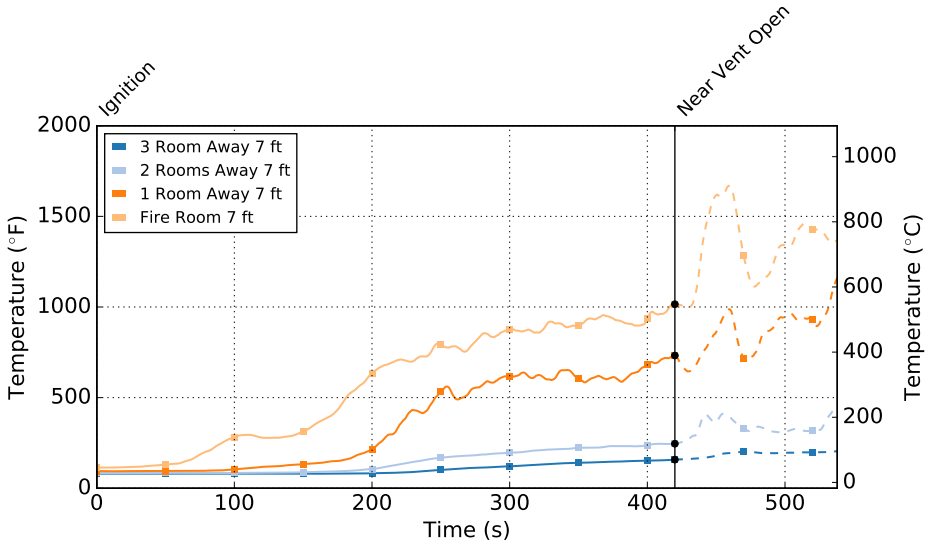

Figure 6.6: 7 ft. Temperature Profiles for Furniture Experiment 2

One reason for the difference in fire behavior between the ranch structure in which previous research on the residential fire environment had been conducted and the concrete live fire training building is the air leakage in the concrete live fire training building. The equivalent leakage area (ELA) for the ranch structure is 1.2 ft^2, and the ELA for a similarly constructed 2-story colonial

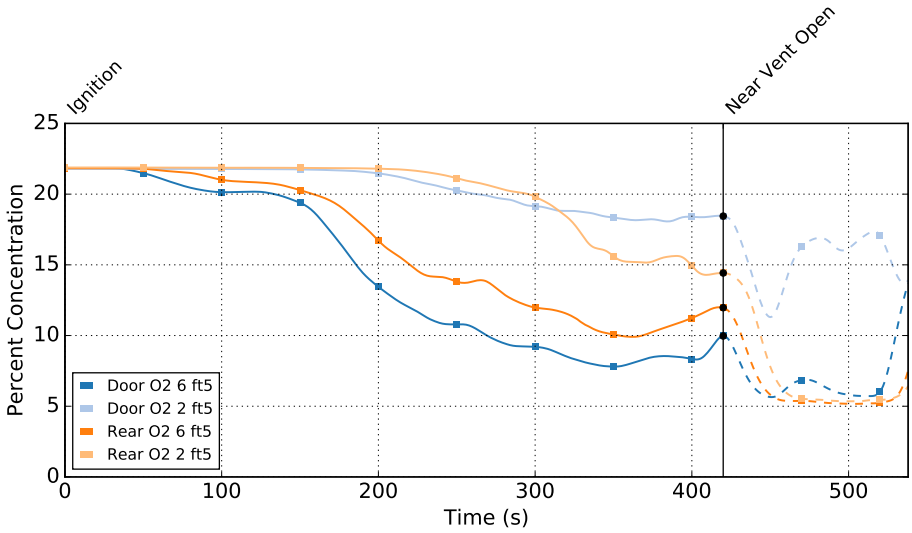

Figure 6.7: Fire room O_2 Concentration (%) for Furniture Experiment 2.

structure is 2.4 ft^2 [42]. While a leakage test could not be conducted on the concrete live fire training building, the surface area of the scuppers themselves was 5.7 ft^2 (5300 cm^2). Thus, without considering any additional leakage through windows, doors, or other means, the leakage into the concrete live fire training building was 3.75 times higher than the ranch structure described above. In the ranch structure, as the fire grows and consumes oxygen, the leakage into the structure is not sufficient to sustain combustion, and as the oxygen concentration in the fire room decreases below the point where burning is possible, the fire begins to choke itself out. The fire in the concrete live fire training building, on the other hand, had a much larger supply of air via leakage. This larger air supply resulted in a constant bi-directional flow through the fire room door for each of the experiments. This air supply is not enough to allow the furniture fuel package to progress to flashover, nor is it too little to result in decay, but rather is enough to reach an oxygen-controlled, fully developed state. Once additional ventilation was provided, flashover occurred sooner than in the ranch house, since the gases in the fire room were already hot, and just needed the additional oxygen to precipitate flashover.

Another difference between the ranch house and concrete building that affects fire dynamics is the high ceilings in the concrete building. Other than the fire room, the ceilings of the rooms on the second floor of the concrete live fire training building are 12 ft. The high ceilings correspond to a larger total volume within the concrete live fire training building. The volume of the second floor, which has a footprint of 938 ft^2, is 14908 ft^3. This volume is 73% larger than the volume of the 1200 ft^2 ranch house, which was 8636 ft^3. This larger volume, combined with the leakage of the concrete live fire training building, prevents a pressure spike due to a buildup of products of combustion. In the ranch house from [6], however, a pressure spike in excess of 75 Pa was observed prior to ventilation, before decreasing to approximately -15 Pa. In the ranch house, with a smaller volume and leakage area, as the fire grows and products of combustion are produced, pressure within the structure is built as the smoke fills the available volume. In the concrete live fire training building, as smoke and hot gases are produced, there is a larger volume that they must

fill in order to build up pressure. Additionally, some of the products of combustion are exhausted from the structure by the leakage as they spread through the building. Thus, the high leakage and volume of the concrete live fire training building prevent the pressure buildup seen in the ranch house. Without a large pressure difference to drive fire flows, it is unlikely that severe thermal conditions would be seen in remote areas of the concrete fire training building, even if a flow path was established through those areas.

The different lining materials between the ranch house and the concrete live fire training building also have an effect on fire dynamics. In any compartment fire, the fire dynamics are driven by the HRR of the fuel. While some of the energy created by the fire acts to heat uninvolved fuel precipitating additional flame spread, some of the heat is also lost to heating the walls and ceiling of the compartment. The amount of energy that is lost to these linings can affect the fire dynamics in the fire room and elsewhere in the structure. The thick concrete walls of the concrete fire training building act as a heat sink. This is because concrete takes considerably more energy to heat up than gypsum board, as evidenced by the thermal inertia values: 2.8 $(kW/m^2K)^2s$ for concrete compared to 0.18 $(kW/m^2K)^2s$ for gypsum board [43]. As the hot gases travel between rooms from the fire room, they lose energy to the concrete block walls and ceiling. In addition to requiring more energy to heat up, the concrete walls also take a longer time to release their energy. Previous research projects have demonstrated that repeated burns in concrete fire training buildings can result in elevated ambient heat conditions [15]. Madrzykowski conducted an experiment in a concrete live fire training building in order to examine the effect of repeated evolutions. The ambient heat flux at 4.9 ft. (1.5 m) from the ceiling before the last evolution was 6 kW/m^2, and the ambient temperature in the burn structure was 302°F (150°C) at 5.02 ft. (1.53 m) below the ceilings.

These building construction differences also have a profound effect on the fire dynamics of the training fuel packages. Since the wood-based training fuels do not have as high of an oxygen demand as the synthetic materials in the furniture fuel package, the same ventilation-controlled behavior was not observed. In the pallets and straw experiments, the density of the straw in the pyramid had a greater effect on fire growth than ventilation. In the OSB experiments, ventilation of the fire room window resulted in an increase in temperatures and heat fluxes because of the efficient flow path that was created. A similar increase in thermal conditions was not noted in the remote vent experiment for the OSB fuel package. In all of the training fuel packages, the oxygen concentrations close to the floor, at the 2 ft. level, remained above 20% for the duration of the experiments. This stands in contrast to the furniture fuel package, where oxygen concentrations at this elevation were 5% in the rear of the room. Just as in the furnished room experiments, no significant pressure spikes were observed in the training fuel package experiments.

Understanding ventilation-controlled fires is among the requirements for live fire training outlined in *NFPA 1403*. Previous research has emphasized that ventilation-controlled fires typically follow a growth curve similar to the one presented on the right in Figure 6.8. This curve is also sometimes referred to as the "modern fire curve." Even the furniture fuel package, which followed a growth trajectory similar to the modern fire curve in the ranch experiments (Figure 6.3), was unable to mirror this growth curve in the concrete live fire training building. While the furniture fires were ventilation-controlled, the air leakage and interior volume prevented them from entering a state of decay. These construction features also prevented any significant pressure buildup, even with all

exterior doors and windows closed. The training fuel packages, which had a lower total fuel weight and oxygen demand due to their wood-based component fuels, demonstrated a growth curve more similar to a fuel-controlled curve, shown on the left in Figure 6.8 and also referred to as the "legacy fire curve." The fresh air provided to the fire room through leakage is enough to prevent the training fuels, and the pallets and straw in particular, from becoming ventilation controlled. Thus, if the objective of a training evolution is to demonstrate the effect of ventilation on fire dynamics or to demonstrate ventilation-controlled fire behavior, using training fuel loads such as these would not meet that objective in a concrete live fire training building.

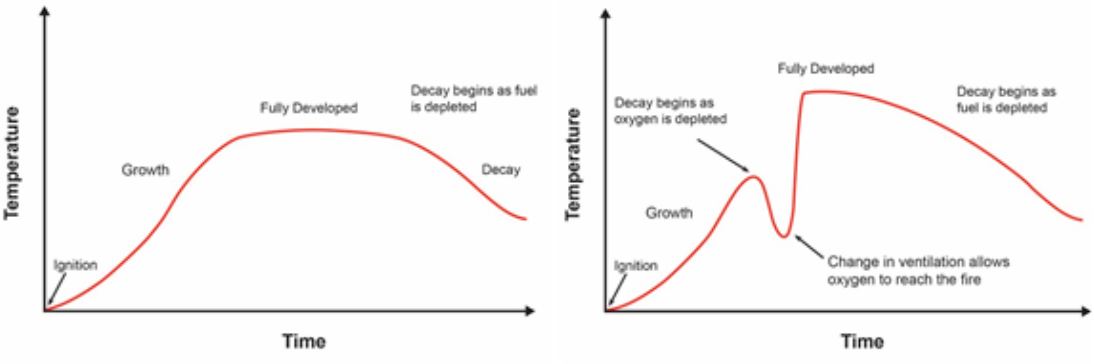

Figure 6.8: Legacy Fire Curve (left) vs. Modern Fire Curve (right)

6.3 Limiting the Fuel Load to Avoid Uncontrolled Flashover Does Not Prevent Thermal Injury

Among the stipulations of *NFPA 1403* is that the fuel load should be limited in an effort to avoid uncontrolled flashover. Several firefighters have died in training-related incidents [11,14] where an excessive or inappropriate fuel load resulted in unexpected fire growth, culminating in flashover. Flashover is typically defined as a transition, usually rapid, from the growth stage to the fully developed stage of fire growth. A hot gas layer temperature of 1112 °F (600°C) or a heat flux of 20 kW/m^2 to the floor are typical benchmarks for the onset of flashover. Temperatures and heat fluxes in excess of these temperatures were measured in each of the furnished room experiments, including the experiment where no windows or doors were opened. This shows that conditions consistent with flashover can be sustained with only the oxygen that is provided via leakage into the structure.

Post-flashover fire conditions were not observed for any of the training fuels. Although none of these fires transitioned to flashover, the peak heat flux and temperature that were observed for the OSB fuel package were 19.3 kW/m^2 and 1320°F (714°C). The failure of the OSB to exhibit flashover conditions, despite floor heat fluxes close to the 20 kW/m^2 and temperatures within the gas layer in excess of 1112°F (600°C), can be attributed to the geometry of the training fuel package. In both training fuel packages, all of the fuel is centralized to a single area of the fire room, and most of the fuel becomes involved during the growth phase of the fire. By the time

that the heat flux has reached a threshold that would typically precipitate flashover, there is a lack of fuel available to contribute to additional fire growth, as shown in Figure 6.9. In the furnished room, most of the fuel is located close to the floor, meaning that as the fire grows, fuels remote from the fire are heated. Eventually, these fuels reach their ignition temperature, precipitating the rapid transition to flashover. In the OSB fuel package, there is no remote fuel, so the radiative heat flux from the gas layer simply heat the concrete floor.

Figure 6.9: Peak Thermal Conditions in OSB Experiment

Although none of the training fires exhibited conditions consistent with flashover, the thermal conditions that were measured were severe, as discussed in the following training consideration. It is important that instructors understand that simply preventing flashover does not necessarily mean that they are preventing thermal injuries from occurring. Care should still be taken to ensure that an inappropriate fuel load is not used, even if that fuel load is not capable of precipitating flashover.

6.4 Time, Distance, and Shielding are Important when Evaluating Thermal Exposure

Among the goals of a successful fire training scenario should be to create a realistic, useful training evolution without injuring any of the participants. The thermal hazard posed by each of the three training fuels was approximated by using the concept of thermal operating zones, proposed by Harvey Utech [19]. This method defines three zones– Routine, Ordinary, and Emergency – based on heat flux and temperature criteria. The floor heat flux gauge and 3 ft. temperature sensors in each room can be used to estimate the thermal threat to firefighters for each of the experiments. It is important to note that the heat flux gauge was directed at the ceiling and was located at an

elevation of 1 ft. from the floor. At this elevation, the fresh air being entrained into the fire room may have cooled the gauge, causing the sensor to underestimate the thermal radiation of the gas layer.

In each of the experiments, thermal conditions were most severe in the fire room. In the OSB and furniture experiments, the peak thermal conditions fell into the emergency operating zone, meaning that the thermal conditions approached or exceeded common failure thresholds for PPE. Firefighters operating in these areas would likely experience equipment failure or thermal injury within seconds. Post-flashover conditions, as were observed in the furnished room fires, fall into the emergency operating zone. The peak conditions in the pallets and straw experiments did not reach the threshold for emergency operating conditions, falling instead into the ordinary operating class. Thermal conditions in the ordinary operating class would not present the immediate threat of thermal injury or equipment failure associated with emergency operating conditions. This is significant in the context of training fires because students participating in a training evolution using pallets and straw as a fuel would have a larger margin of error than if the evolution used OSB or furniture as a fuel load. In the same manner, instructors participating in such an evolution would be able to move more freely without having to worry about the risk of thermal injury to themselves or their students. A visual comparison of the magnitude of the peak thermal conditions against Utech's operating classes is shown in Figure 6.10.

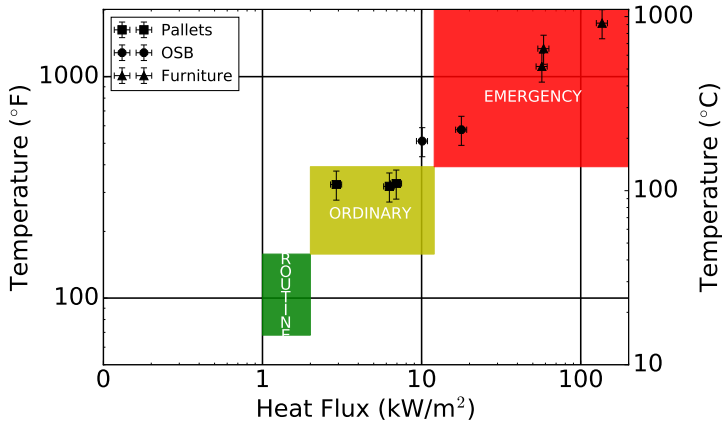

Figure 6.10: Comparison of Peak Thermal Conditions in Fire Room

As the distance from the fire room increased, the severity of thermal conditions decreased substantially, as shown in Figure 6.11, which shows the peak thermal conditions in the fire room for one of the furnished room experiments, compared with conditions one, two, and three rooms away. The chart shows that while the conditions in the room adjacent to the fire room are within the ordinary operating class, conditions in the remainder of rooms on the second floor are within the routine operating class, despite flashover conditions only two or three rooms away. One of the reasons for this drop off in conditions is the high ceilings and thick concrete walls, which remove energy from environment, as discussed in Section 6.2. This reduction in thermal conditions remote from the fire room means that instructors who are operating in these remote rooms may not have a complete understanding of the conditions to which their students are exposed.

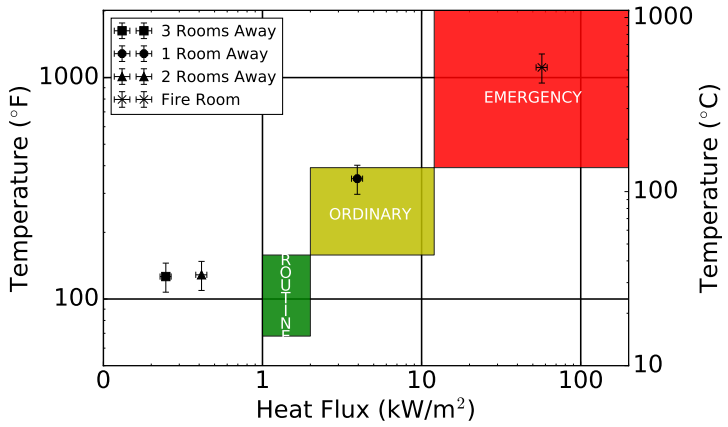

Figure 6.11: Decrease in Thermal Conditions Remote from Fire Room

Location relative to the flow path had a similar effect on thermal conditions. Unlike a typical residential structure, a flow path is always present through the doorway to the fire room because of the leakage into the structure. The gear samples packages placed in and out of the doorway to the fire room can help to characterize the effect of flow path. Just like the floor heat flux gauges, these gear sample packages are elevated 1 ft. off of the floor, rather than 3 ft, which is approximately the height of a crawling firefighter. Thus, the peak heat flux values reported here may be lower than the actual radiative heat flux, due to convective cooling of the gauge.

A firefighter kneeling in the doorway experienced a higher thermal exposure than they would if they had moved a few feet out of the doorway. The exposure is higher in the doorway for a number of reasons. First, the hot gases escaping the fire room increase the radiative and convective heat transfer to the firefighter. Additionally, a firefighter in the doorway has a direct line of sight to the fuel package. Particularly in the training fuels, when obscuration due to smoke was not as high, this means that direct radiation from the fuel package is higher. As the firefighter moves out of the flow path, they move away from the direct radiation from the fire and from the high temperature, high velocity flows escaping the fire room. Instructors or students could take advantage of the lower thermal exposure to reduce the risk of their gear becoming saturated, particularly when operating close to the fire room for an extended period of time. Just as care must be taken when operating close to the fire room, firefighters should not consider themselves out of the danger zone until they are isolated from the flow path as well.

While the magnitude of the peak thermal conditions discussed in previous paragraphs is an important consideration when evaluating the potential for thermal energy, the duration of the exposure is an equally important consideration. To understand this concept, it is first important to appreciate how turnout gear protects firefighters from thermal injury. Consider the simple one-dimensional model presented in Figure 6.13. The turnout gear ensemble is comprised of three parts: an outer shell, a thermal liner, and a moisture barrier, with air gaps between each layer. The firefighter's clothing can also be considered part of the ensemble.

Turnout gear provides thermal protection by delaying the transfer of heat to the skin below. The

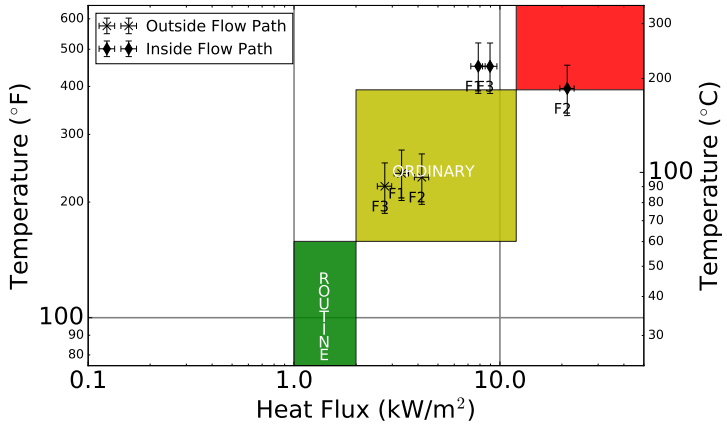

Figure 6.12: Effect of Flow Path on Thermal Exposure

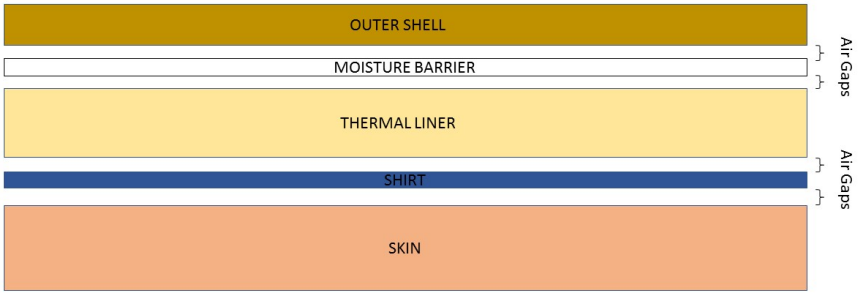

Figure 6.13: Turnout Gear Heat Transfer Model

top graphic in Figure 6.14 shows an external heat flux heating the ensemble. As the exterior flux increases the surface temperature of the outer shell, heat begins to transfer through the rest of the ensemble. The heat transfer occurs via conduction within each layer of the ensemble and by convection within the air gaps. When the heat is first applied, there is not an immediate rise in temperature on the other side. Rather, there is a lag time associated with the transfer of heat through the gear, before which there would not be a significant temperature rise on the interior surface of the turnout gear ensemble. During this time lag, heat is being transferred to the gear, but not to the firefighter through the gear, as shown in the middle graphic in Figure 6.15. After this time lag, the temperature on the back face of the turnout gear ensemble begins to increase. At this point, heat is being transferred to the firefighter, although not at the same rate as it is being transferred to the gear. This scenario is shown by the bottom graphic in Figure 6.16. In both of these scenarios, the turnout gear is still offering protection to the firefighter, because the thermal conditions beneath the gear are less severe than the thermal conditions outside of it.

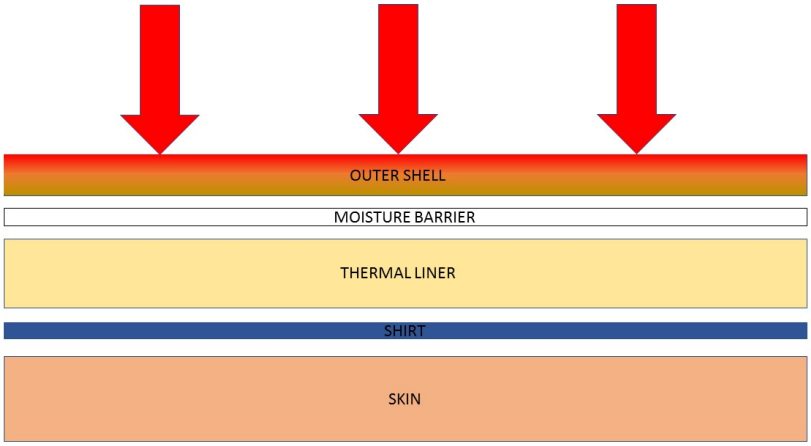

Figure 6.14: Heat Transfer into Ensemble

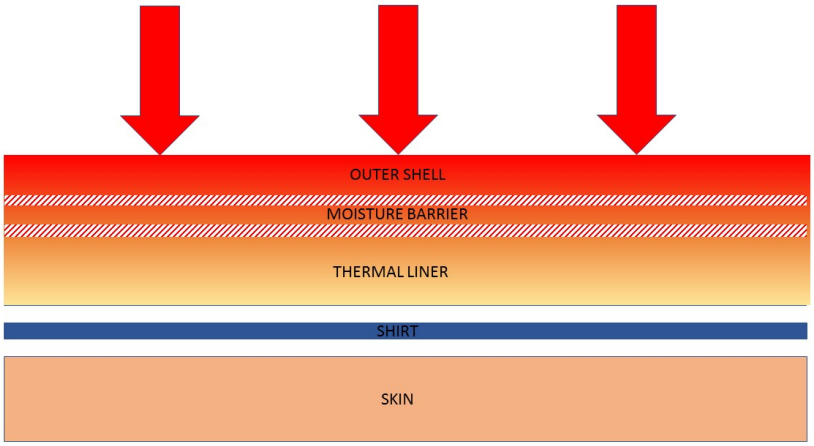

Figure 6.15: Heat Transfer into Ensemble Prior to Temperature Rise on Interior Surface

Heat can continue to be transferred to the gear until the point where the components of the turnout gear ensemble can no longer be heated anymore. At this point, the heat transfer rate to the gear is the same as the heat transfer rate to the firefighter, as shown in Figure 6.17. When this occurs, the turnout gear could be considered "saturated" with heat, much like a sponge which has absorbed as much water as possible, rendering the turnout gear ineffective in protecting the firefighter. In most cases, firefighters would begin to sustain thermal injuries before the gear became saturated, as the amount of heat being transferred through the gear reaches the threshold for thermal injuries. The point at which this threshold is reached is dependent on the amount of heat delivered and the rate at which it is conducted through the gear. The primary driver of the heat transfer rate is the temperature difference between the temperature of the exterior face of the ensemble and the interior face of the ensemble. Thus, in severe thermal conditions, such as a flashover, the heat transfer rate would be quite rapid, meaning that the temperature on the interior surface of the gear

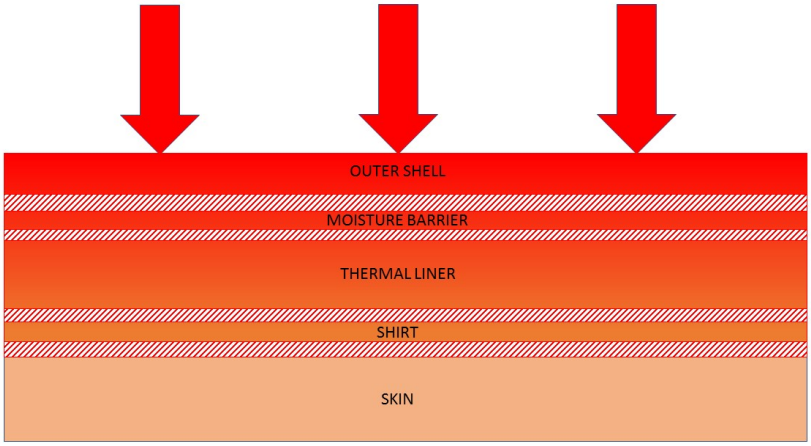

Figure 6.16: Heat Transfer into Ensemble Following Temperature Rise on Interior Surface

would increase more quickly than in less severe thermal conditions. In an environment where thermal conditions were not as severe, the temperature difference would not be as high, and the resultant heat transfer rate would also not be as high. Since heat transfer through turnout gear is a time-dependent process, it would make sense that the time of exposure would be as important to consider as the severity.

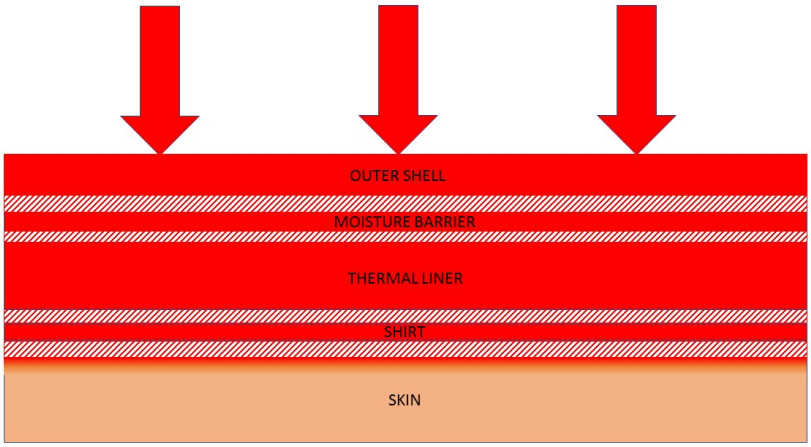

Figure 6.17: Saturated Ensemble

In this series of experiments, temperatures in excess of 111°F (44°C) were observed on the inside surface of the turnout gear for each of the experiments. This is the minimum skin temperature at which pain may be experienced. Both the OSB and furniture experiments had interior surface temperatures in excess of 162°F (72°C), which is the temperature at which skin is instantly destroyed. The maximum interior surface temperatures and heat fluxes are shown in Table 6.2. Although it is difficult to tell exactly the point at which thermal injuries would occur to firefighters due to

differences in station wear, sweat production, blood circulation, and other parameters, the peak thermal conditions beneath the gear were rather severe in some cases. While the experiments with the highest exposures also had high temperatures beneath the turnout gear, several experiments with peak exposures in the ordinary operating zone also had high under-gear temperatures. Thus, while high temperatures and heat fluxes can result in high interior surface temperatures, prolonged exposures to intermediate heat fluxes, as were observed in the OSB experiments, also can result in potentially dangerous conditions beneath turnout gear.

Table 6.2: Peak Under Gear Temperatures and Heat Fluxes Measured in Doorway Gear Sample Package

Experiment	**Surface Temp. °F (°C)**		**Heat Flux (kW/m^2)**	
	Horizontal	**Vertical**	**Horizontal**	**Vertical**
Pallets 1	138 (59)	131 (55)	≤ 1	≤ 1
Pallets 2	140 (60)	136 (58)	≤ 1	≤ 1
Pallets 3	154 (68)	136 (58)	≤ 1	≤ 1
OSB 1	178 (81)	176 (80)	1.7	1.1
OSB 2	171 (77)	154 (68)	≤ 1	≤ 1
Furniture 1	297 (147)	307 (153)	2.1	2.9
Furniture 2	250 (121)	228 (109)	3.1	2.0
Furniture 3	273 (134)	264 (129)	≤ 1	1.9

It is important to note that the heat transfer model discussed above is a simple one, and fails to account for some of the complex movements and geometries associated with a working firefighter in a dynamic fire environment. For example, when certain areas of the turnout gear ensemble are compressed, the air gaps are eliminated, which decreases the effective thickness of the garment and the time required for heat to pass through the ensemble. Nevertheless, it provides a simple, useful model to understand the mechanism by which turnout gear provides protection to the wearer.

Understanding the time-dependent nature of heat transfer through turnout gear is important for several reasons. Since changes in thermal conditions are not immediately reflected underneath turnout gear, a firefighter cannot completely rely on their sense of feel to evaluate the conditions in which they are operating. Since synthetic fuels have the potential for rapid growth, if a firefighter were caught in this period of rapid growth with limited visibility, they may not immediately be able to identify the changing conditions, and by the time that they feel the change, it may be too late to self-rescue from the environment. Although the training fuels used in these experiments exhibited neither the rapid growth nor the severity of conditions, it is still possible for extended exposures to less severe thermal conditions to result in thermal injury because of turnout gear saturation.

7 Summary

The goal of fire service training is to prepare students for the conditions and challenges that they face on the fireground. Among the challenges that firefighters routinely face on the fireground are ventilation-controlled fires. The hazard of these fires has been highlighted by several line-of-duty deaths and injuries in which a failure to understand the fire dynamics produced by these fires has been a contributing factor. The synthetic fuels that commonly fill contemporary homes tend to result in ventilation-controlled conditions.

While synthetic fuels are common on the residential fireground, the fuels that firefighters use for fire training are more often representative of natural, wood-based fuels. In order to better understand the fire dynamics of these training fires, a series of experiments was conducted in a concrete live fire training building in an effort to evaluate the fidelity and safety of two training fuels, pallets and OSB, and compare the fire dynamics created by these fuels to those created by a fuel load representative of a living room set with furniture items with a synthetic components. Additionally, the effects of the concrete live fire training building on the fire dynamics were examined.

7.1 Training Fuels vs. Furniture

NFPA 1403 specifically prohibits the use of fuels, such as rubber, plastic, polyurethane foam, and upholstered furniture. The high energy content of these fuels can cause rapid changes in thermal conditions capable of injuring or killing firefighters in full PPE. Indeed, several training incidents where these materials were incorporated resulted in firefighter deaths following the deterioration of conditions. While synthetic materials such as those described above are restricted from use in training, these materials are the fuels that would be found in a residential structure. The fuels that firefighters use for training are wood-based, and the fire dynamics that they produce are different than those produced by synthetic fuels, such as foams and plastics.

The peak growth period of the wood-based training fuel packages in this series of experiments occurred immediately after ignition. This early growth was facilitated by the straw, which has a high surface-area-to-mass ratio, allowing for rapid fire spread through the straw. In one of the experiments, the straw was packed more densely, resulting in a slower growth than the other two pallets experiments. The addition of the OSB to the pallets fuel package resulted in a higher peak HRR, which corresponded to higher peak temperatures and heat fluxes close to the fire room.

The peak thermal conditions observed in either training fuel package were substantially less than the peak thermal conditions observed for the furnished rooms, which were consistent with post-flashover conditions. This is because of the higher total weight of fuel in the furniture fuel package and the higher heat of combustion of the components.

The higher heats of combustion of the synthetic components of the furniture fuel package correspond to a higher oxygen demand. Since these fuels require more oxygen to sustain combustion, they have an increased propensity to become underventilated. The wood-based training fuels do not have the same high oxygen demand as the synthetics. Among the effects of this is the optically dense, fuel rich smoke that was produced by the furniture experiments was not noted in the training fuel experiments. Thus, if the goal of a training evolution is to replicate ventilation-controlled conditions or to produce optically dense smoke akin to a furniture fire, the use of wood-based training fuels in a concrete live fire training building with high leakage area may not be the most effective means of meeting this goal.

7.2 Effects of Building Construction on Fire Dynamics in Concrete Live Fire Training Buildings

The differences in construction between many concrete live fire training buildings and residential homes have a pronounced effect on the fire dynamics within these buildings and particularly their effectiveness in teaching ventilation-controlled fire behavior. In order to explore these effects, the furniture experiments from this series of experiments were compared to experiments using a similar fuel load in a 1200 ft^2 ranch home. The 12 ft. ceilings in the concrete live fire training building resulted in a larger interior volume than the ranch home. Additionally, the scuppers and other built in leakage points result in a much larger leakage area in the concrete live fire training building than in the ranch house. Further, the thick concrete walls of the concrete live fire training building have different thermal properties than the gypsum board walls in a typical residential structure.

The large interior volume and leakage area prevented products of combustion from building up and causing pressure spikes. Additionally, these features allow for a constant supply of oxygen to the fire room. This constant supply of air was sufficient to maintain a constant bi-directional flow through the fire room door for each of the experiments, and allowed oxygen concentrations in the lower portion of the fire room to remain at ambient for each of the training fuel experiments. Furthermore, a state of decay due to oxygen depletion as observed in previous research conducted in wood-frame, gypsum-lined residential structures was not observed in any of the current experiments.

Because of the high thermal inertia of concrete and the thickness of the walls and floor, the concrete live fire training building requires more energy to heat up and store energy for longer than the gypsum walls of a typical residential structure can hold. This means that earlier burns in the concrete live fire training building may not have as severe of thermal conditions as later burns in

the day, a trend which previous research has emphasized.

The high leakage area and interior volume of the concrete live fire training used in this experiment make it a relatively ineffective prop for teaching ventilation-controlled fire behavior. Previous research and recent line-of-duty deaths and injuries have highlighted that many of the fires that firefighters respond to enter a state of ventilation-limited decay prior to fire department arrival. For this reason and others, *NFPA 1403* lists an understanding of ventilation-controlled fires as requisite knowledge for live fire training. Therefore, instructors conducting training evolutions with the objective of teaching ventilation-controlled fire behavior may want to explore different live fire training props to successfully teach students the characteristics of these fires, or explore creative solutions for reducing the leakage or interior volume during these training evolutions.

7.3 Safety Considerations in Training Fires

Training evolutions are different than the actual incidents to which firefighters respond in the respect that both students and instructors often spend extended periods of time inside the burn structure. Although the peak temperatures and heat fluxes measured in the training fuel package experiments were less than those recorded in the furniture experiments, these lower peak thermal conditions still resulted in elevated interior surface temperatures in the PPE between 131°F (55°C) and 178°F (81°C). Inside the PPE, heat fluxes as high as 1.7 kW/m^2 were measured in the OSB fuel package experiments. Among the job performance requirements in *NFPA 1001: Standard for Fire Fighter Professional Qualifications* is that firefighters understand the methods of heat transfer. It is imperative that this understanding is applied not only to how the methods of heat transfer affect fire dynamics, but also to their effect on the transfer of heat through PPE, and how this time-dependent heat transfer dictates what firefighters feel and their potential for thermal injury. In particular, the potential for thermal injury is driven not only by the magnitude of thermal conditions outside the protective ensemble, but also by the length of time that firefighters are exposed to these conditions. While further research is needed to better characterize the heat transfer through turnout gear and its relationship to thermal injury, the results of these experiments indicated that training fuels can produce thermal conditions with the potential to cause firefighter injuries, particularly in areas close to the fire room. Additionally, firefighters must understand that they cannot completely rely on their sense of feel to monitor conditions, since rapid changes in external conditions are not immediately reflected inside the PPE ensemble.

7.4 Future Work

These experiments examined the fire behavior produced by two training fuel packages and a furniture fuel package with synthetic components in concrete training buildings. Concrete training buildings such as the one in this series of experiments are only one of many types of containers in which firefighters conduct training. The behavior of various fuels in these props should be studied

and compared to their behavior in concrete buildings. Other parts of this study aim to characterize the fire dynamics in other training structures, such as metal structures. The discussion of this study briefly touched upon the effect of wall linings on heat loss from the hot gas layer remote from the fire room. This effect would be useful to understand, not only for training fires, but for fires in all types of compartments.

When considering the safety of firefighters in a thermal environment, the thermal exposure conditions defined by Utech [19] was used. Utech considered the thermal threat to the firefighter in terms of two components: a radiant component and a convective component. The convective component is approximated by the temperature in the area that the firefighter is operating, but this neglects an important facet: the gas velocity. Higher gas velocities would result in higher convective heat transfer coefficients and a higher convective heat flux. Furthermore, the thermal threat of the firefighter should not be considered as an isolated peak event, but rather as a fractional dose, dependent on both the thermal load and the time of exposure. Thus, future work should focus on better evaluating the thermal hazard to firefighters and the heat transfer through PPE ensembles. This work should focus not only on training exposures, but also on thermal exposures representative of those that firefighters would encounter on the fireground.

References

[1] S. Wertman. F2010-10: One career fire fighter/paramedic dies and a part-time fire fighter/paramedic is injured when caught in a residential structure flashover - Illinois. Report, National Institute for Occupational Safety and Health, March 2010.

[2] M. Loflin. F2014-09: Lieutenant and fire fighter die and 13 fire fighters injured in a wind-driven fire in a brownstone - Massachusetts. Report, National Institute for Occupational Safety and Health, March 2014.

[3] S. Wertman. F2013-04: Two career lieutenants killed and two career fire fighters injured following a flashover at an assembly hall fire - Texas. Report, National Institute for Occupational Safety and Health, February 2013.

[4] M. Loflin J. Tarley, S. Miles and T. Merinar. F2011-02: Volunteer fire fighter caught in a rapid fire event during unprotected search, dies after facepiece lens melts - Maryland. Report, National Institute for Occupational Safety and Health.

[5] S. Kerber. Impact of Ventilation on Fire Behavior in Legacy and Contemporary Residential Construction. Report, Underwriters Laboratories, Northbrook, Illinois, December 2012.

[6] S. Kerber. Study of the Effectiveness of Fire Service Vertical Ventilation and Suppression Tactics in Single Family Homes. Report, Underwriters Laboratories, Northbrook, Illinois, June 2013.

[7] E. Meltzer. Boulder fire training deaths remembered on 30th anniversary. *Daily Camera*, January 2012.

[8] F. Reeder. The NFPA 1403 Debate. *Fire Rescue*, July 2013.

[9] J. Tarley. F2007-09: Career Probationary Fire Fighter Dies While Participating in a Live-Fire Training Evolution at an Acquired Structure - Maryland. Report, National Institute for Occupational Safety and Health, February 2007.

[10] S. Berardinelli. F2005-31: Career officer injured during a live fire evolution at a training academy dies two days later - Pennsylvania. Report, National Institute for Occupational Safety and Health, October 2005.

[11] J. Tarley and T. Mezzanotte. F2001-38: Volunteer fire fighter dies and two others are injured during live-burn training - New York. Report, National Institute for Occupational Safety and Health, September 2001.

[12] National Fire Protection Association, Quincy, Massachusetts. *NFPA 1403: Standard on Live Fire Training Evolutions*, 2018.

[13] National Fire Protection Association, Quincy, Massachusetts. *NFPA 1001, Standard for Fire Fighter Professional Qualifications*, 2013.

[14] S. Bernadelli N.T. Romano, J. Tarley. Career lieutenant and fire fighter die in a flashover during a live-fire training evolution - Florida. Report, National Institute for Occupational Safety and Health, July 2002.

[15] D. Madrzykowski. Fatal Training Fires: Fire Analysis for the Fire Service. Report, National Institute of Standards and Technology, Gaithersburg, MD, 2007.

[16] G. Horn J. Willi and D. Madrzykowski. Characterizing a Firefighter's Immediate Thermal Environment in Live-Fire Training Scenarios. *Fire Technology*, 52:1667–1696, 2016.

[17] Rene Rossi. Fire Fighting and its Influence on the Body. Report, National Institute for Occupational Safety and Health, August 2003.

[18] J.R. Lawson M.J. Selepak M. K. Donnely, W. D. Davis. Thermal Environment for Electronic Equipment Used by First Responders . Report, National Institute of Standards and Technology, 2006.

[19] H. Utech. Status report on research programs for firefighters protective clothing. In *Proceedings of the Fire Deparment Instructor's Conference*, Indianapolis, Indiana, 1973.

[20] National Fire Protection Association. *NFPA 1971: Standard on Protective Ensembles for Structural Fire Fighting and Proximity Fire Fighting*, 2013.

[21] National Fire Protection Association, Quincy, Massachusetts. *NFPA 1981: Standard on Open-Circuit Self-Contained Breathing Apparatus (SCBA) for Emergency Services*, 2013.

[22] N. Bryner G. Braga A. Putorti, A. Mensch. Thermal Performance of Self-Contained Breathing Apparatus Facepiece Lenses Exposed to Radiant Heat Flux. Technical Report NIST TN 1785, National Institute of Standards and Technology, Gaithersburg, MD, 2013.

[23] D. Madrzykwoski. Fire Fighter Equipment Operational Environment: Evaluation of Thermal Conditions. Technical report, Fire Protection Research Foundation, Quincy, MA, August 2017.

[24] R.A. Bryand and George Mullholland. A guide to characterizing heat release rate measurement uncertainty for full-scale fire tests. *Fire and Materials*, 32:121–139, 2008.

[25] *The Temperature Handbook*. Omega Engineering, 7 edition, 2010.

[26] L.G. Blevins. Behavior of Bare and Aspirated Thermocouples in Compartment Fires. In *Proceedings of the 33rd National Heat transfer Conference*, Albuquerque, New Mexico, August 1999.

[27] R.D. Peacock H.E Mitler E.L. Johnsson P.A. Reneke L.G. Blevins W.M. Pitts, E. Braun. Temperature Uncertainties For Bare-Bead and Aspirated Thermocouple MEasurements in Fire Environments. In *14th Meeting of the United States-Japan Conference on Devlopment of Natural Resources (UJNR) Panel on Fire Research and Safety*, University of Maryland, College Park, Maryland, USA, May 1998.

[28] J.L. De Ris J. Filtz K. Nygard D. Smith I. Wetterlund W.M. Pitts, A.V. Murthy. Round Robbin Study of Total Heat Flux Gauge Calibration at Fire Laboratories. *Fire Safety Journal*, 41.6:459–475, 2006.

[29] R.A. Bryant. A comparison of gas velocity measurements in a full-scale enclosure fire. *Fire Safety Journal*, 44:793–800, 2009.

[30] M. Bundy, A. Hamins, E.L. Johnsson, S.C. Kim, G.H. Ko, and D.B. Lenhart. Measurements of Heat and Combustion Products in Reduced-Scale Ventilated-Limited Compartment Fires. NIST Technical Note 1483, National Institute of Standards and Technology, Gaithersburg, MD, 2007.

[31] A. Lock, M. Bundy, E.L. Johnsson, A. Hamins, G.H. Ko, C. Hwang, P. Fuss, and R. Harris. Experimental study of the effects of fuel type, fuel distribution, and vent size on full-scale underventilated compartment fires in an ISO 9705 room. NIST Technical Note 1603, National Institute of Standards and Technology, Gaithersburg, MD, 2008.

[32] *Fire Protection Handbook*. National Fire Protection Association, Quincy, Massachusetts, 18th edition, 1997.

[33] International Energy Conservation Code. Report, International Code Council, Country Club Hills, Illinois, 2012.

[34] T. Tanaka and T. Yamana. Reduced Scale Experiments For Convective Heat Transfer In the Early Stage of Fires. *International Journal on Engineering Performance-Based Codes*, 1(3):196–203, 1999.

[35] K.J. Overholt, C.G. Weinschenk, and D. Madrzykowski. Simulation of a Fire in a Hillside Residential Structure – San Francisco, CA. NIST Technical Note 1856, National Institute of Standards and Technology, Gaithersburg, Maryland, 2014.

[36] S.K. Hoglander and S. Conver-White. House Fire with Significant Firefighter Injuries – Riverdale Heights, MD. Safety Investigation Team Report, Prince George's County Fire/Emergency Medical Services Department, Lanham, Maryland, 2013.

[37] W.H. Twilley J.R. Lawson. Development of an Apparatus for Measuring the Thermal Performance of Fire Fighters' Protective Clothing. Report, National Institute of Standards and Technology, 1999.

[38] National Fire Protection Association, Quincy, Massachusetts. *NFPA 1971, Standard on Protective Ensembles for Structural Fire Fighting and Proximity Fire Fighting*, 2013.

[39] International Organization for Standardization (ISO), Geneva, Switzerland. *ISO 17492, Clothing for protection against heat and flame – Determination of heat transmission on exposure to both flame and radiant heat*, 2003.

[40] American Society for Testing and Materials, West Conshohocken, Pennsylvania. *ASTM C 1055-03, Standard Guide for Heated System Surface Conditions that Produce Contact Burn Injuries*, 2003.

[41] IFSTA. *Essentials of Fire Fighting and Fire Department Operations*. Prentice Hall, 5th edition, 2008.

[42] R Zevotek and S. Kerber. Study of the Effectiveness of Fire Service Positive Pressure Ventilation During Fire Attack in Single Family Homes Incorporating Modern Construction Practices. Report, UL Firefighter Safety Research Institute, Columbia, MD, 2016.

[43] J. Quintere. *Fundamentals of Fire Phenomena*. Wiley, 2008.

Appendix A: Training Fire Fuel Weights

Experiment	Pallet Weights lbs. (kg)	Straw Weight lbs. (kg)	Total OSB Weight lbs. (kg)
3	n.r.	n.r.	-
4	39.6, 44.3, 42.1 (18.0, 20.1, 19.1)	n.r.	n.r.
6	39.9, 37.7, 37.3 (18.1, 17.1, 16.9)	n.r.	-
7	38.4, 45.0, 34.8 (17.4, 20.4 15.8)	32.4 (14.7)	-
8	41.0, 42.1, 43.0 (18.6, 19.1, 19.5)	30.6 (13.9)	93.3 (42.3)

Appendix B: Thermal Conditions Remote from Fire Room

B.1 Summary of Peak Thermal Conditions in Remote Areas

Table B.1: Peak Heat Fluxes Remote From Fire Room

Experiment	Room 202		Room 203		Room 204	
	Pre-Vent	Post-Vent	Pre-Vent	Post-Vent	Pre-Vent	Post-Vent
1	1.34	5.57	0.16	0.47	0.11	0.40
2	4.72	-	0.46	-	0.37	-
3	0.63	0.96	0.04	0.09	0	0.23
4	0.88	1.17	0.06	0.12	0	0.08
5	1.82	4.73	0.18	0.46	0.14	0.46
6	0.71	-	0.07	-	0.08	-
7	0.53	0.79	0.03	0.04	0	0.02
8	0.97	1.86	0.06	0.17	0.02	0.18

Table B.2: Peak 3 ft. Temperatures Remote From Fire Room

Experiment	Room 202		Room 203		Room 204	
	Pre-Vent	Post-Vent	Pre-Vent	Post-Vent	Pre-Vent	Post-Vent
1	105.3	245.0	45.0	78.1	43.7	60.5
2	176.6	-	53.7	-	52.4	-
3	55.1	72.2	31.1	42.6	30.2	46.7
4	46.9	57.6	31.9	34.2	30.7	31.6
5	100.4	164.0	43.4	67.7	46.1	56.5
6	74.5	-	39.9	-	39.4	-
7	55.1	71.0	33.1	45.4	32.3	41.3
8	67.3	113.8	33.9	56.4	33.3	53.3

B.2 Pallets Experiment Results

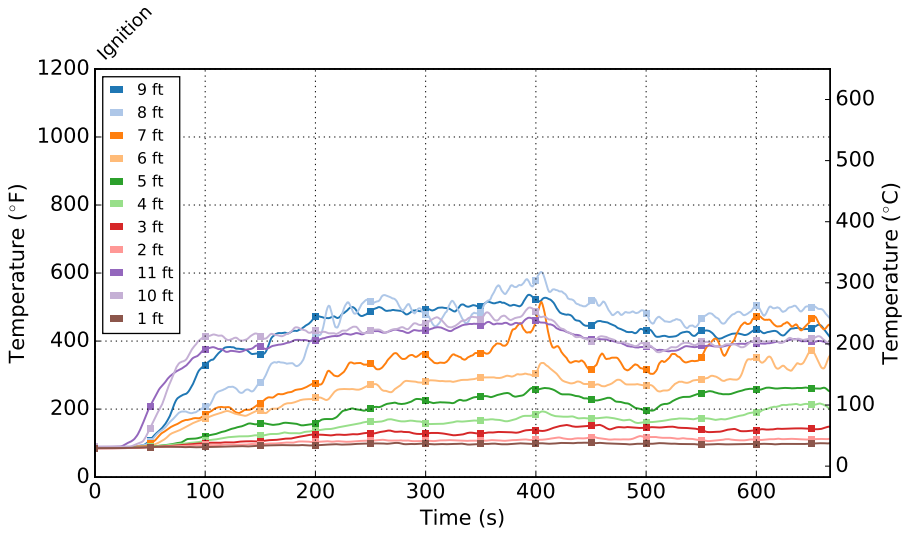

Figure B.1: Room 202 Temperatures for Pallets Experiment 1

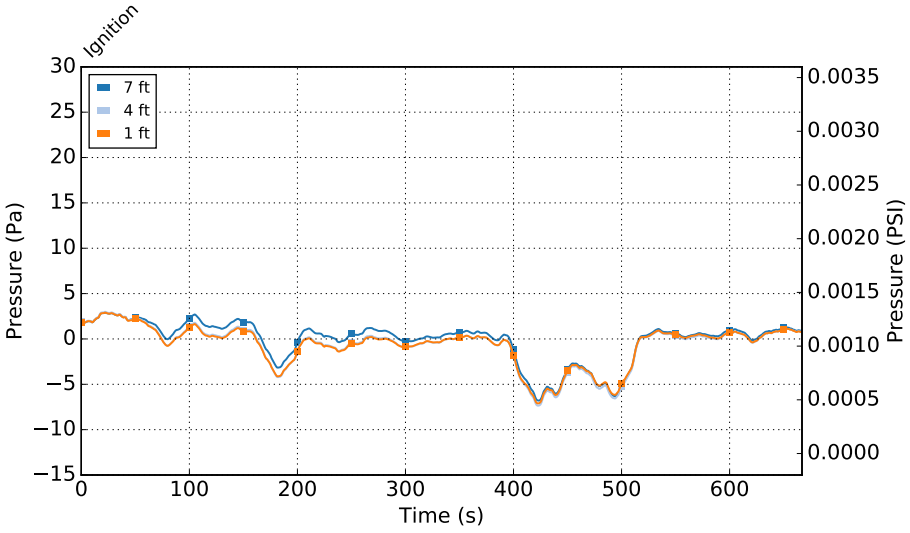

Figure B.2: Room 202 Pressure for Pallets Experiment 1

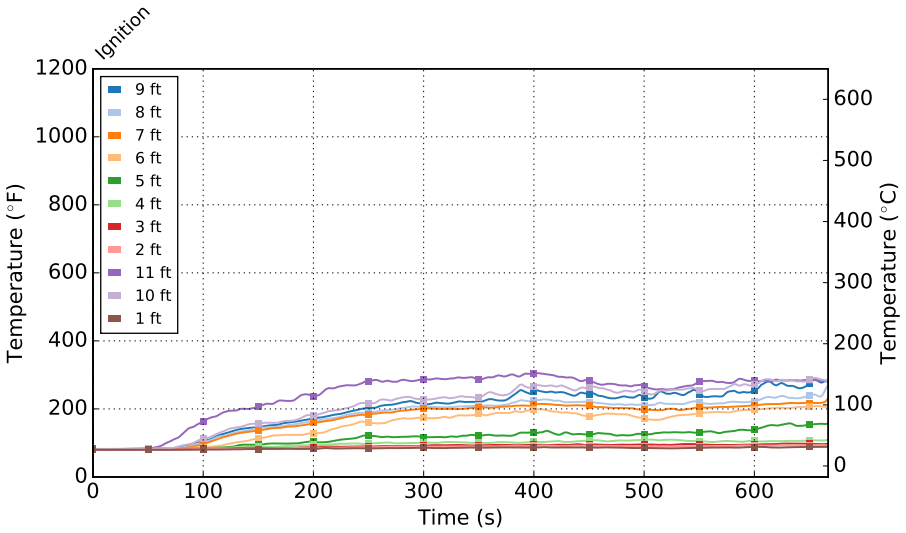

Figure B.3: Room 203 Temperatures for Pallets Experiment 1

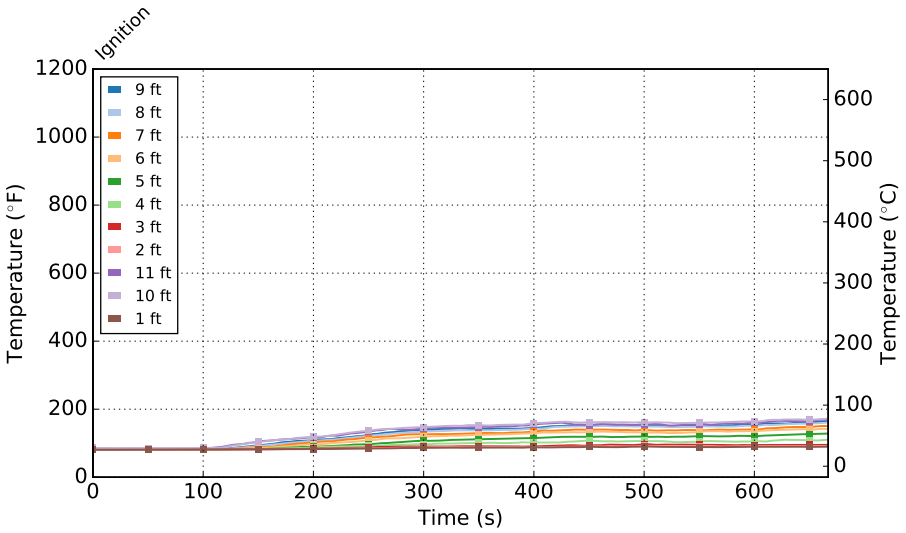

Figure B.4: Room 204 Temperatures for Pallets Experiment 1

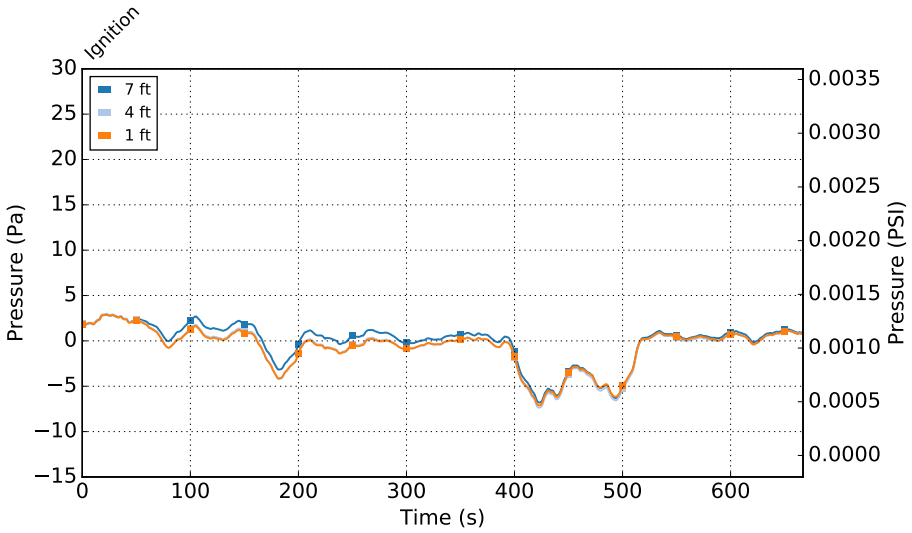

Figure B.5: Room 204 Window Velocity for Pallets Experiment 1

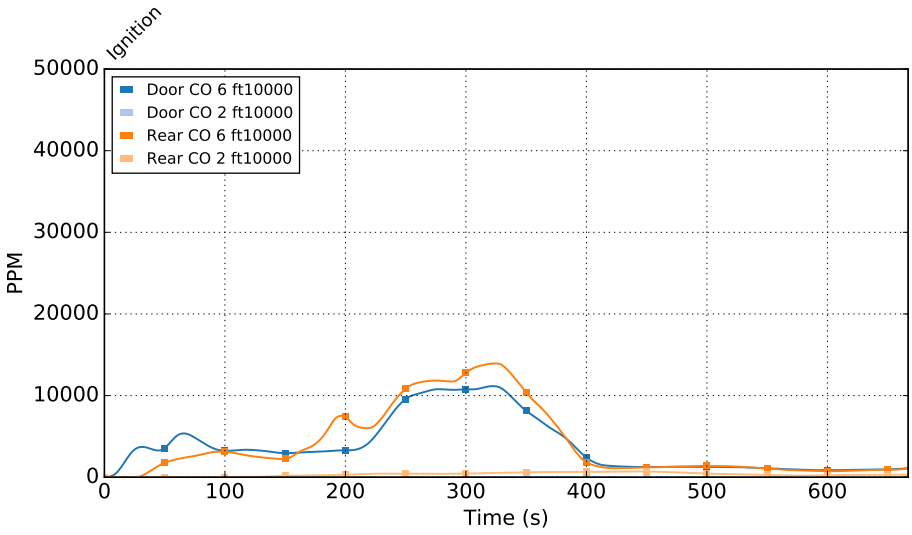

Figure B.6: Room 201 CO Concentrations for Pallets Experiment 1

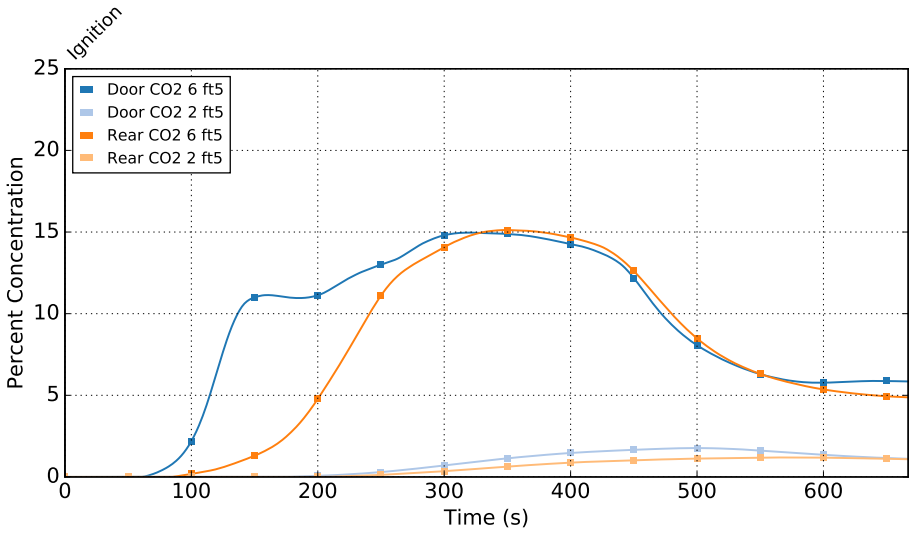

Figure B.7: Room 201 CO_2 Concentrations for Pallets Experiment 1

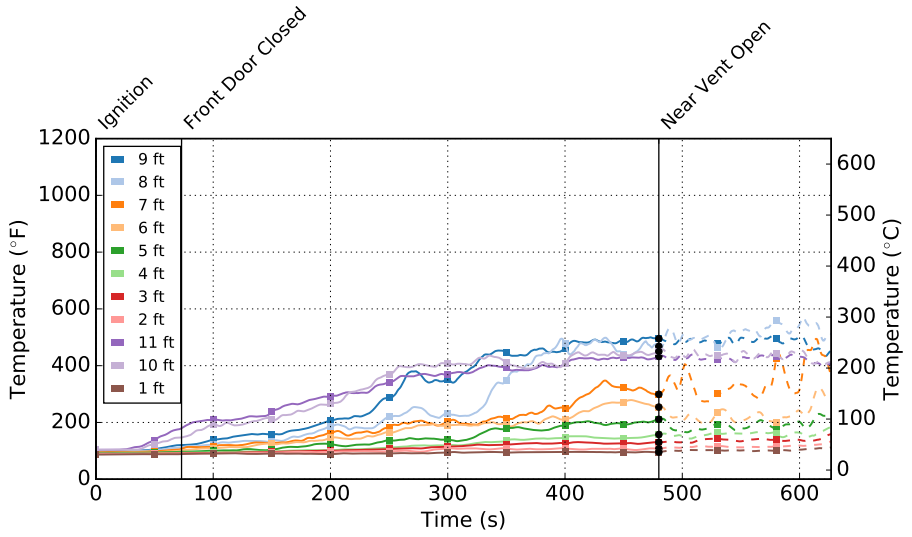

Figure B.8: Room 202 Temperatures for Pallets Experiment 2

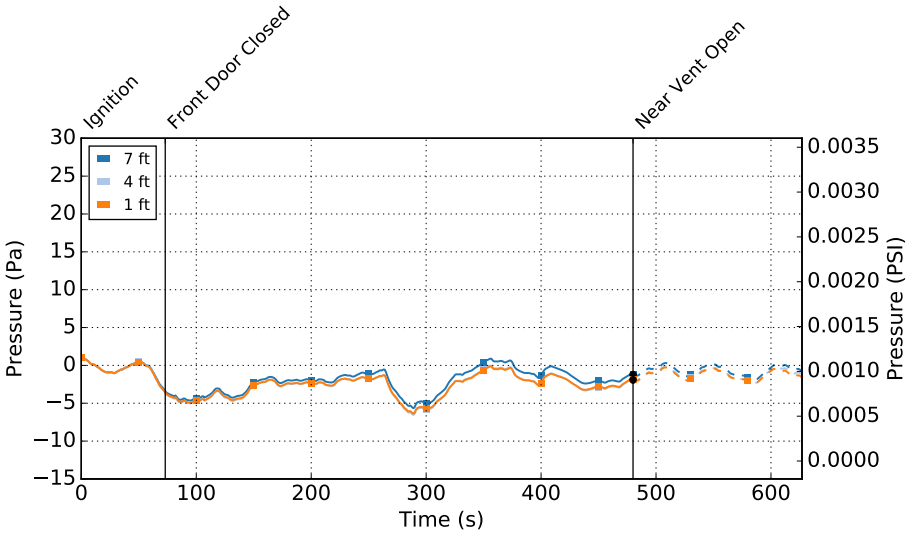

Figure B.9: Room 202 Pressure for Pallets Experiment 2

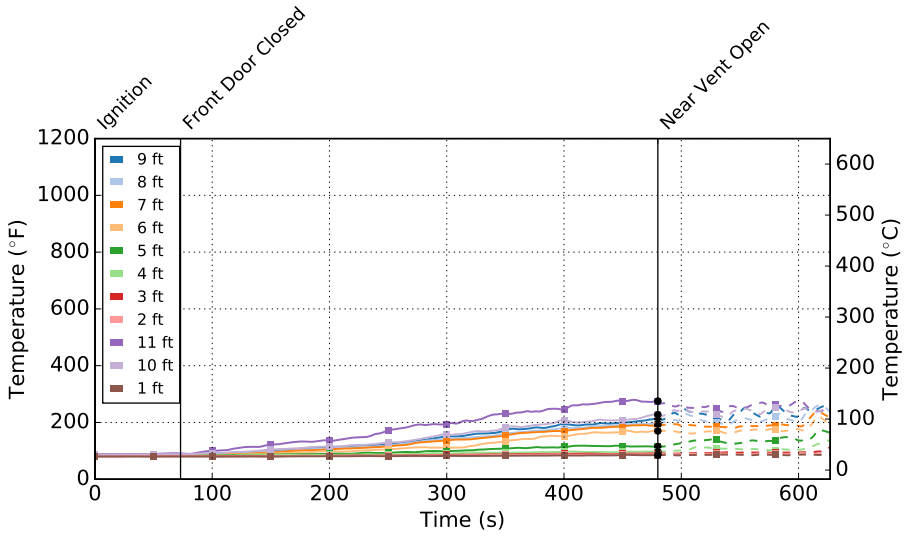

Figure B.10: Room 203 Temperatures for Pallets Experiment 2

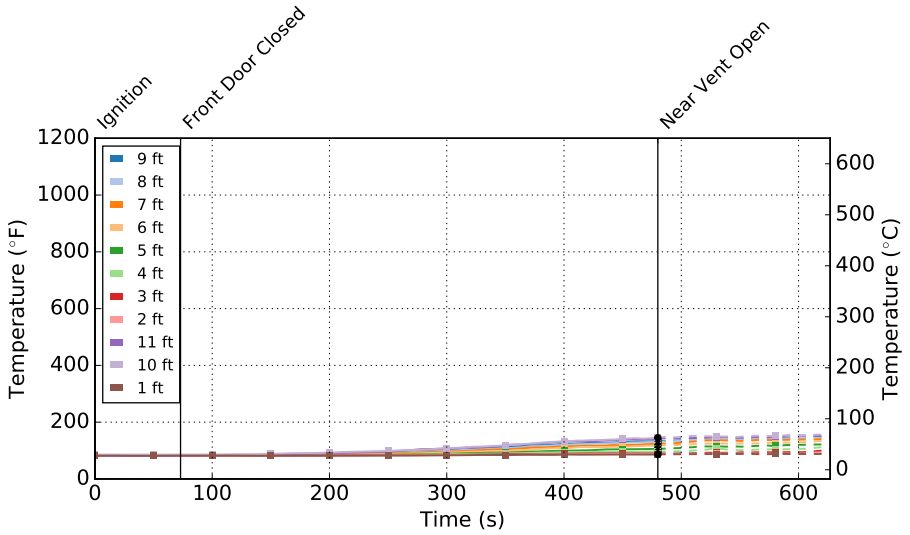

Figure B.11: Room 204 Temperatures for Pallets Experiment 2

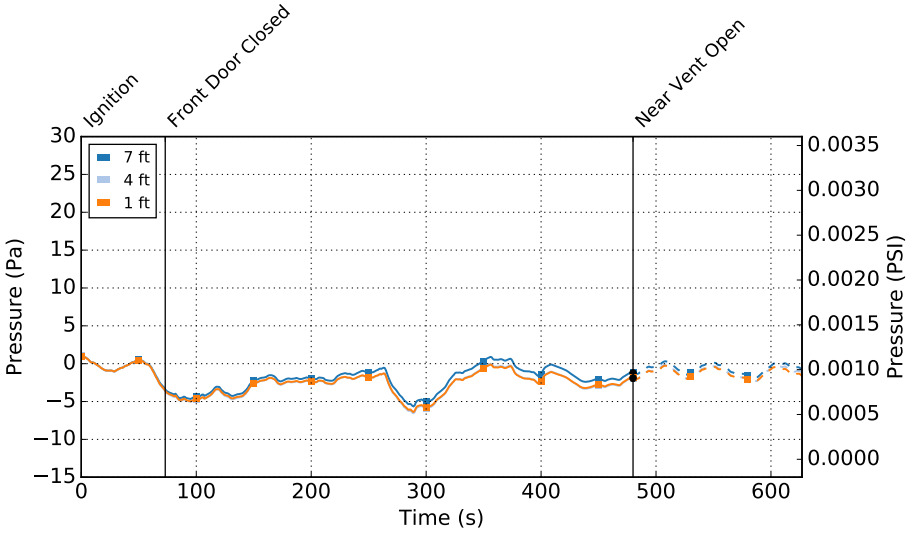

Figure B.12: Room 204 Window Velocity for Pallets Experiment 2

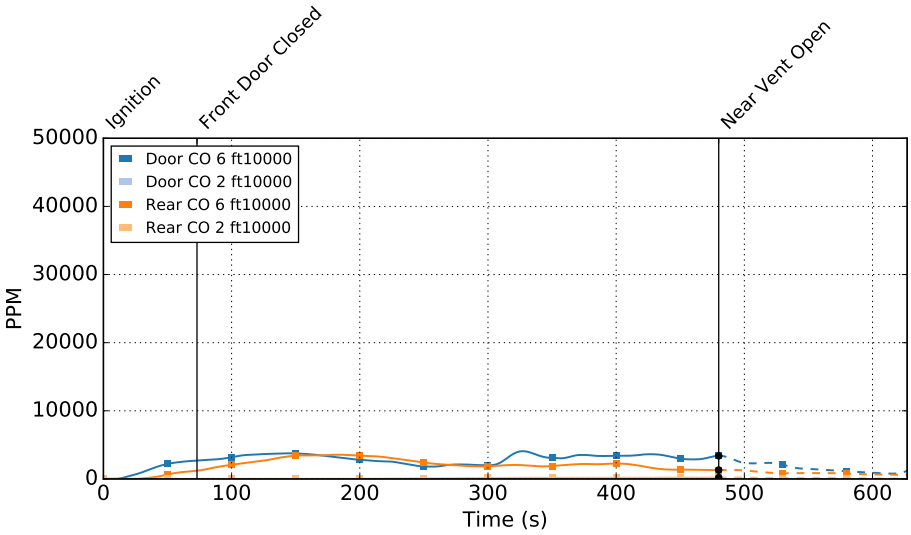

Figure B.13: Room 201 CO Concentrations for Pallets Experiment 2

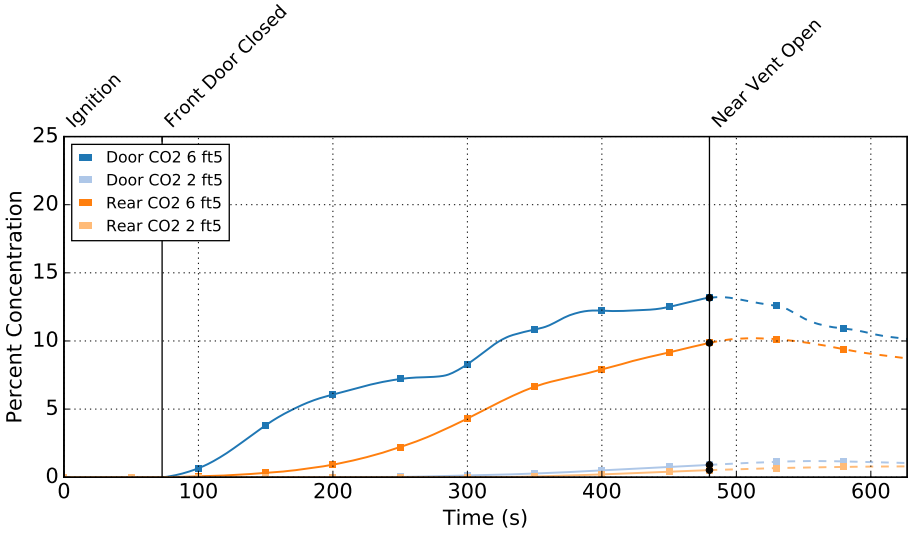

Figure B.14: Room 201 CO_2 Concentrations for Pallets Experiment 2

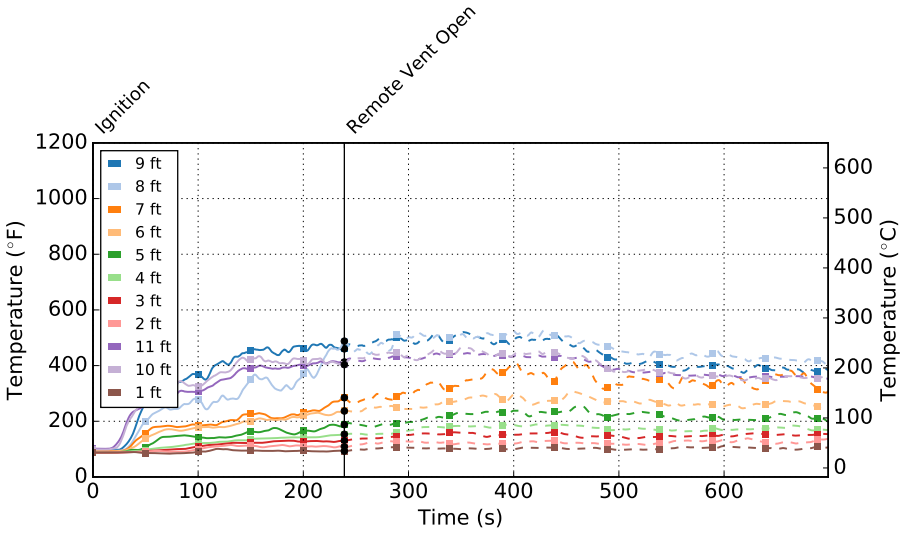

Figure B.15: Room 202 Temperatures for Pallets Experiment 3

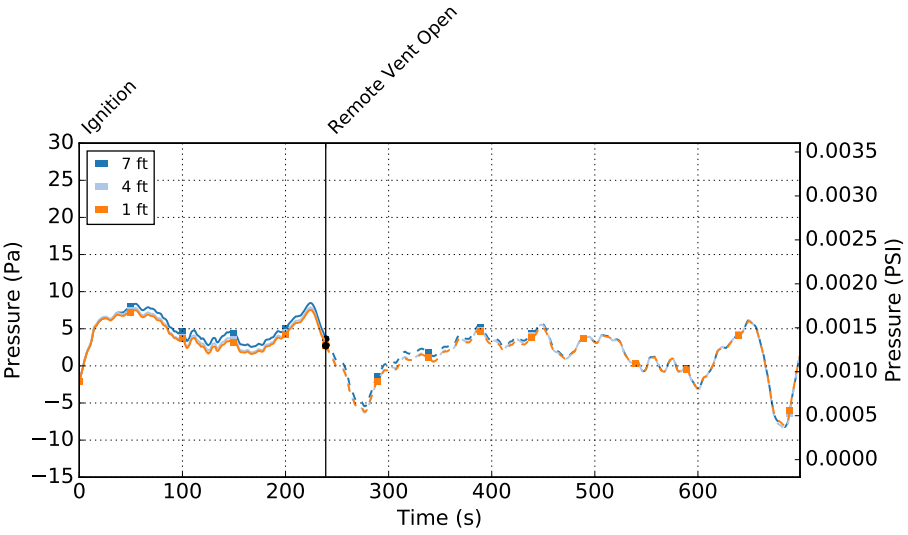

Figure B.16: Room 202 Pressure for Pallets Experiment 3

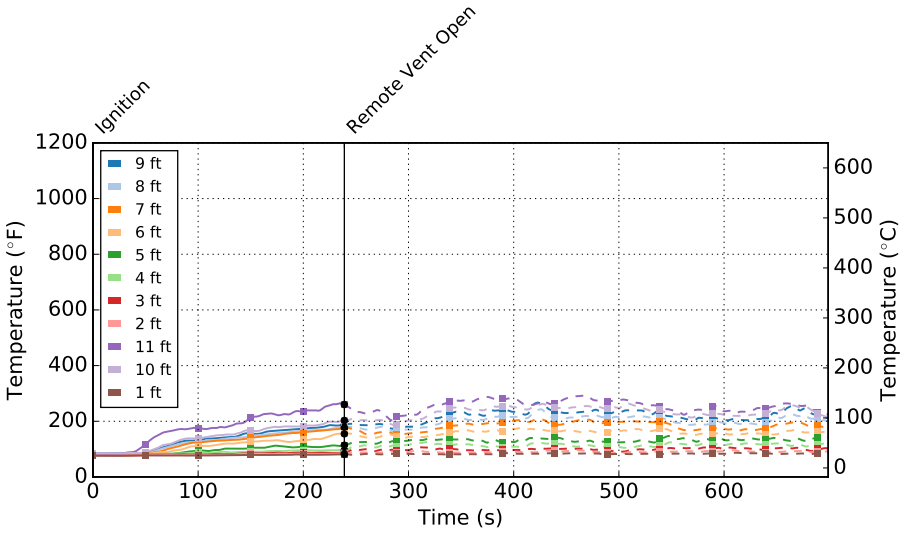

Figure B.17: Room 203 Temperatures for Pallets Experiment 3

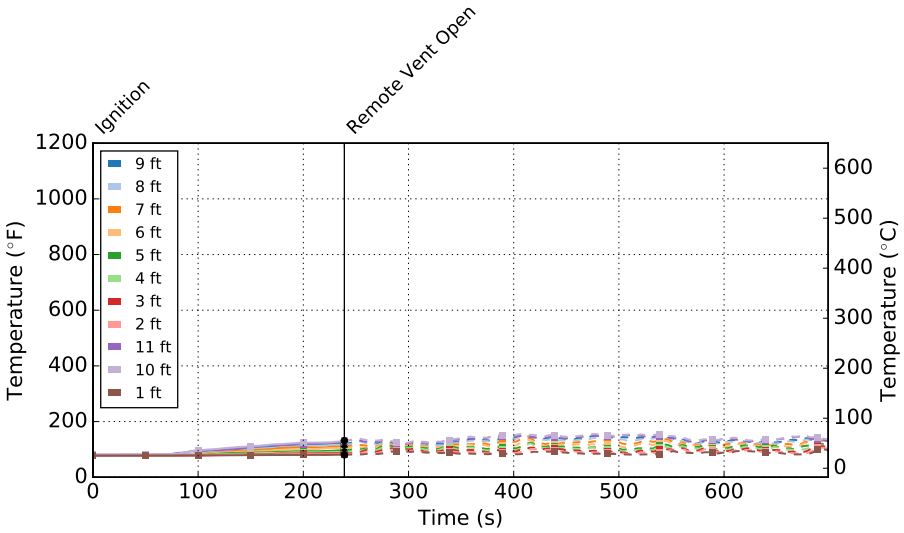

Figure B.18: Room 204 Temperatures for Pallets Experiment 3

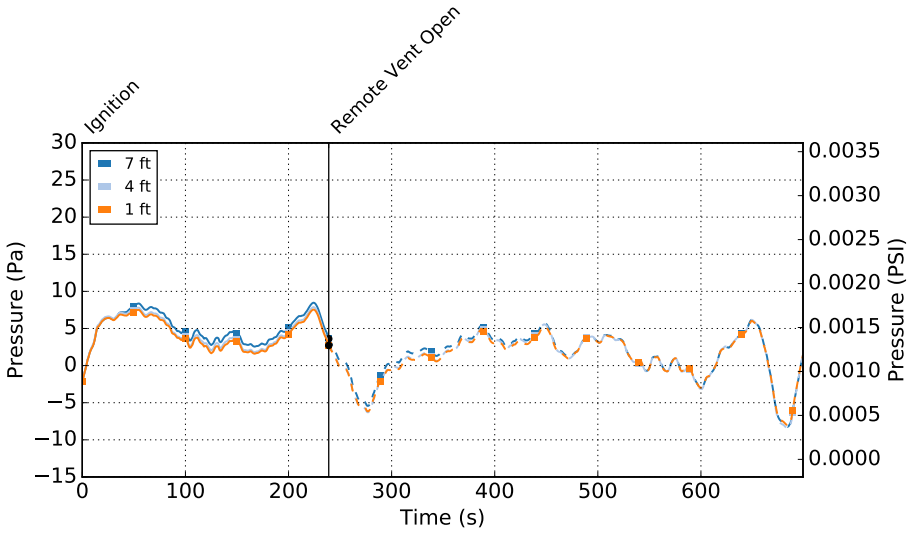

Figure B.19: Room 204 Window Velocity for Pallets Experiment 3

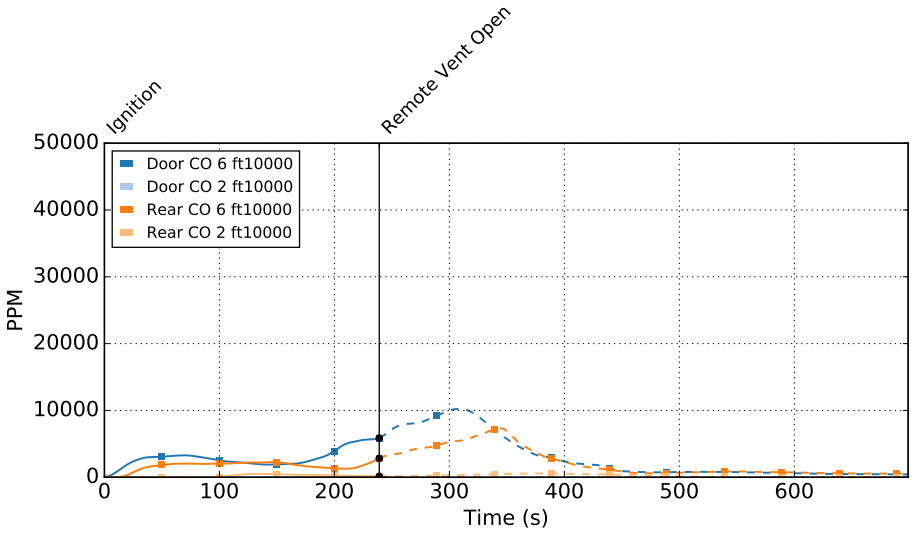

Figure B.20: Room 201 CO Concentrations for Pallets Experiment 3

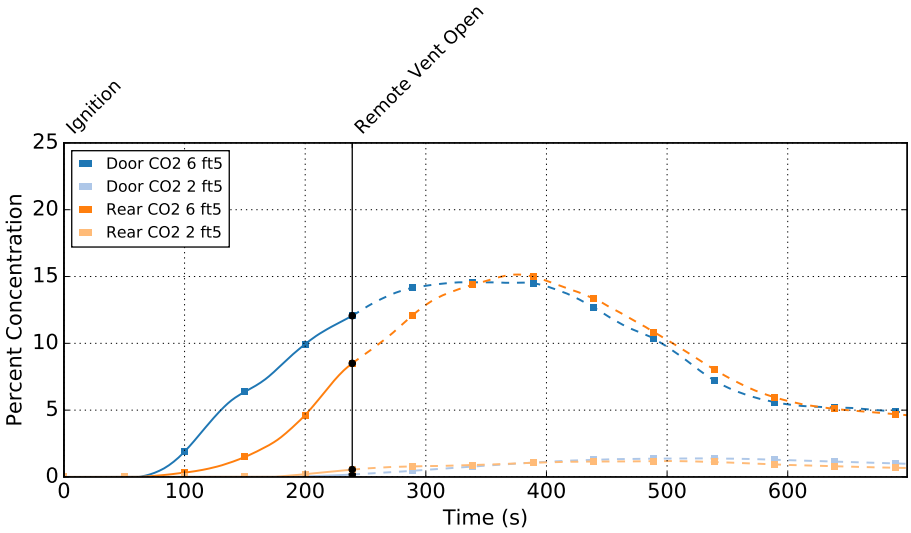

Figure B.21: Room 201 CO_2 Concentrations for Pallets Experiment 3

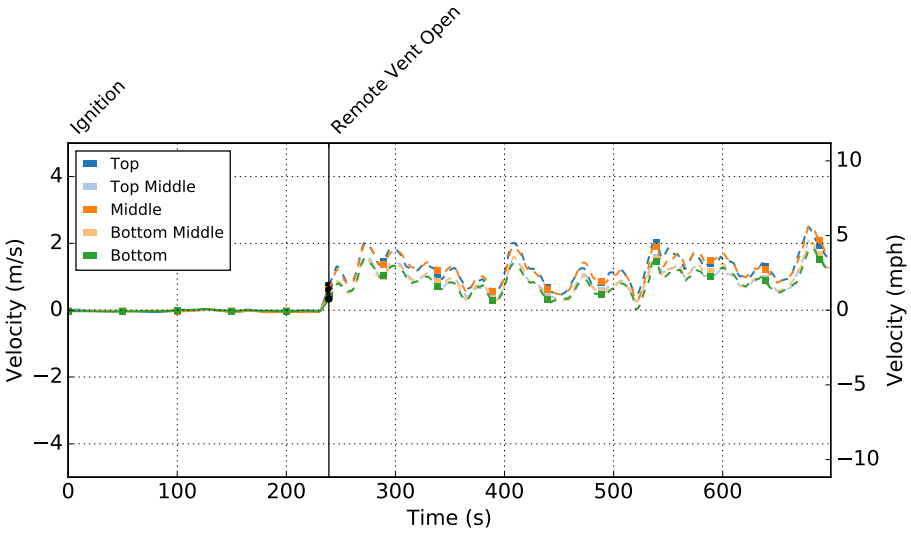

Figure B.22: Room 204 Window Velocity for Pallets Experiment 3

B.3 OSB Experiment Results

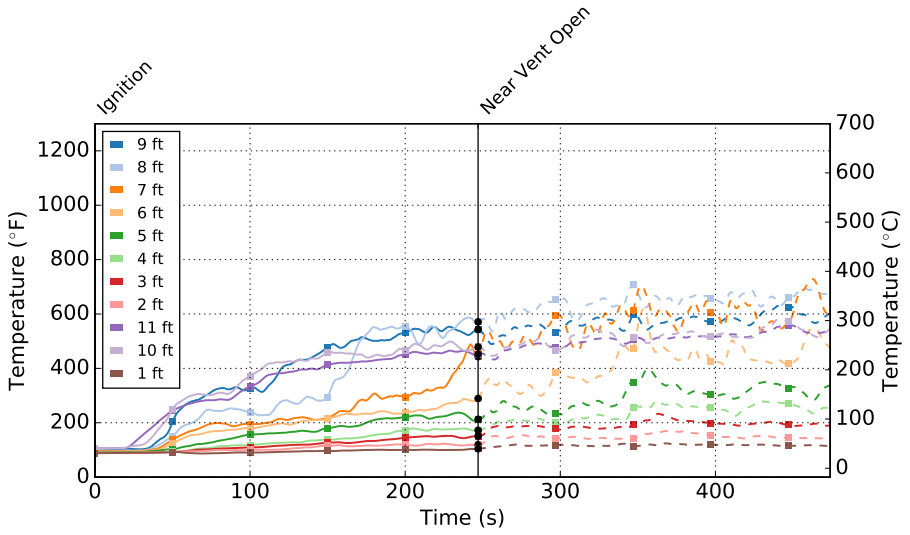

Figure B.23: Room 202 Temperatures for OSB Experiment 1

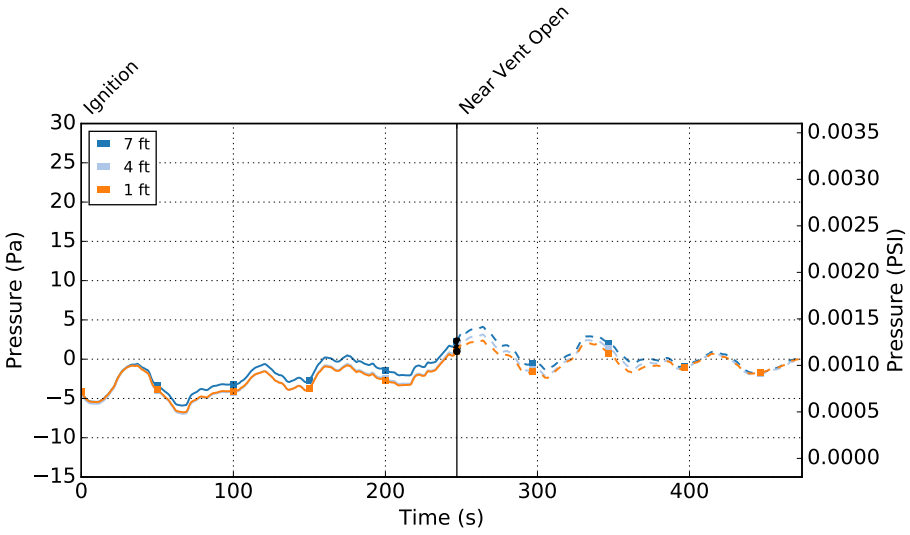

Figure B.24: Room 202 Pressure for OSB Experiment 1

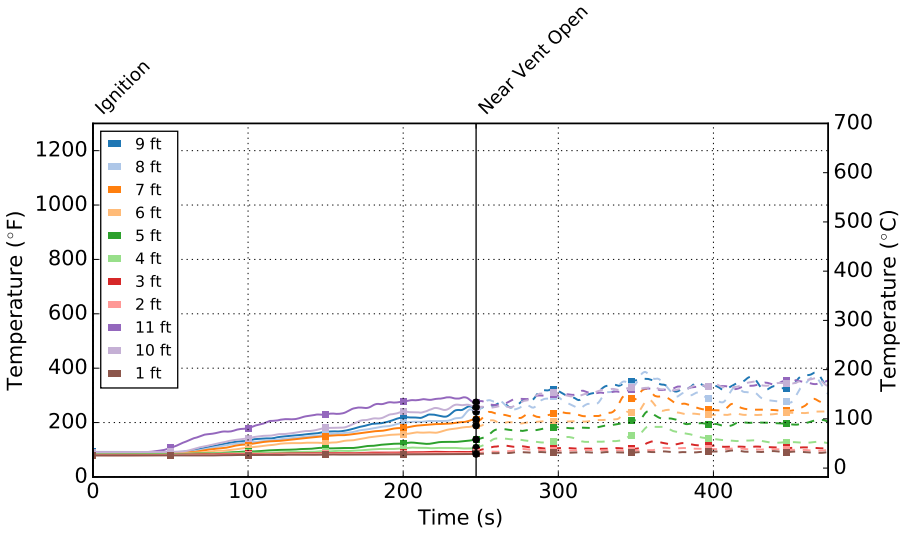

Figure B.25: Room 203 Temperatures for OSB Experiment 1

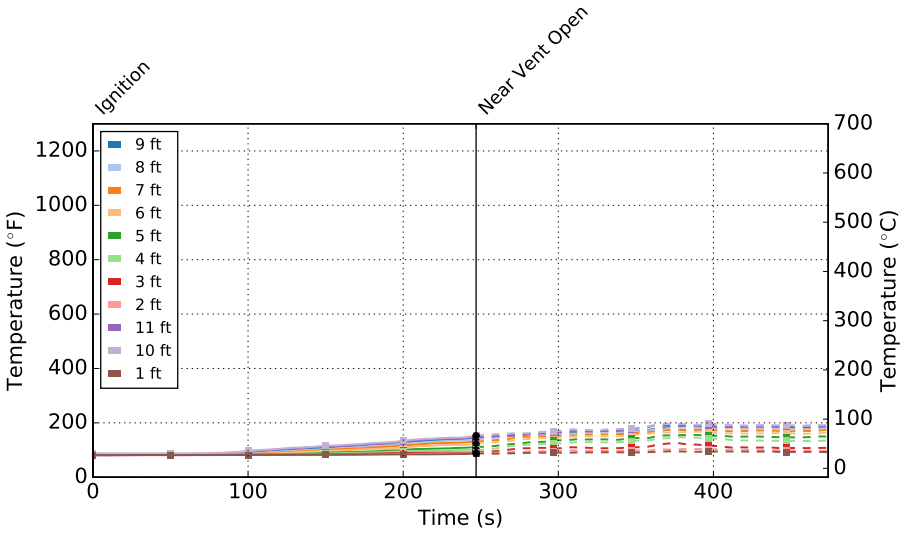

Figure B.26: Room 204 Temperatures for OSB Experiment 1

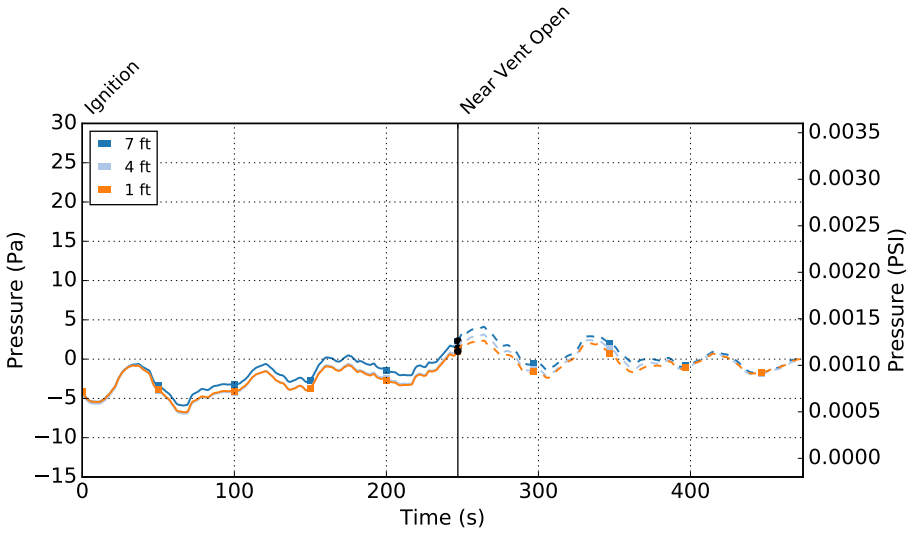

Figure B.27: Room 204 Window Velocity for OSB Experiment 1

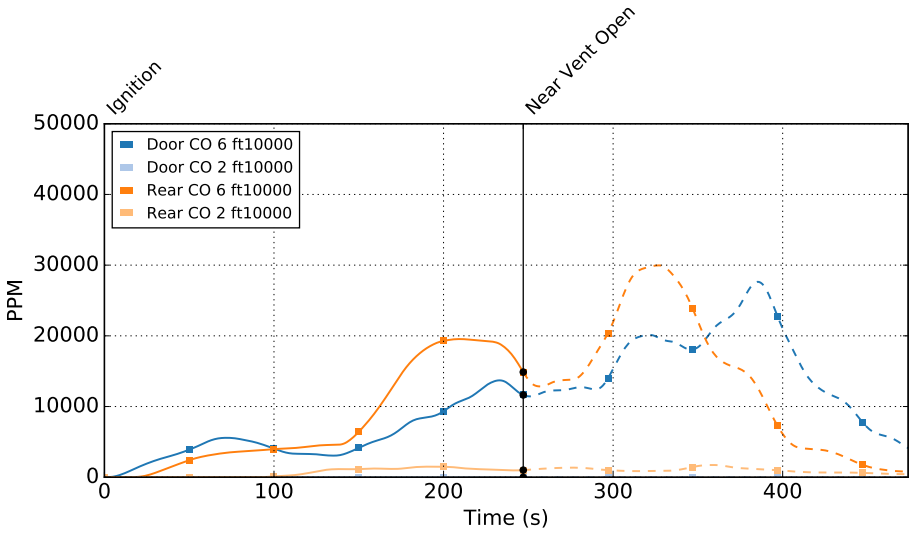

Figure B.28: Room 201 CO Concentrations for OSB Experiment 1

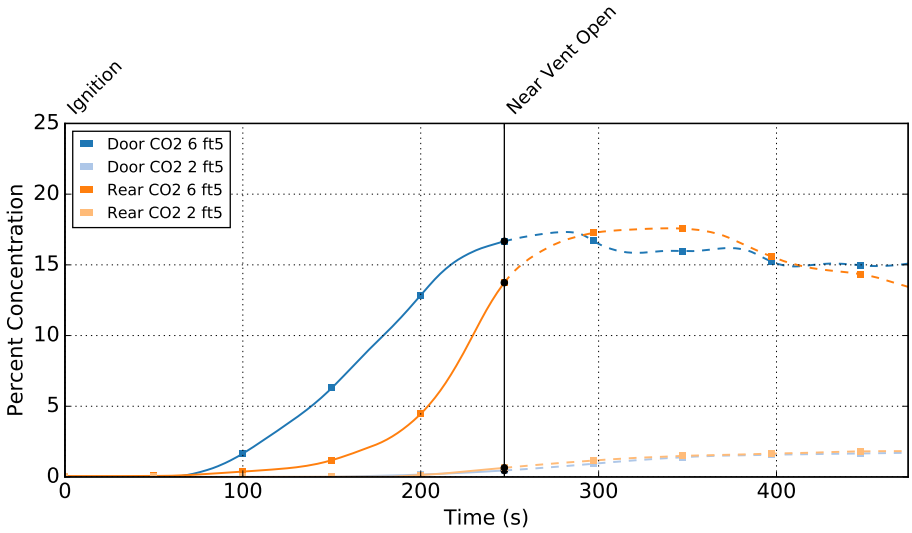

Figure B.29: Room 201 CO_2 Concentrations for OSB Experiment 1

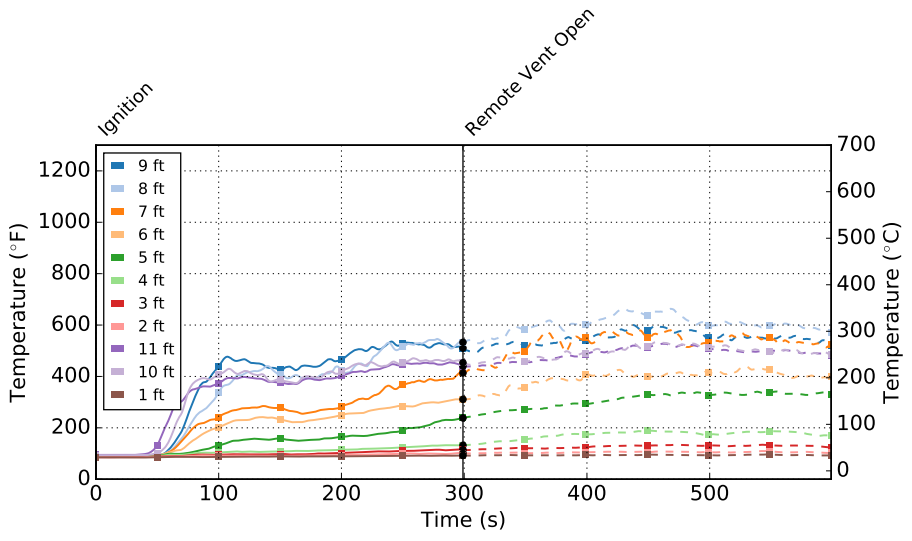

Figure B.30: Room 202 Temperatures for OSB Experiment 2

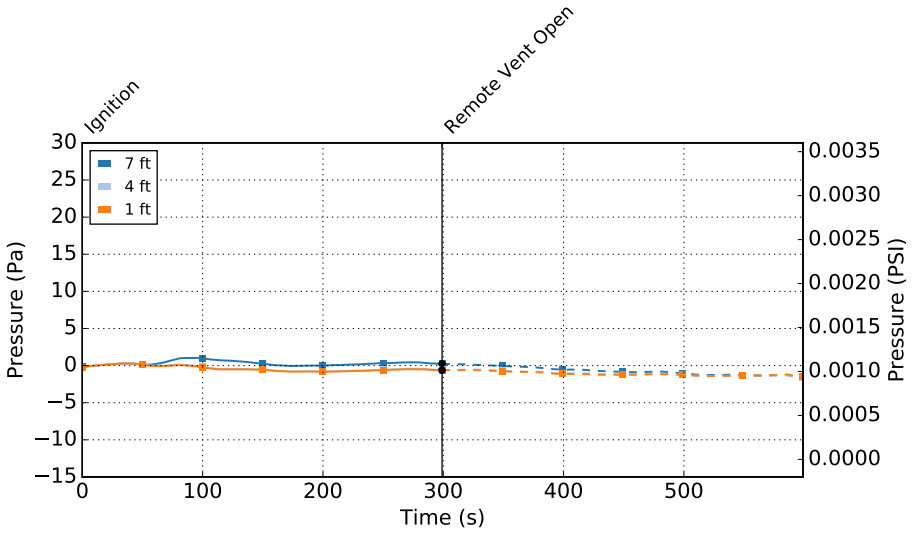

Figure B.31: Room 202 Pressure for OSB Experiment 2

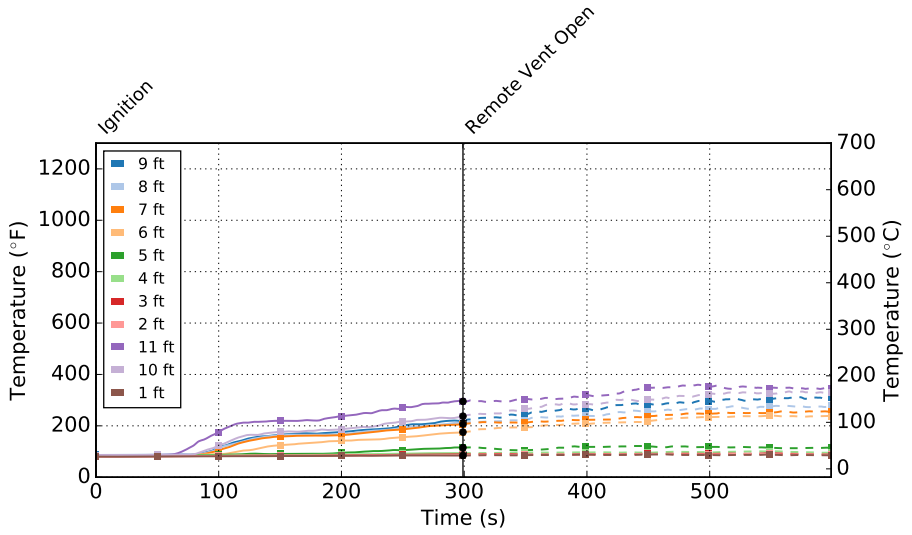

Figure B.32: Room 203 Temperatures for OSB Experiment 2

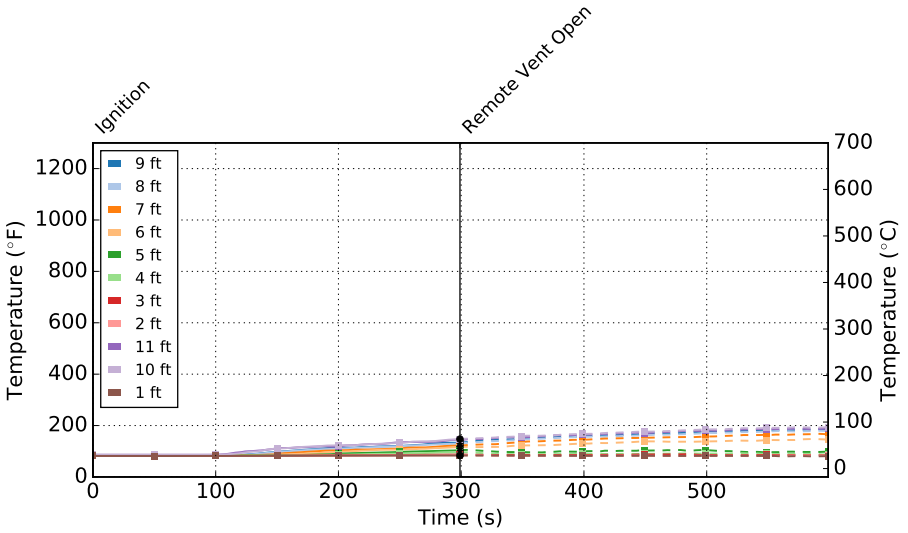

Figure B.33: Room 204 Temperatures for OSB Experiment 2

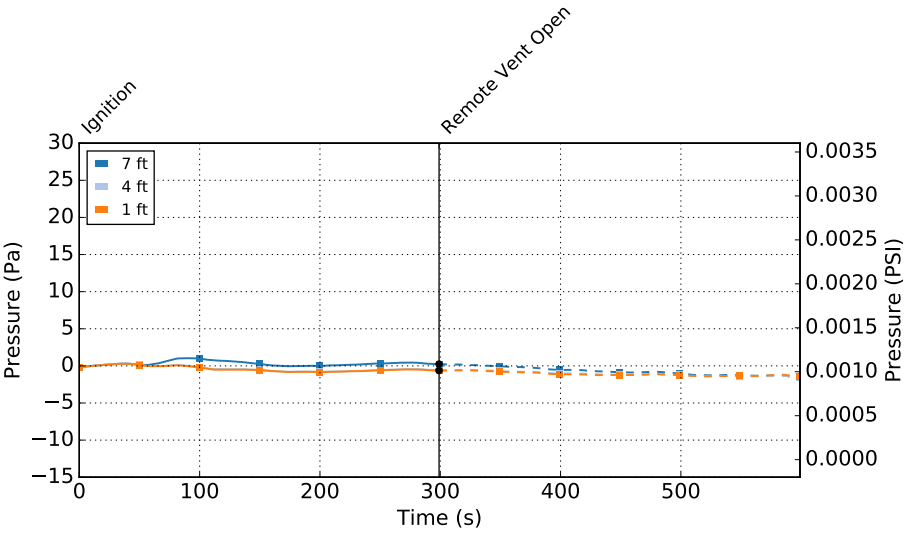

Figure B.34: Room 204 Window Velocity for OSB Experiment 2

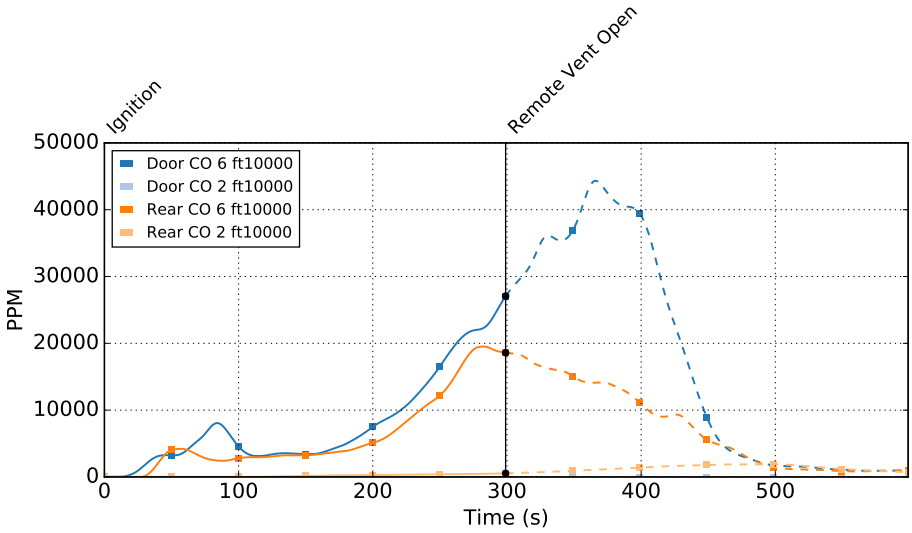

Figure B.35: Room 201 CO Concentrations for OSB Experiment 2

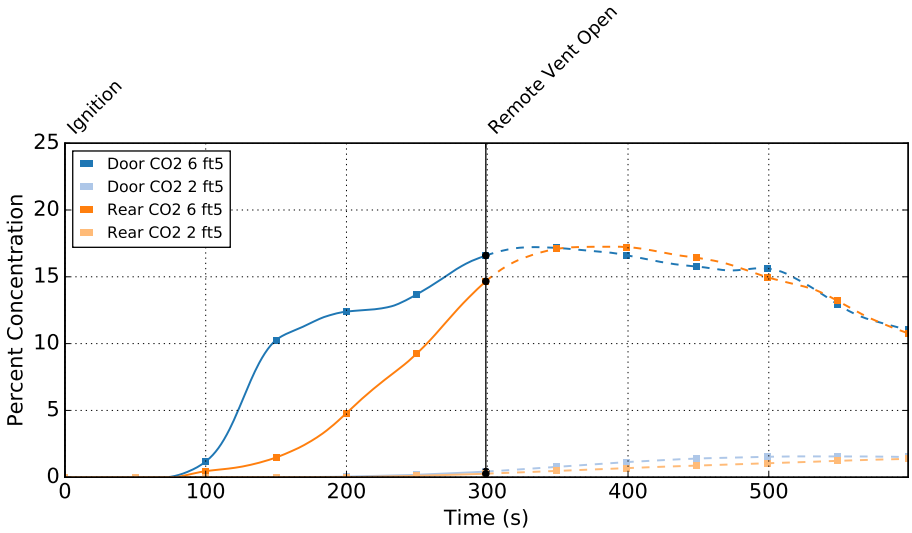

Figure B.36: Room 201 CO_2 Concentrations for OSB Experiment 2

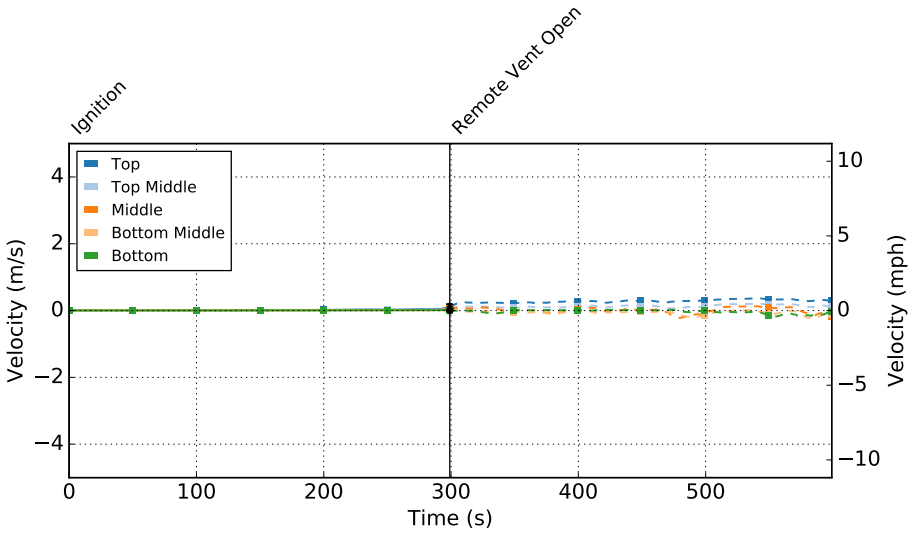

Figure B.37: Room 204 Window Velocity for OSB Experiment 2

B.4 Furniture Experiment Results

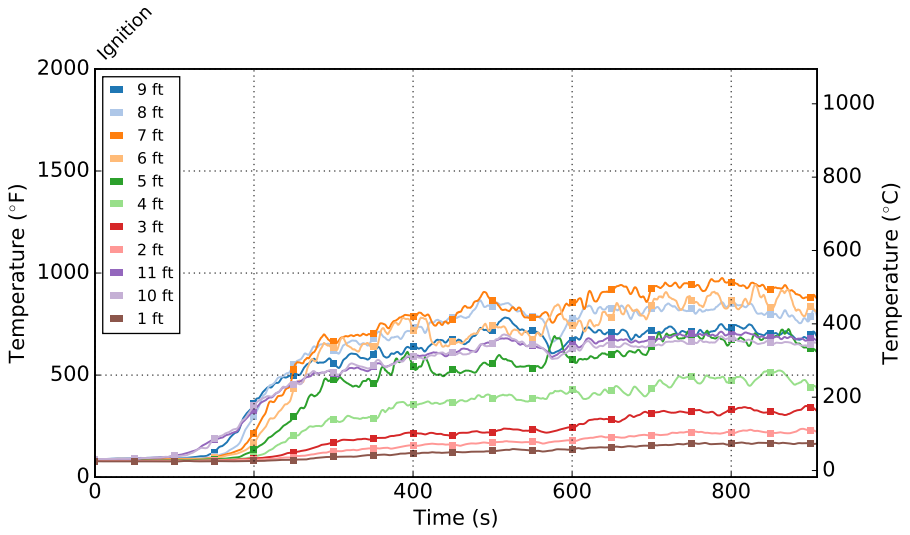

Figure B.38: Room 202 Temperatures for Furniture Experiment 1

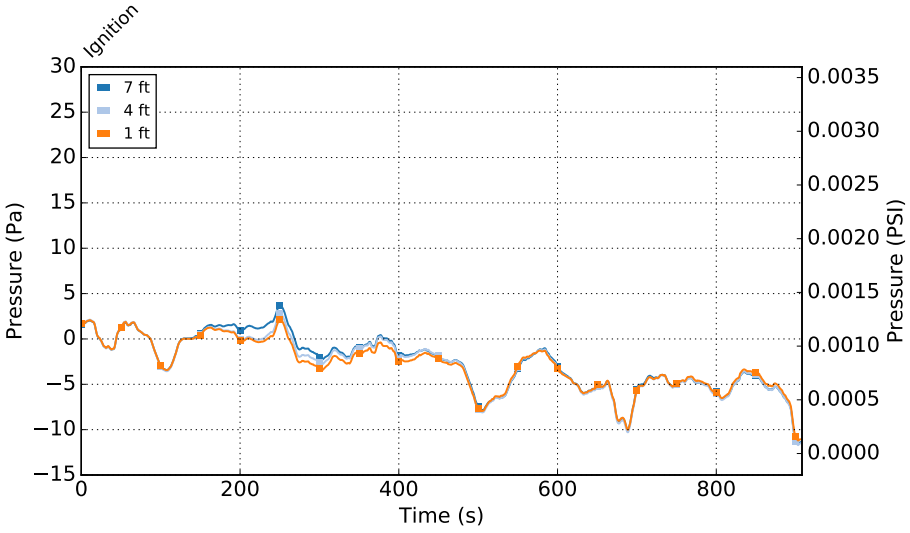

Figure B.39: Room 202 Pressure for Furniture Experiment 1

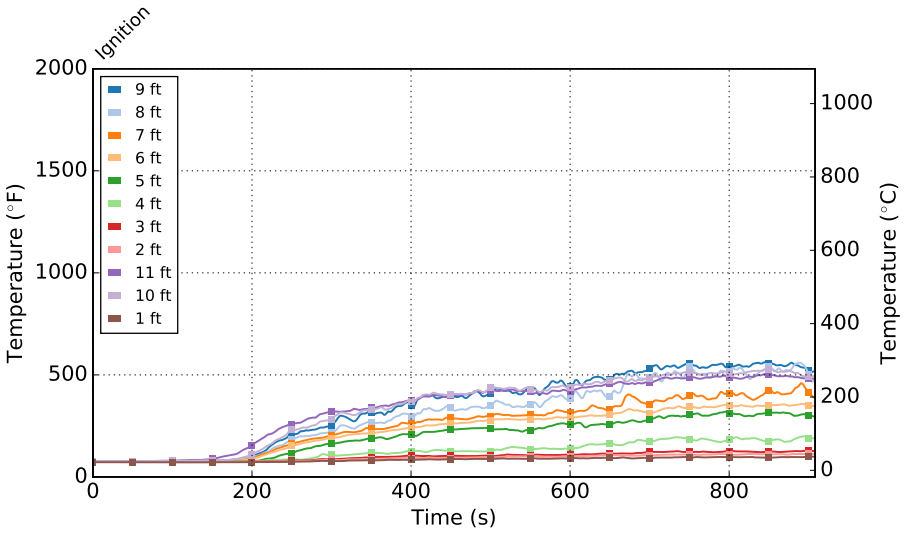

Figure B.40: Room 203 Temperatures for Furniture Experiment 1

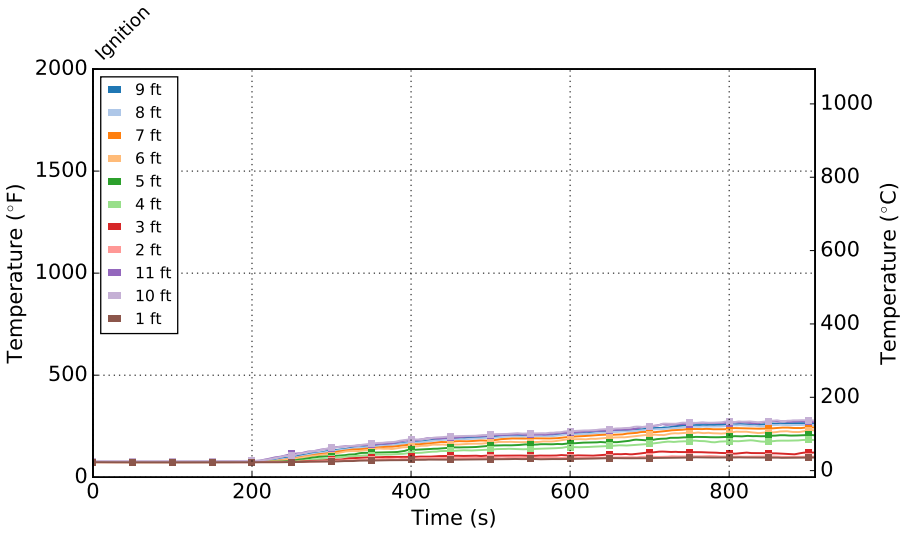

Figure B.41: Room 204 Temperatures for Furniture Experiment 1

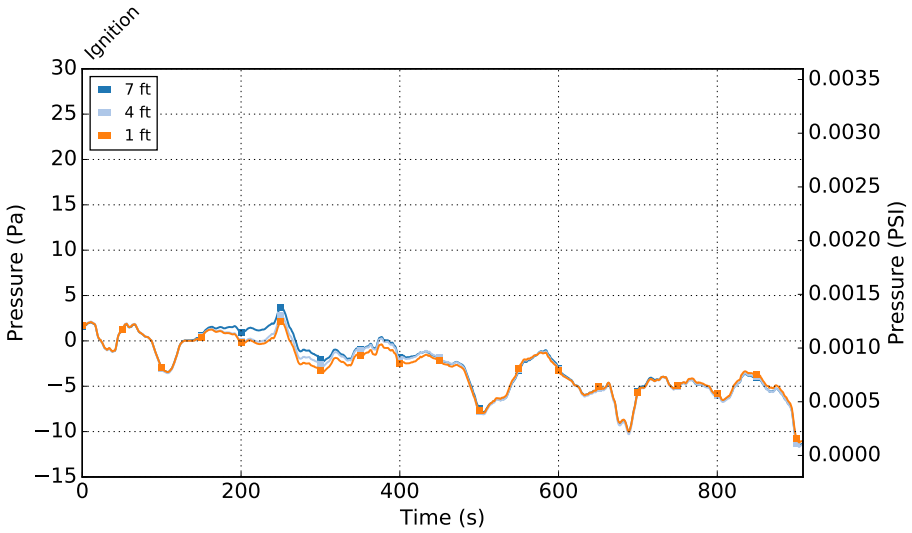

Figure B.42: Room 204 Window Velocity for Furniture Experiment 1

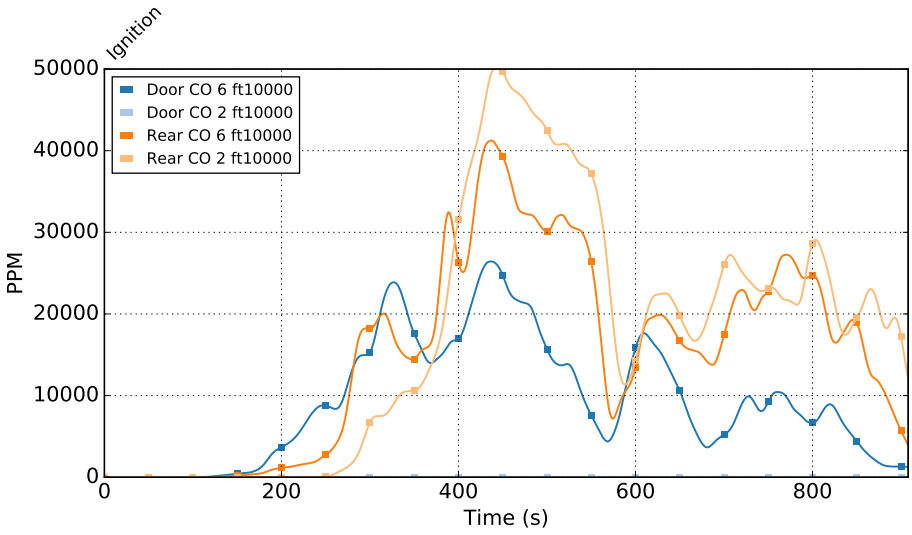

Figure B.43: Room 201 CO Concentrations for Furniture Experiment 1

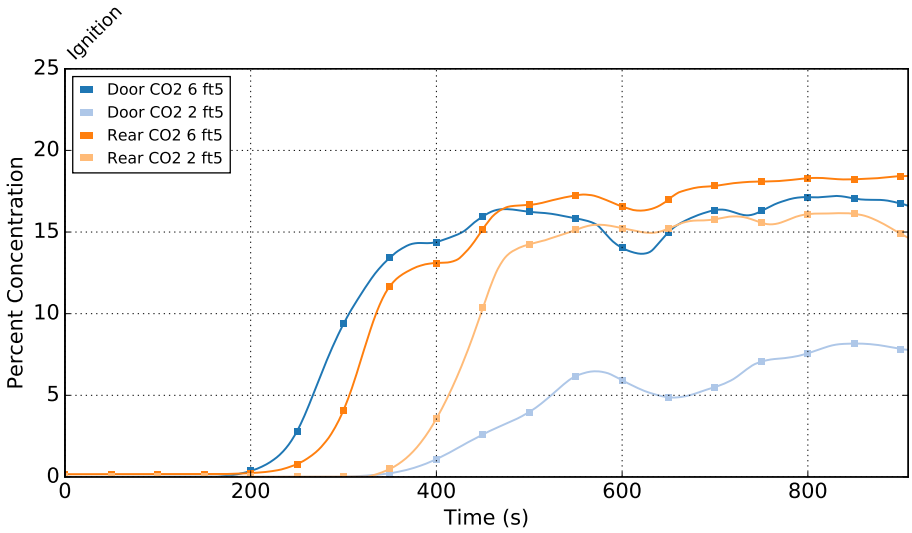

Figure B.44: Room 201 CO_2 Concentrations for Furniture Experiment 1

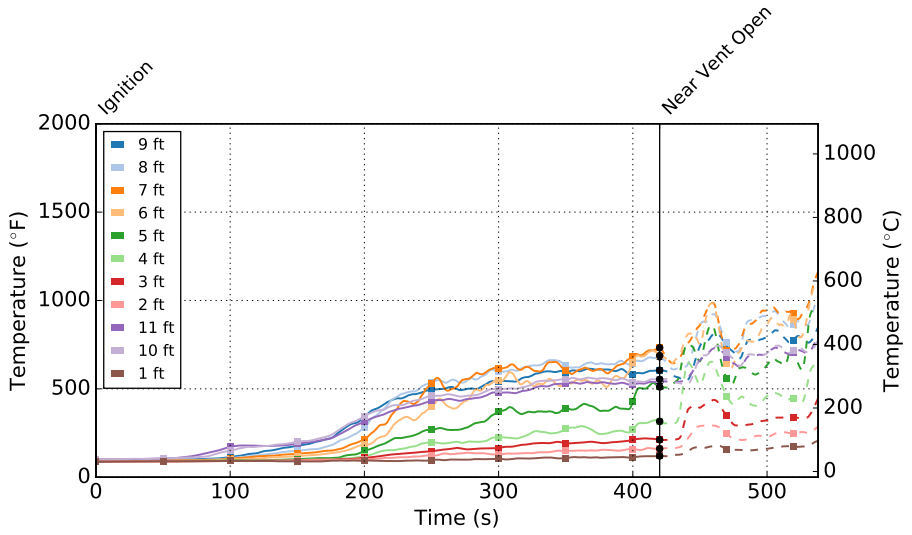

Figure B.45: Room 202 Temperatures for Furniture Experiment 2

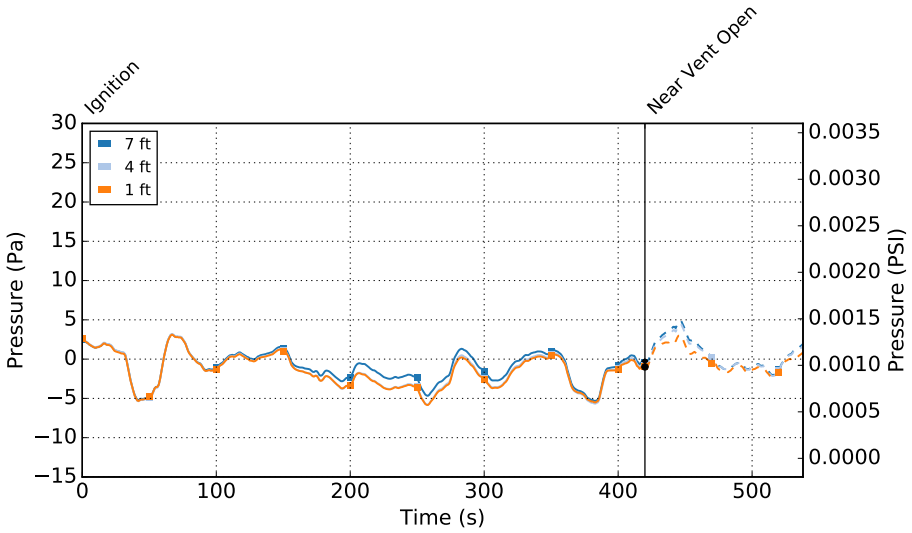

Figure B.46: Room 202 Pressure for Furniture Experiment 2

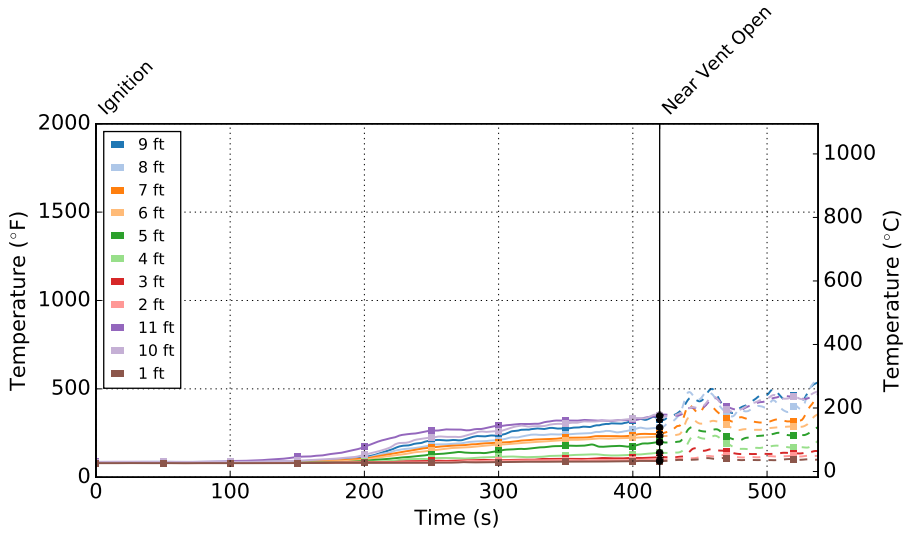

Figure B.47: Room 203 Temperatures for Furniture Experiment 2

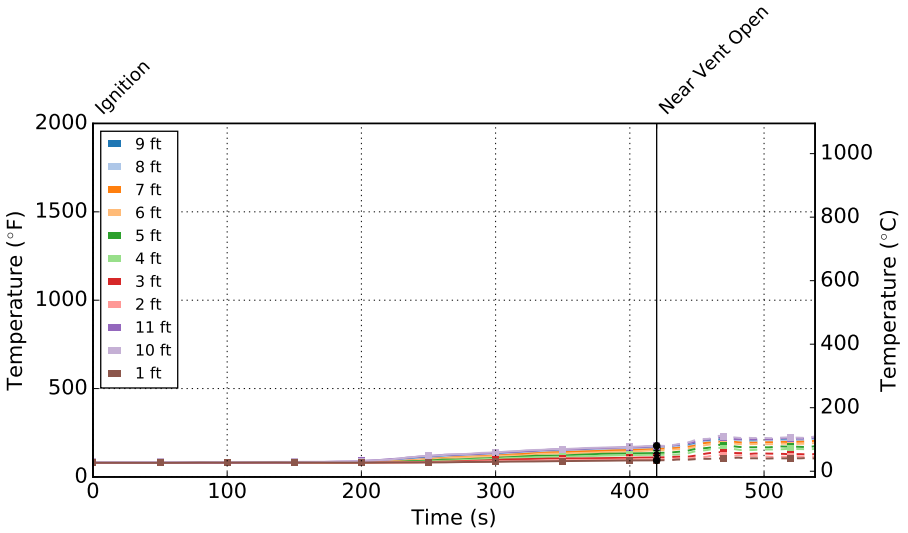

Figure B.48: Room 204 Temperatures for Furniture Experiment 2

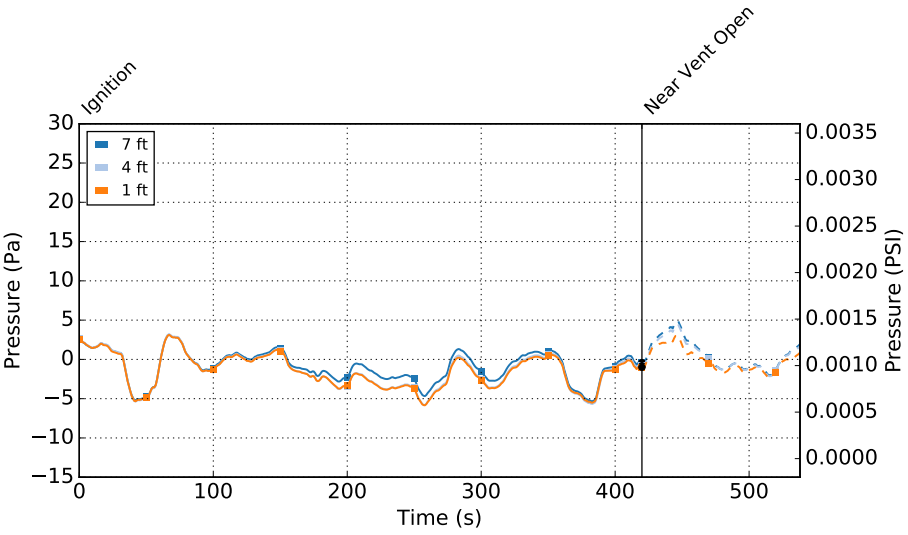

Figure B.49: Room 204 Window Velocity for Furniture Experiment 2

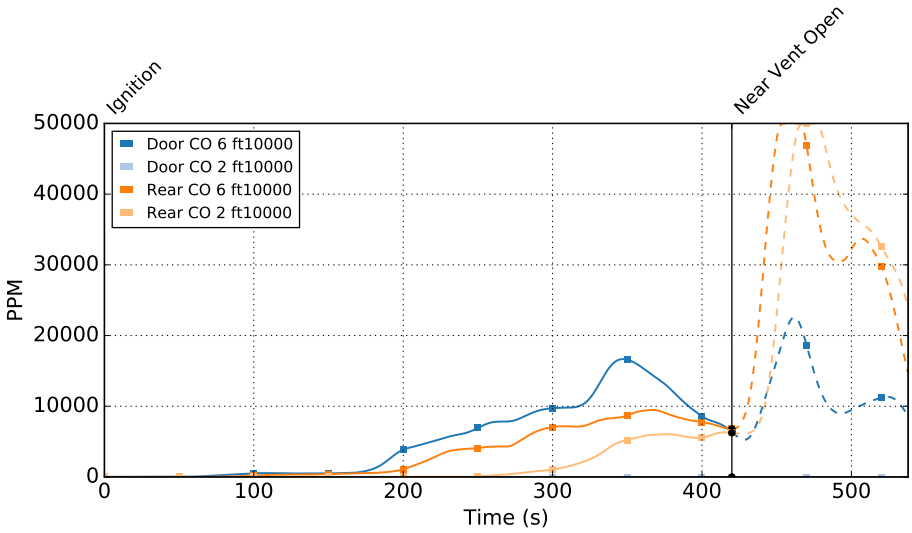

Figure B.50: Room 201 CO Concentrations for Furniture Experiment 2

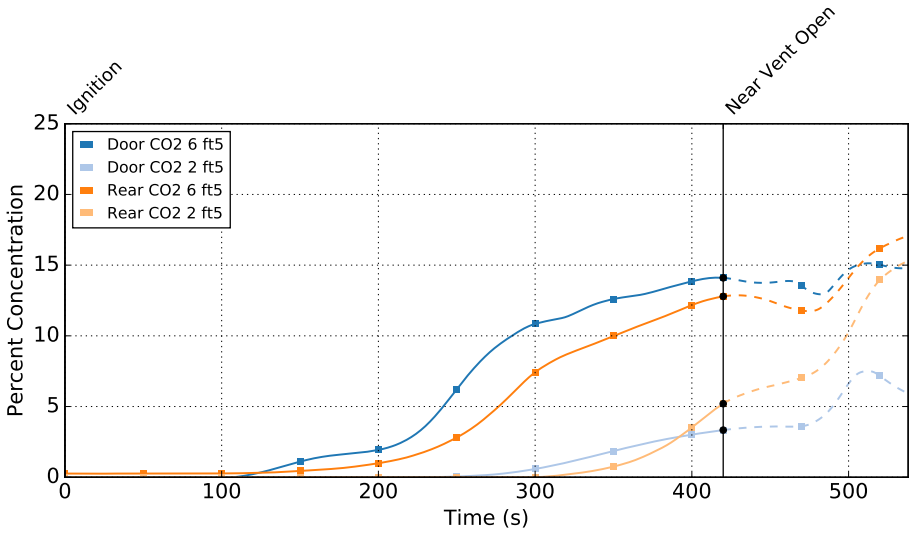

Figure B.51: Room 201 CO_2 Concentrations for Furniture Experiment 2

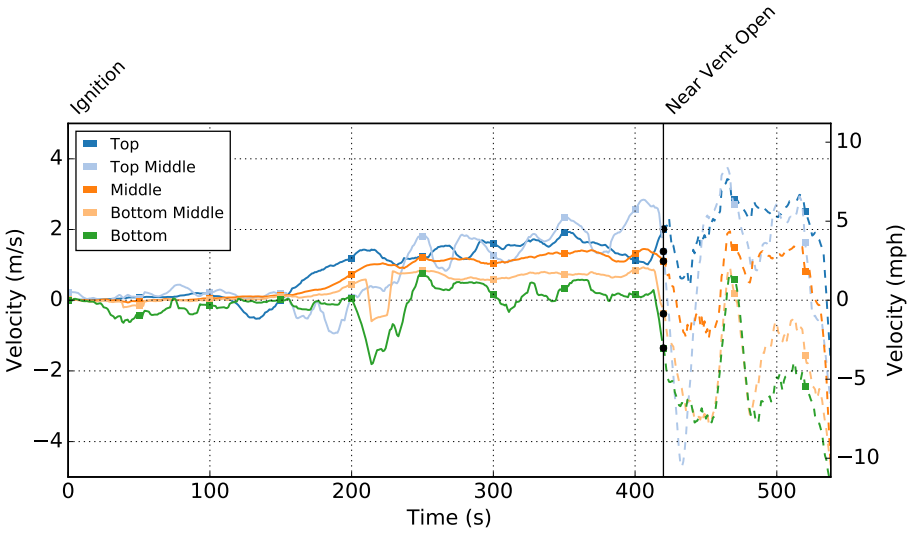

Figure B.52: Room 201 Window Velocity for Furniture Experiment 2

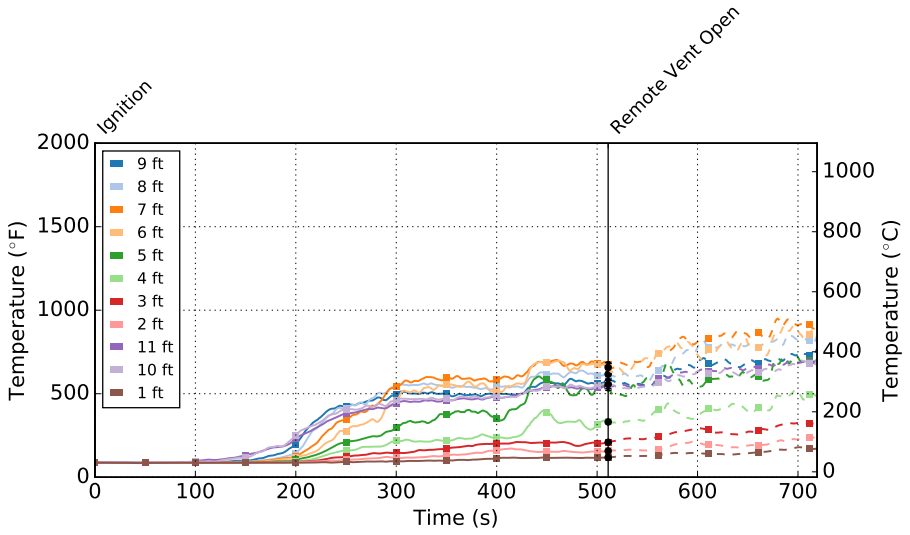

Figure B.53: Room 202 Temperatures for Furniture Experiment 3

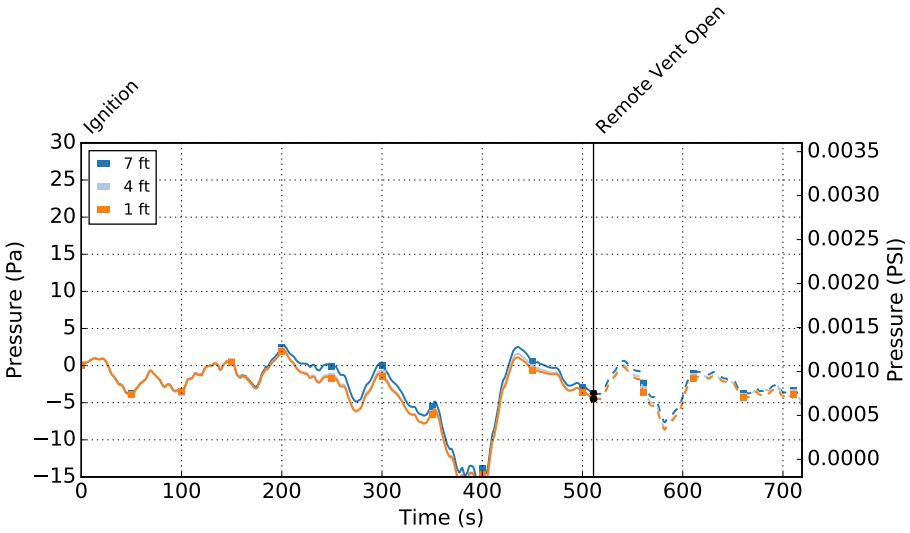

Figure B.54: Room 202 Pressure for Furniture Experiment 3

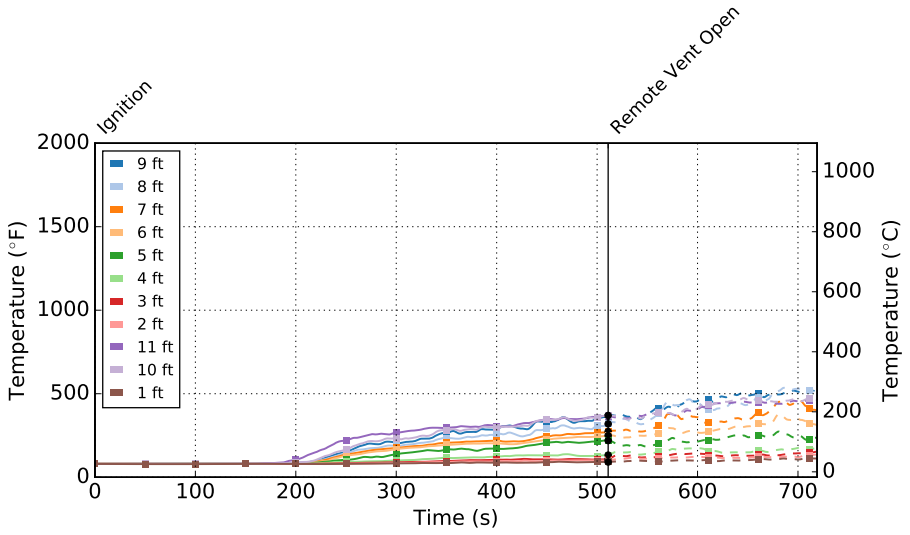

Figure B.55: Room 203 Temperatures for Furniture Experiment 3

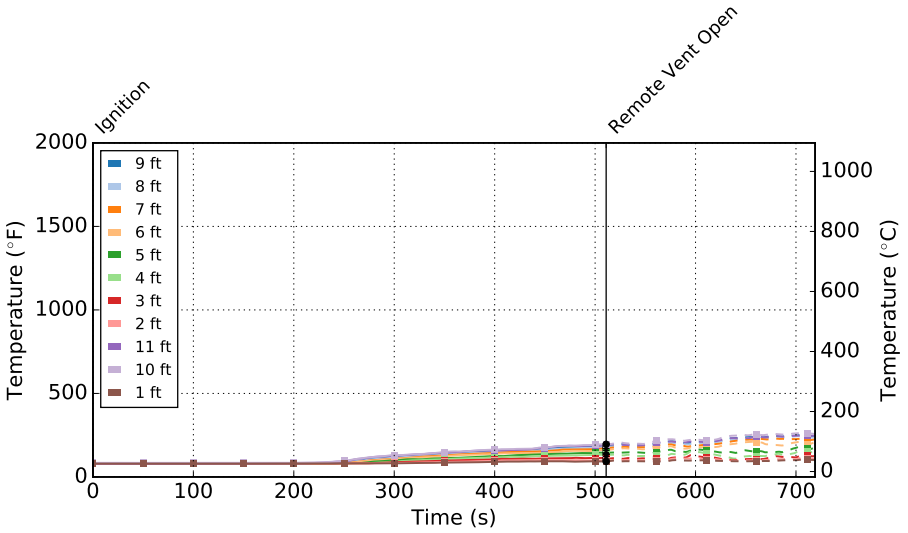

Figure B.56: Room 204 Temperatures for Furniture Experiment 3

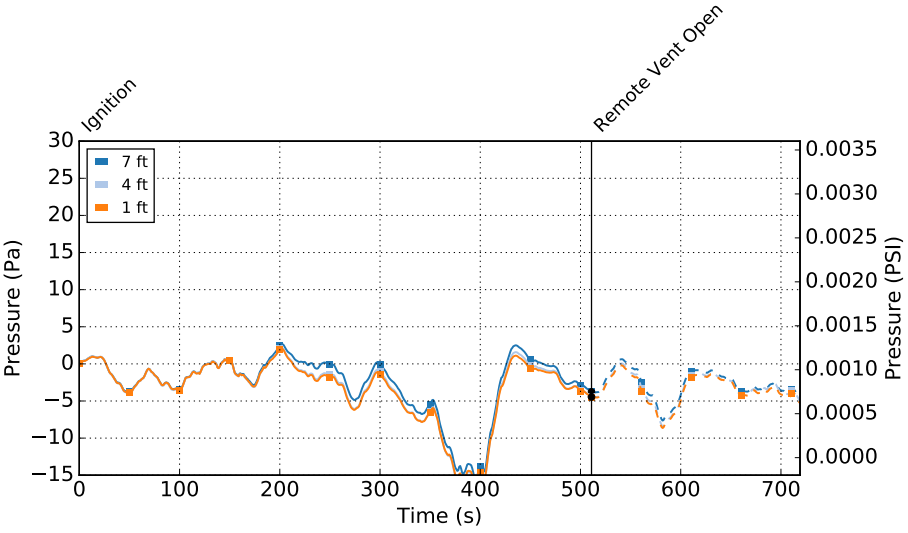

Figure B.57: Room 204 Window Velocity for Furniture Experiment 3

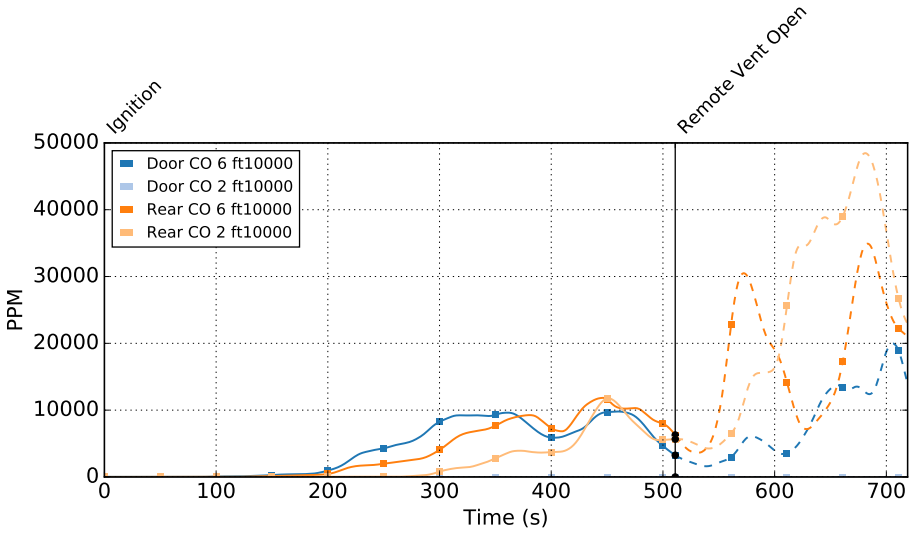

Figure B.58: Room 201 CO Concentrations for Furniture Experiment 3

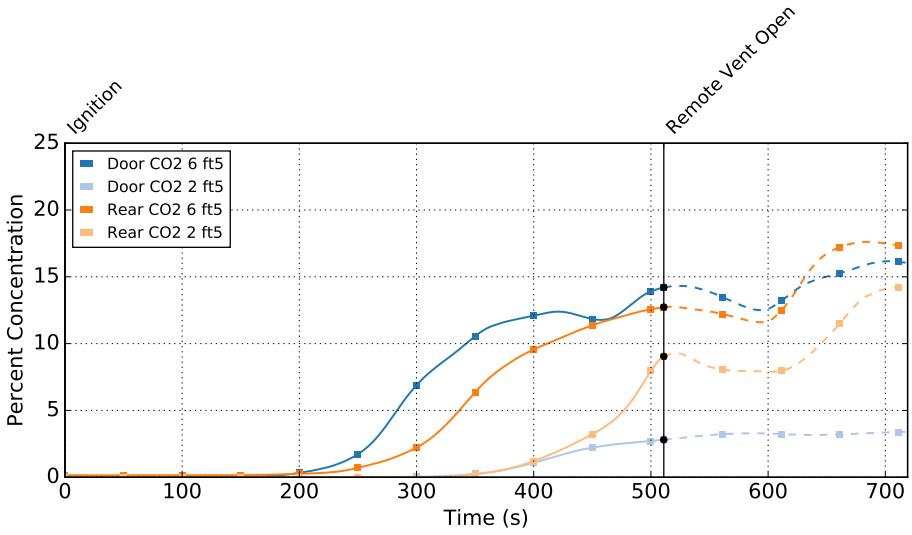

Figure B.59: Room 201 CO_2 Concentrations for Furniture Experiment 3

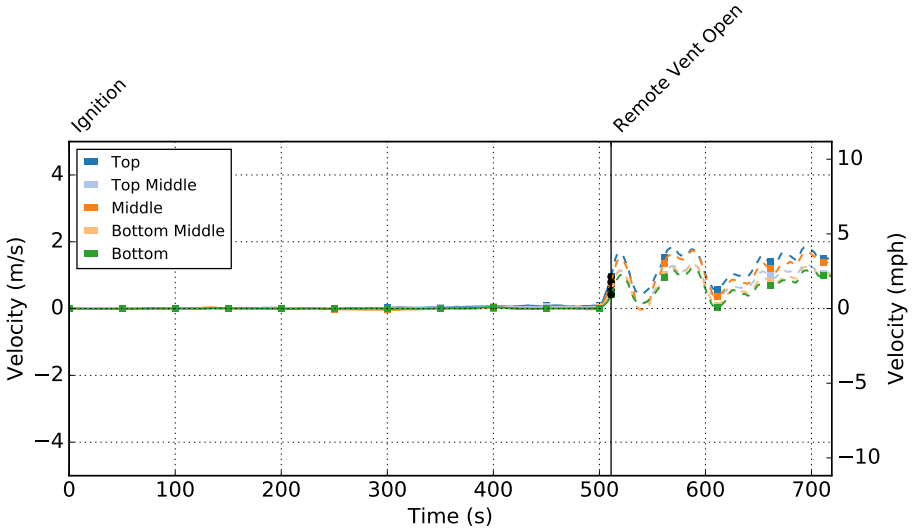

Figure B.60: Room 204 Window Velocity for Furniture Experiment 3

Appendix C: Gear Sample Results

C.1 Gear Sample Results for Pallets and Straw Experiments

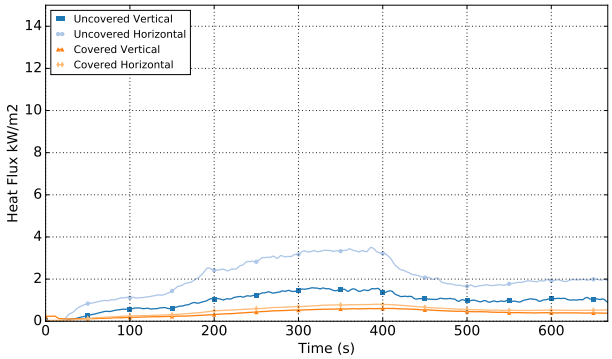

Figure C.1: Gear Sample Heat Flux in Doorway for Pallets Experiment 1

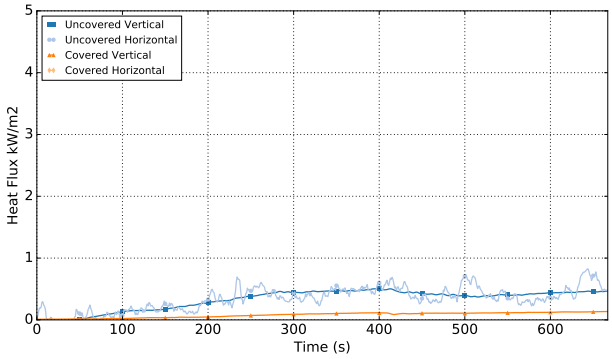

Figure C.2: Gear Sample Heat Flux out of Doorway for Pallets Experiment 1

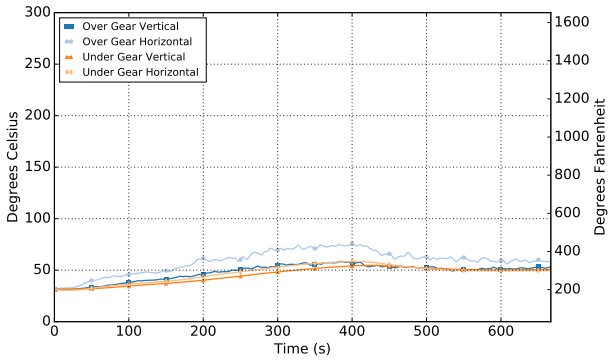

Figure C.3: Gear Sample Temperature in Doorway for Pallets Experiment 1

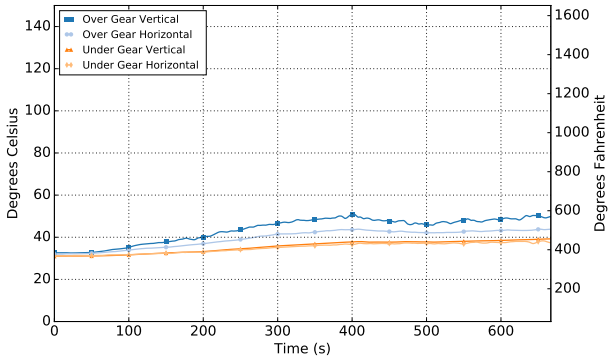

Figure C.4: Gear Sample Temperature out of Doorway for Pallets Experiment 1

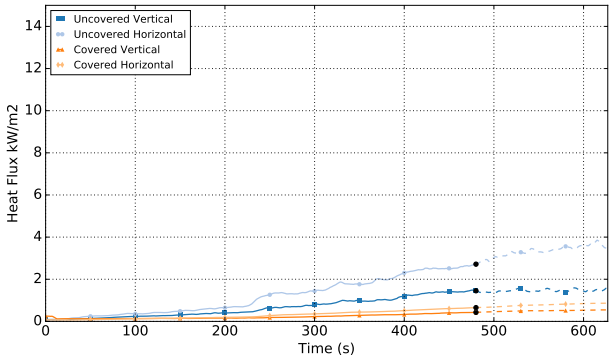

Figure C.5: Gear Sample Heat Flux in Doorway for Pallets Experiment 2

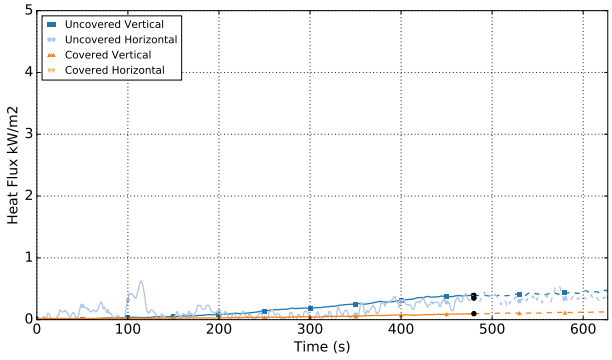

Figure C.6: Gear Sample Heat Flux out of Doorway for Pallets Experiment 2

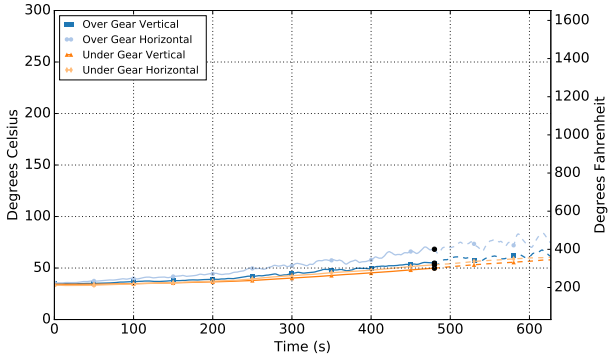

Figure C.7: Gear Sample Temperature in Doorway for Pallets Experiment 2

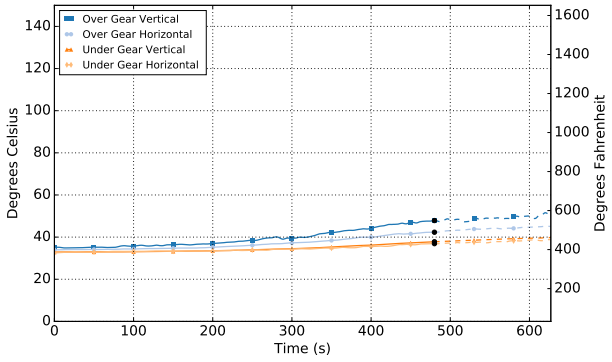

Figure C.8: Gear Sample Temperature out of Doorway for Pallets Experiment 2

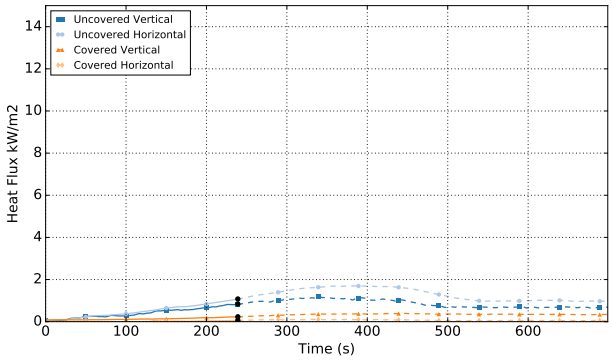

Figure C.9: Gear Sample Heat Flux in Doorway for Pallets Experiment 3

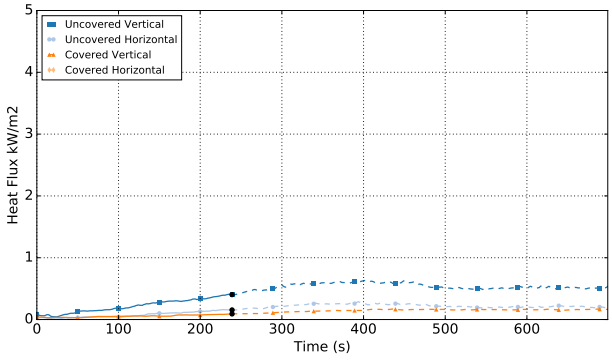

Figure C.10: Gear Sample Heat Flux out of Doorway for Pallets Experiment 3

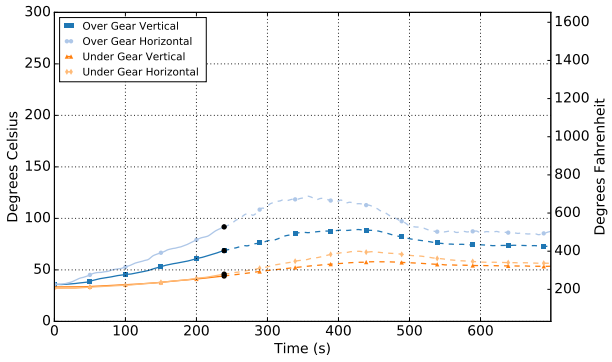

Figure C.11: Gear Sample Temperature in Doorway for Pallets Experiment 3

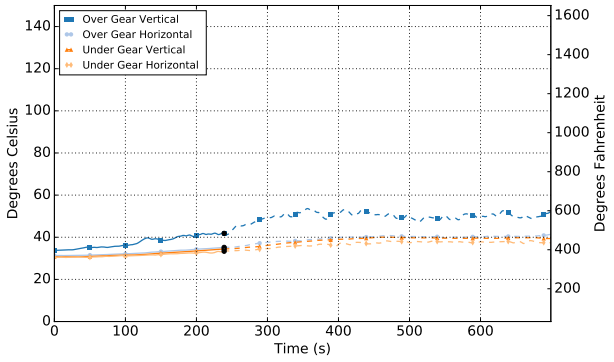

Figure C.12: Gear Sample Temperature out of Doorway for Pallets Experiment 3

C.2 Gear Sample Results for OSB Experiments

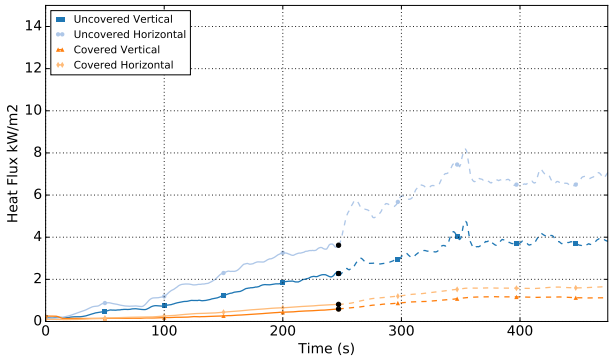

Figure C.13: Gear Sample Heat Flux in Doorway for OSB Experiment 1

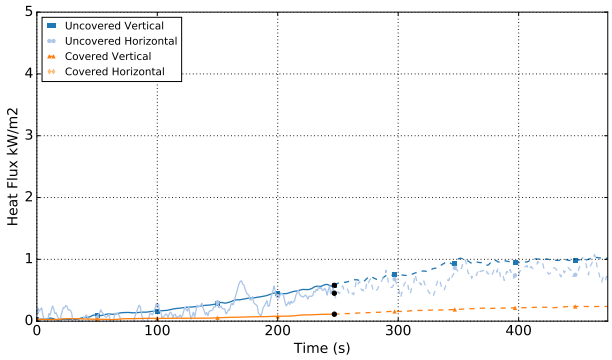

Figure C.14: Gear Sample Heat Flux out of Doorway for OSB Experiment 1

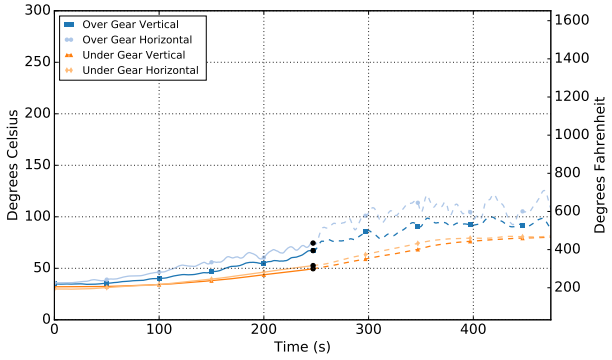

Figure C.15: Gear Sample Temperature in Doorway for OSB Experiment 1

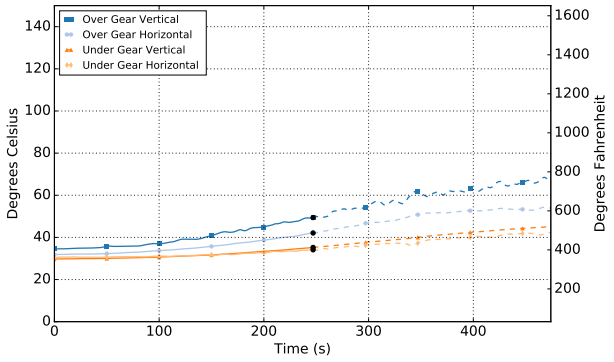

Figure C.16: Gear Sample Temperature out of Doorway for OSB Experiment 1

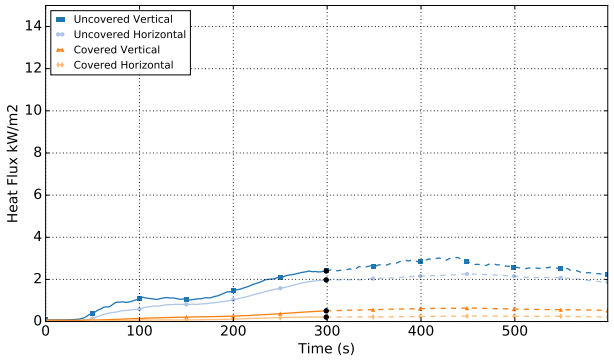

Figure C.17: Gear Sample Heat Flux in Doorway for OSB Experiment 2

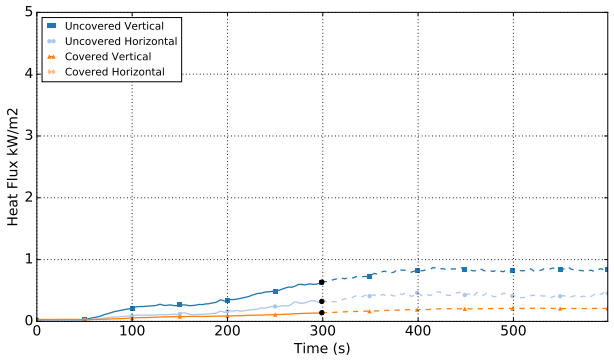

Figure C.18: Gear Sample Heat Flux out of Doorway for OSB Experiment 2

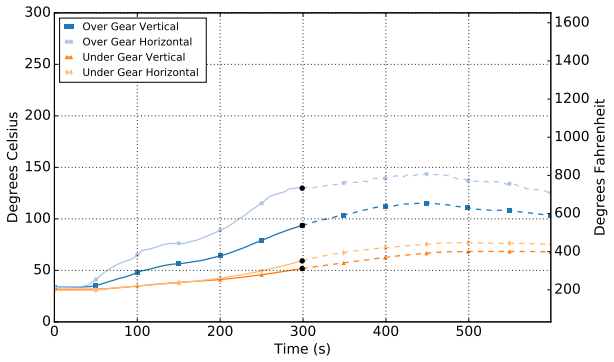

Figure C.19: Gear Sample Temperature in Doorway for OSB Experiment 2

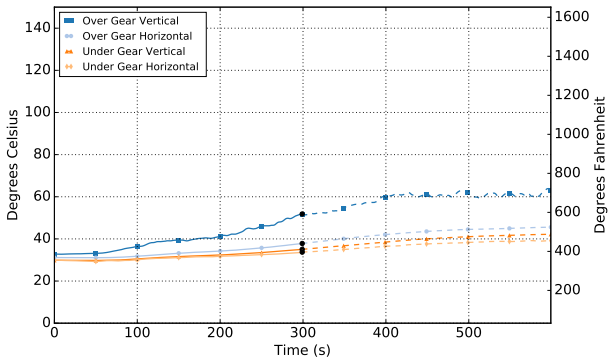

Figure C.20: Gear Sample Temperature out of Doorway for OSB Experiment 2

C.3 Gear Sample Results for Furnished Room Experiments

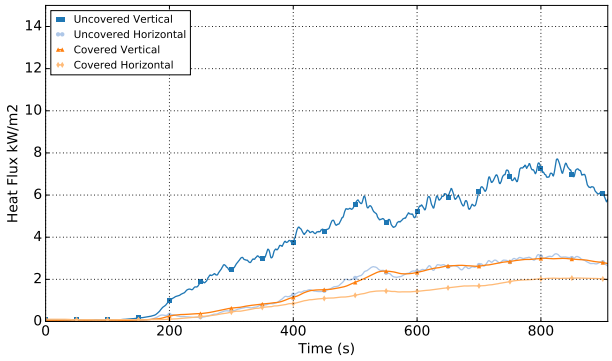

Figure C.21: Gear Sample Heat Flux in Doorway for Furniture Experiment 1

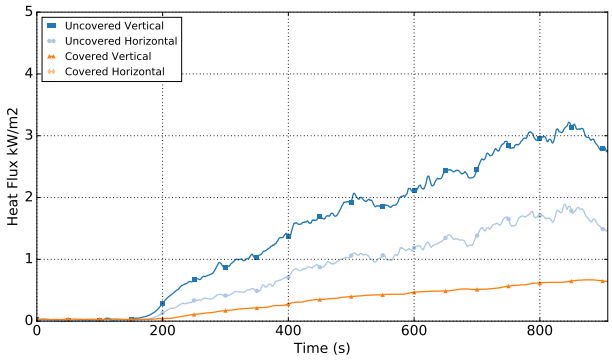

Figure C.22: Gear Sample Heat Flux out of Doorway for Furniture Experiment 1

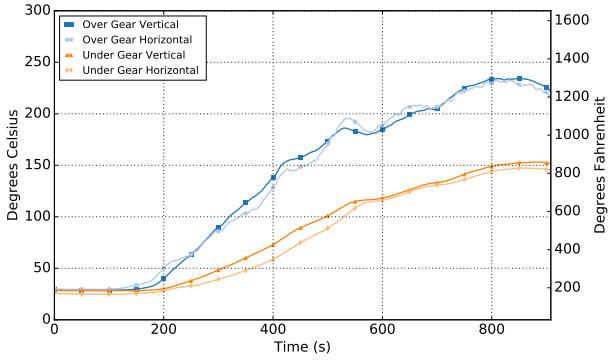

Figure C.23: Gear Sample Temperature in Doorway for Furniture Experiment 1

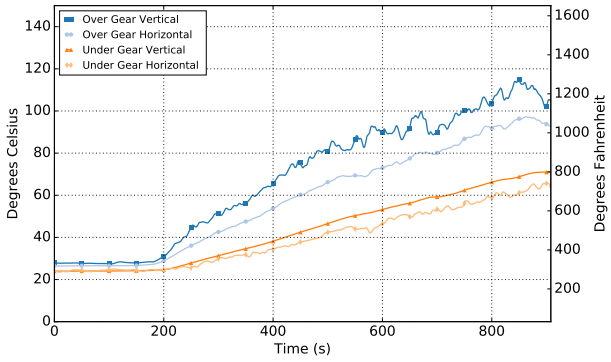

Figure C.24: Gear Sample Temperature out of Doorway for Furniture Experiment 1

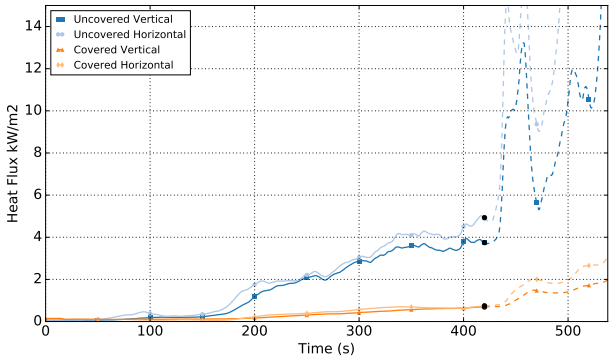

Figure C.25: Gear Sample Heat Flux in Doorway for Furniture Experiment 2

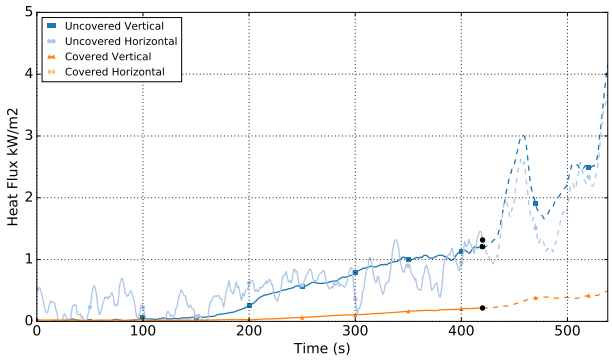

Figure C.26: Gear Sample Heat Flux out of Doorway for Furniture Experiment 2

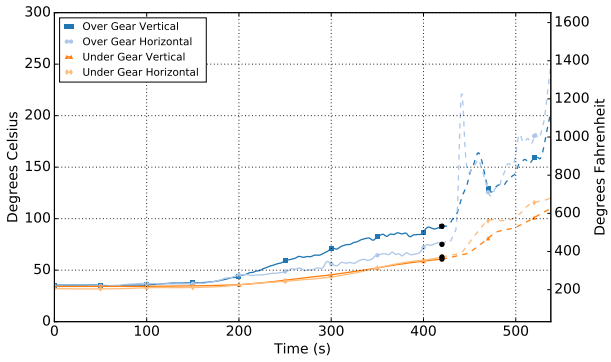

Figure C.27: Gear Sample Temperature in Doorway for Furniture Experiment 2

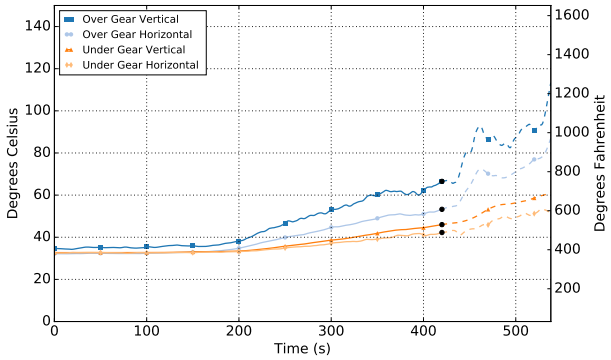

Figure C.28: Gear Sample Temperature out of Doorway for Furniture Experiment 2

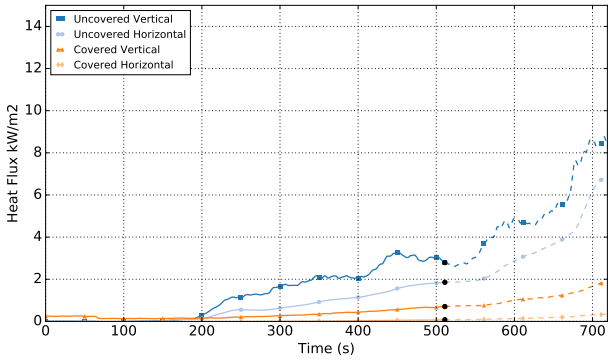

Figure C.29: Gear Sample Heat Flux in Doorway for Furniture Experiment 3

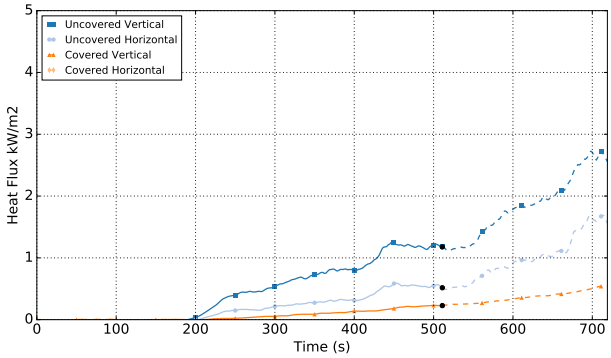

Figure C.30: Gear Sample Heat Flux out of Doorway for Furniture Experiment 3

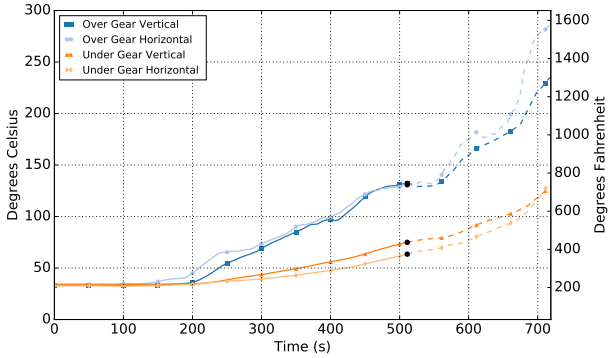

Figure C.31: Gear Sample Temperature in Doorway for Furniture Experiment 3

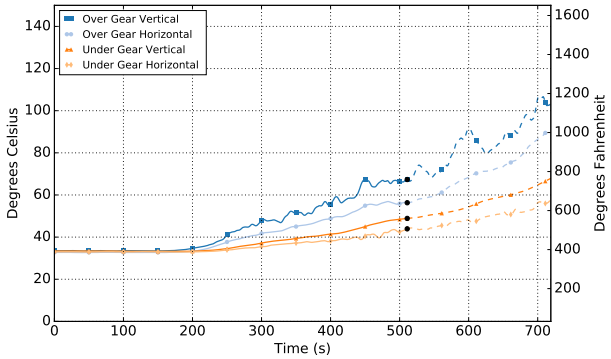

Figure C.32: Gear Sample Temperature out of Doorway for Furniture Experiment 3